Early evolution of titanosauriform sauropod dinosaurs

by

Michael Daniel D’Emic

A dissertation submitted in partial fulfillment
of the requirements for the degree of
Doctor of Philosophy
(Geology)
in The University of Michigan
2011

Committee:

Associate Professor Jeffrey A. Wilson, chair
Assistant Professor Catherine Badgley
Professor Tomasz K. Baumiller
Professor Daniel C. Fisher
Professor Rob van der Voo

ACKNOWLEDGEMENTS

First, I would like to thank my dissertation committee: C. Badgley, T. Baumiller, D. Fisher, R. van der Voo, and J. A. Wilson for advice and guidance during the project. Special thanks to J. A. Wilson for constant support, guidance, and research opportunities over the years.

Thanks for field assistance and support from P. Christenson, T. Churchill, B. Dauksewicz, B. Foreman, P. Gingerich, A. Hayden, D. Klein, S. Macone, C. Manz, K. Melstrom, D. Raisanen, A. Tillett, and C. Youngs. Thanks to M. Fox (YPM), D. Nixon (SMU), C. Manz, K. Melstrom, and B. Sanders (UM) for preparation. Special thanks to A. Pan, L. Ballinger (FWMSH) and D. Colodner (ASDM) for permission to destructively sample limb bones for histology, and M. Sander and K. Stein for helpful technical information about drilling sauropod bones. Thanks to D. C. Fisher for use of thin-sectioning equipment and K. M. Smith for assistance. J. A. Wilson, M. Wedel and R. Barnes kindly provided parts of figures 4.1, 4.6 and 4.7, respectively. Thanks to the administrative staff of the UM Geological Sciences Department, especially N. Kingsbury and A. Hudon for much help over the years.

Collections managers and curators at the following institutions are thanked for their help and hospitality, without which this dissertation certainly would not have been possible: C. Mehling and M. Norell (American Museum of Natural History, New York City), W. Joyce and D. Brinkman (Yale Peabody Museum, New Haven), M. Carrano, C. Ito, and M. Brett-Surman (United States National Museum, Washington, D.C.), R. Sullivan (State Museum of Pennslyvania, Harrisburg), M. Lamanna and A. Henrici (Carnegie Museum of Natural History, Pittsburgh), B. Simpson (Field Museum of Natural History, Chicago), P. Sereno, B. Masek, and T. Keillor (University of Chicago Paleontology Laboratory, Chicago), K. Curry Rogers (Science Museum of Minnesota, St. Paul), P. M. Sander, N. Klein, K. Remes, and N. Klein (Universitat Bonn, Bonn), R. Cifelli, J. Person, and K. Davies (Oklahoma Museum of Natural History, Norman), T. Rowe and L. Murray (Texas Memorial Museum, Austin), D. Winkler and L. Jacobs (Southern Methodist University, Dallas), A. Pan and L. Ballinger (Ft. Worth Museum of Science and Nature, Ft. Worth), T. Williamson and S. Lucas (New Mexico Museum of Natural History, Albuquerque), D. Colodner (Arizona-Sonora Desert Museum, Tucson), M. Getty (Utah Museum of Natural History), B. Brooks and R. Sheetz (Brigham Young University, Provo), K. Carpenter and L. Ivy (Denver Museum of Nature and Science, Denver), D. Schwarz-Wings (Museum für Naturkunde, Berlin), R. Allain (Muséum national d'Historire naturelle, Paris), A. Kramarz (Museo Argentino de Ciencias Naturales, Buenos Aires), J. Powell (Instituto Miguel Lillo, Tucumán), B. González Riga (IANIGLA, Mendoza), R.

Coria (Museo Carmen Funes, Plaza Huincul), D. Pol and P. Puerta (Museo Paleontológico Egidio Feruglio, Trelew), V. and S. Suteethorn (Sirindhorn Museum, Phu Kum Khao, Thailand), and B. Khenthavong (Musée des Dinosaures, Savannakhet, Laos).

I have also had the privilege of serving as a teaching assistant for several exceptional professors, including J. A. Wilson, G. Dick, D. C. Fisher, J. Blum, D. Zak, T. Baumiller, B. Kennedy, M. Clark, D. Lund, S. Simmons, K. Webber, and R. van der Voo. Thanks to all for showing me how to teach by your example.

Discussions with J. Carballido, B. Z. Foreman, T. Ikejiri, D. Ksepka, P. D. Mannion, J. S. McIntosh, P. Rose, P. M. Sander, P. Sereno, K. M. Smith, K. Stein, S. Suteethorn, P. Upchurch, M. J. Wedel, J. A. Whitlock, D. Winkler, and A. Wood greatly helped me in writing this dissertation — thanks to everyone for advice and input. Special thanks to T. Ikejiri and J. A. Whitlock for advice early and throughout my graduate career — life would have been a lot more difficult without their kind and consistent help. I would also like to thank the many UM graduate students and friends who have kept life in Ann Arbor interesting and fun. Thanks also to my family, especially my Mom, for support and encouragement over the years.

TABLE OF CONTENTS

Chapter

LIST OF FIGURES

Figure

LIST OF TABLES

Table

ABSTRACT

Titanosauriformes was a globally-distributed, long-lived clade of dinosaurs that contains both the largest and smallest known sauropods. In an effort to understand the phylogenetic relationships of their early (Late Jurassic–Early Cretaceous) members, this dissertation presents a taxonomic revision of Early Cretaceous North American titanosauriforms and a lower-level cladistic analysis of basal titanosauriforms worldwide.

Taxonomic revision renders some Early Cretaceous North American sauropods nomina dubia, substantially augments the hypodigm of others, and recognizes a new genus and species. This revision reinforces the similarity among Early Cretaceous North American dinosaur faunas; this homogeneity stands in marked contrast to the latitudinal variation in dinosaur faunas that developed later in the Cretaceous. Reports of titanosaurs in the Early Cretaceous of North America are unsubstantiated. The latest register of Early Cretaceous North American sauropods (before the 'sauropod hiatus') occurs in the coastal units marking transgression of the Western Interior Seaway, whereas eight ecologically disparate dinosaur lineages are present just below and above this boundary in the same geologic units that sauropods are found in. I thus interpret the start of the sauropod hiatus as the result of a continent-wide extinction, coincident with and perhaps attributable to competition with ornithischian herbivores, rather than the result of preservation or sampling bias.

Cladistic analysis of 25 taxa and 114 characters results in the recovery of three main titanosauriform clades: Brachiosauridae, Euhelopodidae, and Titanosauria. A re-evaluation of the phylogenetic affinities of fragmentary taxa and footprints based on synapomorphies recovered in this analysis finds no evidence for titanosaurs before the Early Cretaceous, in contrast to previous reports of Middle and Late Jurassic forms. The origin of Titanosauria is enigmatic because the geologically oldest titanosaurs are derived forms (lithostrotians) found penecontemporaneously on both Laurasian and Gondwanan continents.

Finally, I explore the bone histology (osteocyte morphology) of recent birds in an attempt to discover proxies of bone growth rate that can be applied to Titanosauriformes. Characterization of osteocyte shape and size reveals substantial intra-bone, intra-individual, and intra-specific variation, and highlights the need for sampling control in studies of fossil bone histology.

CHAPTER 1

INTRODUCTION

Titanosauriformes is a large clade of sauropod dinosaurs whose members are common in many Mesozoic ecosystems. The smallest, largest, geologically youngest, and most geographically-widespread sauropods are titanosauriforms. Some genera are known from complete skeletons (e.g., Janensch, 1950) and a few are known from ontogenetic series (Curry Rogers, 2005), but most named species are poorly known. In particular, skulls are exceedingly rare in Titanosauriformes, though recent discoveries have begun to remedy this situation (Curry Rogers, 2005; Chure et al., 2010). Despite the patchy sampling of much of their fossil record, several evolutionary patterns are apparent in titanosauriform evolution, including a trend towards decreasing tooth size (Chure et al., 2010), development of a 'wide gauge' posture and concomitant appendicular specializations (Wilson and Carrano, 1999), and several episodes of dwarfing (Sander et al., 2006; Stein et al., 2010). More derived titanosauriforms — lithostrotian titanosaurs — are characterized by a number of apomorphies that might seem counterintuitive for giant animals, including non-ossification of the carpus and manual phalanges (Salgado et al., 1997; Wilson and Sereno, 1998), increased skeletal pneumaticity (Wedel et al., 2000b), and the development of osteoderms (Bonaparte and Powell, 1980; D'Emic et al., 2009).

Since the first titanosauriform was named by Richard Lydekker in 1877, the number of named titanosauriforms has swelled to include more than 90 named genera, as have the number of taxonomic revisions adding information to previously named genera (e.g., Wilson and Upchurch, 2003; Wilson et al., 2009; D'Emic and Wilson, 2011; Carballido et al., 2011; Carballido et al., in press; Mannion and Calvo, in press). The bulk of new discoveries has come from Asia and South America, but several North American, African, and Australian forms have come to light as well (see genus lists in Mannion and Calvo, in press).

Titanosauriformes evolved during the Late Jurassic and Cretaceous, which was a complex time in terms of faunal turnover, changing paleogeography, and the expansion of new floras (Ostrom, 1970; Cifelli et al,. 1997; Jacobs and Winkler, 1998). Because of its long collecting history and well-dated sediments, North America has been important to shaping our view of dinosaurs in general, and Titanosauriformes in particular. Numerous authors have proposed that Early Cretaceous North American dinosaur faunas are relicts of those of the Late Jurassic, being predominated by sauropods, allosauroids, and primitive iguanodonts (Jacobs and Winkler, 1998). In contrast, the Late Cretaceous of North America is predominated by taxa such as ceratopsians, hadrosaurids, and tyrannosaurids, which are thought to represent an Asian paleobiogeographic influence (Sereno, 1999). The period of turnover between the earlier, 'relictual' faunas and later, Asian faunas may have been as short as 2 Myr around the Albian–Cenomanian boundary based on the record in Texas and Oklahoma (Jacobs and Winkler, 1998).

The place of sauropods in this turnover has been controversial. Definitive sauropod fossils are absent from North America from the mid-Cenomanian until the Maastrichtian (D’Emic et al., 2010). This mid-Cretaceous period of absence is termed the ‘sauropod hiatus’ (Lucas and Hunt, 1989). Some authors have suggested that sauropod disappearance is an artifact of biases in the fossil record perhaps related to a lack of the appropriate type of sauropod-bearing environments into the Late Cretaceous (e.g., Lehman, 2001; Mannion and Upchurch, 2011). Other authors have considered the disappearance of sauropods around the Early–Late Cretaceous boundary (ca. 100 Ma) to represent a regional extinction, and their reappearance to represent paleobiogeographic immigration from another landmass (e.g., Lucas and Hunt, 1989; Cifelli et al., 1997; D’Emic et al., 2010). Whereas discerning which of these scenarios (bias versus genuine extinction) is correct depends on knowledge of titanosauriform interrelationships, discerning the cause(s) of titanosauriform success or extinction on various landmasses is informed by titanosauriform paleobiology.

Titanosauriform paleobiology attracts much research attention because they were the largest terrestrial animals that ever evolved. Attempts to reconstruct sauropod growth rates have been made using skeletochronology, wherein annual growth rings in long bones are plotted against body mass to create a growth curve (Lehman and Woodward, 2008). These attempts have yielded varying results, as they are sensitive to the sampled bone and methodology chosen (see Lehman and Woodward, 2008). Furthermore, most large sauropods lack growth rings and so skeletochronology is inapplicable (Klein and Sander, 2008). A novel proxy for growth rate or metabolism is needed for estimating growth rates in sauropods.

In this dissertation, I apply taxonomic revision, geologic fieldwork, cladistic analysis, and bone histology to investigate (1) the interrelationships of basal titanosauriforms, (2) the cause(s) of the sauropod hiatus in North America, and (3) possible proxies for growth rate in titanosauriforms.

Chapter 2 presents taxonomic revision of titanosauriforms from the Early Cretaceous Trinity Group of Texas. These sauropods were historically referred to ‘*Pleurocoelus*’; instead I show that they represent other previously named and novel genera and species. I conclude by discussing the distribution of dinosaur faunas in the Early Cretaceous of North America.

Chapter 3 presents taxonomic revision of titanosauriform material from the Early Cretaceous Cloverly Formation of Wyoming and Montana, as well as the results of paleontological and geological fieldwork. I discuss the start of the sauropod hiatus in terms of the relative roles of bias and extinction.

Chapter 4 presents a lower-level cladistic analysis of basal titanosauriforms. This analysis is aimed at understanding the phylogenetic relationships of early (Late Jurassic–Early Cretaceous) titanosauriforms. Chapter 4 employes the augmented operational taxonomic units forged in chapters 2 and 3. This analysis establishes robust synapomorphies for many titanosauriform subclades, and provides a foundation for future study of basal titanosauriform phylogeny and the origin of Titanosauria.

Chapter 5 explores the utility of osteocytes as proxies for the metabolic or growth rates of sauropods. This chapter is motivated by the question of how fast sauropods grew, which has eluded determination in most species because their long bones (that scale with mass) lack growth lines. To explore these relationships, I first investigate patterns of variation in osteocyte volume and surface area within individuals and species of modern birds. I then attempt to discover predictive relationships between osteocyte morphology and physiological parameters such as growth rate and basal metabolic rate.

Chapter 6 summarizes the conclusions and interpretations of the previous chapters.

REFERENCES

Bonaparte JF, Powell JE. 1980. A continental assemblage of tetrapods from the Upper Cretaceous beds of El Brete, northwestern Argentina (Sauropoda–Coelurosauria–Carnosauria–Aves). *Mémoires de la Société Geólogique de France, nouvelle séries* **139**: 19–28.

Carballido JL, Pol D, Cerda I, Salgado L. 2011. The osteology of *Chubutisaurus insignis* Del Corro, 1975 (Dinosauria: Neosauropoda) from the ‘middle’ Cretaceous of central Patagonia, Argentina. *Journal of Vertebrate Paleontology* **31**: 93–110.

Carballido JL, Pol D, Rauhut O. in press. Osteology and phylogenetic relationships of *Tehuelchesaurus benitezii* (Dinosauria, Sauropoda) from the Upper Jurassic of Patagonia. *Zoological Journal of the Linnean Society.*

Chure D, Britt BB, Whitlock, JA, Wilson, JA. 2010. First complete sauropod dinosaur skull from the Cretaceous of the Americas and the evolution of sauropod dentition. *Naturwissenschaften* **97**: 379–391.

Cifelli, R, Kirkland JI, Weil A, Deino A, Kowallis BJ. 1999. High-precision ^{40}Ar/^{39}Ar geochronology and the advent of North America's Late Cretaceous terrestrial fauna. *Proceedings of the National Academy of Sciences* **94**: 11163–11167.

Curry Rogers K. 2005. Titanosauria: a phylogenetic overview. In: Curry Rogers K, Wilson JA, eds. *The Sauropods: Evolution and Paleobiology*. Berkeley: University of California Press, 50–103.

D'Emic MD, Wilson JA. 2011. New remains attributable to the holotype of the sauropod dinosaur *Neuquensaurus australis*, with implications for saltasaurine systematics. *Acta Palaeontologica Polonica* **56**: 61–73.

D'Emic MD, Wilson JA, Chatterjee S. 2009. The titanosaur (Dinosauria: Sauropoda) osteoderm record: review and first definitive specimen from India. *Journal of Vertebrate Paleontology* **29**: 165–177.

D'Emic MD, Wilson JA, Thompson R. 2010. The end of the sauropod dinosaur hiatus in North America. *Palaeogeography, Palaeoclimatology, Palaeoecology* **297**: 486–490.

Jacobs LL, Winkler DA. 1998. Mammals, archosaurs, and the Early to Late Cretaceous transition in north-central Texas. In: Tomida Y, Rich TH, Vickers-Rich P, eds. *Proceedings of the second Gondwanan dinosaur symposium*. Tokyo: National Science Museum Monographs, 253–280.

Janensch W. 1950. Die Wirbelsaule von *Brachiosaurus brancai*. Palaeontographica (Suppl. 7) 3:27–93.

Klein N, Sander PM. 2008. Ontogenetic stages in the long bone histology of sauropod dinosaurs. *Paleobiology* **34**: 248–264.

Lehman T. 2001. Late Cretaceous dinosaur provinciality; in Tanke, D. H. and K. Carpenter (eds.), Mesozoic Vertebrate Life. Indiana University Press, Bloomington, Indiana. pp. 310–328.

Lehman T, Woodward H. 2008. Modeling growth rates for sauropod dinosaurs. *Paleobiology* **34**: 264–281.

Lucas SG, Hunt AP. 1989. *Alamosaurus* and the sauropod hiatus in the Cretaceous of the North American western interior. Geological Society of America Special Paper **238**: 75–85.

Mannion PD, Upchurch P. 2011. A re-evaluation of the 'mid-Cretaceous sauropod hiatus' and the impact of uneven sampling of the fossil record on patterns of regional dinosaur extinction. *Palaeogeography, Palaeoclimatology, Palaeoecology* **299**: 529–540.

Mannion PD, Calvo JO. In press. Anatomy of the basal titanosaur (Dinosauria, Sauropoda) *Andesaurus delgadoi* from the mid-Cretaceous (Albian–early Cenomanian) Río Limay Formation, Neuquén Province, Argentina: implications for titanosaur systematics. *Zoological Journal of the Linnean Society*.

Ostrom JH. 1970. Stratigraphy and paleontology of the Cloverly Formation (Lower Cretaceous) of the Bighorn basin area, Wyoming and Montana.

Peabody Museum Bulletin **35**: 1–234.

Sander PM, Mateus O, Laven T, Knötschke N. 2006. Bone histology indicates insular dwarfism in a new Late Jurassic sauropod dinosaur. *Nature* **441**: 739–741.

Sereno PC. 1999. Dinosaurian biogeography: vicariance, dispersal and regional extinction. In: Tomida Y, Rich TH, Vickers-Rich P, eds. *Proceedings of the second Gondwanan dinosaur symposium*. Tokyo: National Science Museum Monographs, 249–257.

Stein K, Cziki Z, Curry Rogers K, Weishampel DB, Redelstorff R, Carballido JL, Sander PM. 2010. Small body size and extreme cortical bone remodeling indicate phyletic dwarfism in *Magyarosaurus dacus* (Sauropoda: Titanosauria). *Proceedings of the National Academy of Sciences* **107**: 9258–9263.

Upchurch P. 1995. The evolutionary history of sauropod dinosaurs. Philosophical Transactions of the Royal Society of *London* **349:** 365–390.

Upchurch P. 1998. The phylogenetic relationships of sauropod dinosaurs. *Zoological Journal of the Linnean Society* **124:** 43–103.

Upchurch P, Barrett PM, Dodson P. 2004. Sauropoda. In: Weishampel DB, Dodson P, Osmólska H, eds. *The Dinosauria*, 2nd edition. Berkeley: University of California Press, 259–322.

Wedel MJ, Cifelli RL, Sanders RK. 2000. *Sauroposeidon proteles*, a new sauropod from the Early Cretaceous of Oklahoma. *Journal of Vertebrate Paleontology* **20**: 109–114.

Wilson JA, Carrano MT. 1999. Titanosaurs and the origin of 'wide-gauge' trackways: a biomechanical and systematic perspective on sauropod locomotion. *Paleobiology* **25**: 252–267.

Wilson JA, Upchurch P. 2003. A revision of *Titanosaurus* Lydekker (Dinosauria-Sauropoda), the first dinosaur genus with a 'Gondwanan' distribution. *Journal of Systematic Palaeontology* **1**: 125–160.

Wilson JA, Upchurch P. 2009. Redescription and reassessment of the phylogenetic affinities of *Euhelopus zdanskyi* (Dinosauria: Sauropoda) from the Early Cretaceous of China. *Journal of Systematic Palaeontology* **7**: 199–239.

CHAPTER 2

REVISION OF THE SAUROPOD DINOSAURS OF THE TRINITY GROUP (COMANCHEAN SERIES, EARLY CRETACEOUS), USA, WITH THE DESCRIPTION OF A NEW GENUS

Introduction

Sauropod dinosaurs were common and diverse megaherbivores in many Mesozoic ecosystems. Their status as the largest land animals that ever evolved, as well as their unique body plan with a long neck and tail set on an elephantine body, has fuelled studies of their evolution and palaeobiology (e.g., Wilson 2002; Sander & Clauss, 2008). Their extreme size has also hindered such studies, contributing to the incompleteness of most fossil sauropod individuals and the difficulty of excavating and working with them. Nonetheless, better fossil material and many systematic revisions in the last decade have greatly increased the amount of information available to sauropod researchers (e.g., McIntosh 2005; Rose 2007; Taylor 2009; Carballido *et al.* 2011; Mannion, in press).

The first sauropods described from North America were found in the Arundel Formation of Maryland (Johnston 1859), which was originally thought to be Late Jurassic in age (e.g., Marsh 1897), but is now recognized as Early Cretaceous (e.g., Ostrom 1970). *Astrodon* (Leidy 1865) and *Pleurocoelus* (Marsh 1888) were based on isolated, incomplete type specimens, to which later-discovered specimens from Maryland and elsewhere were referred. The validity, hypodigms, and inferred affinities of these two genera have varied widely since they were named over a century ago (Table 2.1; see below). Sauropods from several other regions of the world have been referred to *Pleurocoelus* and *Astrodon* (e.g., Langston 1974), but new discoveries and analyses have challenged some of these referrals (e.g., Rose 2007). The controversial or ambiguous taxonomy of many fragmentary Early Cretaceous North American sauropods and the discovery of substantial new material (e.g., Wedel et al., 2000a; Rose, 2007) prompts a comprehensive reevaluation of Early Cretaceous North American sauropods.

Cretaceous Sauropods of North America. The presence of sauropods into the Cretaceous of North America was confirmed by Larkin (1910), who reported the discovery of a sauropod coracoid in the Early Cretaceous Antlers Formation of Oklahoma (a lateral equivalent of the Trinity Group of Texas). Several decades later, more complete excavations and exploration in the Trinity Group were undertaken by the Field Museum of Natural History, Harvard University, and Southern Methodist University. These excavations yielded the remains of a diverse vertebrate fauna, including sauropods (Bilelo 1969). Additional Trinity

Group sauropod remains were reported from Texas, including a hind limb from the Paluxy Formation at Walnut Creek in Wise County (Bilelo 1969) and a partial skeleton from the underlying Glen Rose Formation near Blanco (Langston 1974; Tidwell & Carpenter 2003).

The Trinity Group sauropods collected by the Field Museum teams and reported by Bilelo (1969) were referred to *Pleurocoelus sp.* by Langston (1974), a taxonomic decision that was followed for some time (e.g., Gallup 1975, 1989; McIntosh 1990), but not by more recent authors (e.g., Gomani *et al.* 1999, Upchurch *et al.* 2004; Carpenter & Tidwell 2005; Rose 2007). Authors have also disagreed on the phylogenetic affinities of these Early Cretaceous Texan materials referred to *Pleurocoelus*, with some referring them to Brachiosauridae, and others regarding it as more closely related to titanosaurs (e.g., McIntosh 1990; Salgado *et al.* 1995). Figure 2.1 depicts a cladogram of the major clades and taxa discussed in this paper, based on recent analyses (Upchurch *et al*. 2004; Rose 2007).

The Early Cretaceous North American sauropod fossil record has improved greatly in the last decade, as several more complete skeletons have been described from Early Cretaceous strata, especially in the Trinity Group and Antlers Formation of Texas and Oklahoma, respectively. Two monospecific genera have been named from these strata — *Sauroposeidon proteles* (Wedel *et al.* 2000a) and *Paluxysaurus jonesi* (Rose 2007). Comparatively little has been discussed regarding the taxonomy or phylogenetic affinities of other sauropod

Trinity fossils, although a sauropod partial skeleton reported by Bilelo (1969; SMU 61732) has been mentioned as a genus distinct from other Early Cretaceous Trinity sauropods (e.g., Tidwell *et al.* 1999; Wedel *et al.* 2000b). Herein I provide a name, diagnosis, description, and comparisons for this skeleton. I then examine the anatomy and affinities of the hind limb from the Paluxy Formation described by Gallup (1975, 1989) and evaluate the validity and diagnoses of other Early Cretaceous sauropods from the Trinity Group. Finally, I evaluate the similarity of these revised Trinity Group faunas to those of similar age, such as from the Cloverly Formation of Wyoming and Montana and the Cedar Mountain Formation of Utah.

Note on the taxonomy of *Astrodon* and *Pleurocoelus*. The taxonomy of *Astrodon* and *Pleurocoelus* has varied widely according to different authors (Table 3.1). The type series of *Astrodon johnstoni* consists of two teeth (YPM 798) from the Arundel Formation in Maryland, USA (Johnston 1859; Leidy 1865). The type series of *P. altus* consists of a left tibia and fibula from one individual (USNM 4971), and the type series of *P. nanus* consists of a cervical (USNM 5678), dorsal (USNM 4968), sacral (USNM 4969), and caudal (USNM 4970) centrum, all of which are unfused to their respective neural arches and ribs (Marsh, 1988; Lull *et al.* 1911). The type series of *Pleurocoelus nanus* is of the appropriate size to belong to one individual, but the exact provenance of each bone is uncertain. These bones could represent a chimera of individuals or taxa

(Hatcher 1903).

Referrals of new material to *Pleurocoelus* and *Astrodon* and revisions of the Arundel Formation fauna drastically changed the taxonomy of these sauropods during the twentieth century. Hatcher (1903, 12) believed that the Arundel Formation remains were found "...in essentially, and perhaps identically, the same locality and horizon..." and, given the lack of substantial variation among those sauropod remains, suggested *Astrodon johnstoni* was the only sauropod genus and species present in the formation*.* Lull *et al.* (1911) agreed with Hatcher (1903) that *Astrodon* and *Pleurocoelus altus* represented the same taxon, but thought that *Pleurocoelus nanus* was a different taxon, based on the relative frequency of small and large sauropod bones in the formation. Gilmore (1921) reviewed the Arundel Formation fauna and agreed with former workers that more than one species of sauropod was present in the Arundel Formation. However, he differed from previous authors in assigning taxonomic value to the observed differences among the material, referring all of the material to a single genus, *Astrodon*, and creating the new species *Astrodon nanus* and *Astrodon altus*. Gilmore's (1911) taxonomy was preferred for several decades—for example, the subsumation of *Pleurocoelus* into *Astrodon* was followed by the influential work of Romer (1956). Kingham (1962) also referred all of the Maryland species to *Astrodon*; in addition, he referred several species of *Brachiosaurus* to *Astrodon,* creating *Astrodon atalaiensis, Astrodon brancai, and Astrodon altithorax.* Kingham (1962) also named *Astrodon fraasi.* Kingham's

(1962) referrals have not been followed by subsequent authors (e.g., McIntosh 1990; Upchurch *et al.* 2004; Carpenter & Tidwell 2005).

Carpenter & Tidwell (2005) re-described much of the Arundel Formation sauropod material and concluded that the low degree of variability in the available skeletal elements indicates that only one species is present, which would be *Astrodon johnstoni* based on priority. Carpenter & Tidwell (2005) presented ten autapomorphies in their diagnosis of *Astrodon johnstoni* (based on all of the sauropod material from the Arundel Formation): (1) supraoccipital crest low and wide; (2) tall, narrow foramen magnum; (3) short, wide camerate cervical vertebrae with very large pleurocoels; (4) deep pleurocoels in the dorsal vertebrae; (5) deep pleurocoels in the sacral vertebrae; (6) posterior sacral vertebrae with a prominent groove on the ventral surface; (7) anterior caudal vertebrae with short centra; (8) coracoid thick with prominent lip; (9) radius with distinct oblique ridge; and (10) two small postero-distal condyles on the radius. Many of these features are indistinguishable compared to the situation exhibited in other sauropods such as *Camarasaurus* (characters 1, 2, 7–10; Osborn & Mook, 1921; Ostrom & McIntosh, 1966, pl. 46, 51; Madsen *et al.* 1995, fig. 23), or are related to the juvenile nature of the material (characters 1, 3–5; Wedel *et al.* 2000b; Curry Rogers & Forster 2004).

None of these autapomorphies deals with teeth, which make up the type series elements of *Astrodon johnstoni*. Like *Astrodon johnstoni*, the type series of *Pleurocoelus altus* and *P. nanus* bears no unique features, making all three taxa nomina dubia (pers. obs., 2010).

Carpenter & Tidwell (2005) present an example of the ‘laissez-faire’ approach outlined by Wilson *et al.* (2009). Employing the laissez-faire approach in the case of the Arundel Formation involves (1) ascribing no taxonomic meaning to the range of variation in the sample, (2) assuming the coeval nature of the various horizons of the Arundel Formation, and (3) inferring ontogenetic transformations among specimens in the sample. Currently these assumptions are large owing to a lack of data surrounding them. For the taxonomy of *Astrodon* and *Pleurocoelus*, I advocate the opposite viewpoint, the ‘tabula rasa’ approach (Wilson *et al.* 2009), in which taxa whose holotypes are non-diagnostic are deemed nomina dubia. I employ the tabula rasa approach in the Arundel Formation case because of (1) the especially fragmentary and non-diagnostic type series involved and (2) the paucity of provenance or quarry data for nearly all specimens.

However, the ventral groove on the sacral vertebra (character 6) may be unique (USNM 5666, pers. obs. 2010), but cannot be observed in the syntype of *Pleurocoelus nanus*. Indeed, other sauropod material from the Arundel Formation does have unique features, including a groove below the ectopterygoid and palatine articular facets on the maxilla and laterally curved pedal unguals (pers. obs., 2010). However, the lack of association among these materials limits their systematic utility. Furthermore, some bones in the sample display marked variation, such as the deeply divided versus flat distal ends of the first metatarsals (pers. obs., 2010), suggesting that more than one taxon is present. Future discoveries may yield associated skeletons in the Arundel Formation bearing these or other diagnostic features.

Anatomical abbreviations

acdl, anterior centrodiapophyseal lamina; cprl, centroprezygapophyseal lamina; pcdl, posterior centrodiapophyseal lamina; pl, pleurocoel; pocdf, postzygapophyseal centrodiapophyseal fossa; podl, postzygapophyseal diapophyseal lamina; posdf, postzygapophyseal spinodiapophyseal fossa; prdl, prezygapophyseal diapophyseal lamina; sdf, spinodiapophyseal fossa; sprf, spinoprezygapophyseal fossa; spol, spinopostzygapophyseal lamina.

Institutional abbreviations

ASDM, Arizona-Sonora Desert Museum, Arizona, USA; DMNS, Denver Museum of Nature and Science, Denver, USA; FMNH, Field Museum of Natural History, Chicago, USA; FWMSH, Ft. Worth Museum of Science and History, Ft. Worth, USA; HMN MB. R, Humboldt Museum für Naturkunde, Berlin; OMNH, Oklahoma Museum of Natural History, Norman, USA; SMU, Southern Methodist University, Dallas, USA; TMM, Texas Memorial Museum, Austin, USA, USNM, United States National Museum (Smithsonian Institution), Washington, D.C., USA.

Systematic palaeontology

DINOSAURIA Owen, 1842

SAUROPODA Marsh, 1878

NEOSAUROPODA Bonaparte, 1986

TITANOSAURIFORMES Salgado *et al.,* 1997

Astrophocaudia gen. nov.

1974 *‘Pleurocoelus’* sp. Langston

1997 ‘*Pleurocoelus’* Salgado and Calvo

Type species. *Astrophocaudia slaughteri*, sp. nov. (Figs. 2.3–2.10).

Holotype. SMU 61732 and 203/73655; a tooth (SMU 203/73655), two cervical vertebrae, fragments of dorsal vertebrae, 24 caudal vertebrae, approximately 20 fragmentary dorsal ribs, two chevrons, a distal scapular blade, part of a right ilium, and numerous fragments. The two associated teeth mentioned by Rose (2007) are instead prezygapophyses of middle caudal vertebrae; these were glued onto their appropriate vertebrae during preparation in August 2009. The appropriate size and lack of duplication of elements suggest that only one sauropod individual was present in the quarry.

Diagnosis. Autapomorphies include: anterior-middle caudal vertebrae with planar hyposphene-hypantrum articulations set off from zygapophyses; anterior-middle caudal vertebrae with prespinal lamina contacting intraprezygapophyseal lamina. Unlike *Astrophocaudia*, *Sauroposeidon proteles* (see below) has wide spinoprezygapophyseal fossae (sprf) that are bounded by strongly developed spinoprezygapophyseal laminae (sprl) in anterior caudal vertebrae. *Giraffatitan*, *Abydosaurus*, *Venenosaurus*, and *Cedarosaurus* are differentiated from *Astrophocaudia* by the presence of sporadically distributed fossae below the transverse processes in caudal vertebrae and forward-leaning neural spines in the latter two genera. *Sonorasaurus* is differentiated from *Astrophocaudia* by the reduction of the spinoprezygapophyseal laminae (spol) in the anterior-middle caudal vertebrae that cause each postzygapophysis to project far beyond the posterior margin of the neural spine. The ilium of *Astrophocaudia* is not complete enough to compare meaningfully with that of *Brontomerus mcintoshi*.

Derivation of name. *A*-, non- (Greek); *stropho*-, twisting or turning (Greek); *caud*-, tail (Greek). The name is in reference to the tightly articulating hyposphene-hypantrum system in the anterior and middle caudal vertebrae, which also resembles a star (*astron*; Greek) in posterior view. The generic name is also a reference to *Astrodon*, the first Early Cretaceous North American sauropod. The specific name honors Dr. Robert H. Slaughter, who excavated the specimen in the 1960s.

Locality, horizon, and age. Walnut Creek, southeast of Decatur, Wise County, Texas. 33° 09’ N, 97° 34’ W (Thurmond 1974; Fig. 2). This locality also preserves the semionontid fish *Lepidotes* (some scales of which were found in contact with the bones of *Astrophocaudia*), a theropod claw (SMU 62723), a theropod squamosal (SMU 61741), and the turtle *Naomichelys*. Bilelo (1969) reported the sauropod as coming from Wall, Texas. There is a city called “Wall” in Texas, but it is several hundred miles from Wise County. Dr. Wann Langston visited the Walnut Creek sauropod site in 1984 (D. Winkler, pers. comm., 2009), and noted the location as occurring “5.6 miles south and 0.9 miles west of Decatur” (which is in Wise County). In addition, Thurmond (1974: appendix) gives latitude and longitude coordinates for a “Walnut Creek B local fauna” that includes a sauropod and is in accordance with the locality given in Langston’s notes. SMU 61732 comes from the Trinity Group, uppermost part of the middle unit of the Paluxy Formation (Thurmond 1974), which is lower Albian (112.2–106 Ma) in age (Jacobs & Winkler 1998).

Description and comparisons

In the following description, abbreviations for vertebral laminae and fossae follow Wilson (1999) and Wilson *et al*. (2011), respectively. Comparisons are made where relevant; other comparative information can be found in the differential diagnosis or Discussion below.

Tooth

SMU 203/73655 (Fig. 2.3) is missing its enamel, but details of its morphology and wear are still evident. It is uncertain what part of the jaw the tooth comes from. The tooth is 17 mm long, 5.6 mm deep labiolingually and 6.4 mm wide mesiodistally. The tooth is slightly spatulate, with a midline longitudinal groove on its lingual face (Fig. 2.3). Its wear facet is nearly planar and is angled either mesially or distally, but not labiolingually. There is a very slight axial twist towards the apex of the tooth, though not as great as in the upper teeth of *Abydosaurus* (Chure *et al.* 2010).

Presacral vertebrae

One partial middle-to-posterior cervical vertebra and fragments of several posterior cervical or anterior dorsal vertebrae are accessioned as part of SMU 61732. Little can be said about the morphology of the more fragmentary vertebrae, so description will focus on the middle-to-posterior cervical vertebra.

The mid-cervical vertebra has been sheared dorsally on its right side, exposing the ventral face of the centrum in right lateral view (Fig. 2.4). Its centrum is 48 cm long, and the partially fused neurocentral suture is still visible anteriorly and posteriorly as well-defined furrows offsetting the neural arch pedicles. The posterior centrum is 24 cm wide and 15 cm tall, but it is sheared, so the actual measurements would have been closer to 22 x 17 cm. The elongation index (EI = centrum length/posterior centrum height; Wilson & Sereno

1998) cannot be determined reliably due to the deformation mentioned above, but is between 2.8 and 3.2. The average EI (aEI = centrum length divided by average of posterior width and height; Chure *et al*. 2010) equals 2.5. The aEI varies along the vertebral column in sauropods; it is generally highest in the middle cervical vertebrae. The aEI of this vertebra of *Astrophocaudia* is intermediate between the low values observed in basal macronarians (e.g., *Camarasaurus*, 1.5) and the high values (above 4.0) observed in many titanosauriforms (e.g., *Giraffatitan*, *Malawisaurus*; Chure et al., 2010).

The centrum of the mid-cervical vertebra is strongly opisthocoelous and has a flat to slightly concave bottom. Pneumaticity is extensive in the centrum, and its lateral face is highly subdivided into pneumatic camerae and camellae that are about 1–8 cm in their longest dimension, ramify into decreasingly smaller cavities, and are separated by 1–3 mm thick bony walls. A sharp ridge on the dorsolateral face of the centrum delimits the pneumatic areas of the centrum from those of the neural arch. The mid-posterior cervical vertebra appears to possess the camellate or somphospondylous condition sensu Wedel (2003), with a several generations of sub-centimeter branching chambers that permeate the centrum. Much of the neural arch is damaged, and the neural spine is largely missing. The acdl and prdl are well developed, and the fossa between them (prcdf) is subdivided.

Caudal vertebrae

Langston (1974) listed twenty-one caudal vertebrae as belonging to SMU 61732. In addition to these, three vertebrae were located in a drawer with other materials of SMU 61732, along with a notecard, which reads: “Walnut Creek Loc. Paluxy Fm. Sauropod Loc. Turtle vertebrae” (pers. obs., 2009). These caudal vertebrae and the 21 presented by Langston (1974) are from a single quarry and are appropriate in morphology, size, and preservation to represent a single series. With these additional vertebrae, the holotypic caudal vertebral series includes a total of 24 vertebrae (Figs 2.5–2.7). Additional fragments, including zygapophyses, neural spines, and transverse processes, were recovered from boxes of fragments from the site and reattached to their respective vertebrae in August 2009.

All regions of the tail are well-represented aside from the anteriormost caudal vertebrae. The anteriormost preserved caudal vertebra is likely the 8th in the series, based on comparisons with *Giraffatitan brancai* and *Cedarosaurus weiskopfae*. After this, there is a gap of 1–2 vertebrae and then a series of five consecutive caudal vertebrae. The rest of the preserved tail is made up of series of one to six vertebrae with gaps between. Estimated vertebral positions are given in Figures 2.5 and 2.7. In the description below, vertebrae are numbered according to their most likely anatomical position.

All centra have a width:height ratio of roughly 1:1 (Table 3.2). In caudal vertebra eight, the lateral walls of the centrum angle inwards ventrally and are delimited from the flat ventral face by a weak ridge. This ridge persists to about caudal vertebra 25, distal to which caudal centra are cylindrical in cross section. There are no fossae on the lateral or ventral faces of any of the caudal vertebral centra, and all of the caudal vertebral centra have a solid (i.e., non-camerate or camellate) bone texture. With the neural canal held horizontally, the centrum and neural spines of the anterior and middle caudal vertebrae are nearly vertically oriented (Fig. 2.5).

The anterior face of the first preserved (eighth) caudal centrum is concave, and the posterior face is irregular in shape, but essentially flat (Fig. 2.5). The second and fourth caudal vertebral centra have concave anterior faces, and posterior faces that are flat or weakly concave. In the next vertebra, both faces are concave, but the anterior concavity is greater than the posterior. This type of articulation, termed “plani-concave” by Tidwell *et al.* (2001) has been proposed as an autapomorphy of *Cedarosaurus*. However, this condition is present in several sauropods, including *Camarasaurus* (YPM 1905, pers. obs., 2007), *Brachiosaurus altithorax* (FMNH P 25107; pers. obs., 2008), and *Sauroposeidon* (FWMSH 93-B; see below; pers. obs., 2009). The rest of the vertebrae, excepting the last few, have equally weakly concave anterior and posterior faces (i.e., weakly amphicoelous). The last few are a mix of procoelous and biconvex centra as in some vertebrae referred to *Giraffatitan brancai* (HMN MB.R 5000, pers. obs., 2008) and some titanosaurs (e.g., Trotta *et al.* 2002; Calvo & González Riga 2003).

The neural spines of the more anterior caudal vertebrae are composed anterolaterally of sprls. In caudal vertebrae 8–15, the prsl rugosity reaches all the way to the tprl. The spinoprezygapophyseal fossa (sprf) is narrow and shallow. In the tenth caudal vertebra in the series, there is a slight transverse expansion of the neural spine distally. In all other caudal vertebrae, the lateral faces of the neural spine are parallel. In the tenth caudal vertebra of the series, the neural spine has a “saddle” at its midpoint (Figure 2.5), as in some vertebrae of *Venenosaurus* (DMNH 40392; pers. obs., 2010) and *Camarasaurus* (Ostrom & McIntosh 1966: pl. 37). Some mid-posterior caudal vertebrae have a slight anterior projection on the neural spine (Fig. 2.7). On the neural arch, there is a small fossa in front of the postzygapophyses that represents a combined postzygapophyseal spinodiapophyseal fossa plus a postzygapophyseal centrodiapophyseal fossa (= posdf + pocdf; see Wilson *et al.* 2011). The remnants of this fossa persist as a subtle depression until caudal vertebra 15.

The zygapophyses and hyposphene-hypantrum articulations undergo dramatic morphological changes along the caudal vertebral series. In the first caudal vertebra that preserves zygapophyses (caudal vertebra 10), the pre- and postzygapophyses are large and subhorizontally oriented, and the hyposphene is subequal in size to the postzygapophysis. The postzygapophyses and hyposphene are both planar and meet at an angle of about 80 degrees (Figure 2.5). More posteriorly in the caudal vertebral series, the zygapophyseal articular surfaces decrease in size faster than the hyposphene-hypantrum articular surfaces. By the caudal vertebra 20, the intervertebral neural arch articulation is represented by a single, vertical plane, as in other sauropods (e.g., *Camarasaurus*, *Giraffatitan*, *Mendozasaurus*).

Dorsal ribs

A total of about 20 fragmentary dorsal ribs are present; none are “plank-like” (cross- section more than three times wider anteroposterioly than mediodistally). Some of the preserved ribs approach this condition (cross-sectional ratio 2.8), so *Astrophocaudia* may have plank-like ribs as titanosauriforms do (Wilson 2002). The largest dorsal rib is pneumatic, again as in Titanosauriformes (Fig. 2.8). There is an oval, ridged tubercle on the anterior half of the proximolateral part of the largest dorsal rib (Figure 2.8A). This feature is absent in the only other dorsal rib that preserves this portion of the shaft.

Chevrons

Langston (1974) reported a single chevron with SMU 61732. In the process of studying the material, a second was discovered. Both come from the anterior region of the tail. The more complete chevron is only missing its distalmost blade (Fig. 2.9). It is 24.2 cm long, and has an open hemal canal that measures 9.1 cm deep dorsoventrally. On the anterior face of the blade, there is a flattened oval boss measuring 1.2 x 4 cm that has a texture of ridges and grooves (Fig. 2.9). Each arm of the chevron bears a single articular facet with a medially pointed process.

Scapula

A distal scapular blade (Fig. 2.10) has complete anterodorsal and posteroventral margins and is almost complete distally. It could represent a left or right scapula, as the preserved part is symmetrical about its long axis. The preserved length is 70 cm. Its breadth ranges from 17 to 38.5 cm, giving a minimum-to maximum width ratio of about 2.3. The scapular blade is less than 1 cm thick distally and about 3 cm thick at the center of the broken base of the blade. The base of the blade is flat in cross section as in *Euhelopus* and titanosaurs, rather than D-shaped with a broad lateral ridge as in non-somphospondylans (Wilson and Sereno, 1998). The bone has a texture of subtle, axially oriented ridges and grooves on the exterior face of the bone.

Ilium

The acetabular region and part of the preacetabular process of the left ilium are present. The preacetabular lobe of the ilium flares outward at about 45 degrees. No evidence of pneumaticity exists in the ilium. A subtle ridge extends anteroposteriorly above the pubic peduncle, as in some other sauropods (e.g., *Camarasaurus*, Ostrom & McIntosh 1966). The total preserved length of the element is 45 cm.

DINOSAURIA Owen, 1842

SAUROPODA Marsh, 1878

NEOSAUROPODA Bonaparte, 1986

TITANOSAURIFORMES Salgado *et al.,* 1997

Cedarosaurus Tidwell *et al.* 1999 Figs. 2.11–2.14

1974 *Pleurocoelus* sp. Langston

1989 *Pleurocoelus* sp. Gallup

1997 *Pleurocoelus* Salgado and Calvo

Type species. *Cedarosaurus weiskopfae* Tidwell *et al.* 1999 (Figs. 2.11–2.14).

Holotype. DMNH 39045, a partial skeleton consisting of dorsal and caudal vertebrae, dorsal ribs, chevrons, partial left and right scapulae, coracoids, and sternal plates, a right humerus, radius, ulna, and metacarpal IV, partial right and left pubes, ischia, and femora, a right tibia and right metatarsals I, II, and V.

Holotype locality, horizon, and age. Early Cretaceous Yellowcat Member of the Cedar Mountain Formation, Utah, USA, Barremian–Aptian (Tidwell *et al.* 1999; Greenhalgh and Britt, 2006).

Referred material. FMNH PR 977, a partial hind limb including an incomplete tibia and fibula, an astragalus, five metatarsals, and 11 phalanges.

Referred material locality, horizon, and age. Referred material comes from the Paluxy Formation, 20 km south of Decatur, Texas, USA, which is Aptian–Albian in age (Jacobs & Winkler 1998).

Revised diagnosis. Autapomorphies of *Cedarosaurus weiskopfae* include: radius with hypertrophied longitudinal flange lateral to ulnar articulation on the posterior side of the distal end (Tidwell *et al.*, 1999), radius with tubercle on anterior face of shaft, one-third of the way from proximal end, metatarsal II with well-developed medial and lateral tubercles at mid-shaft (pers. obs., 2010). FMNH PR 977 is referable to *Cedarosaurus* on the basis of two additional autapomorphies: metatarsal V only slightly expanded proximally (length/proximal transverse breadth > 2), and metatarsal V around 1.5 times longer than metatarsal I. Also, FMNH PR 977 possesses four well-developed pedal unguals and a phalanx on metatarsal V, providing two additional autapomorphies for *Cedarosaurus.*

Description

The following description focuses on material referred to *Cedarosaurus weiskopfae*, which consists of a partial hind limb described by Gallup (1989). For description and comparisons of the holotype of *Cedarosaurus*, see Tidwell *et al.*

(1999). The crus was found vertically over the astragalus and pes (Gallup, 1989). Consequently, deformation in the astragalus and metatarsals is dorsoventral. Some of the distal ends of the metatarsals are broken/eroded away, and much of the bone was restored with plaster.

Crus and tarsus

About three-quarters of the middle section of the tibia and fibula are preserved in several pieces (Gallup 1975). The preserved lengths of the tibia and fibula are about 71 and 95 cm, respectively. The tibia is oval in cross-section, and its midshaft measures 16.1 cm anteroposteriorly by 8.4 cm transversely. The mid-shaft of the fibula is roughly D-shaped in cross section with a slightly concave medial margin, and its midshaft measures 11.6 cm anteroposteriorly by 5.7 cm transversely. The astragalus is extremely crushed dorsoventrally. The astragalus is roughly two-thirds as broad anteroposteriorly as transversely and rugose, as in most sauropods (e.g., *Camarasaurus*, Ostrom and McIntosh, 1966). No calcaneum was found with the specimen.

Metatarsals

Five metatarsals are preserved (Figs. 2.11–2.12). Metatarsal I is nearly complete and undeformed, but metatarsals II–IV are incomplete distally, and metatarsals II and V are crushed dorsoventrally (Fig. 2.11). The proximal articular surface is largest on metatarsal I, and it is slightly smaller or subequal for metatarsals II–IV. All of the metatarsals have slightly concave proximolateral faces for the articulation of the adjacent metatarsal. In dorsal view, the lateral margin of each metatarsal is more tightly curved than the medial, as in most sauropods. The metatarsals increase in length laterally, such that metatarsal V is the longest and about 1.8 times longer than metatarsal I. The long axis of the proximal ends of metatarsals I and III are oriented dorsoventrally and roughly orthogonal to the long axis of their distal ends, which are oriented mediolaterally (Figs. 2.11–2.12).

Metatarsal I is subtriangular in proximal view, coming to a point dorsally. The articular facet for ungual I.1 is beveled dorsomedially (Figs. 2.11 and 2.12). Metatarsals II–IV are subrectangular proximally. Little can be said about their distal ends due to deformation and extensive plaster reconstruction (Fig. 2.11). Metatarsal V is much broader transversely than dorsoventrally, and is only slightly narrower transversely at its midshaft than at its distal ends (Fig. 2.11).

Phalanges

Eleven phalanges were preserved with the foot, including four unguals (Fig. 2.11). The first digit is the only one for which an exact phalangeal count (two) is known. Three are definitively the proximal-most phalanges of digits 2–4 based on fit, and a small phalanx belongs to metatarsal V because it is too small to be the penultimate phalanx on any of the other digits, which bear unguals. The best-estimate phalangeal formula is 2*-3*-3*-3*-1, but there is a range of possibilities based on other sauropods (e.g., 2*-(2-3)*-(2-4)*-(2-4)*-1; González Riga *et al.* 2008). Phalanx I.1 is wedge-shaped such that the ungual of digit I is directed laterally (Fig. 2.12). The remaining non-terminal unguals are roughly trapezoidal in dorsal view, with constricted midshafts and oval proximal faces. The innermost three unguals are about 1.7 times longer than tall and each has a dorsally acuminate oval proximal face (Fig. 2.13). Each bears variably developed nail-grooves. The presence of a large claw on metatarsal IV is regarded as an autapomorphy among eusauropods (Wilson 2002).

DINOSAURIA Owen, 1842

SAUROPODA Marsh, 1878

NEOSAUROPODA Bonaparte, 1986

TITANOSAURIFORMES Salgado *et al.*, 1997

Sauroposeidon Wedel *et al.*, 2000 Fig. 2.14

2007 *Paluxysaurus jonesi* Rose

Type species. *Sauroposeidon proteles* Wedel *et al.*, 2000 (Fig. 2.14).

Holotype. OMNH 53062, four articulated middle (?5th–8th) cervical vertebrae.

Holotype locality, horizon, and age. Early Cretaceous (Aptian–Albian) Antlers Formation of southern Oklahoma, USA. Referred materials come from the Twin

Mountains Formation of north-central Texas, USA.

Referred material. Referred material (see below) includes holotypic (FWMSH 93B-10-18) and referred (FWMSH 93B-10-1 through FWMSH 93B-10-17; FWMSH 93B-10-19 through FWMSH 93B-10-51; TMM 42488) materials of *Paluxysaurus jonesi* Rose 2007. Some of the material reported by Ostrom (1970) from the Cloverly Formation is likewise referable to *Sauroposeidon* (e.g., YPM 5449, YPM 5147), the details of which will be dealt with in future work (see also Wedel & Cifelli 2005, who tentatively referred a cervical vertebra from the Cloverly Formation (YPM 5294) to *Sauroposeidon proteles*).

Referred material locality, horizon, and age. FWMSH 93B-10-1 through FWMSH 93B-10-51 comes from the Early Cretaceous (Aptian–Albian) Twin Mountains Formation of north-central Texas, USA (Winkler *et al.* 1990). The Twin Mountains Formation is laterally equivalent to the Antlers Formation.

Revised diagnosis. Extreme elongation of the middle cervical vertebrae (length/posterior centrum height > 6), middle cervical vertebrae with posterior expansion of the pneumatic fossa to the cotyle, neural spines perforated in middle cervical vertebrae, top of neural spine with broad midline ridge flanked by small fossae at its anterior and posterior ends, middle and posterior dorsal neural spines that taper distally, anterior caudal vertebral centra roughly square in cross-section, anterior caudal vertebrae with divergent spinoprezygapophyseal laminae (sprl) (angle greater than 50 degrees) forming wide spinoprezygapophyseal fossae (sprf), scapula with two processes at the base of the ventral edge of the blade, humerus gracile, length/midshaft width > 7.5.

Comments. *Sauroposeidon proteles* and *Paluxysaurus jonesi* are from laterally equivalent units and have been hypothesized to be closely related to the brachiosaurids *Brachiosaurus* and *Giraffatitan* (Wedel *et al*. 2000b; Rose 2007). Because of their close spatiotemporal similarity and proposed close phylogenetic affinity, it is possible that *Sauroposeidon* and *Paluxysaurus* represent a single species. Several features have been cited as unique for *Sauroposeidon* and *Paluxysaurus*, or useful for distinguishing them. Some cited diagnostic features of *Sauroposeidon* have a broader phylogenetic distribution, such as the 'centroparapophyseal lamina' (Wedel *et al.* (2000a, b), which is similarly developed in some large vertebrae of *Giraffatitan brancai* (e.g., Janensch 1950, figs 40, 42; pers. obs., 2008) and *Euhelopus* (Wiman 1929, pl. 3). Some proposed autapomorphies of *Sauroposeidon* (Wedel *et al.* 2000b) are shared with *Paluxysaurus*, such as the posterior placement of the diapophyses in larger cervical vertebrae (Rose 2007).

Rose (2007) proposed three features to distinguish *Sauroposeidon* from *Paluxysaurus*: absence of an acdl, wider neural arches, and a wider prdl than *Sauroposeidon*. However, re-examination of the vertebrae of both exemplars indicates that these features do not distinguish them. There are multiple laminae beneath the arm of the prdl in both exemplars (see Wedel *et al.* 2000, fig. 6, and Rose 2007, figs. 7 and 8; pers. obs., 2009). The acdl appears unusually large on the sixth cervical vertebra of *Paluxysaurus* (Rose 2007, fig. 8) because this vertebra has been sheared upwards and backwards on its right side. Despite this shearing, it is apparent that the vertebrae of the two taxa do not differ in breadth or the width of the prdl.

Although there are no substantive morphological differences between their exemplars, the two taxa differ substantially in size: the sixth through eighth cervical vertebrae of *Sauroposeidon* have centra whose length (including condyles) are ca. 1.25 m, whereas the largest known vertebra of *Paluxysaurus* (FWMSH 93B-10-30) was estimated to have a centrum length of 0.83 m (Rose 2007). In order to evaluate the meaning of this size difference, morphological and histological features relevant to its ontogenetic status are described below.

Description

The following description focuses on demonstrating the juvenile nature of exemplars of '*Paluxysaurus jonesi'* in order to evaluate its possible referral to *Sauroposeidon proteles*. For description and comparisons of the holotype of *Sauroposeidon proteles*, see Wedel et al. (2000a, b), and for description and comparisons of '*Paluxysaurus jonesi'* see Rose (2007).

The neurocentral sutures and cervical ribs of the holotypic cervical vertebrae of *Sauroposeidon* are fully fused, suggesting that it may have been at or near skeletal maturity (Ikejiri 2003). In contrast, some cervical and dorsal vertebrae referred to *Paluxysaurus* (e.g., FWMSH 93B-10-8, -13, -30) have slight furrows representing the original position of the neurocentral sutures near their condyles and cotyles (pers. obs., 2009). In addition, the last sacral vertebra and ilia of one specimen of *Paluxysaurus* are not fully fused to the other sacral vertebrae or ilia (pers. obs., 2009), and one of the coracoids is not fused to a scapula (Rose 2007). This suggests that these individuals were not skeletally mature, because these bones tend to fuse over ontogeny (Schwarz et al., 2007). The femora and humeri in the Jones Ranch quarry do not differ by more than 10% in size (Rose 2007), so all of the quarry individuals were likely of similar ontogenetic age.

In order to more precisely determine the ontogenetic age of the *Paluxysaurus* specimens, midshaft samples of a referred fragmentary humerus (FWMSH 93-B-10-7; Rose 2007, fig. 23, 8-11) and left femur (FWMSH 93-B-10) were taken with a diamond-tipped drill according to the methodology of Stein & Sander (2009). Due to the impermeable but friable nature of the femur, stabilization with glue and extraction of the core was difficult, and the outermost few millimeters of bone were lost. It is uncertain whether or not the femur and humerus belonged to a single individual.

Thin-sections of the humeral and femoral cores reveal a cortex composed of fibrolamellar bone, as in most other sauropods (Figure 2.14; Klein & Sander 2008). Most of the bone texture is parallel-fibered, and vascular canals are relatively open. Only one line of arrested growth is visible in each section. The presence of an external fundamental system is equivocal in the humerus due to damage, but it was absent in the femur. Some secondary osteons are present within the outer centimeter of both cortices, but these do not form a solid remodeling front.

The bone represented in the outer cortex of the humerus represents types D and E of Klein & Sander (2008), which approximates those authors' histological ontogenetic stage 8 or 9. This indicates that this individual was not at adult size. Femora and humeri of *Giraffatitan brancai* at histological ontogenetic stage 8–9 can be one-half to three-quarters the size the largest known individuals of that species (see Klein & Sander 2008: fig. 4G).

In sum, lack of substantial morphological or definitive size differences and shared unique features (see diagnosis above) suggest that *Paluxysaurus* and *Sauroposeidon* represent the same species.

Discussion

Phylogenetic affinities of sauropod remains from the Trinity Group and Antlers Formation

The proposed phylogenetic affinities of sauropods from Trinity–Antlers strata have not been as historically complex as their taxonomic identities, with all authors agreeing that they represent basal titanosauriforms or titanosaurs. As shown above, most of the material making up '*Pleurocoelus*' from Texas discussed by Salgado *et al.* (1997) and other authors (Langston 1974; McIntosh 1990; Upchurch *et al.* 2004) is instead attributable to *Astrophocaudia* (SMU 61732), *Cedarosaurus* (FMNH PR 977), or *Sauroposeidon* (FWMSH 93B-10). Salgado *et al.* (1995, 1997) suggested that '*Pleurocoelus nanus*' is the sister taxon to Titanosauria, and '*Pleurocoelus* sp.' from Texas is a basal titanosaur. The characters listed as supporting titanosaur or near-titanosaur affinities — for example, a single prespinal lamina in dorsal vertebrae — are now recognized as features characterizing a wider clade than Titanosauria (Carballido *et al.* 2011). *Sauroposeidon* was described as a brachiosaurid (Wedel *et al.* 2000a) and recovered as such (as *Paluxysaurus*) in the phylogenetic analysis of Rose (2007). In contrast, Ostrom (1970) pointed out some features shared between sauropod material from the Cloverly Formation (now = *Sauroposeidon*, see Chapter 3) and titanosaurs, such as a robust ulna.

The taxonomic revisions presented above augment, combine, and redistribute some apomorphies of the Trinity Group sauropods and prompt reevaluation of their phylogenetic affinities. Chapter 4 investigates those affinities in detail, but brief comments will be made here. *Astrophocaudia* and *Sauroposeidon* are recognized as a titanosauriforms based on the presence of camellate presacral vertebrae, pneumatic dorsal ribs, a flared iliac preacetabular process, and caudal vertebrae with neural arches situated anteriorly. Somphospondylan features of *Astrophocaudia* and *Sauroposeidon* include somphospondylous vertebral pneumaticity (sub-centimeter cells with sub-millimeter walls that permeate the vertebra) and a scapular blade with a flat cross-section at its base. *Sauroposeidon* possesses numerous other somphospondylan synapomorphies including a medially beveled scapular glenoid, an ischial blade that is shorter than the pubic blade, and a proximally embracing tibia and fibula (Wilson and Upchurch, 2009). *Cedarosaurus* is a brachiosaurid titanosauriform on the basis of a high humerus-to-femur ratio and gracile humerus (Wilson, 2002).

Several sauropod remains that are indeterminate to the genus level have been reported from Trinity–Antlers strata, including a coracoid (Larkin 1910), ischium (Gallup 1975), and teeth (Gallup 1975, Maxwell & Cifelli 2000). Langston (1974) mentioned a partial skeleton from the Glen Rose Formation of Blanco County, Texas (TMM 40435; see also Tidwell and Carpenter, 2003). This specimen is a juvenile based on the lack of neurocentral fusion in some vertebrae, and the lack of fusion among the laterosphenoids, prootics, parietals, and frontals (pers. obs., 2008). This skeleton represents a titanosauriform based on the presence of camellate presacral vertebral pneumaticity, but is not diagnostic to the genus level.

Latitudinal homogeneity in Early Cretaceous North American dinosaur

faunas

The referral of *Paluxysaurus* and the Cloverly Formation sauropod material (Ostrom 1970; in prep.) to *Sauroposeidon,* as well as the referral of the hind limb from the Glen Rose Formation to *Cedarosaurus*, reinforces proposed faunal links among the Trinity Group, Antlers Formation, Ruby Ranch Member of the Cedar Mountain Formation, and Cloverly Formation (Langston 1974; Winkler *et al.* 1990; Jacobs & Winkler 1998). Nydam & Cifelli (2002) challenged the temporal correlation of the Cloverly and Antlers Formations on the basis of their disparate lizard faunas, but noted similarity between the Cloverly and Twin Mountains Formations. However, at the spatiotemporal scale of sampling in these formations, paleoenvironmental biases can also explain the observed differences in faunal compositions (Winkler *et al*. 1990).

Though separated by over 15 degrees of palaeolatitude (1,500 km; Fig. 2.2), four dinosaur genera are shared between the penecontemporaneous Twin Mountains/Antlers and Cloverly Formations: *Tenontosaurus*, *Deinonychus*, *Sauroposeidon*, and *Acrocanthosaurus* (D’Emic and Melstrom, in review). The formations also share multiple non-dinosaur genera, as well as some suprageneric dinosaur taxa such as nodosaurids (Jacobs & Winkler 1998). This degree of faunal similarity over 15 degrees of palaeolatitude stands in contrast to the latitudinal variation present in dinosaur faunas observed in the Late Cretaceous (Lehman 1987; 2001). Decades of exploration and analyses of Late Cretaceous North American strata have reinforced this latitudinal variation (Gates *et al*. 2010), whereas increased data and study of Early Cretaceous faunas has reenforced its latitudinal homogeneity. Proposed explanations for Late Cretaceous latitudinal variation (e.g., climate) could be tested against the more homogenous pattern observed in the Early Cretaceous.

Conclusions

Historically, Early Cretaceous sauropods from North America were referred to the genera *Pleurocoelus* or *Astrodon* from the Early Cretaceous Arundel Formation of Maryland. A lack of associations and non-diagnostic type specimens means that species of *Astrodon* and *Pleurocoelus* (Table 3.1) are nomina dubia.

Because these Maryland species are invalid, materials previously referred to them were reexamined. A single partial skeleton previously referred to '*Pleurocoelus* sp.' from the Trinity Group represents a new taxon, *Astrophocaudia slaughteri*. Materials from the Trinity Group designated as *Paluxysaurus jonesi* are morphologically similar to and bear autapomorphies of *Sauroposeidon*, have a similar spatiotemporal provenance, and were not at their adult body size. *Paluxysaurus* is a junior synonym of *Sauroposeidon*, which is also represented in the Cloverly Formation of Wyoming (Ostrom 1970; Chapter 3). A hind limb from the Trinity Group previously referred to '*Pleurocoelus*' (Langston 1974) is referred to *Cedarosaurus weiskopfae* on the basis of pedal synapomorphies.

Cedarosaurus is a brachiosaurid, whereas *Astrophocaudia* and *Sauroposeidon* are members of the Somphospondyli.

The sauropod dinosaurs *Sauroposeidon* and *Cedarosaurus* were widespread in western North America in the Early Cretaceous, reinforcing links among northern and southern faunas first drawn based on other dinosaurs (Jacobs & Winkler 1998). This relative homogeneity suggests that provincialism among dinosaur faunas with respect to latitude developed only later in the Cretaceous.

REFERENCES

Bilelo, M. M. 1969. The Fossil Fish *Lepidotes* in the Paluxy Formation. North-central Texas. *American Midland Naturalist* **81**, 405–411.

Bonaparte, J. F. 1986. The early radiation and phylogenetic relationships of sauropod dinosaurs, based on vertebral anatomy. Pp. 247–258 *in* K. Padian (ed.) *The Beginning of the Age of Dinosaurs.* Cambridge University Press, Cambridge.

Brochu, C. A. 1996. Closure of neurocentral sutures during crocodilian ontogeny: implications for maturity assessment in fossil archosaurs. *Journal of Vertebrate Paleontology* **16**, 49–62.

Calvo, J.O. & González Riga, B. J. 2003. *Rinconsaurus caudamirus* gen. et sp nov., a new titanosaurid (Dinosauria, Sauropoda) from the Late Cretaceous of Patagonia, Argentina. *Revista Geologica de Chile* **30**, 333–353.

Calvo, J. O., Porfiri, J. D., González Riga, B. J. & Kellner, A. W. A., 2008. Anatomy of *Futalognkosaurus dukei* Calvo, Porfiri, González Riga & Kellner, 2007 (Dinosauria, Titanosauridae) from the Neuquén Group (Late Cretaceous), Patagonia, Argentina. *Arquivos do Museu Nacional, Rio de Janeiro* **65**, 511–526.

Canudo, J. Royo-Torres, R. & Cuenca-Bescós, G. 2008. A new sauropod: *Tastavinsaurus sanzi* gen et. sp. nov. from the Early Cretaceous (Aptian) of Spain. *Journal of Vertebrate Paleontology* **28**, 712–731.

Carballido, J.L., Pol, D., Cerda, I., & Salgado, L. 2011. The osteology of *Chubutisaurus insignis* Del Corro, 1975 (Dinosauria: Neosauropoda) from the ‘middle’ Cretaceous of central Patagonia, Argentina. *Journal of Vertebrate Paleontology* **31**, 93–110.

Carpenter, K. & Tidwell, V. 2005. Reassessment of the Early Cretaceous sauropod *Astrodon johnstoni* Leidy 1865 (Titanosauriformes). Pp. 78–114. *in* V. Tidwell & K. Carpenter (eds) *Thunder Lizards: the sauropodomorph dinosaurs*. Indiana University Press, Bloomington.

Chure, D. Britt, B. B, Whitlock, J. A & Wilson, J. A. 2010. First complete sauropod dinosaur skull from the Cretaceous of the Americas and the evolution of sauropod dentition. *Naturwissenschaften* **97**, 379–391.

Cifelli, R., Kirkland, J. I., Weil, A., Deino, A. & Kowallis, B. J. 1999. High-precision ^{40}Ar/^{39}Ar geochronology and the advent of North America’s Late Cretaceous terrestrial fauna. *Proceedings of the National Academy of Sciences* **94**, 11163–11167.

Curry Rogers, K. A. 2005. Titanosauria: a phylogenetic overview. Pp. 50–103 *in* Curry K. A. Rogers & J. A. Wilson (eds) *The Sauropods: Evolution and Paleobiology.* University of California Press, Berkeley and Los Angeles.

Curry Rogers, K. A. & Forster, C. 2004. The skull of *Rapetosaurus krausei* (Sauropoda, Titanosauria) from the Late Cretaceous of Madagascar. *Journal of Vertebrate Paleontology* **24**: 121–144.

D’Emic, M. D. & Britt, B. B. 2008. Reevaluation of the phylogenetic affinities and age of a basal titanosauriform (Sauropoda: Dinosauria) from the Early Cretaceous Cloverly Formation of North America. Journal of Vertebrate Paleontology **28**, 68A.

D’Emic, M. D. & Melstrom, K. M. in review. A juvenile specimen of *Acrocanthosaurus atokensis* (Dinosauria: Theropoda): implications for Early Cretaceous North American ecosystems. Palaeogeography, Palaeoclimatology, Palaeoecology.

Gallup, M. R. 1975. Lower Cretaceous dinosaurs and associated vertebrates from north-central Texas in the Field Museum of Natural History. Unpublished M.A. thesis, University of Texas, Austin.

Gallup, M. R. 1989. Functional morphology of the hindfoot of the Texas sauropod *Pleurocoelus* sp. indet. Pp. 71–74 *in* J. O. Farlow (ed), Paleobiology of the Dinosaurs. *Geological Society of America Special Paper* 238.

Galton, P. 1981. A juvenile stegosaur, “*Astrodon pusillus*,” from the upper Jurassic of Portugal, with comments on upper Jurassic and lower Cretaceous biogeography. *Journal of Vertebrate Paleontology* **1**, 245–256.

Gates T. A., Sampson, S. D., Zanno, L. E., Roberts, E. M., Eaton, J. G., Nydam, R. L., & Hutchinson, J. H., Smith, J. A., Loewen M. A., & M. A. Getty. 2010. Biogeography of terrestrial and freshwater vertebrates from the Late Cretaceous (Campanian) Western Interior of North America. Palaeogeography, Palaeoclimatology, Palaeoecology **291**, 371–387.

Gilmore, C. W. 1921. The fauna of the Arundel Formation of Maryland. *U.S. National Museum Proceedings* **59**: 581–594.

Gomani, E., Jacobs, L. L. & Winkler, D. A. 1999. Comparison of the African titanosaurian, *Malawisaurus*, with an Early Cretaceous North American sauropod. Pp. 223–233 *in* Y. Tomida, T. H. Rich, & P. Vickers-Rich (eds) *Proceedings of the Second Gondwanan Dinosaur Symposium*, National Museum of Tokyo Monograph 15.

Hatcher, J. B. 1903. Discovery of *Astrodon* (*Pleurocoelus*) in the *Atlantosaurus* beds of Wyoming. *Annals of the Carnegie Museum of Natural History,* **2**, 9–14.

Hatcher, J. B., Marsh, O. C. & Lull, R. S. 1907. The Ceratopsia. *U.S. Geological Survey Monograph* **49**, 1–300.

Haq, B. U., Hardenbol, J. & Vail, P. 1987. Chronology of Fluctuating Sea Levels since the Triassic. *Science* **235**, 1156–1167.

He, X., Li, K., & Cai, K. 1988. *[The Middle Jurassic Dinosaur fauna from Dashanpu, Zigong, Sichuan, Vol. IV. Sauropod dinosaurs (2), Omeisaurus tianfuensis]*. Chengdu: Sichuan *Scientific and Technical Publishing House. (In Chinese.)*

Ikejiri, T. 2003. Sequence of closure of neurocentral sutures in *Camarasaurus* (Sauropoda) and implications for phylogeny in Reptilia. *Journal of Vertebrate Paleontology* **23**, 65A.

Ikejiri, T., Tidwell, V. & Trexler, D. L. 2005. New adult specimens of *Camarasaurus lentus* highlight ontogenetic variation within the species. Pp. 154–186 *in* V. Tidwell & K. Carpenter (eds) *Thunderlizards: the Sauropodomorph Dinosaurs.* Indiana University Press, Bloomington.

Jacobs, L. L. & Winkler, D. A. 1998. Mammals, archosaurs, and the Early to Late Cretaceous transition in north-central Texas. Pp. 253–280 *in* Y. Tomida, T. H. Rich, & P. Vickers-Rich (eds) Proceedings of the Second Gondwanan Dinosaur Symposium, *National Museum of Tokyo Monograph* **15**.

Janensch, W. 1950. Die wirbelsäule von *Brachiosaurus brancai. Palaeontographica* (Supplement 7) **2**, 27–93.

Johnston, C. J. 1859. Note upon odontology. *American Journal of Dental Science (new series)* **9**, 337–343.

Kingham, R. F. 1962. Studies of the sauropod dinosaur *Astrodon* Leidy. *Proceedings of the Washington Junior Academy of Sciences* **1**, 38–43.

Klein, N. & Sander, M. 2008. Ontogenetic stages in the long bone histology of sauropod dinosaurs. *Paleobiology* **34**, 247–263.

Krantz, P. M. 1998. Mostly dinosaurs: a review of the vertebrates of the Potomac Group (Aptian Arundel Formation), USA. Pp. 235–238 *in* S. G. Lucas, J. I. Kirkland, and J. W. Estep (eds) Lower and Middle Cretaceous Terrestrial Ecosystems. *New Mexico Museum of Natural History and Science Bulletin* **14**.

Langston, W. 1974. Nonmammalian Comanchean tetrapods. *Geoscience and Man* **8**, 77–102.

Lapparent, A. F. de. & Zbyszewski, G. 1957. Les dinosauriens du Portugal.

Mémoires des Services Géologiques du Portugal, nouvelle série **2**, 1–63.

Larkin, P. 1910. The occurrence of a sauropod dinosaur in the Trinity Cretaceous of Oklahoma. *Journal of Geology* **28**, 93–98.

Leidy, J. 1865. Cretaceous reptiles of the United States. *Smithsonian Contributions to Knowledge* **14**, 1–135.

Lovelace, D., M., Hartman, S. A. & Wahl, W. R. 2007.Morphology of a specimen of *Supersaurus* (Dinosauria, Sauropoda) from the Morrison Formation of Wyoming, and a re-evaluation of diplodocoid phylogeny. *Arquivos do Museu Nacional, Rio de Janeiro* **65**, 527–544.

Lull, R. S. 1911. The reptilian fauna of the Arundel Formation. *Maryland Geological Survey:* 173–178.

Lydekker, R. 1877. Notices of new and other Vertebrata from Indian Tertiary and Secondary rocks. *Records of the Geological Survey of India* **10**, 30–43.

Lydekker, R. 1890. Contributions to our knowledge of the dinosaurs of the Wealden, and the Sauropterygia of the Purbeck and Oxford Clay. *Quarterly Journal of the Geological Society of London* **46**, 182–184.

Maddison, W.P. & Maddison, D. R. 1992. MacClade, Version 3.0. Sunderland, Massachusetts: Sinauer.

Madsen, J. M., McIntosh, J. S. & Berman, D. S. 1995. The skull and atlas-axis complex of the Upper Jurassic sauropod *Camarasaurus* Cope (Reptilia: Saurischia). *Bulletin of the Carnegie Museum* **31**: 1–115.

Mannion PD. In press. A reassessment of *Mongolosaurus haplodon* Gilmore, 1933, a titanosaurian sauropod dinosaur from the Early Cretaceous of Inner Mongolia, People's Republic of China. *Journal of Systematic Palaeontology*.

McIntosh, J. S. 1990. Sauropoda. Pp. 345–401 *in* D. B. Weishampel, P. Dodson & H. Osmólska (eds) *The Dinosauria.* University of California Press, Berkeley.

McIntosh, J. S. 2005. The genus *Barosaurus* Marsh (Sauropoda, Diplodocidae). Pp. 38–77 *in* V. Tidwell & K. Carpenter (eds) *Thunder-Lizards: the Sauropodomorph Dinosaurs.* Indiana University Press, Bloomington.

Marsh, O. C. 1878. Principal characters of American Jurassic dinosaurs. Pt. I. *American Journal of Science* **16**, 411–416.

Marsh, O. C. 1888. Notice of a new genus of Sauropoda and other new dinosaurs from the Potomac Formation. *American Journal of Science, series 3,* **35**, 89–94.

Marsh, O. C. 1896. Dinosaurs of North America. *U.S. Geological Survey Annual Report* **16**, 133–244.

Marsh, O. C. 1897. Recent observations on European dinosaurs. *American Journal of Science* **4**, 413–416.

Martin, V., Suteethorn, V. & Buffetaut, E. 1999. Description of the type and referred material of *Phuwiangosaurus sirindhornae* Martin, Buffetaut and Suteethorn 1994, a sauropod from the Lower Cretaceous of Thailand. *Oryctos* **2**, 29–91.

Maxwell, W. D. & Cifelli, R. L. 2000. Last evidence of sauropod dinosaurs (Saurischia: Sauropodomorpha) in the North American mid-Cretaceous. *Brigham Young University Geology Studies* **45**,19–25.

McIntosh, J. S. & Berman, D. S. 1975. Description of the palate and lower jaw of *Diplodocus* (Reptilia: Saurischia) with remarks on the nature of the skull of *Apatosaurus*. *Journal of Paleontology* **49**, 187–199.

McIntosh, J. S. & Williams, M. 1988. A new species of sauropod dinosaur, *Haplocanthosaurus delfsi* sp. nov., from the Upper Jurassic Morrison Formation of Colorado. *Kirtlandia* **43**, 3–26.

McIntosh, J. S., Coombs Jr.,W. P. & Russell, D. A. 1992. A new diplodocid sauropod (Dinosauria) from Wyoming, U.S.A. *Journal of Vertebrate Paleontology* **12**, 158–167.

Nydam, R. L. & Cifelli, R. L. 2002. Lizards from the Lower Cretaceous (Aptian–Albian) Antlers and Cloverly Formations. Journal of Vertebrate Paleontology **22**, 286–298.

Osborn H. F. & Mook C. C. 1921. *Camarasaurus*, *Amphicoelias*, and other sauropods of Cope. *Memoirs of the American Museum of Natural History* **3**, 247–387.

Ostrom, J. H. 1970. Stratigraphy and paleontology of the Cloverly Formation (Lower Cretaceous) of the Bighorn basin area, Wyoming and Montana. *Peabody Museum Bulletin* **35**, 1–234.

Ostrom, J. H. & McIntosh, J. S. 1966. Marsh's Dinosaurs. Yale University Press, New Haven, 388 pp.

Owen, R. 1842. A description of a portion of the skeleton of *Cetiosaurus*, a gigantic extinct saurian occurring in the Oolitic Formation of different parts of England. *Proceedings of the Geological Society of London* **3**, 457–462.

Owen, R. 1875. Monographs of the fossil Reptilia of the Mesozoic formations Part II (genera *Bothriospondylus*, *Cetiosaurus*, *Omosaurus*). *Palaeontographical Society Monograph* **29**, 15–94.

Patterson, B. 1956. Early Cretaceous mammals and the evolution of mammalian molar teeth. *Fieldiana: Geology,* **13**, 1–105.

Powell, J. 2003. Revision of South American titanosaurid dinosaurs: palaeobiological, palaeobiogeographical, and phylogenetic aspects. *Records of the Queen Victoria Museum* 1–173.

Romer, A. S. 1956. *Osteology of the reptiles*. University of Chicago Press, Chicago, 772 pp.

Rose, P. 2007. A titanosauriform (Dinosauria: Saurischia) from the Early Cretaceous of Central Texas and its phylogenetic relationships. *Palaeontologica Electronica* **10**, 1–65.

Ruiz-Omeñaca, J. I. & Canudo, J. I. 2005. "*Pleurocoelus*" *valdensis* Lydekker, 1889 (Saurischia, Sauropoda) en el Cretácico Inferior (Barremiense) de la Península Ibérica. *Geogaceta* **38**, 43–46.

Salgado, L., Calvo, J. & R. A. Coria. 1995. Phylogenetic relationships of *Pleurocoelus* Marsh (Sauropoda). *Resúmenes 11th Jornadas Argentinas* *de Paleontología de Vertebrados*: **34**.

Salgado, L., & Calvo, J. O. 1997a. Evolution of titanosaurid sauropods. II: The cranial evidence. *Ameghiniana* **34**, 33–48.

Salgado, L., Coria, R. & Calvo, J. O. 1997b. Evolution of titanosaurid sauropods. I: phylogenetic analysis based on the postcranial evidence. *Ameghiniana* **34**, 3–32.

Sander, P.M. & Clauss, M. 2008. Sauropod gigantism. *Science* 322: 200–201.

Sanz, J. Buscalioni, A. D., Casanovas, M. L. & Santafé, J. V. 1987. Dinosaurios del Cretacico inferior de Galve (Teruel, España). *Estudios geologicos, vol. extr. Galve-Tremp* 45–64.

Schwarz, D., Ikejiri, T., Breithaupt, B. H., Sander, P. M. & Klein, N. 2007. A nearly complete skeleton of an early juvenile diplodocid (Dinosauria: Sauropoda) from the Lower Morrison Formation (Late Jurassic) of north central Wyoming and its implications for early ontogeny and pneumaticity in sauropods. *Historical Biology* **19**, 225–253.

Sereno P. C., Beck, A. L., Dutheil, D. B., Larssen, H. C. E., Lyon, G. H., Moussa, B., Sadleir, R. W., Sidor, C. A., Varricchio, D. J., Wilson, G. P. & Wilson J. A. 1999. Cretaceous sauropods from the Sahara and the uneven rate of skeletal evolution among dinosaurs. *Science* **286**, 1342–1347.

Simpson, G. G. 1948. The beginning of the age of mammals in South America, 1. *Bulletin of the American Museum of Natural History* **91**, 1–232.

Stein, K, Csiki, Z., Rogers, K. C., Weishampel, D. B., Redelstorff, R., Carballido, J. & Sander, P. M. 2010. Small body size and extreme cortical bone

remodeling indicate phyletic dwarfism in *Magyarosaurus dacus* (Sauropoda: Titanosauria). *Proceedings of the National Academy of Sciences* **107**: 9258–9263.

Stein, K. & M. Sander. 2009. Histological core drilling: a less destrcutive method for studying bone histology. Pp. 69–80 *in* M. A. Brown, J. F. Kane, & W. G. Parker (eds) *Methods In Fossil Preparation: Proceedings of the First Annual Fossil Preparation and Collections Symposium*.

Swofford, D.L. 2002. *PAUP*: phylogenetic analysis using parsimony (*and other methods), Version 4.0b10*. Sunderland: *Sinauer Associates.*

Tang, F., Jing, X., Kang, X., & Zhang, G. 2001. *[Omeisaurus maoianus*: a complete sauropod from Jingyuan, Sichuan]. Beijing: China Ocean Press. (In Chinese.)

Thurmond, J. T. 1974. Lower vertebrate faunas of the Trinity division in North-Central Texas. *Geoscience and Man* **8**, 103–129.

Taylor, M. 2009. A reevaluation of *Brachiosaurus altithorax* Riggs, 1903 (Dinosauria, Sauropoda) and its generic separation from *Brachiosaurus brancai* (Janensch, 1914). *Journal of Vertebrate Paleontology* **29**, 787–806.

Tidwell, V. & Carpenter, K. 2003. Braincase of an Early Cretaceous titanosauriform sauropod from Texas. *Journal of Vertebrate Paleontology* **23**, 176–180.

Tidwell, V., Carpenter, K. & Brooks, W. 1999. New sauropod from the Lower Cretaceous of Utah, USA. *Oryctos* **2**, 21–37.

Tidwell, V., Carpenter, K. & Meyer, S. 2001. New titanosauriform (Sauropoda) from the Poison Strip Member of the Cedar Mountain Formation (Lower Cretaceous), Utah. Pp. 139–165 *in* D. Tanke & K. Carpenter (eds) *Mesozoic Vertebrate Life: New Research Inspired by the Paleontology of Phillip J. Currie.* Indiana University Press, Bloomington.

Trotta, M. N. F., Campos, D. A. & Kellner, W. A. 2002. Unusual caudal vertebral centra of a titanosaurid (Dinosauria, Sauropoda) from the Continental Upper Cretaceous of Brazil. Boletim do Museu Nacional **64**, 1–11.

Upchurch, P., Barrett, P. M. & Dodson, P. 2004. Sauropoda. Pp. 259–324 *in* D. B. Weishampel, P. Dodson & H. Osmólska (eds) *The Dinosauria.* 2nd Edition. University of California Press, Berkeley.

van der Voo, R., Spakman, W. & Bijwaard, H. 1999. Tethyan subducted slabs under India. *Earth and Planetary Science Letters* **171**, 7–20.

Wedel, M. J., Cifelli, R. L. & Sanders, R. K. 2000a. *Sauroposeidon proteles*, a new sauropod from the Early Cretaceous of Oklahoma. *Journal of Vertebrate Paleontology* **20**, 109–114.

Wedel, M. J., Cifelli, R. & Sanders , R. K. 2000b. Osteology, paleobiology, and relationships of the sauropod dinosaur *Sauroposeidon*. *Acta Palaeontologica Polonica* **45**, 343–388.

Wedel, M. J. 2003. The evolution of vertebral pneumaticity in sauropod dinosaurs. *Journal of Vertebrate Paleontology* **23**, 344–357.

Wedel, M. J. & Cifelli, R. 2005. *Sauroposeidon*: Oklahoma's Native Giant. *Oklahoma Geology Notes* **65**, 40–57.

Wilson, J. A., D'Emic, M. D., Ikejiri, T., Moacdieh, E., & J. A. Whitlock. 2011. A nomenclature for vertebral fossae in sauropods and other saurischian dinosaurs. PLOS One. 19 pp.

Wilson, J. A. 1999. A nomenclature for vertebral laminae in sauropods and other saurischian dinosaurs. *Journal of Vertebrate Paleontology* **19**, 639–653.

Wilson, J. A. 2002. Sauropod dinosaur phylogeny: critique and cladistic analysis. *Zoological Journal of the Linnean Society* **136**, 217–276.

Wilson, J. A. & Sereno, P. C. 1998. Early evolution and higher-level phylogeny of sauropod dinosaurs. *Journal of Vertebrate Paleontology* **18**, 1–68.

Wiman, C. 1929. Die Kreide-Dinosaurier aus Shantung. *Palaeontologia Sinica (series C)* **6**, 1–67.

Winkler, D. A., Murray, P. A. & Jacobs, L. L. 1989. Vertebrate Paleontology of the Trinity Group, Lower Cretaceous of Central Texas*. in* D. A. Winkler, P. A. Murry, and L. L. Jacobs (eds) Field guide to the vertebrate paleontology of the Trinity Group, Lower Cretaceous of central Texas: *Field Guide, Society of Vertebrate Paleontology 49th Annual Meeting*, Austin, Texas, 1–22.

Winkler, D. A., Murray, P. A. & Jacobs, L. L. 1990. Early Cretaceous (Comanchean) vertebrates of Central Texas. Journal of Vertebrate Paleontology **10**, 95–116.

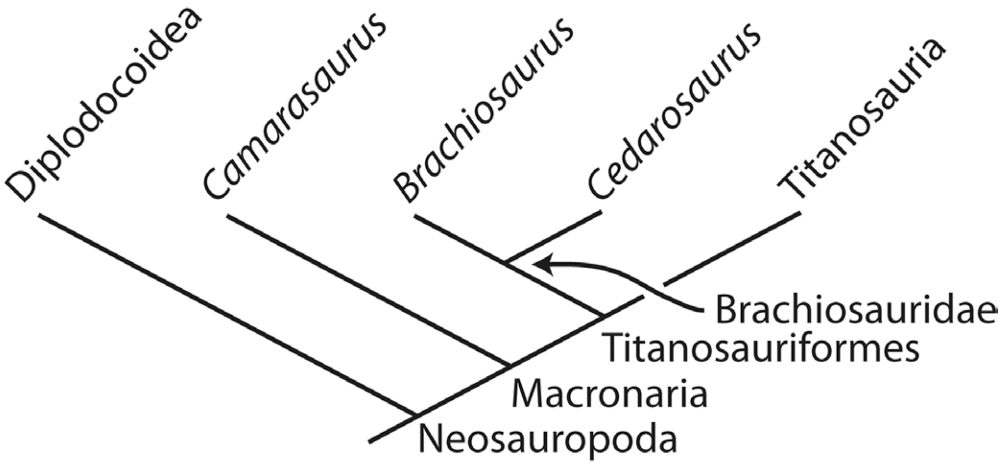

Figure 2.1. Simplified cladogram depicting the relationships of relevant sauropod clades. Based on the phylogeny of Upchurch *et al.* (2004).

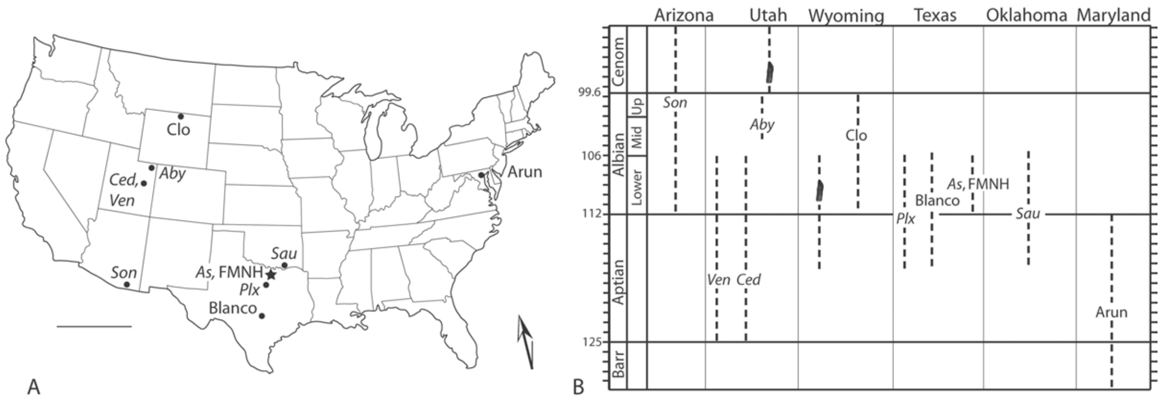

Figure 2.2. A, Holotypic locality of *Astrophocaudia slaughteri* in Wise County, Texas, USA (star), with locations of other Early Cretaceous North American sauropods (dots). Arrow indicates the direction of north during the Albian (taken from www.pbdb.org). **B,** Stratigraphic position of *Astrophocaudia slaughteri* relative to other Early Cretaceous North American sauropods. Placement of the abbreviated name indicates the most likely age for the taxon, and the dotted lines represent age uncertainty. Abbreviations: ***Aby***, *Abydosaurus*; **Arun**, Arundel Formation sauropod material, including '*Astrodon*' and '*Pleurocoelus*'; ***As***, *Astrophocaudia* gen. et. sp. nov.; **Blanco**, TMM 40435, partial sauropod skeleton from the Glen Rose Formation (Tidwell and Carpenter, 2003); ***Ced***, *Cedarosaurus*; **Clo**, Cloverly Formation sauropod material (Ostrom, 1970); **FMNH**, FMNH PR 977, hind limb of a sauropod from the Paluxy Formation referable to *Cedarosaurus weiskopfae* (Gallup, 1989); ***Plx***, *Paluxysaurus*; ***Sau***, *Sauroposeidon*; ***Son***, *Sonorasaurus*. Tooth figures indicate localities that preserve indeterminate sauropod teeth. Scale bar in **A** equals 500 km.

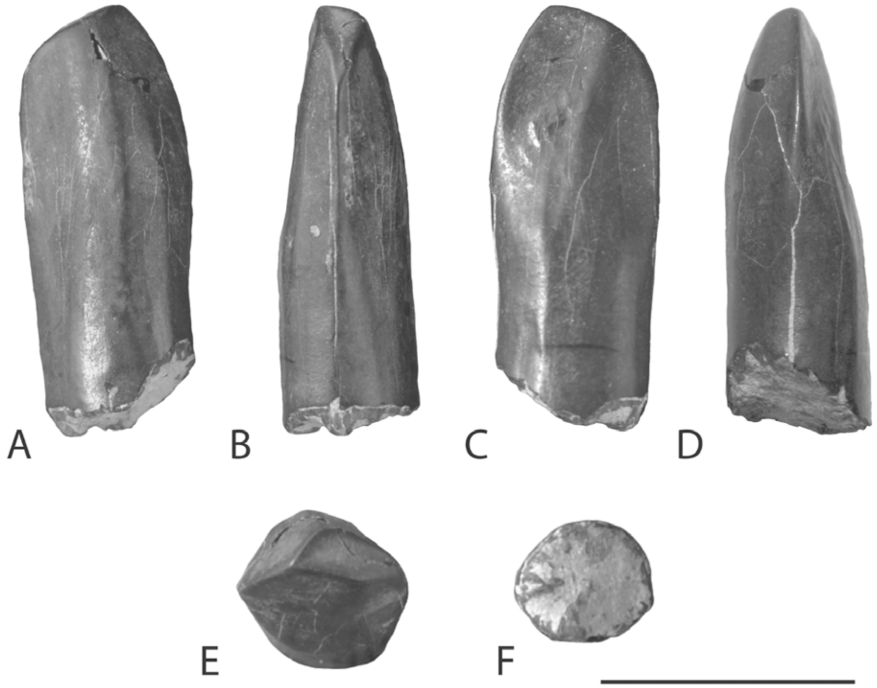

Figure 2.3 Holotypic tooth of *Astrophocaudia slaughteri* (SMU 203/73655) in **A,** labial, **B,** ?mesial, **C,** lingual, **D,** ?distal, **E,** occlusal, and **F,** proximal views. Orientation is uncertain because of uncertainty in tooth position within the jaw. Abbreviations: **wf,** wear facet. Scale bar = 1 cm.

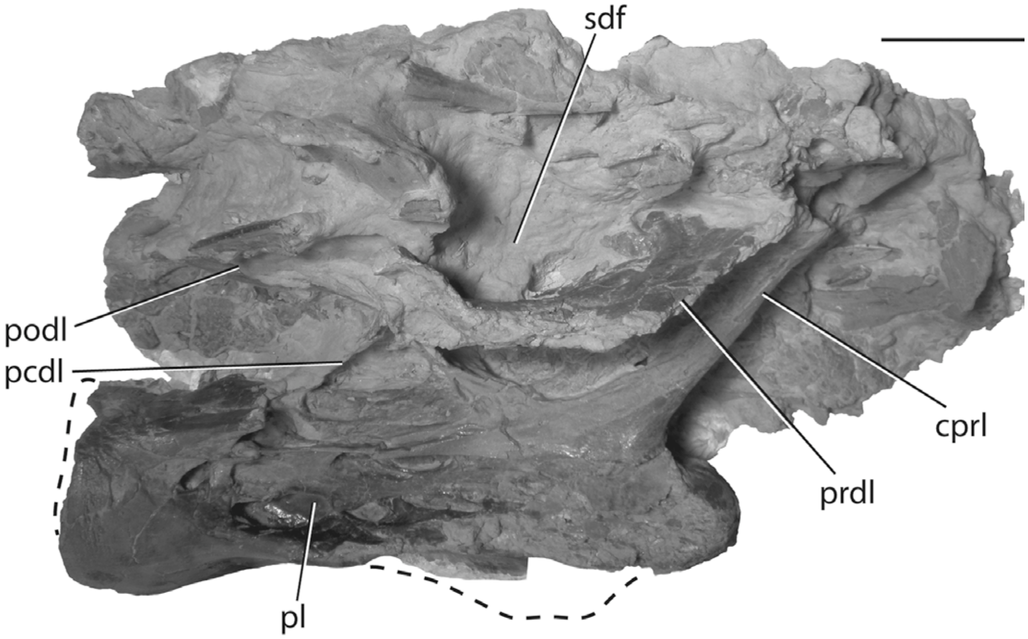

Figure 2.4. Holotypic middle to posterior cervical vertebra of *Astrophocaudia slaughteri* (SMU 61732) in lateral view. Abbreviations: **cprl**, centroprezygapophsyeal lamina; **pcdl**, posterior centrodiapophyseal lamina; **pl**, pleorucoel; **prdl**, prezygodiapophyseal lamina; **podl**, postzygapophyseal diapophyseal lamina; **sdf**, spinodiapophyseal fossa. Dashed lines indicate missing bone. Scale bar = 10 cm.

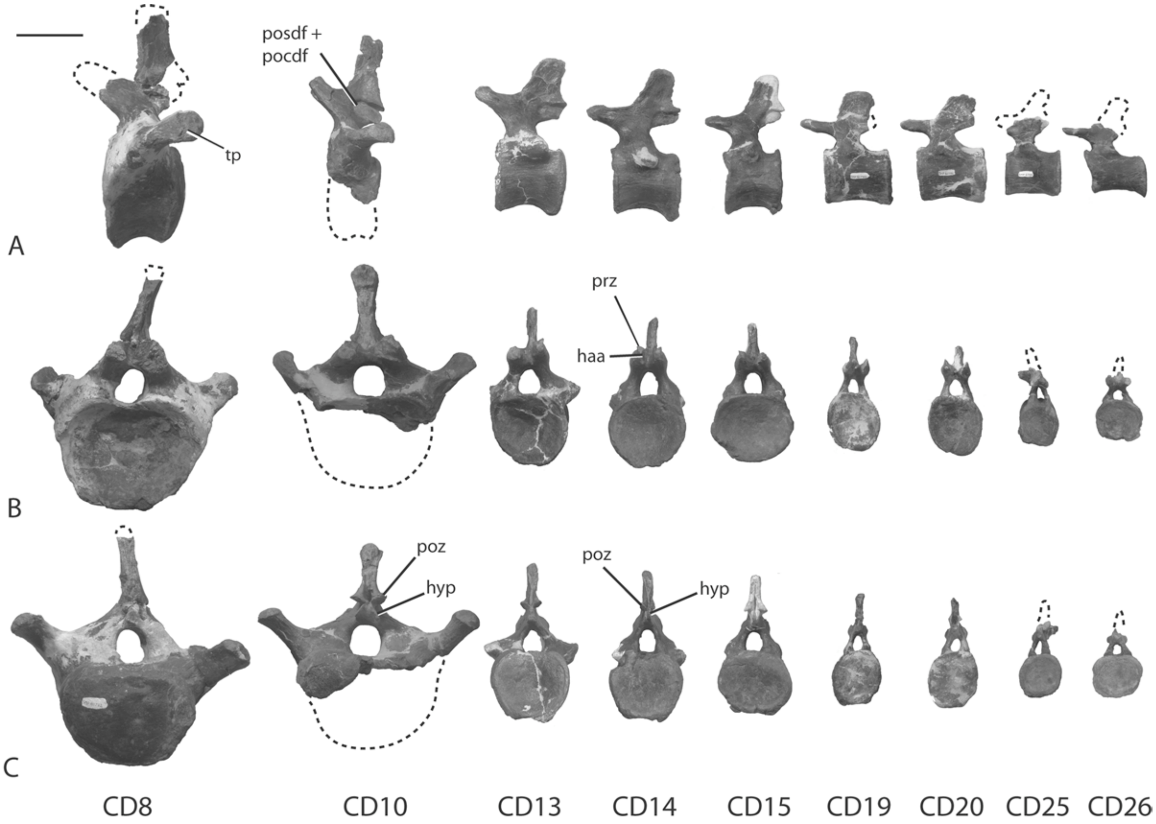

Figure 2.5. Selected vertebrae of the holotypic anterior-middle caudal vertebral series of *Astrophocaudia slaughteri* (SMU 61732) in **A,** left lateral, **B,** anterior, and **C,** posterior views. Numbers below each vertebra indicate its likely position in the caudal sequence. The 10th caudal vertebra is reversed in **A**. Abbreviations: **pocdf**, postzygapophyseal centrodiapophyseal fossa; **posdf**, postzygapophyseal spinodiapophyseal fossa; **CD**, caudal vertebra; **poz**, postzygapophysis; **prz**, prezygapophysis; **tp**, transverse process. Dashed lines indicate missing bone. Scale bar = 10 cm.

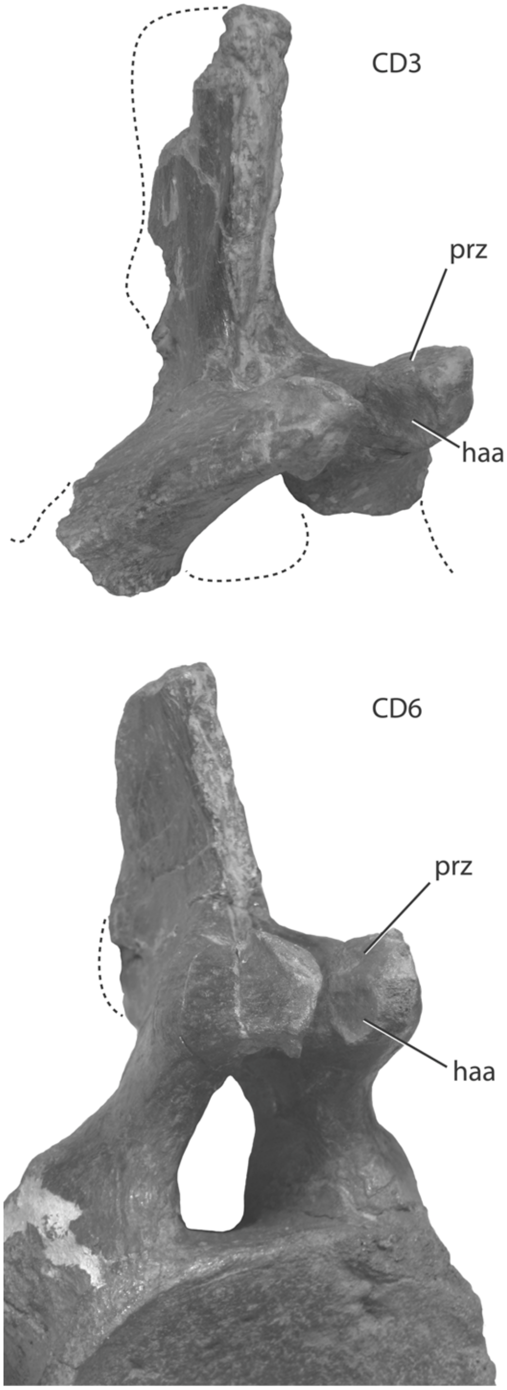

Figure 2.6. Prezygapophyses and hypantra of the 3rd and 6th preserved caudal vertebrae of the holotype of *Astrophocaudia slaughteri* (SMU 61732) in anterolateral view. Abbreviations: **CD**, caudal vertebra; **haa**, hypantrum articulation surface; **prz**, prezygapophyseal articulation surface. Dashed lines indicate missing bone. Not to scale.

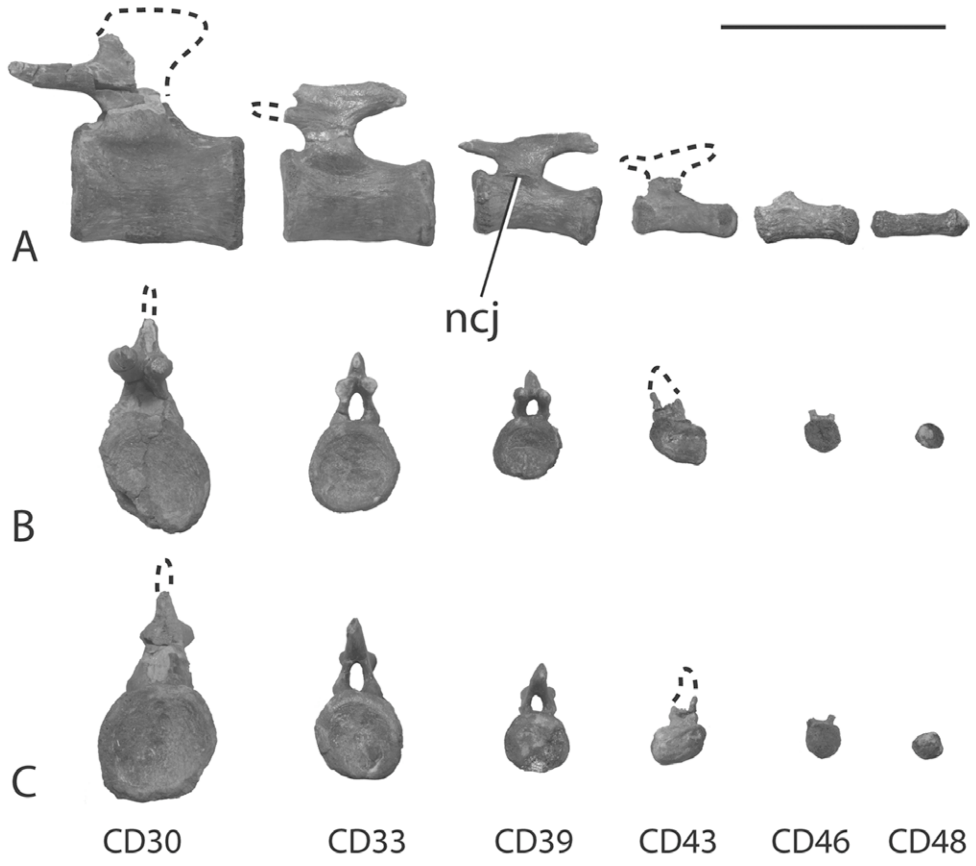

Figure 2.7. Selected vertebrae of the holotypic posterior caudal vertebral series of *Astrophocaudia slaughteri* (SMU 61732) in **A,** left lateral, **B,** anterior, and **C,** posterior views. Numbers below each vertebra indicate likely position of the vertebra in the caudal sequence. Abbreviations: **CD**, caudal vertebra; **ha,** hypantrum; **ncj,** location of fused neurocentral junction. Dashed lines indicate missing bone. Scale bar = 10 cm.

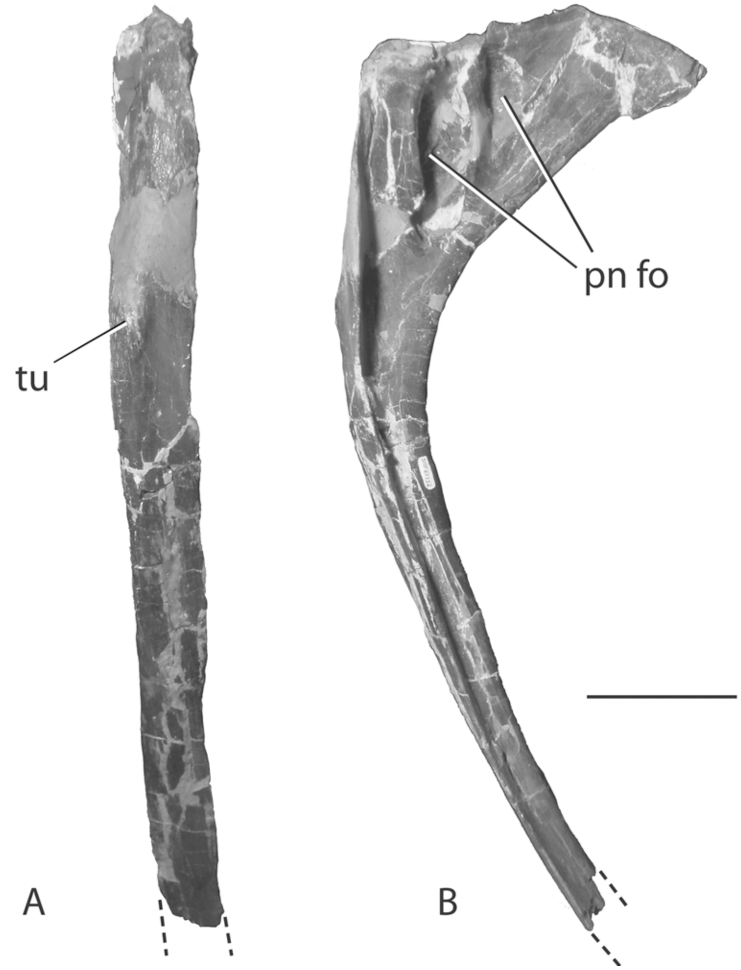

Figure 2.8. Holotypic dorsal rib of *Astrophocaudia slaughteri* (SMU 61732) in **A,** lateral and **B,** posterior views. Abbreviations: **pn fo,** pneumatic fossa; **tu,** tubercle. Dashed lines indicate missing bone. Scale bar = 10 cm.

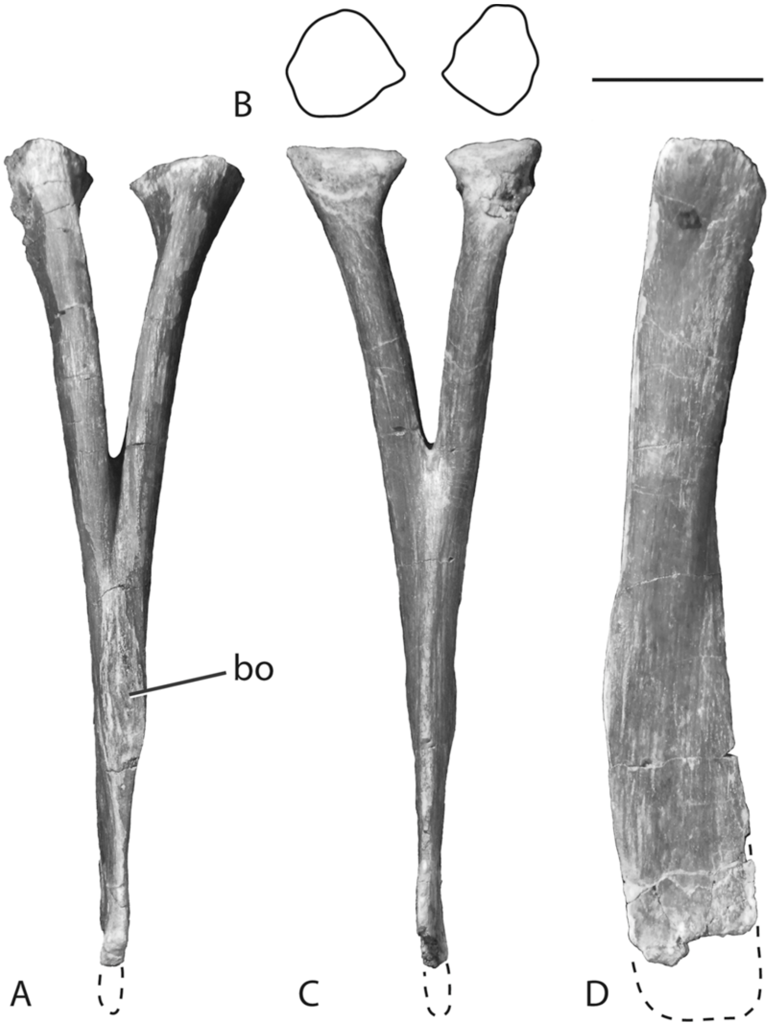

Figure 2.9. Holotypic chevron of *Astrophocaudia slaughteri* (SMU 61732) in **A,** anterior, **B,** proximal (line drawing), **C,** posterior, and **D,** lateral views. Abbreviations: **bo,** boss. Dashed lines indicate missing bone. Scale bar = 5 cm.

Figure 2.10. Holotypic partial scapula of *Astrophocaudia slaughteri* (SMU 61732) in lateral, with cross section indicated. Dashed lines indicate missing bone. Scale bar = 10 cm.

Figure 2.11. Metatarsals I–V referable to *Cedarosaurus weiskopfae* (FMNH PR 977). in dorsal (top row) and lateral (bottom row) views. Dashed lines indicate missing bone. Scale bar = 10 cm.

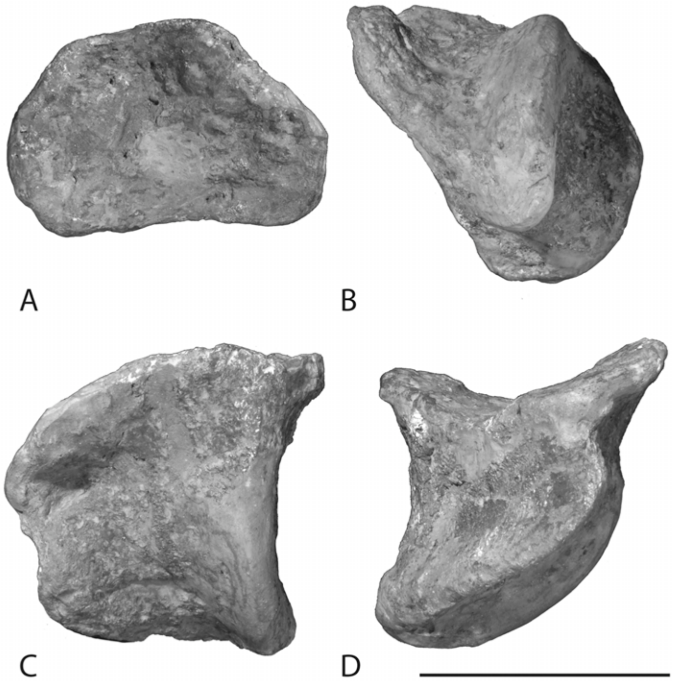

Figure 2.12. Phalanx I.1 referable to *Cedarosaurus weiskopfae* (FMNH PR 977) in **A,** proximal, **B,** distal, **C,** ventral, and **D,** lateral views. Scale bar = 5 cm.

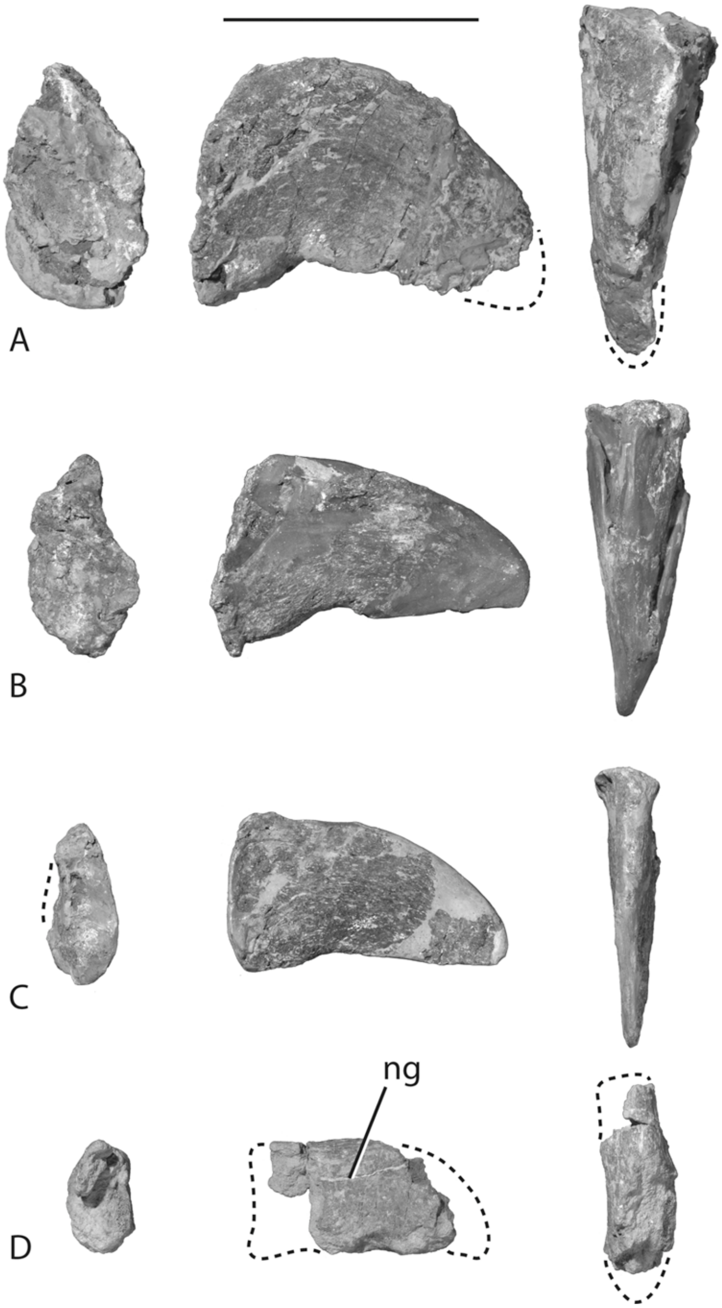

Figure 2.13. Unguals referable to *Cedarosaurus weiskopfae* (FMNH PR 977). **A,** ungual of digit I in proximal, medial, and dorsal views. **B,** ungual of digit II in proximal, medial, and dorsal views. **C,** ungual of digit III in proximal, medial, and dorsal views. **D,** ungual of digit IV in proximal, medial, and dorsal views. Scale bar = 10 cm. Abbreviations: **ng,** nail groove. Dashed lines indicate missing bone.

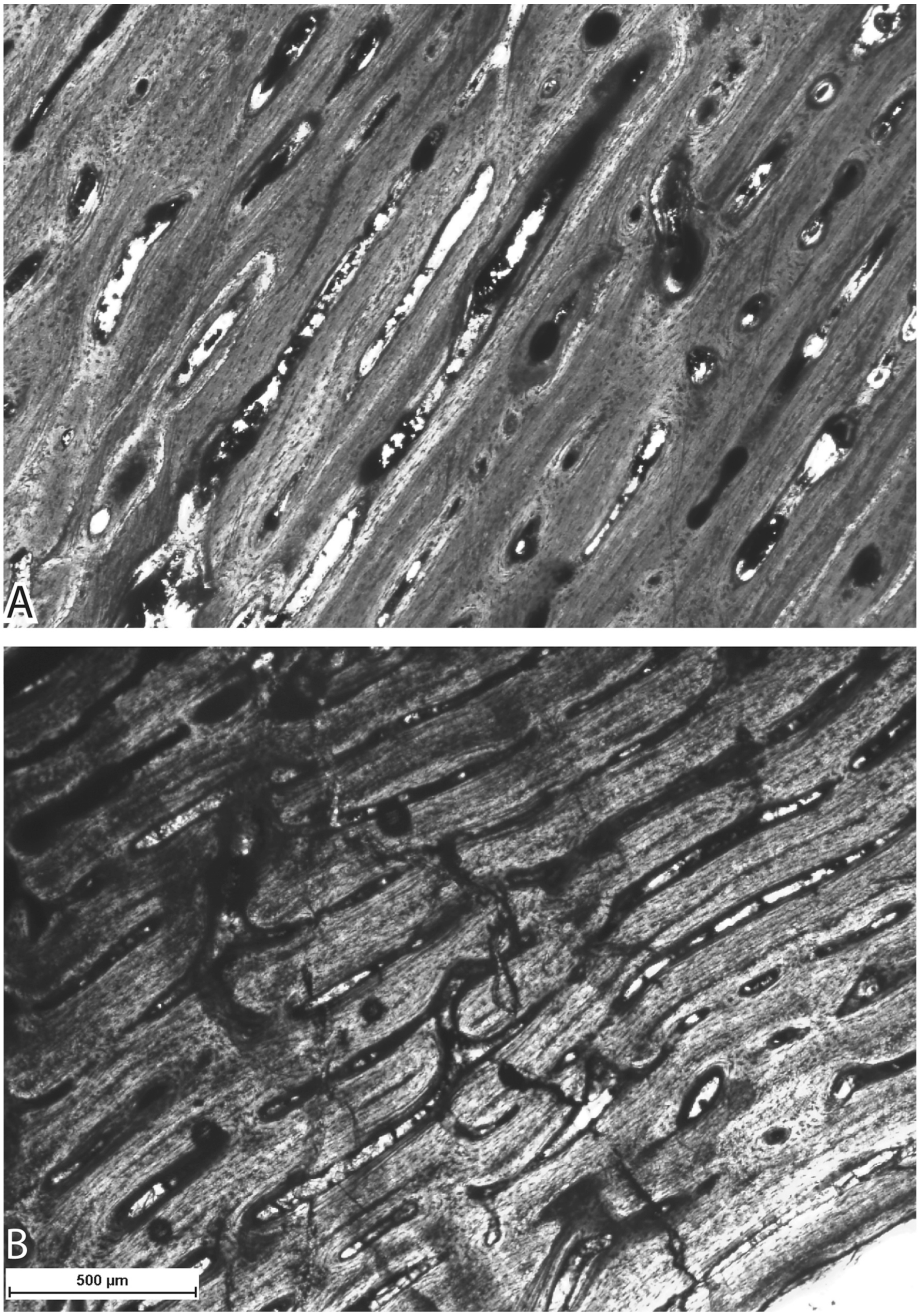

Figure 2.14. Bone histology of *Sauroposeidon proteles.* **A,** microphotograph of a thin section of the humerus (FWMSH 93B-10). **B,** microphotograph of a thin section of the femur (FWMSH 93B-10). Thin-sections reveal primarily laminar fibrolamellar bone, which indicates that these individuals were not at adult size at death. Scale bar is the same for **A** and **B**.

Table 2.1. Novel genus-species combinations of *Astrodon* and *Pleurocoelus* in order of publication, with taxonomic action taken at the time of naming.

author	taxa named	action
Johnston, 1859	*Astrodon*	new genus
Leidy, 1865	*Astrodon johnstoni*	new species
Marsh, 1888	*Pleurocoelus nanus,* *Pleurocoelus altus*	new genus, two new species
Marsh, 1896	*Pleurocoelus montanus*	new species
Lydekker, 1890	*Pleurocoelus valdensis*	new species
Marsh, 1897	*Pleurocoelus suffosus*	new species
Hatcher, 1903	*Astrodon suffosus*	new species
Gilmore, 1921	*Astrodon nanus, Astrodon altus*	subsumed *P. nanus* and *P. altus* into *Astrodon*
Lapparent and Zbyszewski, 1957	*Astrodon pusillus,* *Astrodon montanus*	new species; subsumed *P. montanus* into *Astrodon*
Kingham, 1962	*Astrodon altithorax,* *Astrodon atalaiensis,* *Astrodon brancai,* *Astrodon fraasi*	four new species

Table 2.2. Measurements of the holotypic caudal vertebrae of *Astrophocaudia slaughteri* (SMU 61732) in cm. e = estimated measurement; d = measurement influenced by distortion. Centrum width and height measured at posterior face.

Estimated position in series	Centrum Length	Centrum width	Centrum height
8	—	—	—
10	7.2	15.6e	—
11	—	—	—
12	9.7	10.2e	10e
13	9.1	10.3	9.2
14	8.7	9.4	8.9
15	7.4	10.2	8.6
19	8.8	6.8	7.1
20	9.1	6.6	7.4
22	8.6	6.4	6.7
23	8.7	7.4d	5.9d
24	8	6e	6.2
25	7.3	6.5d	6.3
26	7.2	6.8	5.8
27	8.1	6.4	5.5
30	7.8	5.4	5.2

31	7.2	5.4	5.2
33	6.8	4.3	4.3
37	6.9	—	—
38	6.5	—	—
39	5.7	3.4	3.1
43	5.1e	2.6e	1.8e
46	4.5	1.5	1.6
48	—	1.3	1.2

CHAPTER 3

the beginning of the sauropod dinosaur hiatus in north america: insights from the early cretaceous cloverly formation of wyoming

INTRODUCTION

The Early–Late Cretaceous boundary in North America was a complex time in terms of faunal turnover, changing paleogeography, and the rise of new floras (Ostrom, 1970; Cifelli et al., 1997; Jacobs and Winker, 1998). Numerous authors have proposed that Early Cretaceous North American dinosaur faunas are relicts of those of the Late Jurassic, predominated by sauropods, allosauroids, and primitive iguanodonts (Jacobs and Winkler, 1998). In contrast, the Late Cretaceous of North America is predominated by taxa such as ceratopsians, hadrosaurids, and tyrannosaurids, which are thought to represent an Asian paleobiogeographic influence (Sereno, 1999). The period of turnover between the earlier, 'relictual' faunas and later faunas of Asian origin is thought to have been as short as 2 Myr, around the Albian–Cenomanian boundary (Winker and Jacobs, 1998).

The place of sauropods in this turnover has been controversial. Definitive sauropod fossils are absent from North America from the mid-Cenomanian until the Maastrichtian (D’Emic et al., 2010). This mid-Cretaceous period of absence is termed the ‘sauropod hiatus’ (Lucas and Hunt, 1989). Most authors have considered the disappearance of sauropods around the Early–Late Cretaceous boundary (ca. 100 Ma) to represent a local (continental) extinction, perhaps related to the incursion of the Western Interior Seaway, competition with more ‘advanced’ ornithischian herbivores, or the spread of angiosperms (e.g., Lucas and Hunt, 1989; Cifelli et al., 1997). Other authors have challenged this notion, suggesting that the sauropod disappearance is the result of biases in the fossil record, perhaps related to a dearth of appropriate sauropod-bearing ‘inland’ environments in the Late Cretaceous (e.g., Lehman, 2001; Mannion and Upchurch, 2011). Some authors have suggested that post-hiatus sauropods could represent the descendants of pre-hiatus sauropods, that is, Early Cretaceous North American titanosaurs (e.g., Lehman, 2001).

Central to resolving the role of local extinction and bias in producing the mid-Cretaceous sauropod hiatus (Lucas and Hunt, 1989) are the taxonomic and phylogenetic affinities of Early and Late Cretaceous North American sauropod specimens. The presence of titanosaurs in the Early Cretaceous of North America (Ostrom, 1970; Britt et al., 1996, 1997, 1998; Tidwell and Carpenter, 2007) would decrease support for the local extinction/reinvasion scenario and raise the possibility of the existence of an unsampled lineage of titanosaurs leading to *Alamosaurus*. Many recent discoveries and descriptions have substantially augmented the amount of comparable sauropod material from the Early Cretaceous of North America (e.g., Rose, 2007), which allow reexamination of claims for titanosaurs. Revision of the Early Cretaceous sauropods from Texas, Oklahoma, and Maryland have revealed the presence of both brachiosaurid (e.g., *Cedarosaurus*) and somphospondylan (e.g., *Astrophocaudia*) sauropods (see Chapters 2 and 4), rendered some genera nomina dubia (*Astrodon*, *Pleurocoelus*), and synonymized other genera (*Paluxysaurus* and *Sauroposeidon*).

Sauroposeidon proteles is one of the largest known sauropods, and is one of the best known from the Early Cretaceous of North America with several individuals representing various ontogenetic stages (Wedel et al., 2000a, b; Rose, 2007). The holotype of *Sauroposeidon* and abundant referred material come from Early Cretaceous sediments of Oklahoma and Texas. Wedel et al. (2000a, b) suggested that *Sauroposeidon proteles* was also present in the Cloverly Formation, tentatively referring a cervical vertebra originally described by Ostrom (1970) to the taxon. Below, we confirm this referral and augment it with other sauropod material from the Cloverly Formation. In addition, fieldwork at the original sauropod site of Ostrom (1970) has yielded geological information relevant to the age and paleoenvironment of the site as well as new materials referable to *Sauroposeidon*. I discuss the phylogenetic relationships of *Sauroposeidon* and their implications for the paleobiogeographic history of Cretaceous North American sauropods. Finally, I evaluate the role of bias at the start of the sauropod hiatus by examining the occurrence data of coexisting dinosaur groups before and after the disappearance of sauropods in light of the wealth of new data that has accumulated in the last decades.

Institutional Abbreviations—**ASDM**, Arizona-Sonora Desert Museum, Tucson, U.S.A.; **DMNS**, Denver Museum of Nature and Science, Denver, U.S.A.; **FMNH**, Field Museum of Natural History, Chicago, U.S.A.; **FWMSH**, Fort Worth Museum of Science and History, Fort Worth, U.S.A.; **HMN**, Humboldt Museum für Naturkunde, Berlin, Germany; **OMNH**, Oklahoma Museum of Natural History, Norman, U.S.A.; **SMU**, Southern Methodist University, Dallas, U.S.A.; **TMM**, Texas Memorial Museum, Austin, U.S.A.; **YPM**, Yale Peabody Museum, New Haven, U.S.A.; **UM**, University of Michigan Museum of Paleontology, Ann Arbor, U.S.A.

SYSTEMATIC PALEONTOLOGY

DINOSAURIA Owen, 1842
SAUROPODA Marsh, 1878
NEOSAUROPODA Bonaparte, 1986
TITANOSAURIFORMES Salgado, Calvo, and Coria, 1997
SOMPHOSPONDYLI Wilson and Sereno, 1998
SAUROPOSEIDON Wedel, Cifelli, and Sanders, 2000a
SAUROPOSEIDON PROTELES Wedel, Cifelli, and Sanders, 2000a

Figures 3.3–3.14

Referred material—All materials listed by Rose (2007: 5) as pertaining to *Paluxysaurus jonesi* (FWMSH 93B-10-1 to 10-51), TMM 42488 (see Chapter 2). Referred material also includes specimens reported by Ostrom (1970) from the Cloverly Formation of Wyoming and Montana (see YPM numbers below) and newly excavated specimens (see UM numbers below).

Exemplar A (at locality YPM 63-18)—a middle cervical vertebra (YPM 5294), six dorsal vertebrae (YPM 5449; Fig. 3.3–3.7), two sternal plates (YPM 5449), four ribs, (YPM 5449, 5126, and 5100), a left ulna (YPM 5449; Fig. 3.11), a distal left radius (YPM 5449; Fig. 3.11), two partial pubes (YPM 5449; Fig. 3.12).

Exemplar B (at locality YPM 63-19)—a posterior dorsal vertebra (YPM 5147; Fig. 3.8), two coossified anterior caudal vertebrae (YPM 5147; Fig. 3.9A).

Additional materials from localities YPM 63-18 and YPM 63-19 may pertain to exemplar A or B, but this cannot be known with certainty. They are referred to *Sauroposeidon* because of their similarity to the *Sauroposeidon* exemplars from Jones Ranch, Texas (= ‘*Paluxysaurus*’, Rose, 2007). At locality YPM 63-18, the following bones are referred: a posterior caudal vertebra (YPM 5152); a chevron (YPM 5123); a right scapula and coracoid (UM 20800); a left femur (YPM 5451). At locality YPM 63-19, the following bones are referred: two middle-posterior caudal vertebrae (YPM 5103, 5104); four chevrons (YPM 5089, 5096, 5097, 5087); a left tibia (YPM 5450).

Indeterminate material—The teeth from YPM 63-18 and YPM 63-19 vary substantially in size and form, and so cannot confidently be referred to

Sauroposeidon. These include three teeth from locality YPM 63-18 (YPM 5149, YPM 5347, YPM 5375) and five teeth from locality YPM 63-19 (YPM 5349, YPM 5360, YPM 5365, YPM 5374).

Emended diagnosis—Middle cervical vertebral elongation index greater than 6; pneumatic fossa developed posteriorly to the cotyle in middle cervical vertebrae, middle and posterior dorsal neural spines that taper distally, anterior caudal vertebral centra roughly square in cross-section, middle caudal vertebrae with wide spinoprezygapophyseal fossa and spinoprezygapophyseal laminae that meet at an angle greater than 50 degrees, scapula with two processes at the base of the blade on the ventral side, humerus gracile (length/midshaft width > 7.5). (Wedel et al., 2000a, b; see Chapter 2).

Comments—As originally suggested by Wedel et al. (2000a, b), *Sauroposeidon proteles* is present in the Cloverly Formation. Wedel et al. (2000a, b) only referred the mid-cervical vertebra of exemplar A to *Sauroposeidon*, but I refer additional sauropod remains from the same localities (YPM 63-18 and 63-19; see above). Rose (2007) cast doubt on the conspecificity of '*Paluxysaurus*' (= *Sauroposeidon*) and the Cloverly sauropod. Below, I show that proposed differences between *Sauroposeidon* and '*Paluxysaurus*' are minor, and that they share several unique features that support their conspecificity.

Several of the autapomorphies that were reported for '*Paluxysaurus jonesi'* by Rose (2007) are more widespread among titanosauriforms, including material from the Cloverly Formation referred to *Sauroposeidon*. These features include: (1) the presence of accessory laminae on dorsal neural arches, (2) dorsal vertebrae that lack a postspinal lamina, (3) middle caudal vertebral centra with forward-sloping anterior and posterior faces, (4) presence of a spinoprezygapophyseal fossa in anterior and middle caudal vertebrae. Feature (1) is present in several other taxa including *Brachiosaurus, Giraffatitan, Epachthosaurus, Euhelopus,* and *Malawisaurus*, (2) is shared with *Brachiosaurus*, and (3) is present in *Cedarosaurus*, *Venenosaurus*, and several titanosaurs. The presence of a spinoprezygapophyseal fossa in anterior and middle caudal vertebrae (4) is not unique, but its width and depth are unique to *Sauroposeidon*

Rose (2007) listed five differences between '*Paluxysaurus'* and the Cloverly sauropod that are unsupported upon further inspection: anterior dorsal vertebrae of '*Paluxysaurus*' with (1) taller neural arches and broader neural spines, (2) a caudoventral lip on the centrum, and (3) inclined postzygapophyses, and posterior dorsal vertebrae of '*Paluxysaurus*' with (4) a more upright neural spine and (5) "eye" shaped pleurocoels. These differences are either minor (1, 3, 4), affected by preservation (4), or are as variable within each sample as between them (1–5; see 'Description' and figures below).

Rose (2007) also noted differences between the humeri of of '*Paluxysaurus'* and the humerus from the Cloverly Formation (YPM 5452); however, the humerus was found in isolation and does not necessarily pertain to *Sauroposeidon*. Another difference listed by Rose (2007) as distinguishing the Cloverly sauropod from '*Paluxysaurus'* is a much shorter and more robust ulna in the former specimen. As noted by Rose (2007: 38), the Texas ulna is about 20 cm longer than the Wyoming specimen, even though “the dorsal vertebrae of YPM 5449 are close to the size of dorsals of *P. jonesi*.” However, the complete posterior dorsal vertebrae of the Texas and Wyoming specimens are markedly different in size, for example FWMSH 93-B-10-13 is 70 cm tall, but YPM 5449-D is only 48 cm tall, making the Texas vertebra 45% larger. This is the same relative difference in size between the ulnae of ‘*Paluxysaurus’* and the Cloverly *Sauroposeidon* (87 cm vs 60 cm). The perceived difference in robustness of the ulnae is also minimal and is accentuated by the crushing of the ‘*Paluxysaurus’* ulna. For example, the proximal anteromedial process:total length ratio is 0.33 in ‘*Paluxysaurus*,’ versus 0.36 in the Cloverly *Sauroposeidon* exemplar. Likewise, the midshaft anteroposterior width: total length ratio in ‘*Paluxysaurus’* is 0.18, versus 0.19 in the Cloverly *Sauroposeidon*. In sum, several autapomorphies, the absence of substantial differences, and their similar geologic age support referral of the Cloverly Formation sauropod material to *Sauroposeidon* (= ‘*Paluxysaurus*’).

Locality—Referred FWMSH and TMM specimens come from the W.W. Jones Ranch, SMU Locality 282 (FWMSH 93B-10), north-central Texas. YPM and UM specimens come from YPM localities 63-18 and 63-19, near Crooked Creek, about 10 miles northeast of Lovell, Big Horn County, Wyoming, USA (Fig. 3.1A).

Horizon and Age—Referred FWMSH and TMM materials come from the Twin Mountains Formation, dated to about the Aptian–Albian boundary (Fig. 3.1). YPM and UM materials come from Units VI and VII of the Cloverly Formation, which were regarded as middle Albian by Ostrom (1970:fig. 5). These units are referred to as the Himes Member of the Cloverly Formation by some authors (e.g., Moberly, 1960, Winslow and Heller, 1987), or as part of the "C" interval of the Cloverly Formation by others (e.g., Zahela, 2006). Zahela (2006) suggested that the upper Cloverly Formation is Albian in age based on palynological evidence. Laser-ablation multi-collector ICP-MS U/Pb ages of detrital zircons from fine sandstones subjacent to the quarry at YPM 63-18 have yielded an age of 104.4 Ma, making the bone-bearing horizon younger than middle Albian (D'Emic and Britt, 2008).

Depositional environment and taphonomy—In discussing the association of these sauropod remains, Ostrom (1970:77) stated that: "the possibility exists that these bones do not all belong to the same individual, but they were so closely associated—in some instances in contact—that this seems a remote possibility." A field sketch discovered in the collections of the YPM supports Ostrom's (1970) report of contact between many of the bones (Fig. 3.1B), and would appear to support Ostrom's claim of only a single individual at the site. However, a juvenile sauropod dorsal vertebra (YPM 5151) and sacral vertebra (YPM 5107) from the same site (YPM 63-18) are similar in size to each other and much smaller than the other vertebrae from YPM 63-18 (centrum lengths ca. 10 cm), making the minimum number of individuals at the site two. Additionally, larger elements—an associated dorsal vertebra and two caudal vertebrae (YPM 5147), and a tibia (YPM 5450)—at site YPM 63-19 indicate that a third individual was present as well. The two sites also host a diverse assemblage of other taxa including turtle, crocodile, theropod, ankylosaur, and ornithopod fossils (Ostrom, 1970).

Fossil sites 63-18 and 63-19 are located approximately 110 m above the contact between the Sundance and Cloverly Formations, near the base of Unit VII in the Crooked Creek section of Ostrom (1970) (Fig. 3.2A). The sites represent a multitaxic, macrofossil bonebed (sensu Behrensmeyer, 1991, 2007), and can be classified genetically as a sedimentologic concentration (sensu Rogers and Kidwell, 2007). The two sites are hosted within a paleosol profile ca. 2.3 m thick (Fig. 3.2). The weathered surface of this profile is pale reddish brown (10R-5/4), and sharply overlies a fine- to medium-grained fluvial sandstone, which weathers to a light olive gray (5Y-6/1) color. The various fossil elements are constrained to a 0.5 meter thick interval located ~0.2 m from the top of the underlying fluvial sandstone. The paleosol profile itself consists of four units within a single, fining upward sedimentary package (Fig. 3.2B). The dominant color and mottling features change among the units, and correspond to variations in the soil moisture and water table during pedogenesis (Fig. 3.2C; Duchaufour, 1982; Fanning and Fanning, 1989; Vepraskas, 1994). The top of this paleosol profile is delimited by the presence of rhizoliths (i.e., root traces). These and other fossils in Units VI and VII of the Cloverly Formation were likely deposited on floodplains close to the margin of the encroaching Western Interior Seaway (Kvale and Vondra, 1993). Some sauropod fossils (e.g., UM 20809; sauropod ribs) from the upper third of the formation are found within horizons that feature meter-scale slickensides indicative of vertisols, which commonly occur in wet, coastal settings today (Driese et al., 2005).

The multitaxic composition, disarticulation, and variable degree of surface cracking and compression of the fossil elements support moderate (at least weeks to months) subaerial exposure (Toots, 1965; Behrensmeyer, 1978; Hill, 1979). A few small sauropod teeth recovered from the sites lack much of their enamel, a feature consistent with passage through a digestive tract (Fisher, 1981). Elements smaller than ~20 cm in length are rare in the bonebed, with the exception of the few sauropod and crocodile teeth. The bones present are predominantly vertebrae and appendicular elements, which correspond to Voorhies Group I/II and suggest moderate transport and sorting in an active flow (Voorhies, 1969). Anatomically disjunct elements are commonly found in direct contact with one another, indicating at least some degree of hydrologic movement (Eberth et al., 2007). However, there is little evidence of abrasion, polishing, or rounding that would be expected with extensive hydrologic transport and delicate vertebral laminae are preserved, whereas many neural spines and transverse processes are broken off. This combination of taphonomic features suggests hydrologic sorting (i.e. removal of small elements), and minimal transport of large and/or dense elements (Wolff, 1973; Behrensmeyer, 1988; Wood et al., 1988; Eberth, 1990). This sorting likely occurred during a crevasse splay event that preferentially filled the topographic low on the floodplain and entombed the fossil elements at the base of a fining-upward sedimentary package. Eventually, a soil formed from this parent material and further altered the fossil material, as observed by mottling and discoloration of fossil surfaces.

DESCRIPTION

General comments

Nomenclature for vertebral laminae and fossae follow Wilson (1999) and Wilson et al. (2011), respectively. Orientational terms and regional anatomical descriptors are “Romerian” following those traditionally applied to sauropods (Wilson, 2006). A minimum of three individuals are present at sites YPM 63-18 and 63-19: a young juvenile represented by two centra, a partial skeleton of an older juvenile (exemplar A), and an older individual represented by a large dorsal vertebra, two large co-ossified caudal vertebrae, and a tibia (exemplar B). Comparisons are included where appropriate.

Mid-cervical vertebral centrum

An opisthocoelous, elongate, cervical vertebral centrum (YPM 5294; Wedel et al. 2000b; 2005) was recovered from site YPM 63-18. The centrum is unfused to its neural arch. Ostrom (1970:82) reported it as being “widely separated” from the other bones, but its exact proximity to the majority of other bones in the quarry is unknown. However, Ostrom’s entire quarry at YPM 63-18 was less than 4 x 2 meters wide (MDD., pers. obs. 2008), so it seems plausible that it pertains to exemplar A. Ostrom’s (1970) suggestion that the cervical vertebra is of the right size to belong to exemplar A is corroborated by the anatomy of other titanosauriforms; for example, the mid-cervical centrum length and total posterior dorsal vertebral heights are subequal in *Malawisaurus* (Gomani, 2005); as in YPM 5294 and YPM 5449.

The vertebra is dorsoventrally crushed, but even in its uncrushed state, it would have a minimum elongation index (total length: posterior cotyle height) around 6.9 (48.5 cm: ~7 cm restored) and average elongation index (average of posterior condyle width and height divided by centrum length; Chure et al., 2010) of 5.2. This vertebra likely belongs to a juvenile because its neurocentral junction is unfused (Ikejiri, 2003). The neural canal is constant in width along its length, unlike the medially constricted (hourglass or 'butterfly-shaped') neural canals of some titanosaurs (e.g., *Rapetosaurus*, Curry Rogers, 2009). The ventral margin of the centrum is weakly concave anteriorly, flat posteriorly, and lacks ridges. Parapophyses are set just behind the condyle and a lamina projects posteriorly from them (referred to as the 'centroparapophyseal lamina' by Wedel et al., 2000b), as in other sauropods (e.g., *Euhelopus*, Wiman, 1929, *Giraffatitan*, Janensch, 1950). The pleurocoel extends to the cotyle, which is an autapomorphy of *Sauroposeidon* (Wedel et al., 2000a, b).

Anterior dorsal vertebrae

Three anterior dorsal vertebrae of YPM 5449 (Figs. 3.3–3.5) likely represent the second, third, and fourth dorsal vertebrae, respectively, as evidenced by the positions of the dorsoventrally-elongate parapophyses near the dorsal edge of the centrum and in front of the pleurocoel. These vertebrae are largely undistorted, but some are missing parts of their neural spines and/or diapophyses and others are only visible in a single view (e.g., anterior) because they are too fragile to remove from their plaster jacket.

The centrum is wider than tall at both the condyle and the cotyle, but the cotyle is greater in diameter. The centrum is strongly opisthocoelous with a distinct notch in the dorsal lip of the cotyle. This notch was described as an autapomorphy of *Europasaurus* (Sander et al., 2006), but is present in many sauropods (e.g., *Camarasaurus*, Ostrom and McIntosh, 1966). Pleurocoels expand and ramify to fill the centrum with subcentimeter-scale pneumatic chambers (‘somphospondylan’; Wilson and Sereno, 1998). The neural arch is low, with the distance from the base neurocentral junction to the base of the neural spine less than or equal to the height of the centrum. The neural canal is subrectangular and is about the same diameter through its entire length in the vertebra. The intraprezygapophyseal (tprl) laminae are well-developed, but the intrapostzygapophyseal lamina (tpol) are absent, as in the anterior dorsal vertebrae of most sauropods (e.g., *Camarasaurus*, Osborn and Mook, 1921; *Ligabuesaurus*, Bonaparte et al., 2006). The pre- and post zygapophyses are well-separated, large, elliptical, and angled about 30 degrees from the horizontal. The centroprezygapophyseal laminae (cprl) have their greatest relief near the centrum, and become more subtle dorsally.

All neural spines show some evidence of distal expansion, although only the neural spine of one of the vertebrae (Fig. 3.5) is complete. The neural spine of the anterior dorsal vertebrae is anteroposteriorly compressed, laterally expanded, and rounded distally, as in the somphospondylans *Ligabuesaurus*

(Bonaparte et al., 2006), *Malawisaurus* (Gomani, 2005), *Mendozasaurus* (González Riga, 2005), and *Futalognkosaurus* (Calvo et al., 2008). When the base of the neural canal is held horizontally, the neural spine is inclined anteriorly about 10 degrees from vertical. In cross-section the neural spine is subrectangular with the transverse dimension about four times the anteroposterior. Pre- and postspinal laminae are only weakly developed as low ridges that extend from the base of the neural spine to a point about halfway up the spine. Low-relief secondary spinodiapophyseal laminae (spdl) extend from the midpoint of the neural spine to an area between the prezygapophyses and diapophysis, as in titanosaurs and their relatives (Salgado et al., 1997).

The diapophyses extend laterally and slightly downward out to a distance about equal to the width of the centrum. The posterior centrodiapophyseal laminae (pcdl) form a thin, dorsoventrally deep web that hosts other laminae, subdividing the prezygapophyseal centrodiapophyseal fossa (prcdf) and postzygapophyseal centrodiapophyseal fossa (pocdf). On the posterior side of the diapophyses there are sharp-lipped circular cavities 2–3 cm in diameter (Fig. 3.3). These excavations are variably present on the dorsal vertebrae of some sauropods such as *Cetiosaurus* (Upchurch and Martin, 2002, 2003); *Camarasaurus*, (Osborn and Mook, 1921:pl. 70), *Sauroposeidon* (Rose, 2007:fig. 12), and *Giraffatitan* (Janensch 1950:fig. 54).

Posterior dorsal vertebrae

Four posterior dorsal vertebrae were listed by Ostrom (1970): three at site

YPM 63-18 that pertain to exemplar A, (YPM 5449, Figs. 3.5–3.7) and one at locality YPM 63-19 that pertains to exemplar B (YPM 5147, Fig. 3.8). The relative positions of the vertebrae in the series are unknown, so they will be described in one section here, following the order in which Ostrom (1970) described them. There were likely at least two vertebrae missing in the series between the anterior and posterior dorsal vertebrae based on comparisons with *Brachiosaurus*, *Giraffatitan*, and *Camarasaurus*, so the posterior dorsal vertebrae of YPM 5449 likely belong somewhere in the series between dorsal vertebrae 8 and 13.

Two of the posterior dorsal vertebrae (Figs. 3.6, 3.7) have been laterally compressed and sheared forward on their right sides, causing the numerous cavities on the right side of the vertebrae to appear larger than those on the left (Figs. 3.6, 3.7). On both sides the pleurocoels are gently acuminate posteriorly as occurs in many sauropods (with some serial variation; e.g., *Camarasaurus*, Osborn and Mook, 1921; *Brachiosaurus*, Riggs, 1903; *Giraffatitan*, Janensch, 1950; *Neuquensaurus*, Salgado et al., 2005). The development of laminae on the neural arches of the posterior dorsal vertebrae is asymmetric: on the right side of the vertebrae, the anterior centrodiapophyseal lamina (acdl), posterior centrodiapophyseal lamina (pcdl), centropostzygapophyseal lamina (cpol), and centroprezygapophyseal lamina (cprl) are present and distinguishable from their origin to their terminus near the neurocentral junction (e.g., Fig. 3.6). In contrast, on the left side these laminae are absent around the base of the neural arch (Fig. 3.6).

One posterior dorsal vertebra is crushed and overlain by an anterior dorsal vertebra (Fig. 3.5). The close association of these two vertebrae suggests that they belong to the same individual. Ostrom (1970:78) noticed the disparity in width between the centra of these vertebrae: “A surprising feature is that the greatest diameters of the centra are significantly less than those of the associated anterior centra, a condition that has not been reported in any other sauropod.” However, at the time, such a feature had been reported in one sauropods: *Euhelopus* (Wiman, 1929:pl. 3) in which the width of the posterior centra of the anterior dorsal vertebrae is over 150% the width of the posterior centra of the middle dorsal vertebrae. The centra of the posterior dorsal vertebrae are strongly opisthocoelous and taller than wide. The pleurocoel is set into a shallow fossa posteriorly.

The zygapophyses of the posterior dorsal vertebrae are large and elliptical, with their long axis directed approximately 55 degrees from the horizontal. The prezygapophyses are set close to the midline and connected to other parts of the vertebra by robust centroprezygapophyseal laminae (cprl), prezygodiapophyseal laminae (prdl), and spinoprezygapophyseal laminae (sprl), but are not connected to one another by an intraprezygapophyseal lamina (tprl). The prezygapophyses have flaring, pendant hypantra under the prezygapophyses and a small, rhomboidal hyposphene sits below the postzygapophyses (Fig. 3.7). The area between the postzygapophyses is bounded by the dorsally-tapering spinopostzygapophyseal laminae (spol) and contains a dorsoventrally elongate, sharp-lipped cavity, the spinopostzygapophyseal fossa (spof). Dorsal to the spof, the spol is wide and rugose as in *Sauroposeidon* (Rose, 2007).

Spinoprezygapophyseal laminae (sprl) unite to form a prespinal lamina halfway up the neural spine, unlike in the anterior dorsal vertebrae. The diapophyses of the posterior dorsal vertebrae are dorsally directed, though this has been enhanced by distortion. Extending alongside the diapophyses is a small lateral centropostzygapophyseal lamina (cpol) that connects the postzygapophyseal diapophyseal lamina (podl) and the posterior centrodiapophyseal lamina (pcdl), dividing the postzygapophyseal centrodiapophyseal fossa (pocdf).

YPM 5147 (Fig. 3.8) is substantially larger than any of the dorsal vertebrae of exemplar A (YPM 5449), and it comes from site YPM 63-19 rather than YPM 63-18, so it likely belongs to a different individual. It is missing most of its neural spine and diapophyses. The centrum of this vertebra is broken, revealing a camellate texture, similar to that observed in *Brachiosaurus* (Riggs, 1903; Janensch, 1947:fig 4) and *Cedarosaurus* (Tidwell et al., 1999).

Caudal vertebrae

Anterior caudal vertebrae—Two coosified anterior caudal vertebrae from site YPM 63-19 (YPM 5147; Fig. 3.9) were mentioned but not figured by Ostrom (1970). The centra of these caudal vertebrae have widths greater than any of the dorsal vertebrae from site YPM 63-18, but their width and height correspond well with the dorsal vertebra from site YPM 63-19. The posterior dorsal vertebrae and anterior caudal vertebrae are similar in posterior centrum width (within ca. 10%)

in most sauropods (e.g., *Camarasaurus*, Osborn and Mook, 1921; *Tastavinsaurus*, Royo Torres, 2009; *Phuwiangosaurus*, Suteethorn et al., 2009), indicating that the posterior dorsal and anterior caudal vertebrae of YPM 5147 are the appropriate size to belong to the same individual. The exposure of Ostrom's quarry at site YPM 63-19 was less than 4 x 2 meters (MDD pers. obs., 2008). Thus these two caudal vertebrae and the dorsal vertebra are regarded as probably belonging to a single, larger individual than the one at site YPM 63-18 (exemplar B).

These two vertebrae have a solid bone texture, robust laminae and stout neural spines. They likely belong to one of the first several caudal vertebrae based on their large size, well-developed transverse processes and poorly defined chevron facets. The centra are about 1.5 times wider than tall and are nearly flat ventrally. Centra display the concavo-planar articulation type (anterior face convex, posterior face nearly flat) common to many non-lithostrotian sauropods (e.g., *Patagosaurus*, *Camarasaurus*, *Giraffatitan*, *Cedarosaurus*). The centrum is angled forward in lateral view and the neural spines are directed backwards. The transverse processes are directed posteriorly and slightly upwards. The area below the transverse processes is not excavated by fossae nor foramina.

Prezygapophyses are dorsally directed, and their articular facets are steeply angled (approximately 50 degrees above the horizontal). Strongly developed spinoprezygapophyseal laminae (sprl) extend from the prezygapophyses and continue all the way up the neural spine; they do not unite to form a prespinal lamina, but delimit a deep and wide prespinal fossa on the neural spine. Sprl that diverge by more than 50 degrees is an feature known only in *Sauroposeidon* among sauropods. Spinopostzygapophyseal laminae (spol) are short and delimit a broad spinopostzygapophyseal fossa (spof). Within the spof there is a broad, rugose postspinal lamina (posl). The neural spine is longer than wide for most of its length, but strongly expands in width at its distal end.

Ostrom (1970) reported an anterior-middle caudal vertebra (YPM 5116) that may pertain to an ornithopod rather than a sauropod. It has a centrum that is much taller than wide, unlike other anterior-middle caudal vertebrae in the quarry or any of those of *Sauroposeidon,* which are wider than tall (Fig. 2.9). In this and other respects, YPM 5116 is more similar in proportions to the anterior-middle caudal vertebrae of *Tenontosaurus* (Forster, 1990), and more likely represents that genus than a sauropod.

Middle and posterior caudal vertebrae—Middle caudal vertebrae have centra that lean slightly forward, are slightly wider than tall, and are nearly equivalent in length to the centra more anterior and posterior in to them in the tail (Fig. 3.9). The anterior face of the middle caudal centrum is slightly more concave than its posterior face, as in the anterior caudal vertebrae. No fossae are present on the sides or bases of the centrum. Two posterior caudal vertebrae (YPM 5103, 5152) are ‘spool-shaped’ (Langston, 1974) with neural arches displaced to the anterior half of the vertebra. YPM 5152 is weakly procoelous, as in some posterior caudal vertebrae of *Giraffatitan* (HMN MB.R.5000; MDD pers. obs. 2008; see Chapter 4) and *Astrophocaudia* (see

Chapter 2).

Scapula and coracoid

Excavations at YPM 63-18 in 2008 yielded a scapula and coracoid (UM 20800; Fig. 3.10) that likely pertain to exemplar A, but this cannot be verified. The total scapula and scapulocoracoid lengths as preserved are about 1.3 and 1.5 meters, respectively. The scapula is missing some of its coracoid margin, acromion, and parts of its dorsal and distal blade. The blade was found in several pieces and crushed both transversely and proximodistally, such that parts of the blade lay slightly on top of one another. The blade is nearly flat, unlike the laterally expanded (‘D-shaped’) scapular blades of non-somphospondylans (Wilson, 2002). The scapular glenoid measures about 30 cm by 14 cm and is beveled about 30 degrees medially relative to the proximal scapular plate (Fig. 3.10), as in somphospdondylan sauropods (Wilson and Sereno, 1998). Just posterior to the glenoid on the ventral margin of the bone are two processes. A single large process is commonly present in this region in titanosauriformes (e.g., *Chubutisaurus*, *Mendozasaurus*) but some derived titanosaurs also possess two (e.g. *Alamosaurus*, D’Emic et al., in press). Because *Sauroposeidon* and *Alamosaurus* are not regarded as being closely related phylogenetically (see ‘Phylogenetic and paleobiographic history,’ below), the presence of two processes is regarded as a local autapomorphy of *Sauroposeidon*.

The coracoid was found adjacent to the ventral part of the plate of the scapula with its lateral side was face-down, whereas the lateral side of the scapula was found face-up. Part of the coracoid foramen is preserved along the unfused scapular articulation. The coracoid is missing its dorsal margin; its preserved part measures about 46 cm by 30 cm dorsoventrally and proximodistally, respectively. A thin infraglenoid lip is present. The coracoid glenoid measures about 20 cm by 13 cm. The coracoid glenoid is roughly divided into two portions, a larger segment that faces mostly ventrally, and a smaller segment that faces mostly laterally. This is similar to the situation in most sauropods (e.g., *Camarasaurus*, Ostrom and McIntosh, 1966; *Giraffatitan*, Janensch, 1961; *Ligabuesaurus* Bonaparte et al., 2006; see Wilson and Sereno, 1998; contra Taylor, 2009).

Sternal plates and dorsal ribs

Fragments of two sternal plates (YPM 5449) were recovered as part of exemplar A from YPM 63-18, directly below the left pubis (Fig. 3.1). They are approximately 1–2 cm thick and have a tubercle on their anterior internal face as in many other sauropods (e.g., *Omeisaurus*, He et al., 1988; *Giraffatitan*, Janensch, 1961; *Alamosaurus*, Gilmore, 1946). The lateral margins are not complete enough to know their shape. Fragments of three dorsal ribs (YPM 5449 and 5126) were preserved with the assemblage of bones at site YPM 63-18, and one large rib (YPM 5100) was preserved at 63-19. All of the ribs are between two and three times as broad as wide and are strongly curved. Distally, the preserved portions of the ribs are not flat, but are broadly subtriangular in cross section. None of the ribs are preserved proximally, so it is unknown whether or not they were pneumatic.

Ulna

A left ulna (YPM 5449) was found at the site in close proximity to the sternal plates, ischia, and vertebrae (Fig. 3.11). It is nearly complete and undistorted and preserves traces of an articulation surface for the radius distally. The ulna is 60 cm long and slightly less elongate than in brachiosaurids such as *Giraffatitan* and *Cedarosaurus* (e.g., the ratio of the length of the anteromedial arm to total length = 0.36 in YPM 5449 vs 0.33 in the brachiosaurids). The ulna appears to have a more robust shaft and larger olecranon in figures from Ostrom (1970: pl. 14) than it actually does because it was photographed obliquely in that publication. On the anterior and lateral arms of the ulna, the planes of articulation for the radius meet at an angle slightly less than 90 degrees. The medial face of the anterior arm is slightly concave, and the corresponding face on the lateral arm is strongly convex. Measured from the posterior corner of the proximal end, the anterior process is approximately 22 cm long and the lateral process is about 14 cm long. The anterior process is flat proximally, and the lateral process is slightly concave in profile as it slopes gradually away from the slightly raised olecranon. This is similar to the situation present in many titanosauriforms such as *Giraffatitan* (Janensch, 1950), *Venenosaurus* (Tidwell et al., 2001), *Opisthocoelicaudia* (Borsuk-Bialynicka, 1977), and *Alamosaurus* (Gilmore, 1946). The proximal, triradiate end of the ulna tapers toward the midline, which has a triangular cross section. The distal end is subtriangular and beveled upwards anterolaterally. The distal end measures 11.3 and 12.5 cm transversely and anteroposteriorly, respectively.

Radius

A previously uncatalogued bone found in the collections of YPM in a box with other Cloverly sauropod fossils represents the distal end of a sauropod left radius (Fig. 3.11). The radius is slightly eroded on its distal end, nevertheless, it articulates well with the ulna (YPM 5449) from site 63-18, and it is of similar size and preservation, so it is likely that both belong to the same individual. The radius expands markedly towards its distal end. The most proximally preserved part of the radius is subcircular in cross section whereas the distal end is subrectangular except for a small process on the lateral side near the ulnar articular surface. The anterior outline of the distal end is divided into two flat faces that meet at an angle of about 110 degrees. The posterior articular surface for the radius is slightly convex in distal view. Two elongate low ridges extend along the articular surface for the ulna. The first ridge is usually interpreted as an “interosseous ridge,” marking the site where connective tissue binds the radius and ulna together (Borsuk-Bialynicka, 1977). The second ridge has been interpreted as the insertion site of the M. extensor longus digiti I (Borsuk-Bialynicka, 1977). The second ridge is subtle, as in *Venenosaurus* and most sauropods, and not hypertrophied into a flange as in *Cedarosaurus* (Tidwell et al., 1999).

Pubis

Two bones (YPM 5449, Fig. 3.12) that Ostrom referred to as ischia were recovered from site YPM 63-18. Based on their robustness, lack of twisting along their midshaft, and comparisons with *Sauroposeidon* and *Venenosaurus*, these bones more likely represent pubes rather than ischia. As preserved, the more complete, left pubis is 87 cm long, and distally it measures ca. 20 cm by ca. 8 cm. A line drawing of the left pubis can be found in Ostrom (1970: fig.7). The right pubis is extremely fragmentary but similar to the left in its preserved portions. The ambiens process is only subtly developed. The distal end is not expanded anteriorly to a point as in some sauropods (e.g., *Giraffatitan*, Janensch, 1961; *Tastavinsaurus*, Royo Torres, 2009).

Femur

A partial right femur (YPM 5451) was found at site YPM 63-19 (Fig. 3.13). The proximal end is incomplete, and Ostrom (1970) estimated that it would be over 1.5 meters long if complete based on the position of the fourth trochanter. The femur may belong to exemplar B based on its large size, but this is uncertain. Comparisons with the femora of *Brachiosaurus*, *Cedarosaurus*, and *Sauroposeidon* give a similar length estimate of 146 cm for YPM 5451. The fourth trochanter is weakly developed as a ridge bounded medially by a welt (Fig. 3.13). The proximal end preserves the beginnings of a medial deflection and the distal half of a lateral bulge. The tibial condyle is about twice as broad as the fibular condyle and projects about 1.5 times as far posteriorly. In maximum dimensions, the distal end of the femur measures 39.5 cm by 19.5 cm. The transverse dimension of the midshaft equals 220% that of the transverse dimension (24.2 cm by 11 cm), though this is slightly exaggerated by anteroposterior crushing (Fig. 3.13). The least circumference of the femur is about 55 cm.

Tibia

Ostrom (1970) described a left tibia (YPM 5450), found at site 63-19 (Fig. 3.14). The tibia measures 98.5 cm long; other measurements are influenced by distortion. The tibia is strongly crushed transversely. It is the appropriate size to belong to exemplar B and the femur (YPM 5451), but their association is uncertain. The proximal end of the tibia is oval and the cnemial crest is broken. The shaft of the tibia is nearly straight and expands to twice its midshaft width towards its distal end as in many sauropods (e.g., *Camarasaurus*, Ostrom and McIntosh, 1966; *Giraffatitan*, Janensch, 1961; *Erketu*, Ksepka and Norell, 2006). The distal tibia has a deep facet for reception of the astragalus.

Other sauropod remains from the Cloverly Formation

Teeth—Ostrom (1970) reported 13 teeth from the Cloverly Formation including three from site YPM 63-18 and five from site YPM 63-19 (all in Unit VII), and some isolated at other sites in Units V–VII. Teeth from some sites in these units (e.g., YPM 64-3, 64-39) are devoid of enamel but are otherwise intact, possibly indicating passage through a digestive tract (Fisher, 1981). Some of the teeth are twisted along their axis as in the upper teeth of brachiosaurids (e.g., *Abydosaurus,* Chure et al., 2010), but others are straight and chisel-shaped as in titanosaurs and their relatives (Calvo, 1994; Gomani, 2005). None can be confidently referred to *Sauroposeidon*. All of the sauropod teeth from YPM 63-18 and YPM 63-19 are intermediate in slenderness between the broad, spatulate teeth of most non-titanosauriform sauropods and the narrow, peg-like teeth of titanosaurs (slenderness index between 2.6 and 4.3; log slenderness index between 0.41 and 0.63, see Chure et al., 2010: fig. 5). Cross sections are D-shaped on the apical half of the crown, and more circular towards the base. The teeth vary in size from about 1.5 to nearly 4 cm long, though the smallest of these do not bear wear facets and may be replacement teeth. Wear patterns also vary among the teeth: mesio-distal (YPM 5374), lingual (YPM 5360), and apical (YPM 5149) wear is present.

Humerus—Ostrom (1970: pl. 14) described an isolated humerus (YPM 5452) from locality YPM 63-16, 40-50 yards (37-46 m) away from exemplars A and B at YPM 63-18 and -19, respectively. It also comes from a different unit (Unit VI) than the exemplars at the other sites (Unit VII). The humerus possesses a somewhat squared proximolateral corner as in titanosauriformes except for some brachiosaurids (e.g., *Cedarosaurus*, Tidwell et al., 1999). The specimen is crushed antero-posteriorly, exaggerating its eccentricity. There are visible muscle insertion sites on the proximal posterolateral face of the bone and in the deltopectoral fossa, but they are not as pronounced as in titanosaurs (e.g., *Jainosaurus*, Wilson et al., 2009).

Juvenile sauropod bones—One small dorsal centrum and one small sacral centrum that lack neural arches and transverse processes (YPM 5151 and 5107) were found at site 63-19. These vertebral centra belong to a juvenile sauropod dinosaur, as evidenced by the open neurocentral sutures and the presence of large camerae that almost fill the centrum (Wedel et al., 2000a, b). The dorsal and sacral centra are very similar in size, so they may belong to the same individual. It is uncertain whether or not these centra pertain to *Sauroposeidon*.

The juvenile dorsal vertebral centrum (YPM 5151; Fig. 3.16) is 7.3 cm long, 6.9 cm wide, and 6.8 cm tall (measured at the cotyle). The centrum widens posteriorly and possesses a distinct posteroventral lip. The pleurocoel opens on the dorsal half of the centrum, is deepest anteriorly, and is subdivided by a small, subvertical strut at about the mid-length of the vertebra. The centrum is opisthocoelous, spool-shaped, and has a subcircular cross-section. The neurocentral junction is slightly wider posteriorly than anteriorly, measuring 2.1 cm and 1.4 cm wide, respectively. The juvenile dorsal vertebra (YPM 5151) is very similar to juvenile dorsal vertebrae of *Rapetosaurus* (Curry Rogers, 2009), *Apatosaurus* (Carpenter and McIntosh, 1994), and *Eucamerotus* (Blows, 1995) in its shape and extensive pneumaticity.

The juvenile sacral vertebral centrum (YPM 5107, Fig. 3.16) from site YPM 63-19 preserves tall sacral rib facets at its anterior and posterior faces, which are eroded and irregular. It is 9.3 cm long, 10 cm wide, and 6.3 cm tall (measured at the anterior face). A small, thin lamina is present in each pleurocoel, which extends over about half of the length of the centrum and is about 2 cm deep. This sacral centrum is similar to that of ‘*Pleurocoelus’ nanus* (Lull 1911b:pl.15) and *Camarasaurus sp.* (Carpenter and McIntosh, 1994:fig. 17.2) in size of its pleurocoel, but unlike in these taxa, it is distinctly wider than tall.

DISCUSSION

In light of the new information on the anatomy and paleoenvironment of *Sauroposeidon proteles* presented above, I review its phylogenetic relationships and paleobiogeographic history. New information from this reevaluation is also used to evaluate other claims for titanosaurs in the Early Cretaceous of North America. I then evaluate the relative importance of bias versus local extinction in causing the start of the sauropod hiatus, and discuss some possible causes of that extinction.

Phylogenetic and paleobiogeographic history

The absence of a full taxonomic description and paucity of comparative materials have hindered resolution of the phylogenetic relationships of the Cloverly Formation sauropod material. In contrast, *Sauroposeidon proteles* was found to be a brachiosaurid via both comparative anatomy (Wedel et al., 2000a, b) and cladistic analysis (as ‘*Paluxysaurus*’; Rose, 2007). The evidence presented above that the Cloverly Formation material, ‘*Paluxysaurus’*, and

Sauroposeidon represent a single genus prompts reevaluation of its phylogenetic affinities. These affinities are investigated thoroughly in Chapter 4, but will be discussed briefly here.

In discussing the affinities of the Cloverly sauropod, Ostrom (1970:81) concluded that it represented a brachiosaurid or titanosaur, based mostly on the single neural spines in the dorsal vertebrae and that "The relatively thin, unexpanded ischium and the slender, but not elongated ulna suggest titanosaurid rather than brachiosaurid affinities and I have therefore tentatively referred YPM 5449 to the Titanosauridae." However, the ischium is instead a pubis (see above) and is similar to those of other titanosauriforms (e.g., *Giraffatitan*, *Andesaurus*). Likewise, the ulna is similar to those of basal titanosauriforms in proportions (e.g., *Venenosaurus, Phuwiangosaurus*).

In contrast to the titanosaur affinities suggested by Ostrom (1970), Wedel et al. (2000a, b) suggested four characters to link *Sauroposeidon* to brachiosaurids. These include: centrum length more than four times centrum diameter, cervical ribs more than two centra in length, camellate vertebral pneumaticity, and a mid-cervical 'transition point' in neural spine height. However, the first three characters are now recognized in a wider array of sauropods (i.e., Titanosauriformes; Curry Rogers, 2005), and the last is poorly defined and not known with certainty in any specimen of *Sauroposeidon*. Gomani et al. (1999) suggested that '*Paluxysaurus*' was either a brachiosaurid or basal somphospondylan. Rose (2007) presented a cladistic analysis that supported the brachiosaurid affinities of *Paluxysaurus.* However, this relationship was supported by only a single synapomorphy — a highly eccentric femoral cross section — a character with a sporadic phylogenetic distribution in that analysis. In sum, character support for previous hypotheses of relationship between *Sauroposeidon* and titanosaurs or brachiosaurids is weak.

Evidence for a position within Somphospondyli for *Sauroposeidon* is supported by material from the Cloverly Formation, which bears several somphospondylan synapomorphies, such as a single prespinal lamina on anterior dorsal vertebrae and a medially beveled scapular glenoid, a scapular blade that is flat in cross section, an ischial blade that is shorter than the pubic blade, and an interlocking proximal tibia and fibula (Wilson and Upchurch, 2009). *Sauroposeidon* lacks synapomorphies of Titanosauria such as a ventral longitudinal hollow in anterior and middle caudal vertebrae and a plate-like ischium (Wilson, 2002). Likewise, *Sauroposeidon* lacks several brachiosaurid features, including middle and posterior dorsal vertebrae with long, ‘rod-like’ transverse processes or an abbreviate pubic peduncle of the ischium (Janensch, 1950; Wilson, 2002).

As a somphospondylan, *Sauroposeidon* does not represent a relict of a Late Jurassic North American brachiosaurid lineage. The closest relatives of *Sauroposeidon* seem to be Early Cretaceous Gondwanan genera such as *Ligabuesaurus*, suggesting a paleobiogeographic link between Gondwana and Laurasia into the middle Cretaceous. This revised view of the paleobiogeographic history of *Sauroposeidon* parallels that of the contemporaneous theropod *Acrocanthosaurus*, which was once thought to represent a relict of Late Jurassic allosaurs, but is now recognized as having close relatives from Early Cretaceous Gondwanan strata (Brusatte and Sereno, 2008; Eddy and Clarke, 2011).

Although *Sauroposeidon* is not a titanosaur, other reports of Early Cretaceous North American titanosaurs exist. These reports are based on some of the same features previously cited in support of titanosaur affinities for *Sauroposeidon*. Claims for the presence of titanosaurs in the Early Cretaceous of North America are evaluated below.

Early Cretaceous North American titanosaurs?

Reevaluation of the sauropod material described by Ostrom (1970) unequivocally supports its referral to *Sauroposeidon* and placement outside of Titanosauria. Claims of other Early Cretaceous North American titanosaurs are also problematic (Britt et al., 1996, 1997, 1998; Tidwell and Carpenter, 2007). For example, Britt et al. (1996; 1997; 1998) presented a suite of features to support 'titanosaurid' affinities for an Early Cretaceous sauropod from the Dalton Wells quarry, Utah. Many of these features characterize a wider array of sauropods than titanosaurs, for example spatulate teeth (e.g., *Camarasaurus, Turiasaurus*), long sternal plates (e.g., *Cedarosaurus*), a raised ulnar olecranon (e.g., *Tehuelchesaurus*, *Giraffatitan. Venenosaurus*), and procoelous caudal vertebrae (*Turiasaurus, Daxiatitan, Donygangosaurus,* some diplodocids). Likewise, Tidwell and Carpenter (2007: 158A) suggested that a sauropod skeleton from the Yellow Cat Member of the Cedar Mountain Formation was a titanosaur on the basis of "a single, low neural spine, prespinal lamina, and short posterior cervical [vertebra] length”. However, all of these features can also be found in non-titanosaurs (e.g., *Giraffatitan*, Janensch, 1950; *Sauroposeidon,* see above; *Tehuelchesaurus*, Carballido et al., in press).

Thus, there are no demonstrated records of titanosaurs in North America prior to the Maastrichtian. These unsubstantiated reports of Early and middle Cretaceous North American titanosaurs have played a large role in the discussion of the cause of the sauropod hiatus (Lehman, 2001; Mannion and Upchurch, 2011). Below, I reexamine the start of the sauropod hiatus in light of these reevaluated affinities of Early Cretaceous North American sauropods.

The role of bias in the sauropod hiatus

As the best known Early Cretaceous North American sauropod, *Sauroposeidon* is relevant to the sauropod hiatus. Recently, the traditional explanation for the sauropod hiatus as a true local extinction followed by immigration has been challenged (Lehman, 2001; Mannion and Upchurch, 2011). Instead, a combination of sampling and preservation biases are seen as an equally likely explanation for the hiatus, with latest Cretaceous titanosaurs (i.e., *Alamosaurus*) as the descendants of Early Cretaceous North American sauropods. Mannion and Upchurch (2011) used tentative or unsubstantiated reports of Early and early Late Cretaceous North American titanosaurs (see “Early Cretaceous North American titanosaurs?” above) to suggest that the sauropod hiatus was shorter than has been traditionally portrayed, that is from the Turonian–early Campanian (i.e., < 15 Ma) rather than from the Cenomanian–Maastrichtian (i.e., ca. 30 Ma). Furthermore, Mannion and Upchurch (2011) conflated age uncertainty with true stratigraphic range. For example, the single known skeleton of the brachiosaurid *Sonorasaurus thompsoni* (Ratkevitch, 1998) is from strata that are either Albian or Cenomanian in age, but Mannion and Upchurch (2011) cited this skeleton as some of the evidence that the sauropod hiatus did not begin until the Turonian. Based on specimens of known affinities and well-established age, the sauropod hiatus lasted nearly 30 million years, from the middle Cenomanian to the Maastrichtian (D’Emic et al., 2010).

Part of the ‘bias’ explanation of the sauropod hiatus stems from the observations that titanosaurs inhabited more inland settings than other sauropods, and inland paleoenvironments are rare in the Late Cretaceous strata deposited during the sauropod hiatus (Mannion and Upchurch, 2010). The association between titanosaurs and inland paleoenvironments seems robust, but must be treated with caution given that about half of the species used to create the correlation are only known from single individuals (and therefore localities; Mannion and Upchurch, 2011: supplemental information). If a species is only known from a single individual, it is difficult to know the entire paleoenvironment of that species. Discoveries of closely related species in the same paleoenvironment corroborate the idea that the clade to which they belong prefers that environment, but when each species is only known from a single exemplar, each corroboration is weak. New discoveries and referrals will tend to expand the known paleoenvironmental range of a species. For example, *Cedarosaurus* was originally described from the fluvially-deposited Cedar Mountain Formation, but is now also recognized in the marginal marine Glen Rose Formation (see Chapter 2). Likewise, *Sauroposeidon* is recognized from the Antlers, Twin Mountains, and Cloverly Formations, all of which were fluvially deposited, but of varying proximity to the coast (Rose, 2007; see above). In sum, Mannion and Upchurch (2010, 2011) postulated that sampling failures account for some of the perceived patterns in sauropod diversity; these failures may presently *seem* to manifest at the level of large clades, but severer biases likely lie hidden at the species level.

Even if the inland preference of titanosaurs is genuine, it can only explain the *persistence* of the hiatus, not its initiation, because there were no titanosaurs in North America before the hiatus (see above). That is, the “inland bias” explanation for the absence of titanosaurs does not explain the absence of brachiosaurids or other basal titanosauriforms. Early Cretaceous North American sauropods such as *Sauroposeidon* lived on floodplains of varying proximity to the coastline or in coastal settings (Ostrom, 1970; Langston, 1974; see above). Similar paleoenvironments are represented (and bear dinosaurs) into the Late Cretaceous, for example the Cenomanian Blackleaf Formation or Turonian Moreno Hill Formation (Varricchio et al., 2007; Wolfe et al., 2004). Furthermore, the presence of *any* titanosaur in the Early Cretaceous of North America does not support the ‘bias’ explanation for the sauropod hiatus; only the presence of the sister-taxon of *Alamosaurus* would. No cladistic analysis has found such a relationship (e.g., Rose, 2007; Royo Torres, 2009; Carballido et al., 2011;

Mannion and Upchurch, 2011; see chapter 4).

Evaluating biases in the sauropod fossil record can be informed by the fate of other dinosaur lineages that coexisted with sauropods before the start of the hiatus. For example, biases against sauropod recovery would be expected to preferentially affect animals of similar size, habitat, or ecology. I test this expectation by plotting the known stratigraphic ranges of sauropods and other dinosaurs (Fig. 3.17) based on information from the Paleobiology Database (www.pbdb.org, accessed 06/05/11) and the literature. The continent-wide pattern shows that ten ecologically disparate dinosaur groups (neoceratopsians, tyrannosauroid, dromaeosaurid, oviraptorosaur, and ornithomimids theropods, nodosaurid and ankylosaurid ankylosaurs, hypsilophodontid, basal iguanodontian, and hadrosauroid ornithopods) coexisted with sauropods (i.e., were found in the same geologic units) at some time during the Early-middle Cretaceous. Only two ecological groups — titanosauriform sauropods and basal iguanodonts — did not persist past 98 Ma in North America. This pattern has been noted previously (Cifelli et al., 1997; Jacobs and Winkler, 1998), and has persisted even with the intensified fossil collecting in the last fifteen years. This intensified collecting, as well as several redescriptions and revisions, have refined the pattern to show that these two non-persisting ecological groups represent at least five dinosaur lineages (brachiosaurids, basal somphospondylan sauropods, *Tenontosaurus*, and two unnamed basal iguanodontian lineages; see McDonald et al., 2010).

When broken down into geographic regions (Fig. 3.17) the pattern abides:

sauropods and basal iguanodontians disappear from the fossil record in the middle Cretaceous while other dinosaur groups persist. This persistence suggests that suitable brachiosaurid, basal somphospondylan, and basal iguanodont habitat was present long after their disappearance, refuting the paleoenvironmental biases invoked by Mannion and Upchurch (2011) to explain the hiatus. This similar occurrence data among several basins suggest that continental extinction, rather than sampling bias, was the main factor explaining the start of the sauropod hiatus.

The cause of the North American sauropod regional extinction

Several explanations for the cause of sauropods' extirpation from North America in the middle Cretaceous have been proposed. When first recognizing the sauropod hiatus, Lucas and Hunt (1989:83) found "no convincing explanation of this extinction," but tentatively suggested two causes: the incursion of the Western Interior Seaway and competition with hadrosaurs. Another cause for the extirpation was proposed by Salgado and Coria (2005), in which changes in floras and mean annual temperature would have led to substantial sauropod faunal turnover. Additionally, Bakker (1978) linked the decline of sauropods and rise of ornithopods through the Cretaceous to the spread of angiosperms, based mostly on the pattern in North America.

Hypotheses relating changes in floras and climate to sauropod faunal changes (Bakker, 1978; Salgado and Coria, 2005) are difficult to test in light of the spatiotempral vicissitudes of middle-Late Cretaceous sauropod and angiosperm fossil records (Barrett and Willis, 2001). However, some potential causes that have been ruled out by other authors merit further investigation, because their timing coincides well with sauropod disappearance. Below I discuss why two of these causes should not be ruled out.

Incursion of the Western Interior Seaway—The late Albian incursion of the Western Interior Seaway was cited as a possible cause of the start of the sauropod hiatus by Lucas and Hunt (1989). The causal relationship between the incursion and sauropod extinction was not articulated, but the incursion coincided with a fall in marine temperatures and a large marine invertebrate extinction event (Lucas and Hunt, 1989). Mannion and Upchurch (2011) countered this hypothesized cause, arguing that this incursion could not have caused the sauropod hiatus because it predated the last known sauropod fossils by several million years (late Cenomanian in their view). The argument of Mannion and Upchurch (2011) assumes that the incursion occurred entirely in the Albian and before the disappearance of sauropods. However, the incursion took place in irregular transgressions and regressions over several million years in the Albian–Cenomanian before forming a persistent seaway for most of the Late Cretaceous (Kauffman, 1984). Across the western United States, the encroaching of the Western Interior Seaway is marked by a coastal, sandstone-dominated facies (e.g., Dakota Formation, Upper Cloverly/Sykes Mountain Formation, Paluxy Formation); no sauropod fossils are known from above these coastal facies, but a few specimens have been reported from within them (Langston, 1974; K. Carpenter, pers. comm. in Mannion and Upchurch, 2011). Thus, the incursion of the seaway predated or was coincident with sauropod disappearance, which does not preclude it from being a factor in that disappearance (contra Mannion and Upchurch, 2011).

Hadrosauroid competition—Competition between hadrosaurs and sauropods was cast as a doubtful cause of sauropod extinction by Lucas and Hunt (1989: 83), because of their “widely divergent feeding mechanisms.” However, competition may have been present between these groups at different ontogenetic stages, because resource use likely changed during their dramatic change in body size over ontogeny (Whitlock et al., 2010). A scenario of competitive replacement is consistent with the fossil record because the first North American hadrosauroids and last pre-hiatus sauropods are found in the same horizon (Mussentuchit Member, Cedar Mountain Formation; Cifelli et al., 1997; Kirkland, 1998; Maxwell and Cifelli, 2000), whereas each group was more widespread after and before, respectively. These hadrosauroids possessed advanced masticatory capabilities relative to more basal Early Cretaceous taxa (Head, 1997), which may have made them ecologically competitive with sauropods.

The nearly coincident disappearance of sauropods, rise of hadrosauroids, and arrival of the Western Interior Seaway may have been related causally, a hypothesis that awaits refined spatiotemporal sampling for the middle Cretaceous of North America.

CONCLUSIONS

Examination of sauropod fossils from the Early Cretaceous Cloverly Formation of Wyoming, USA, indicates that much of the material is referable to the titanosauriform *Sauroposeidon proteles*. *Sauroposeidon* is neither a brachiosaurid nor a titanosaur as previously proposed, but is instead a basal somphospondylan. *Sauroposeidon* is the best known Early Cretaceous North American sauropod, known from several localities, individuals, and ontogenetic stages. The Early Cretaceous of North America hosted both brachiosaurid and somphospondylan sauropods, but no titanosaurs. These sauropods lived in floodplain and near-coastal settings, paleoenvironments that were present and hosted dinosaurs through the Late Cretaceous in North America. The mid-Cretaceous North American disappearance of sauropods was nearly coincident with the arrival of a persistent Western Interior Seaway and the appearance of hadrosauroid dinosaurs, possibly implicating these events in that disappearance. At least ten dinosaur lineages that coexisted with sauropods before their disappearance persisted well into the Late Cretaceous, suggesting that environmental or sampling bias was not a major factor in the start of the hiatus.

REFERENCES

Barrett, P. M., and K. J. Willis. 2001. Did dinosaurs invent flowers? Dinosaur–angiosperm coevolution revisited. Biological Reviews of the Cambridge Philosophical Society 76:411–447.

Barrett, P. M., and P. Upchurch. 2005. Sauropodomorph diversity through time: paleoecological and macroevolutionary implications; pp. 125–151 in K. A. Curry Rogers and J. A. Wilson (eds.), The Sauropods: Evolution and Paleobiology. University of California Press, Berkeley, California.

Behrensmeyer, A. K. 1978. Taphonomic and ecologic information from bone weathering. Paleobiology 4:150–162.

Behrensmeyer, K. 1988. Vertebrate preservation in fluvial channels: Palaeogeography, Palaeoclimatology, Palaeoecology 63:183–199.

Behrensmeyer, K. 2007. Bonebeds through time; pp. 65–102 in R. R. Rogers, D. A. Eberth, A. R. Fiorillo (eds.), Bonebeds: genesis, analysis, and paleobiological significance. University of Chicago Press, Chicago, Illinois.

Blows, W. T. 1995. The Early Cretaceous brachiosaurid dinosaurs *Ornithopsis* and *Eucamerotus* from the Isle of Wight, England. Palaeontology 38:187–197.

Bonaparte, J. F. 1986. The early radiation and phylogenetic relationships of sauropod dinosaurs, based on vertebral anatomy; pp. 247–258 in K. Padian (ed.), The Beginning of the Age of Dinosaurs. Cambridge University Press, Cambridge.

Borsuk-Bialynicka, M. 1977. New camarasaurid sauropod *Opisthocoelicaudia skarzynskii* gen. n., sp. n. from the upper Cretaceous of Mongolia. Palaeontologica Polonica 37:1–64.

Calvo, J. O. 1994. Feeding mechanisms in some sauropod dinosaurs. Unpublished MSc Thesis, University of Illinois at Chicago.

Canudo, J., R. Royo-Torres, and G. Cuenca-Bescós. 2008. A new sauropod: *Tastavinsaurus sanzi* gen et. sp. nov. from the Early Cretaceous (Aptian) of Spain. Journal of Vertebrate Paleontology 28:712–731.

Carpenter, K. and J. S. McIntosh. 1994. Upper Jurassic sauropod babies from the Morrison; pp. 265–278 in K Carpenter, K. F. Hirsch, and J. R. Horner (eds.), Dinosaur Eggs and Babies. Cambridge University Press, Cambridge.

Carpenter, K. and V. Tidwell. 2005. Reassessment of the Early Cretaceous sauropod *Astrodon johnstoni* Leidy 1865 (Titanosauriformes); pp. 78–114. in V. Tidwell and K. Carpenter, (eds.), Thunder Lizards: the sauropodomorph dinosaurs. Indiana University Press, Bloomington.

Chure, D. B. B. Britt, J. A. Whitlock, and J. A. Wilson. 2010. First complete sauropod dinosaur skull from the Cretaceous of the Americas and the evolution of sauropod dentition. Naturwissenschaften 97:379–391.

Cifelli, R., J. I. Kirkland, A. Weil, A. Deino, and B. J. Kowallis. 1999. High-precision ^{40}Ar/^{39}Ar geochronology and the advent of North America's Late Cretaceous terrestrial fauna. Proceedings of the National Academy of Sciences 94:11163–11167.

Curry Rogers, K. A. 2009. The postcranial osteology of *Rapetosaurus krausei* (Sauropoda: Titanosauria) from the Late Cretaceous of Madagascar. Journal of Vertebrate Paleontology 29:1046–1086.

D'Emic, M. D. and B. B. Britt. 2008. Reevaluation of the phylogenetic affinities and age of a basal titanosauriform (Sauropoda: Dinosauria) from the Early Cretaceous Cloverly Formation of North America. Journal of Vertebrate Paleontology 28, 68A.

D'Emic, M. D., J. A. Wilson, and R. Thompson. 2010. The end of the sauropod dinosaur hiatus in North America. Palaeogeography, Palaeoclimatology, Palaeoecology 297:486–490.

Duchaufour, P., 1982. Pedology. Allen and Unwin, Boston, Massachusetts, 448 pp.

Driese, S. G., L. C. Nordt, W. C. Lynn, C. A. Stiles, C. I. Mora, and L. P. Wilding. 2005. Distinguishing climate in the soil record using chemical trends in a vertisol climosequence from the Texas coast prairie, and application to interpreting Paleozoic paleosols in the Appalachian Basin, U.S.A. Journal of Sedimentary Research 75:339–349.

Eberth, D. A. 1990. Stratigraphy and sedimentology of vertebrate microfossil localities in uppermost Judith River Formation (Campanian) of Dinosaur Provincial Park. Palaeogeography, Palaeoclimatology, Palaeoecology 78:1–36.

Eberth, D. A. 2007. A Bonebeds Database: Classification Biases, and Patterns of Occurence; pp. 103–220 in R. R. Rogers, D. A. Eberth, A. R. Fiorillo (eds.), Bonebeds: genesis, analysis, and paleobiological significance. University of Chicago Press, Chicago, Illinois.

Fanning, D. S. and M. C. B. Fanning. 1989. Soil: Morphology, Genesis, and Classification. John Wiley & Sons, Inc., New York, New York, 395 pp.

Fisher, D. C. 1981. Crocodilian scatology, microvertebrate concentrations, and enamel-less teeth. Paleobiology 7:262-275.

Forster, C. A. 1990. The postcranial skeleton of the ornithopod dinosaur *Tenontosaurus tilletti.* Journal of Vertebrate Paleontology 10:273–294.

Gates, T. A., S. D. Sampson, L. E. Zanno, E. M. Roberts, J. G. Eaton, R. L. Nydam, J. H. Hutchison, J. A. Smith, M. A. Loewen, and M. A. Getty. 2010. Biogeography of terrestrial and freshwater vertebrates from the Late Cretaceous (Campanian) Western Interior of North America. Palaeogeography, Palaeoclimatology, Palaeoecology 291:371–387.

Gomani, E., L. L. Jacobs, and D. A. Winkler. 1999. Comparison of the African titanosaurian, *Malawisaurus*, with an Early Cretaceous North American sauropod.; pp. 223–233 in Y. Tomida, T. H. Rich, and P. Vickers-Rich, (eds.), Proceedings of the Second Gondwanan Dinosaur Symposium, National Museum of Tokyo Monograph 15.

Haq, B. U., J. Hardenbol, and P. Vail. 1987. Chronology of Fluctuating Sea Levels since the Triassic. Science 235:1156–1167.

He, X., K. Li, K. Cai. 1988. [The Middle Jurassic Dinosaur fauna from Dashanpu, Zigong, Sichuan, Vol. IV. Sauropod dinosaurs (2), *Omeisaurus tianfuensis*]. Chengdu: Sichuan Scientific and Technical Publishing House. (In Chinese.)

Hill, A., 1979. Disarticulation and scattering of mammal skeletons: Paleobiology 5:261–274.

Ikejiri, T. 2003. Sequence of closure of neurocentral sutures in Camarasaurus (Sauropoda) and implications for phylogeny in Reptilia. Journal of

Vertebrate Paleontology 23, 65A.

Irmis, R. 2007. Axial skeleton ontogeny in the parasuchia (Archosauria: Pseudosuchia) and its implications for ontogenetic determination in archiosaurs. Journal of Vertebrate Paleontology 270:350–361.

Jacobs, L. L., and D. A. Winkler. 1998. Mammals, archosaurs, and the Early to Late Cretaceous transition in north-central Texas; in Y. Tomida, T. H. Rich, and P. Vickers-Rich, (eds.), Proceedings of the Second Gondwanan Dinosaur Symposium, National Museum of Tokyo Monograph 15:253–280.

Janensch, W. 1947. Pneumatizitat bei Wirbeln von Sauropoden undanderen Saurischiern. Palaeontographica 3:1–25.

Janensch, W. 1950. Die wirbelsäule von *Brachiosaurus brancai*. Palaeontographica (Supplement 7) 2:27–93.

Janensch W. 1961. Die Gliedmaßen und Gliedmassengürtel der Sauropoden der Tendaguru-Schichten. *Palaeontographica (Supplement 7)* 3**:**177–235.

Kvale, E. P., and C. F. Vondra. 1993, Effects of relative sea-level change and local tectonics on a Lower Cretaceous fluvial to transitional marine sequence, Bighorn Basin, Wyoming, USA: Special Publications International Association of Sedimentologists 17:383–399.

Langston, W. 1974. Nonmammalian Comanchean tetrapods. Geoscience and Man 8:77–102.

Lapparent, A. F. de. 1943. Les dinosauriens jurassiques de Damparis (Jura). Mémoires de la Société Géologique de France, nouvelle série 47:1–20.

Larkin, P. 1910. The occurrence of a sauropod dinosaur in the Trinity Cretaceous of Oklahoma. Journal of Geology 28:93–98.

Lehman, T. 2001. Late Cretaceous dinosaur provinciality; pp. 310–328 in Tanke, D. H. and K. Carpenter (eds.), Mesozoic Vertebrate Life. Indiana University Press, Bloomington, Indiana.

Leidy, J. 1865. Cretaceous reptiles of the United States. Smithsonian Contributions to Knowledge 14:1–135.

Lucas, S. G., and A. Hunt. 1989. *Alamosaurus* and the sauropod hiatus in the Cretaceous of the North American western interior; pp. 75–85 in J. O. Farlow (ed.), Geological Society of America Special Paper 238.

Lull, R. S. 1911. Systematic paleontology of the Lower Cretaceous deposits of Maryland: Vertebrata. Lower Cretaceous Volume, Maryland Geological Survey 183–211.

Mannion P.D., and P. Upchurch. 2011. A re-evaluation of the ‘mid-Cretaceous sauropod hiatus’ and the impact of uneven sampling of the fossil record on patterns of regional dinosaur extinction. *P*alaeogeography, Palaeoclimatology, Palaeoecology 299:529–540.

Marsh, O. C. 1878. Principal characters of American Jurassic dinosaurs. Pt. I. American Journal of Science 16:411–416.

Martínez, R. D., O. Giménez, J. Rodríguez, M. Luna, and M. C. Lamanna. 2004. An articulated specimen of the basal titanosaurian (Dinosauria:

Sauropoda) *Epachthosaurus sciuttoi* from the early Late Cretaceous Bajo Barreal Formation of Chubut Province, Argentina. Journal of Vertebrate Paleontology 24:107–120.

Moberly, R. 1960. Morrison, Cloverly, and Sykes Mountain formations, northern Bighorn Basin, Wyoming and Montana. Bulletin of the Geological Survey of America 71:1137–1176.

Osborn, H. F., and C. C. Mook. 1921. *Camarasaurus*, *Amphicoelias*, and other sauropods of Cope. Memoirs of the American Museum of Natural History 3:247–287.

Ostrom, J. H. 1970. Stratigraphy and paleontology of the Cloverly Formation (Lower Cretaceous) of the Bighorn basin area, Wyoming and Montana. Peabody Museum Bulletin 35:1–234.

Ostrom, J. H., and J. S. McIntosh. 1966. Marsh's Dinosaurs. Yale University Press, New Haven, Connecticut, 388 pp.

Owen, R. 1842. A description of a portion of the skeleton of *Cetiosaurus*, a gigantic extinct saurian occurring in the Oolitic Formation of different parts of England. Proceedings of the Geological Society of London 3:457–462.

Paul, G. 1988. The brachiosaur giants of the Morrison and Tendaguru with a description of a new subgenus, *Giraffatitan*, and a comparison of the world's largest dinosaurs. Hunteria 2:1–14.

Rich, T., P. Vickers-Rich, O. Gimenez, R. Cúneo, P. Puerta, and R. Vacca. 1999. A new sauropod dinosaur from Chubut Province, Argentina, in Tomida, Y., T. H. Rich, and P. Vickers-Rich, (eds.), Proceedings of the Second Gondwanan Dinosaur Symposium, National Science Museum of Tokyo Monograph 15: 61–84.

Riggs, E. S. 1903. *Brachiosaurus altithorax*, the largest known dinosaur. American Journal of Science 15:299–306.

Riggs. E. S. 1904. Structure and relationships of the opisthocoelian dinosaurs, part II: the Brachiosauridae. Field Columbian Museum, Publications in Geology 2:229–247.

Rogers, R. R., and S. Kidwell. A Conceptual Framework for the Genesis and Analysis of Vertebrate Skeletal Concentrations. pp. 1–65 in in R. R. Rogers, D. A. Eberth, A. R. Fiorillo (eds.), Bonebeds: genesis, analysis, and paleobiological significance. University of Chicago Press, Chicago, Illinois.

Rose, P. 2007. A titanosauriform (Dinosauria: Saurischia) from the Early Cretaceous of Central Texas and its phylogenetic relationships. Palaeontologica Electronica 10:1–65.

Salgado, L. and J. O. Calvo. 1997a. Evolution of titanosaurid sauropods. II: The cranial evidence. Ameghiniana 34:33–48.

Salgado, L, R. Coria, and J. O. Calvo. 1997b. Evolution of titanosaurid sauropods. I: phylogenetic analysis based on the postcranial evidence. Ameghiniana 34:3–32.

Salgado, L., Apesteguía, S., and S. Heredia. 2005. A new specimen of *Neuquensaurus australis*, a Late Cretaceous saltasaurine titanosaur from North Patagonia. Journal of Vertebrate Paleontology 25: 623–634.

Schwarz, D., T. Ikejiri, B. Breithaupt, P. M. Sander, and N. Klein. 2007. A nearly complete skeleton of an early juvenile diplodocid (Dinosauria: Sauropoda) from the Lower Morrison Formation (Late Jurassic) of north-central Wyoming and its implications for early ontogeny and pneumaticity in sauropods. Historical Biology 19:225–253.

Taylor, M. 2009. A reevaluation of *Brachiosaurus altithorax* Riggs, 1903 (Dinosauria, Sauropoda) and its generic separation from *Brachiosaurus brancai* (Janensch, 1914). Journal of Vertebrate Paleontology 29:787–806.

Tidwell, V., K. Carpenter, and W. Brooks. 1999. New sauropod from the Lower Cretaceous of Utah, USA. Oryctos 2:21–37.

Tidwell, V., K. Carpenter, and S. Meyer. 2001. New titanosauriform (Sauropoda) from the Poison Strip Member of the Cedar Mountain Formation (Lower Cretaceous), Utah; pp. 139–165 in D. Tanke and K. Carpenter, (eds.), Mesozoic Vertebrate Life: New Research Inspired by the Paleontology of Phillip J. Currie. Indiana University Press, Bloomington.

Toots, H., 1965, Sequence of disarticulation in mammalian skeletons: Contributions to Geology, University of Wyoming 4:37–39.

Upchurch, P., and J. Martin. 2002. The Rutland *Cetiosaurus*: the anatomy and relationships of a Middle Jurassic British sauropod dinosaur. Palaeontology 45:1049–1074.

Upchurch, P., and J. Martin. 2003. The anatomy and taxonomy of *Cetiosaurus* (Saurischia, Sauropoda) from the Middle Jurassic of England. Journal of Vertebrate Paleontology 23:208–231.

Vepraskas, M. J., 1994. Redoximorphic Features for Identifying Aquic Conditions. North Carolina Agricultural Research Services Technology Bulletin 301.

Voorhies, M. R., 1969. Taphonomy and population dynamics of an early Pliocene vertebrate fauna, Knox County, Nebraska. University of Wyoming Contributions to Geology 1:1–69.

Wedel, M. J., R. L. Cifelli, and R. K. Sanders. 2000a. *Sauroposeidon proteles*, a new sauropod from the Early Cretaceous of Oklahoma. Journal of Vertebrate Paleontology 20:109–114.

Wedel, M. J., R. L. Cifelli, and R. K. Sanders. 2000b. Osteology, paleobiology, and relationships of the sauropod dinosaur *Sauroposeidon*. Acta Paleontologica Polonica 45:343–388.

Whitlock, J. A., J. A. Wilson, and M. C. Lamanna. 2010. Description of a nearly complete juvenile skull of Diplodocus (Sauropoda: Diplodocoidea) from the Late Jurassic of North America. Journal of Vertebrate Paleontology 30:442–457.

Wilding, L. P., and D. Tessier. 1988. Genesis of Vertisols: shrink-swell phenomena. pp. 55–96 in Wilding, L. P. and R. Puentes (eds.), Vertisols:

Their Distribution, Properties, Classification and Management. Texas A&M University, College Station, Texas.

Wilson, J. A. 1999. A nomenclature for vertebral laminae in sauropods and other saurischian dinosaurs. Journal of Vertebrate Paleontology 19, 639–653.

Wilson, J. A. 2002. Sauropod dinosaur phylogeny: critique and cladistic analysis. Zoological Journal of the Linnean Society 136:217–276.

Wilson, J. A. 2006. Anatomical nomenclature of fossil vertebrates: standardized terms or lingua franca? Journal of Vertebrate Paleontology 26:511–518.

Wilson, J. A. and P .C. Sereno. 1998. Early evolution and higher-level phylogeny of sauropod dinosaurs. Journal of Vertebrate Paleontology 18:1–68.

Wilson, J. A., M. D. D'Emic, K. Curry Rogers, D. M. Mohabey, and S. Sen. 2009. Reassessment of the sauropod dinosaur *Jainosaurus* (= *Antarctosaurus*) *septentrionalis* from the Upper Cretaceous of India. Contributions from the Museum of Paleontology, University of Michigan 32:17–40

Wilson, J. A., M. D. D'Emic, T. Ikejiri, E. Moacdieh, and J. A. Whitlock. 2011. A nomenclature for vertebral fossae in sauropods and other saurischian dinosaurs. PLOS One. 19 pp.

Wiman, C. 1929. Die Kreide-Dinosaurier aus Shantung. Palaeontologia Sinica (series C) 6:1–67.

Winslow, N., and P. Heller. 1987. Evaluation of unconformities in upper Jurassic and Lower Cretaceous nonmarine deposits, Bighorn Basin, Wyoming and Montana, U.S.A. Sedimentary Geology 53:181–202.

Wolfe, D., S. Beekman, S. McGuiness, D. Robira, R. Denton. 2004. Taphonomic characterization of a *Zuniceratopos* bone bed from the Middle Cretaceous (Turonian) Moreno Hill Formation. Journal of Vertebrate Paleontology 24: 131A.

Wolff, R. G. 1973. Hydrodynamic sorting and ecology of a Pleistocene mammalian assemblage from California (U.S.A.). Palaeogeography, Palaeoclimatology, Palaeoecology 13:91–101.

Wood, J., R. Thomas, and J. Visser. 1988, Fluvial processes and vertebrate taphonomy: The Upper Cretaceous Judith River Formation, south-central Dinosaur Provincial Park, Alberta, Canada: Palaeogeography, Palaeoclimatology, Palaeoecology, 66:127–143.

Zaleha, M. 2006. Sevier orogenesis and nonmarine basin filling: Implications of new stratigraphic correlations of Lower Cretaceous strata throughout Wyoming, USA. Geological Society of America Bulletin 118:886–896.

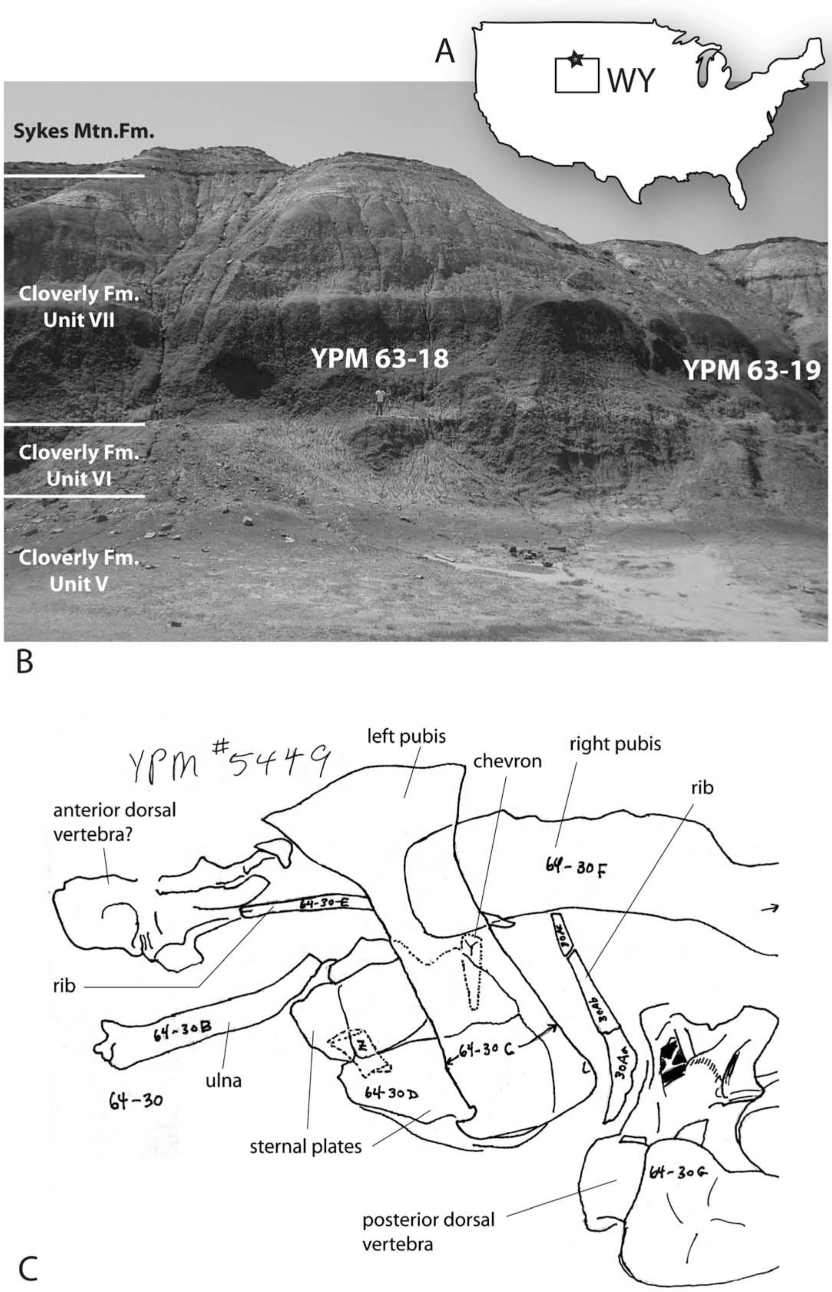

FIGURE 3.1. Field locality and documentation for *Sauroposeidon proteles* from the Cloverly Formation of Wyoming, USA. **A**, Map of USA with quarry location indicated by a star; **B**, Field photograph of YPM localities 63-18 and 63-19 taken in the 2008 field season. Person at YPM 63-18 is 1.8 m tall; **C**, field sketch from the 1963 Yale field season showing the association of many of the specimens in field number YPM 5449 (‘Exemplar A’ in the text).

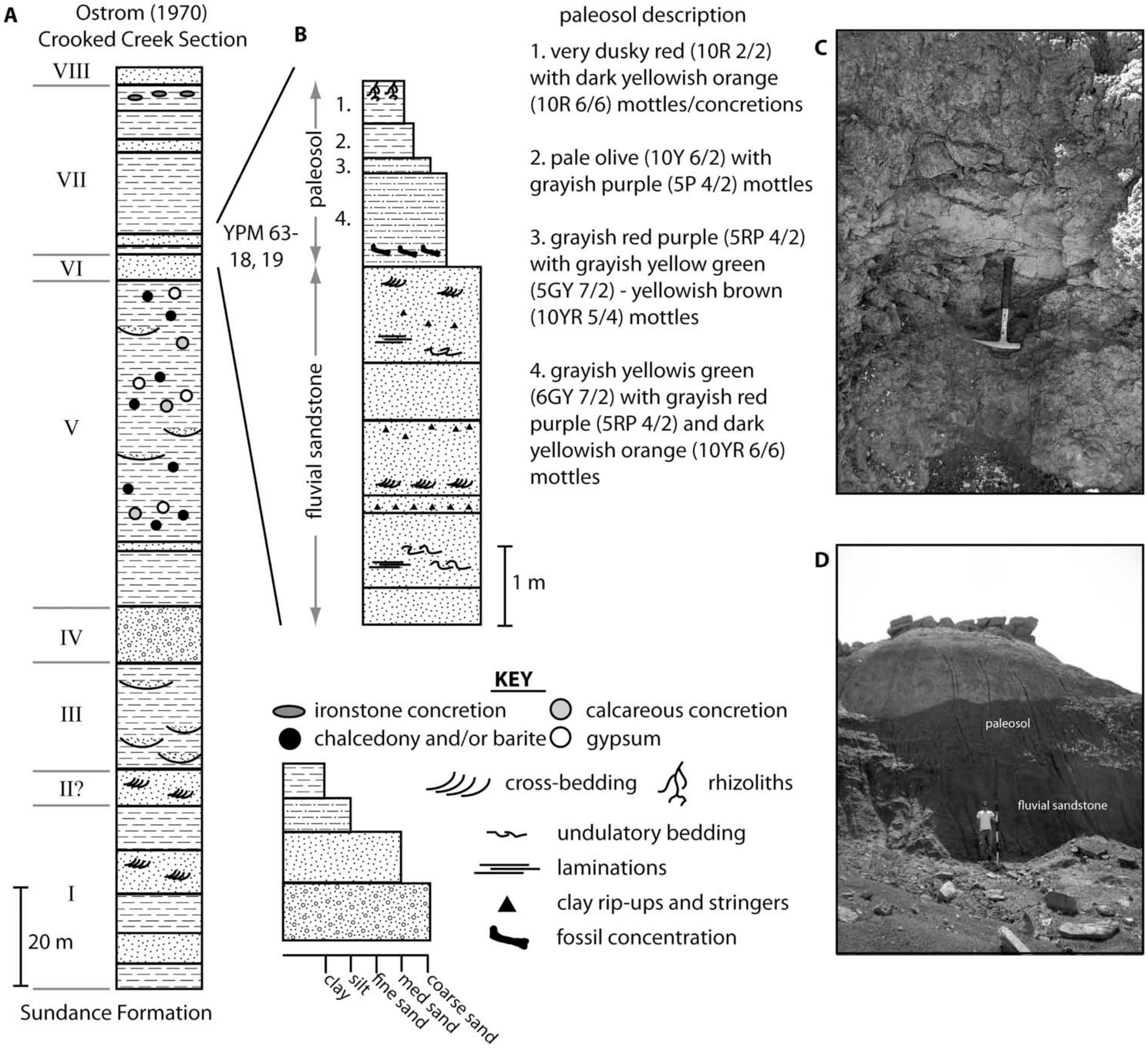

FIGURE 3.2. Sedimentology of the *Sauroposeidon proteles*-hosting units of the Cloverly Formation of Wyoming, USA. **A**, Composite stratigraphic section and lithologic units for the 'Crooked Creek' area (modified from Ostrom [1970]); **B**, Detailed stratigraphic section through sandstone underlying bone bed and hosting paleosol profile; **C**, Photograph of hosting paleosol profile; **D**, Photograph of bone-bearing horizons about 0.5 km northwest of YPM 63-18 and -19, showing preserved floodplain topography. The fossil-hosting stratum is equivalent to the base on the thinnest portion of the red paleosol.

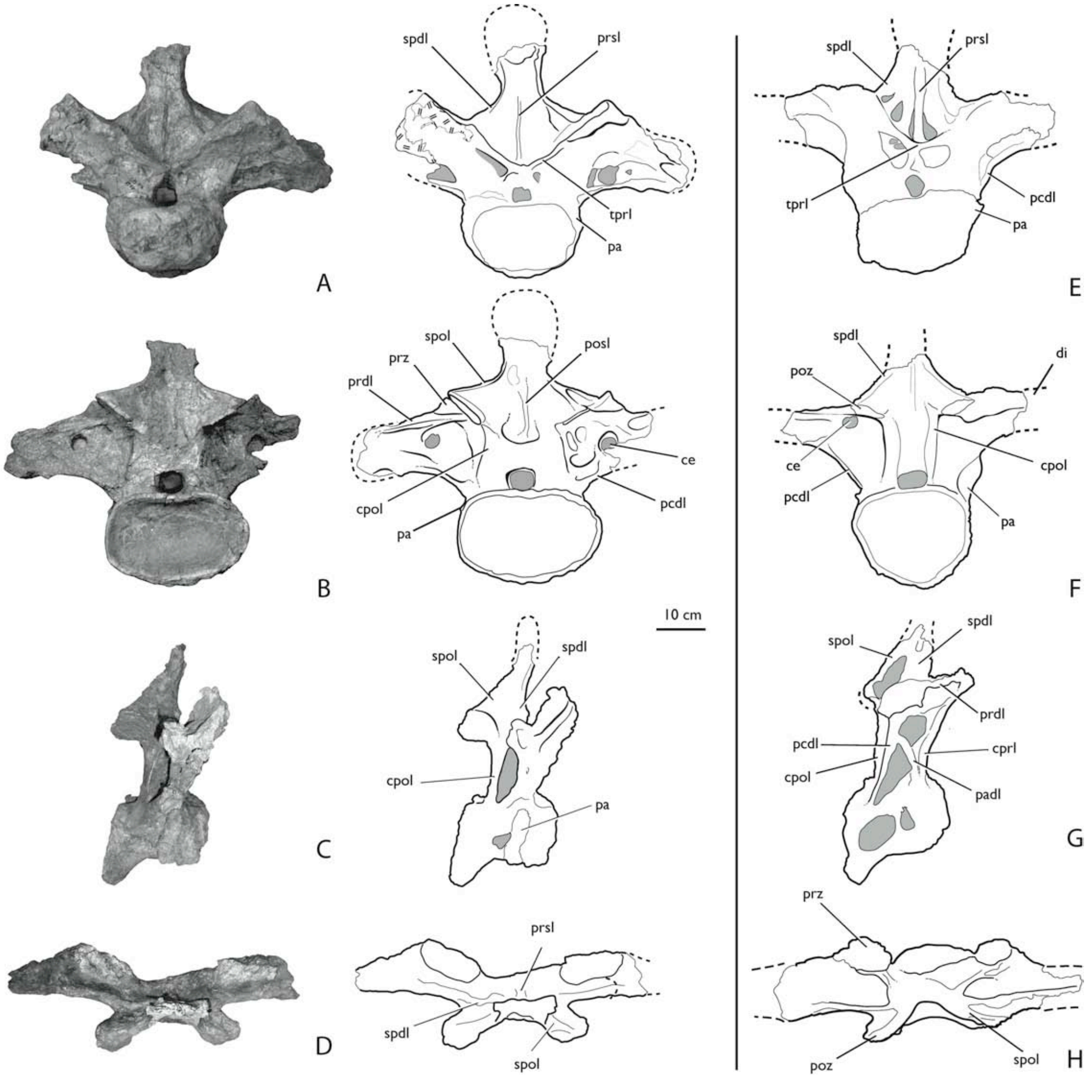

FIGURE 3.3. Anterior dorsal vertebrae from the Cloverly (YPM 5449) and Twin Mountains (FWMSH 93B-10) Formations referred to *Sauroposeidon proteles*. **A–D**, Photographs and interpretive line drawings of *Sauroposeidon* from the Cloverly Formation in **A**, anterior; **B**, posterior; **C**, right lateral, and **D**, dorsal view. **E–H**, Interpretive line drawings of an anterior dorsal vertebra of *Sauroposeidon* from the Twin Mountains Formation (formerly referred to ‘*Paluxysaurus*’ *jonesi*) in **E**, anterior; **F**, posterior; **G**, right lateral (reversed), and **H**, dorsal view. Dotted lines indicate missing bone, and hatched pattern indicates damaged bone. **Abbreviations**: **ce**, circular excavations; **cpol**, centropostzygapophyseal lamina; **pa**, parapophysis; **pcdl**, posterior centrozygapophyseal lamina; **posl**, postspinal lamina; **prsl**, prespinal lamina; **prz**, prezygapophysis; **spdl**, spinodiapophyseal lamina; **spol**, spinopostzygapophyseal lamina; **sprl**, spinoprezygapophyseal lamina; **tprl**, intraprezygapophyseal lamina.

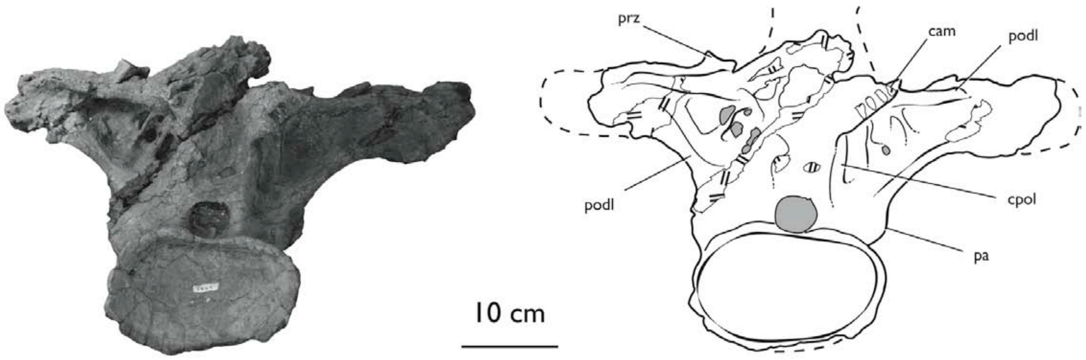

FIGURE 3.4. Anterior dorsal vertebra from the Cloverly Formation referred to *Sauroposeidon proteles* (YPM 5449). Photograph and interpretive drawing in posterior view. Dotted lines indicate missing bone, and hatched pattern indicates damaged bone. **Abbreviations**: **cam**, camellae; other abbreviations as in Figure 3.4.

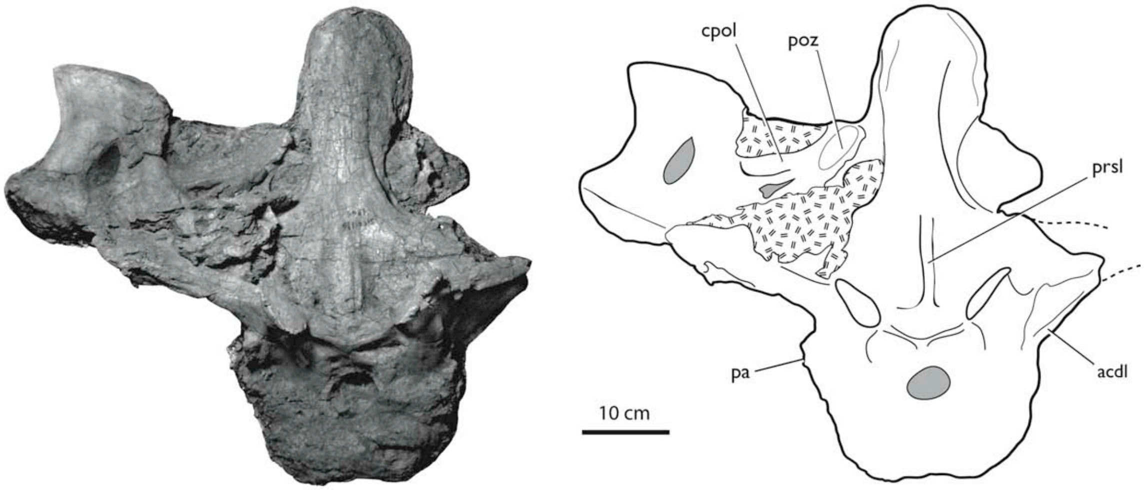

FIGURE 3.5. Anterior and posterior dorsal vertebrae from the Cloverly Formation referred to *Sauroposeidon proteles* (YPM 5449). Photograph and interpretive line drawing of anterior dorsal vertebra in anterior view and crushed posterior dorsal vertebra in right lateral view. Dotted lines indicate missing bone, and hatched pattern indicates damaged bone. **Abbreviations**: **acdl**, anterior centrodiapophyseal lamina; other abbreviations as in Figure 3.4.

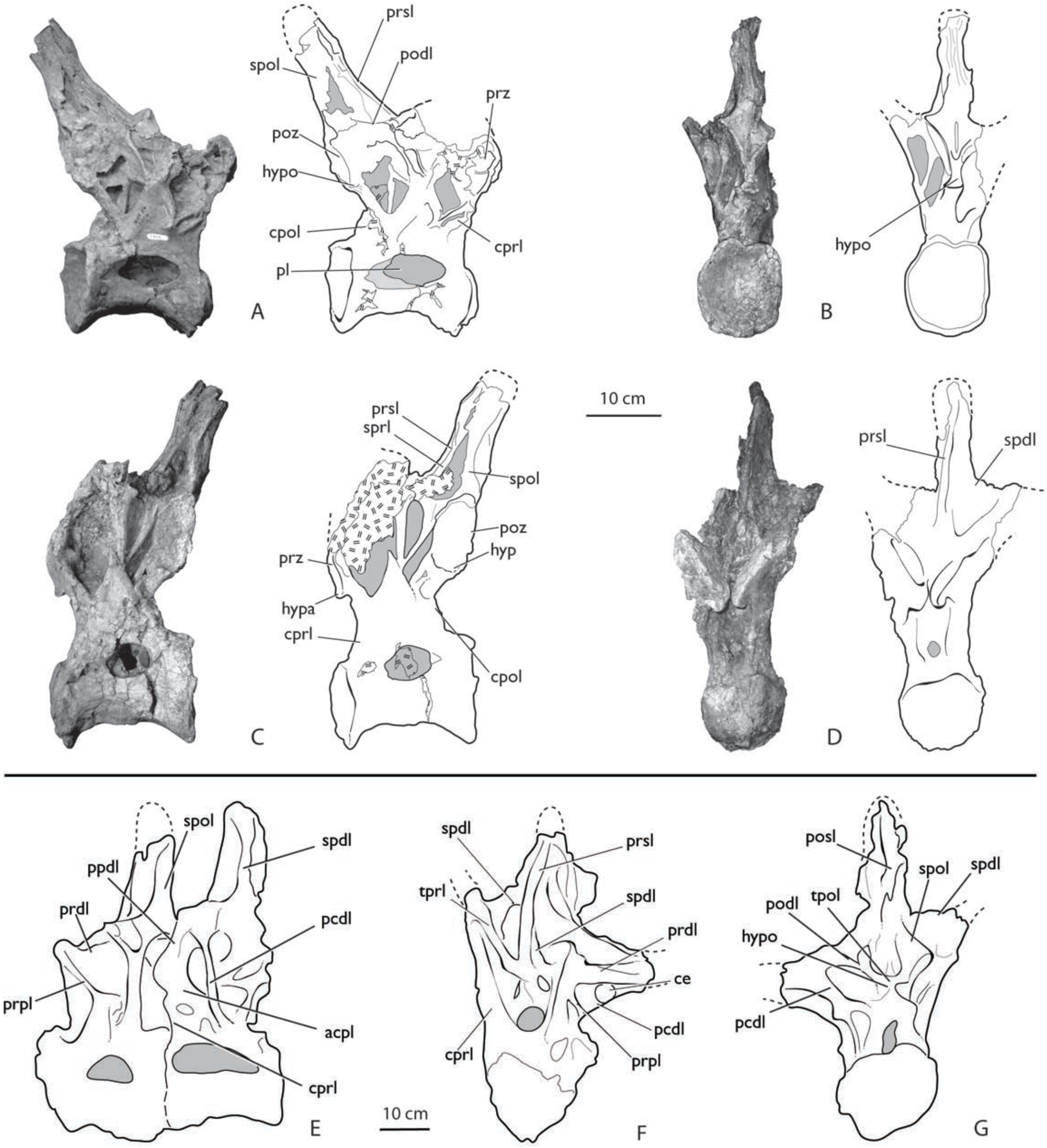

FIGURE 3.6. Posterior dorsal vertebrae from the Cloverly (YPM 5449) and Twin Mountains (FWMSH 93B-10) Formations referred to *Sauroposeidon proteles*. **A–D**, photographs and interpretive line drawings of *Sauroposeidon* from the Cloverly Formation in **A**, right lateral, **B**, posterior, **C**, left lateral, and **D**, anterior views. **E–F**, interpretive line drawings of posterior dorsal vertebrae of *Sauroposeidon* from the Twin Mountains Formation (formerly referred to ‘*Paluxysaurus*’ *jonesi*) in **E**, left lateral; **F**, anterior, and **G**, posterior views. Dotted lines indicate missing bone, and hatched pattern indicates damaged bone. **Abbreviations**: **cprl**, centroprezygapophyseal lamina; **hypa**, hypantrum; **hypo**, hyposphene; **ppdl**, paradiapophyseal lamina; **prpl**, prezygapoparapophyseal lamina.

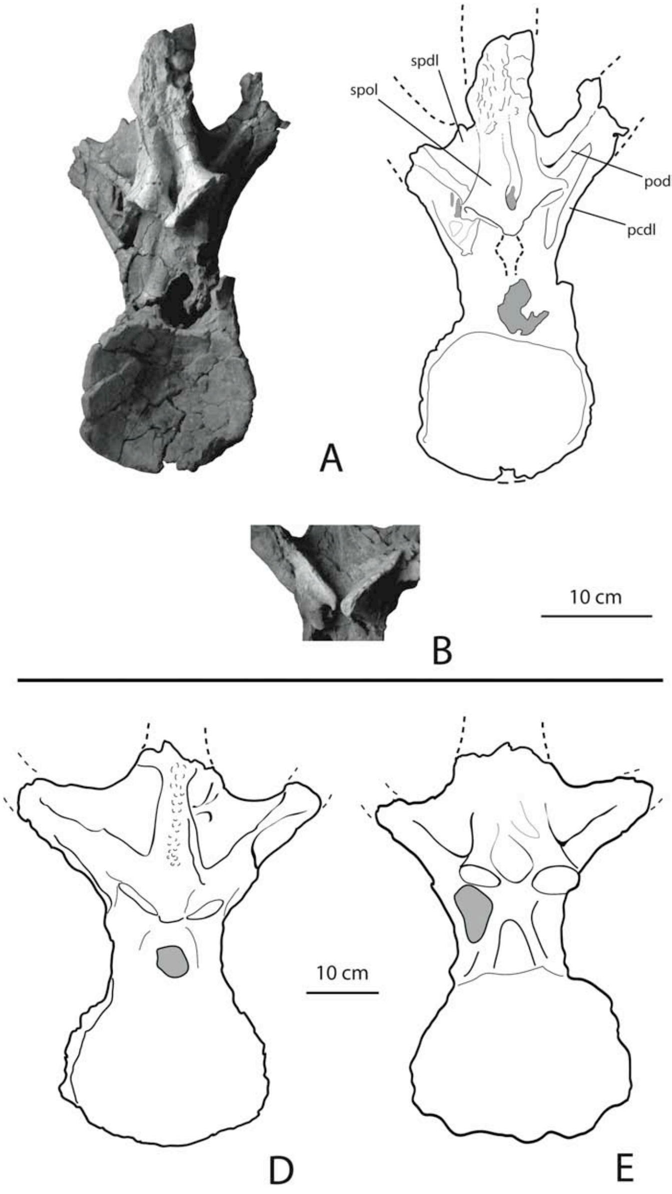

FIGURE 3.7. Posterior dorsal vertebra from the Cloverly (YPM 5449) and Twin Mountains (FWMSH 93B-10) Formations referred to *Sauroposeidon proteles*. Photograph and interpretive line drawing of a posterior dorsal vertebra of *Sauroposeidon* from the Cloverly Formation in **A**, posterior view; **B**, close-up of the same vertebra in anterior view, showing hyposphene. **C–D**, posterior dorsal vertebra of *Sauroposeidon* from the Twin Mountains Formation (formerly referred to ‘*Paluxysaurus*’ *jonesi*) in **C**, anterior, **D**, posterior view. Dotted lines indicate missing bone, and hatched pattern indicates damaged bone. Abbreviations as in Figure 3.4.

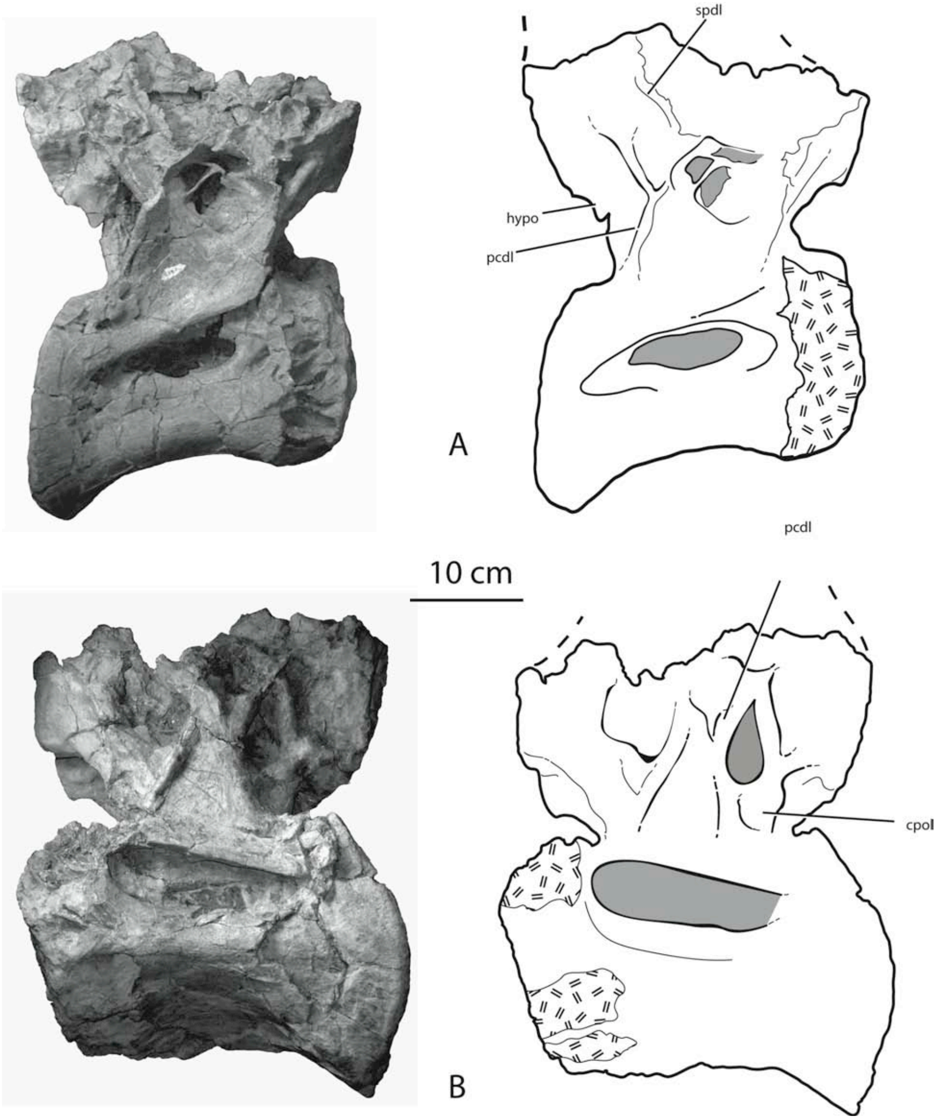

FIGURE 3.8. Posterior dorsal vertebra from the Cloverly Formation (YPM 5147) referred to *Sauroposeidon proteles*. Photographs and interpretive line drawings in **A**, right lateral; and **B**, left lateral views. Dotted lines indicate missing bone, and hatched pattern indicates damaged bone. Abbreviations as in Figure 3.4.

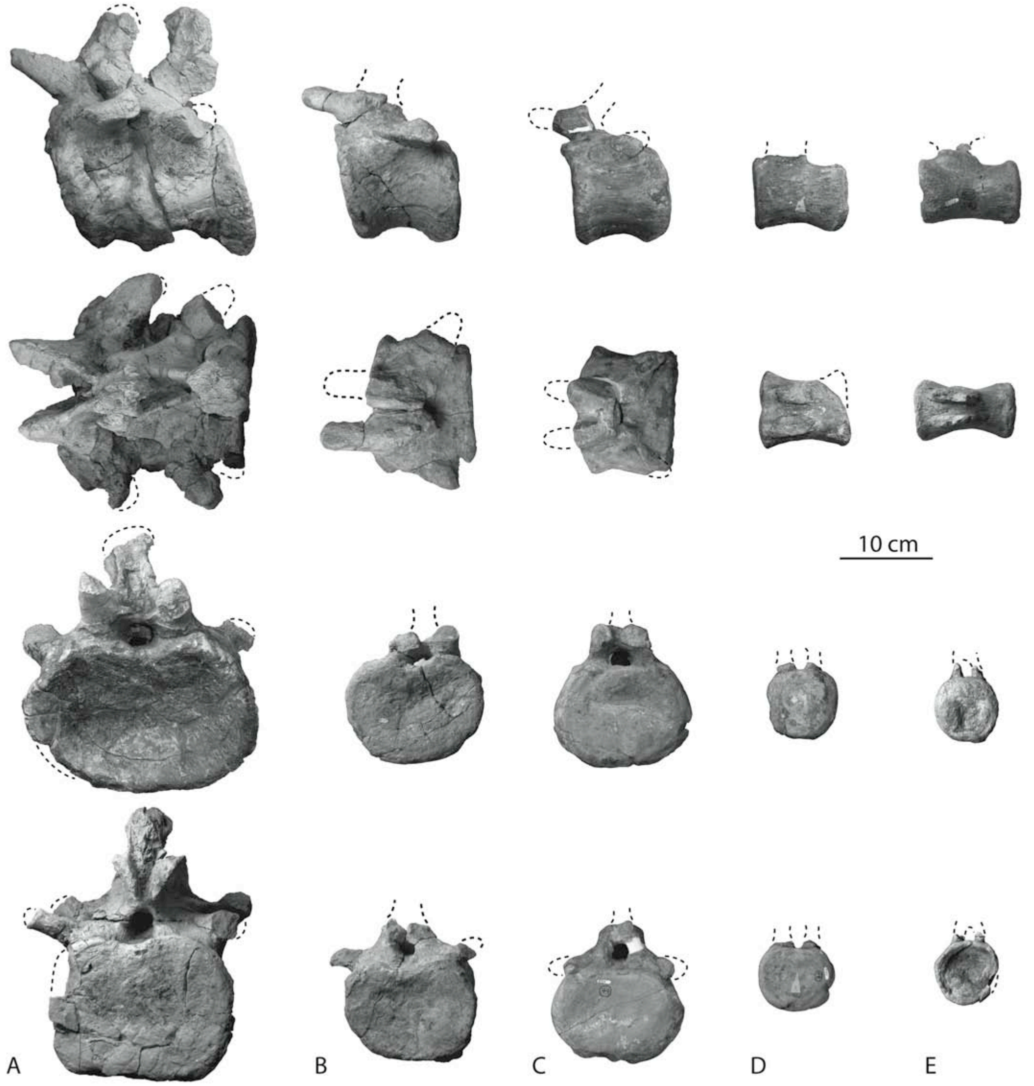

FIGURE 3.9. Caudal vertebrae from the Cloverly Formation referred to *Sauroposeidon proteles*. These vertebrae are arranged in anatomical order from anterior to posterior, but do not necessarily belong to one individual. **A**, YPM 5147, two co-ossified anterior caudal vertebrae; **B**, YPM 5199, middle caudal vertebra; **C**, YPM 5104, middle caudal vertebra; **D**, YPM 5103, distal caudal vertebra; **E**, YPM 5152, distal caudal vertebra. Vertebrae are depicted by row in left lateral (top), dorsal (second row), anterior (third row), and posterior (bottom row) views. The lateral views of YPM 5147, 5104, and 5103 are reversed. Dashed lines indicate missing bone. **Abbreviations**: **fo**, fossa.

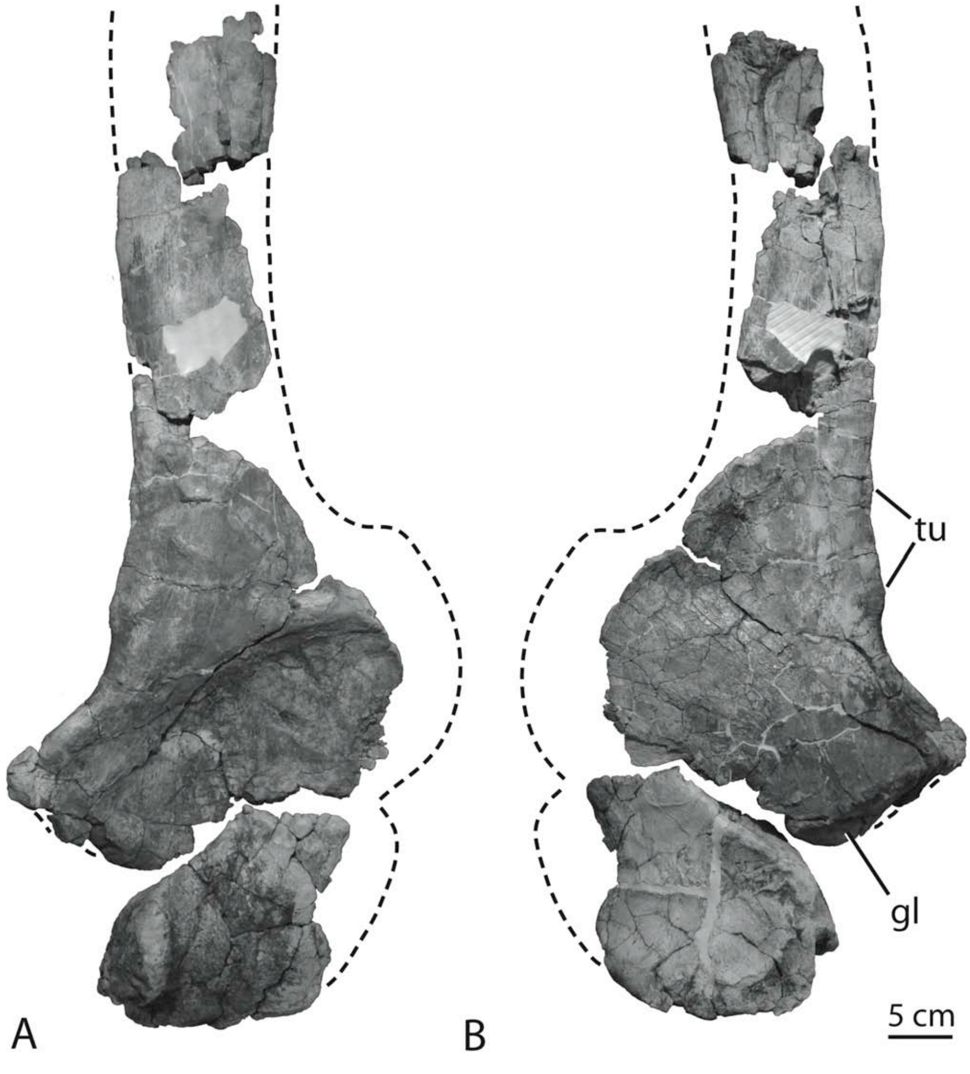

FIGURE 3.10. Scapula and coracoid (UM 20800) from the Cloverly Formation referred to *Sauroposeidon proteles* in A, medial and B, lateral views. Dashed lines indicate missing bone. **Abbreviations**: **gl,** glenoid**; tu**, tubercle.

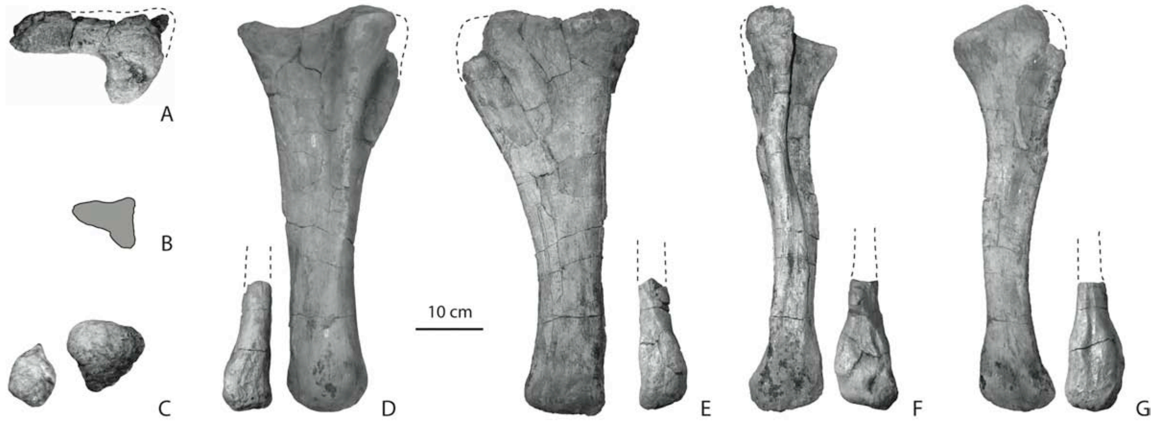

FIGURE 3.11. Left radius and ulna (YPM 5449) from the Cloverly Formation referred to *Sauroposeidon proteles* in **A**, proximal; **B**, mid-shaft cross sectional; **C**, distal; **D**, lateral; **E**, medial; **F**, anterior, and **G**, posterior views. Dashed lines indicate missing bone.

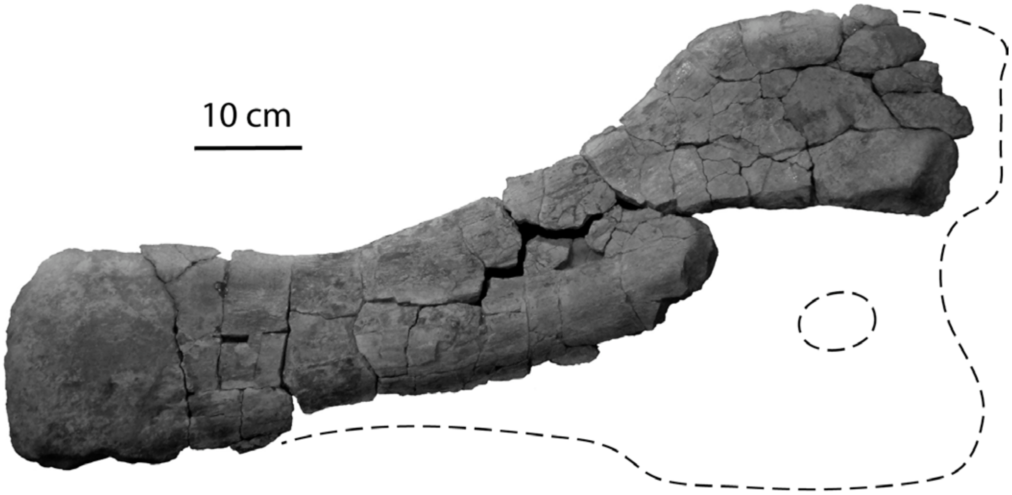

FIGURE 3.12. Left pubis (YPM 5449) from the Cloverly Formation referred to *Sauroposeidon proteles* in anterior view. Dashed lines indicate missing bone.

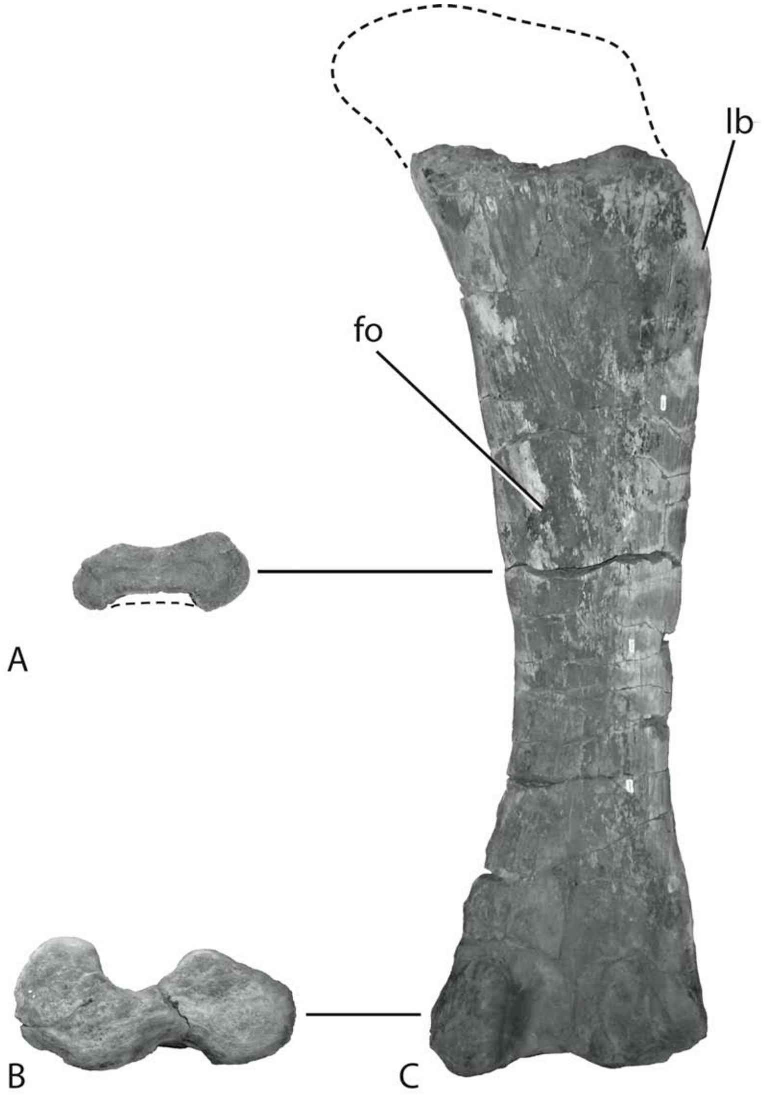

FIGURE 3.13. Right femur (YPM 5451) from the Cloverly Formation, possibly referable to *Sauroposeidon proteles* in **A**, midshaft cross-sectional, **B**, distal, and **C**, posterior views. Dashed lines indicate missing bone. **Abbreviations**: **fo**, fourth trochanter; **lb**, lateral bulge.

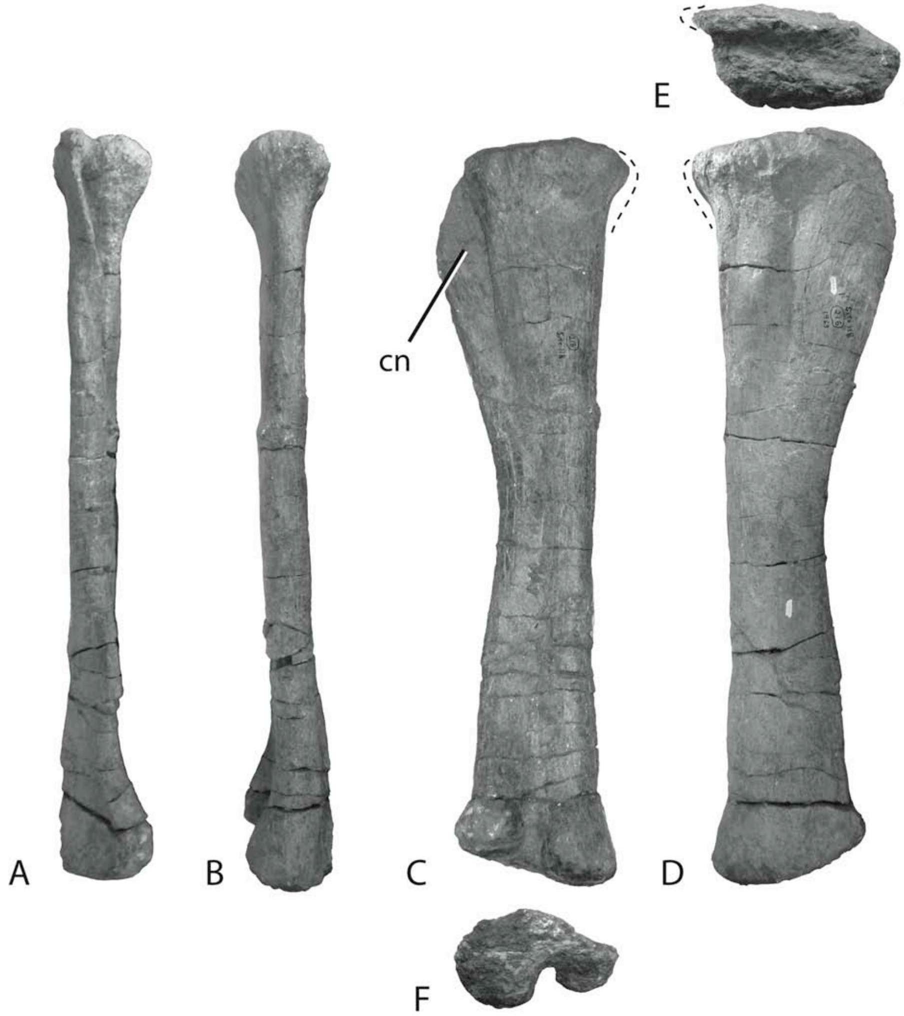

FIGURE 3.14. Left tibia (YPM 5450) from the Cloverly Formation, possibly referable to *Sauroposeidon proteles* in **A**, anterior, **B**, posterior, **C**, lateral, **D**, medial, **E**, proximal, and **F**, distal. Dashed lines indicate missing bone. The tibia has been crushed transversely, increasing its apparent eccentricity. **Abbreviations**: **cn**, cnemial crest.

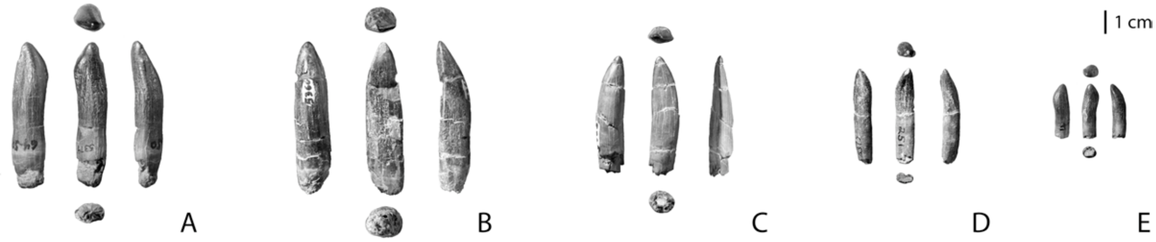

FIGURE 3.15. Teeth from the Cloverly Formation from the Cloverly Formation of Wyoming, USA. These teeth may pertain to *Sauroposeidon proteles*, but the absence of direct associations precludes definitive referral. Teeth are shown in labial (left), lingual (center), mesial or distal (right), occlusal (top) and basal (bottom) views. **A**, YPM 5374; **B**, YPM 5360; **C**, YPM 5365; **D**, YPM 5375; **E**, YPM 5349.

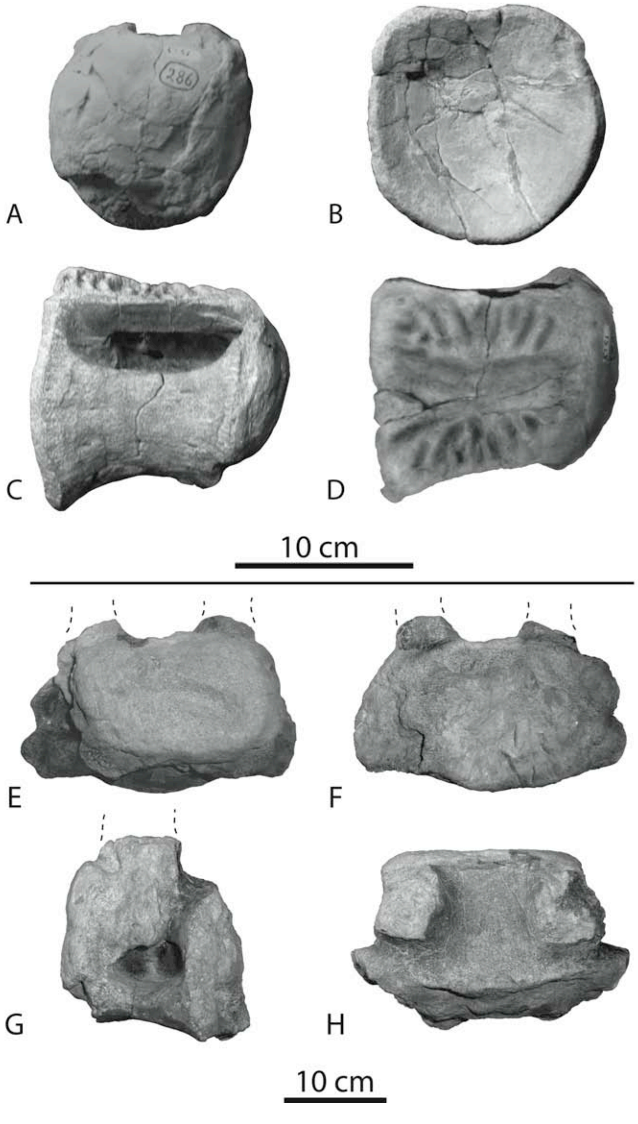

FIGURE 3.16. Juvenile dorsal and sacral vertebrae from the Cloverly Formation. **A**–**D**, middle-posterior dorsal vertebra (YPM 5151); **E**–**H**, sacral vertebra (YPM 5107). **A** and **E**, anterior view, **B** and **F**, posterior view, **C** and **G**, lateral view, **D** and **H**, dorsal view. Dashed lines indicate missing bone.

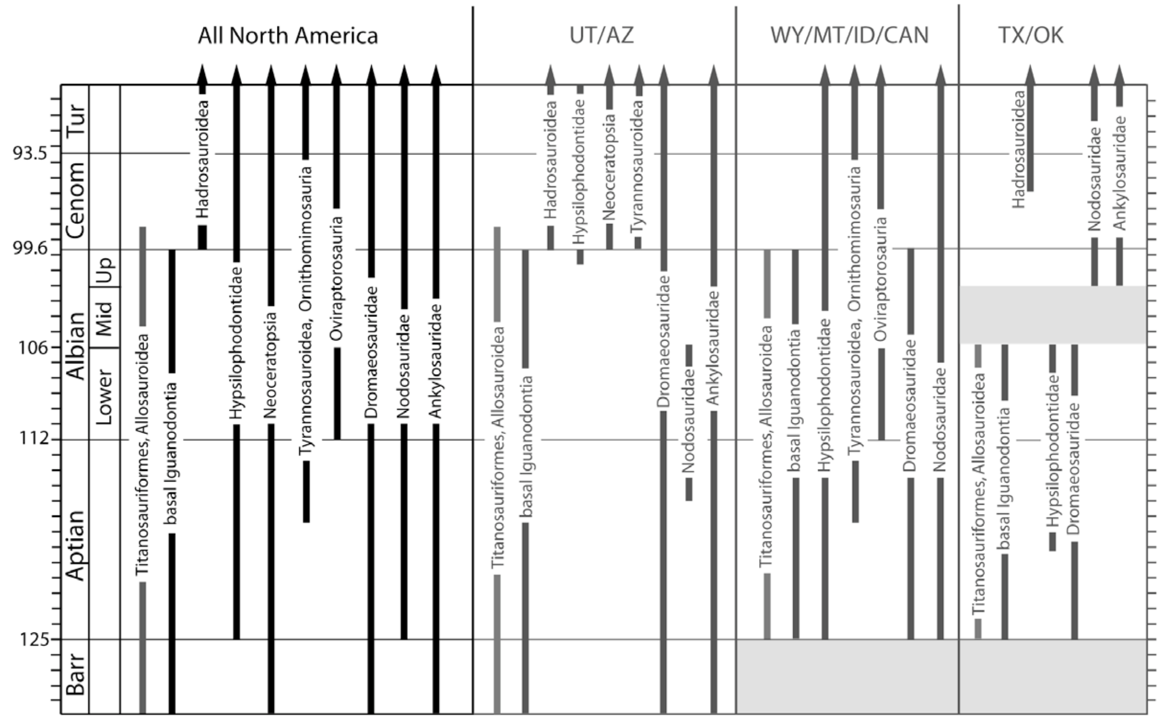

FIGURE 3.17. Stratigraphic distribution of dinosaurs in the Early Cretaceous of North America. Left column indicates the pattern for the entire continent; columns to the right indicate the patter per geographic area. Horizontal bars reflect both stratigraphic range and stratigraphic uncertainty – most groups are only known to the stage level. Note the persistence of all groups except sauropods and basal iguanodontians through the middle Cretaceous. **Abbreviations**: **AZ**, Arizona, **ID**, Idaho, **MT**, Montana, **OK**, Oklahoma, **UT**, Utah, **WY**, Wyoming.

CHAPTER 4

THE PHYLOGENETIC RELATIONSHIPS OF BASAL TITANOSAURIFORM SAUROPOD DINOSAURS

INTRODUCTION

Titanosauriformes is a large clade (ca. 90 named genera) of sauropod dinosaurs whose members are present and common in most Mesozoic ecosystems. The smallest, largest, geologically youngest, and most geographically-widespread sauropods are titanosauriforms. Some genera are well known from complete skeletons and ontogenetic series (Janensch, 1950; Curry Rogers, 2005), but most named species are poorly known. In particular, skulls are exceedingly rare in Titanosauriformes, though recent discoveries have begun to remedy this problem (Curry Rogers, 2005; Chure et al., 2010). Despite the patchy nature of much of their fossil record, several evolutionary patterns are apparent in titanosauriform evolution, including a trend towards decreasing tooth size (Chure et al., 2010), development of a ‘wide gauge’ gait and concomitant appendicular specializations (Wilson and Carrano, 1999), and several episodes of dwarfing (Sander et al., 2006; Stein et al., 2010). More derived titanosauriforms — lithostrotian titanosaurs — are characterized by a number of apomorphies that might seem counterintuitive for giant animals, including non-ossification of the carpus and manual phalanges (Curry Rogers, 2005), increased skeletal pneumaticity (Wedel et al., 2000b), and the development of osteoderms (D'Emic et al., 2009).

The number of named titanosauriforms has dramatically increased in recent years (Fig. 1), as has the number of taxonomic revisions adding information to previously named genera (e.g., Wilson and Upchurch, 2003; Wilson et al., 2009; Mannion, 2010; D'Emic and Wilson, 2011; Carballido et al., 2011; Carballido et al., in press; Mannion and Calvo, in press). The bulk of new discoveries have come from Asia and South America, but several North American, African, and Australian forms have come to light as well (see lists in Mannion, 2010; Mannion and Calvo, in press).

Titanosauriforms are important to Mesozoic paleobiogeography because of their diversity and near-ubiquity, but their impact on paleobiogeography has not been fully realized owing to confusion over their phylogenetic relationships (e.g., Krause et al., 2006). For example, the absence of sauropod fossils in North America for most of the Late Cretaceous followed by the appearance of sauropods just before the close of the Mesozoic has been interpreted as a regional extinction followed by dispersal (Lucas and Hunt, 1989; D'Emic et al., 2010; see Chapter 3), or a bias in the record (Mannion and Upchurch, 2011).

Resolving which of these scenarios is responsible for the ‘sauropod hiatus’ depends on the phylogenetic relationships of the taxa bounding the hiatus. Another salient paleobiogeographic problem for Titanosauriformes is that of East Asian endemism, which has been suggested for sauropods during various time periods, from the Middle Jurassic to the Cretaceous (Wilson and Upchurch, 2009). Recently, all Cretaceous East Asian sauropods have been recognized as titanosauriforms, in contrast to an array of non-neosauropods that characterized the Jurassic (Wilson, 2005). Resolving the role of endemism and the details of this faunal turnover for the sauropods of East Asia also depends on their lower-level phylogenetic relationships.

Titanosauriformes and its subclades are stable because they are defined by phylogenetic nomenclature (e.g., the sister-clades Brachiosauridae and Somphospondyli; Table 4.1), but the content of and interrelationships within these clades vary substantially depending on the analysis. These analyses in turn are sensitive to taxon inclusion, and with the inclusion of characters outpaced by the inclusion of taxa, few topologies are repeatably recovered between analyses (e.g., Royo Torres, 2009).

In the following contribution, I review previous cladistic analyses focusing on basal titanosauriforms in order to identify areas of agreement and conflict. I then present a lower-level cladistic analysis of 25 ingroup taxa using a combination of previously formulated (ca. 2/3) and novel (ca. 1/3) characters. I then explore the phylogenetic affinities of taxa represented by fragmentary specimens and comment on the paleobiogeographic patterns revealed, with a focus on the origins of Titanosauria.

INSTITUTIONAL ABBREVIATIONS

Institutions: FMNH PR, Field Museum of Natural History, Chicago; HMN MB.R, Humboldt Museum für Naturkunde, Berlin, Germany; MACN PV, Museo Argentino de Ciencias Naturales, Buenos Aires; MCF PVPH, Museo Cármen Funes, Paleontología de Vertebrados, Plaza Huincul; NHMUK, British Museum of Natural History, London; YPM, Yale Peabody Museum, New Haven.

Abbreviations for vertebral laminae and fossae follow Wilson (1999) and Wilson et al. (2011), respectively. Anatomical nomenclature is 'Romerian,' following that traditionally applied to reptiles (Wilson, 2006).

PREVIOUS CLADISTIC ANALYSES

'Basal' (non-titanosaur) titanosauriforms have been included in a number of cladistic analyses, including those investigating global sauropod relationships (e.g., Wilson, 2002; Upchurch et al., 2004) and those specifically aimed at resolving the relationships of newly described basal titanosauriforms (e.g., Rose, 2007; Canudo, Royo-Torres & Cuenca-Bescós, 2008). The latter types of analyses employ largely unmodified versions of the data matrices of the two global phylogenetic analyses mentioned above, so their taxonomic and character scope (sensu Sereno, 2009) have been somewhat homogenous. One advantage of these analyses having a similar taxonomic scope and outgroup choice is that their results are more comparable than they would be otherwise. However, the addition of new taxa to analyses has outpaced the addition of characters and thus outpaced discovery of stable (i.e., repeatably-recovered) synapomorphies (Whitlock, D'Emic & WIlson, 2011). Many of the analyses aimed at resolving basal titanosauriform relationships have included a substantial number of characters that were parsimony-uninformative (Table 4.2), or informative only to the relationships of non-titanosauriforms such as diplodocoids. This dilution of the available synapomorphy pool developed for global sauropod analyses (Wilson, 2002; Upchurch et al., 2004) results in reduced phylogenetic resolution and robustness relative to the original global analyses (Whitlock et al., 2011).

Of the many cladistic analyses that have included investigation of early titanosauriform relationships in their scope, six have contributed the bulk of new characters and taxon data (Fig. 2). These analyses show coarse agreement in the phylogenetic relationships of basal titanosauriforms (Fig. 2). Between two and six genera have been resolved as non-titanosaur titanosauriforms in previous analyses (Table 4.2). Brachiosaurids and titanosaurs are always united to the exclusion of *Camarasaurus*, and these three taxa are always united to the exclusion of Diplodocoidea. When included, *Chubutisaurus* and *Ligabuesaurus* are recovered as non-titanosaur somphospondylans (e.g., Royo-Torres, 2009; González Riga Previtera & Pirrone, 2009; Carballido et al., 2011). *Phuwiangosaurus* occupies a variety of positions in these analyses, including a non-titanosaur somphospondylan (Upchurch et al., 2004 rescored by Wilson & Upchurch, 2009; González Riga et al., 2009), a brachiosaurid (Royo-Torres, 2009), and a titanosaur (Carballido et al., 2011). Brachiosauridae is usually only composed of *Brachiosaurus* (including scorings for the now generically separate *Giraffatitan*; Taylor, 2009), but some analyses recover other genera (e.g., *Cedarosaurus*, '*Pleurocoelus*') within the clade as well. Figure 3 shows a strict consensus of simplified versions of the trees (those taxa present in more than half of the six analyses) depicted in Figure 2. This consensus cladogram fails to recover many commonly-recovered sauropod clades as monophyletic, including Titanosauriformes, Macronaria, and Brachiosauridae. The base of Titanosauria is likewise unresolved, as a polytomy between *Andesaurus*, *Ligabuesaurus*, and *Chubutisaurus*. Removing *Euhelopus* from the trees yields a better-resolved cladogram more consistent with previous studies (e.g., Wilson, 2002; Upchurch et al., 2004). In this cladogram, *Tastavinsaurus* is recovered as the sister-taxon to Titanosauriformes, in contrast to its original description as a titanosauriform (Canudo et al., 2008). *Malawisaurus* is consistently recovered as a titanosaur intermediate in position between *Andesaurus* and more derived forms.

Many authors have published more than one iteration of a given matrix, usually varying the taxonomic content to accommodate new discoveries, with changes to characters and/or scoring in some cases (e.g., Calvo & González Riga, 2003; Calvo, González Riga & Porfiri, 2008; González Riga et al., 2009). Each of these sets of analyses will be discussed together, with focus on the most recent analysis of each set that contributed substantial modification to the data matrix. For more detailed comments on previous iterations of the matrices discussed here (e.g., Upchurch, 1995, 1998; Wilson and Sereno, 1998), see Wilson (2002).

Salgado, Coria & Calvo, 1997

The results of Salgado et al. (1997) allied *Camarasaurus*, brachiosaurids, and titanosaurs to the exclusion of diplodocoids (Fig. 4.2). Salgado et al. (1997) coined the node-based clades Titanosauriformes and Camarasauromorpha, and provided a phylogenetic definition for Titanosauria and several included clades. Their analysis included a detailed description of synapomorphies that have been inherited by more recent analyses. Consequently, the analysis of Salgado et al. (1997) served as a higher-level 'backbone' of character data, topology, and phylogenetic nomenclature that has been modified for studies of lower-level titanosauriform affinities. Several synapomorphies were cited as support for each node of Salgado et al. (1997), but decay indices (Bremer, 1994) were not reported. Re-analysis of the matrix of Salgado et al. (1997) produces decay indices of 2 and 3 for Titanosauria and Titanosauriformes, respectively; all other decay indices were equal to 1.

Salgado et al. (1997) included three non-titanosaur titanosauriforms: *Giraffatitan/Brachiosaurus* and *Chubutisaurus*. They recovered *Giraffatitan* and *Andesaurus* as the most basal titanosauriform and titanosaur, respectively, with *Chubutisaurus* as the sister taxon to Titanosauria. They recovered a monophyletic “Titanosauridae” (equivalent to Lithostrotia of Upchurch et al. 2004) and Saltasaurinae, as in most subsequent titanosauriform cladistic analyses.

Wilson, 2002 (Wilson & Upchurch, 2009)

The analysis of Wilson (2002) aimed to study the lower-level relationships of representatives of all major sauropod clades, including basal forms, diplodocoids, and titanosaurs and their relatives (Fig. 2). Wilson (2002) included two non-titanosauriform titanosaurs in his analysis: *Brachiosaurus* (including *Giraffatitan*) and *Euhelopus*, which were recovered as successive sister taxa to Titanosauria, following Wilson & Sereno (1998). Wilson & Sereno (1998) named Somphospondyli, a stem-based node uniting titanosauriforms more closely related to *Saltasaurus* than to *Brachiosaurus* (i.e., non-brachiosaurid titanosauriforms). Wilson & Upchurch (2009) recommended modification for some of the scores for *Euhelopus* in the Wilson (2002) matrix. These alterations do not alter the topology found by Wilson (2002), but do weaken support for the node uniting *Euhelopus* + Titanosauria (Fig. 2). Most of the other titanosauriform nodes in this modified analysis of Wilson (2002) are robustly supported (Fig. 2).

The relationships of most taxa included in both Wilson (2002) and Salgado et al. (1997) are identical. Wilson (2002) did not include *Andesaurus* in his analysis, but like Salgado et al. (1997), recovered *Malawisaurus* in a basal position relative to other titanosaurs.

Upchurch et al., 2004 (Wilson & Upchurch, 2009)

Upchurch et al. (2004) presented an expanded and updated version of the matrices presented in Upchurch (1995, 1998). Like Wilson (2002), the scope of analysis in Upchurch et al. (2004) was broad (Sauropoda). That analysis included a variety of taxa regarded as non-titanosaur titanosauriforms by most authors (e.g., *Euhelopus*, *Phuwiangosaurus*; González Riga et al., 2009, Suteethorn et al., 2010), but only two were recovered as such in Upchurch et al. (2004): *Brachiosaurus* (including *Giraffatitan*) and *Cedarosaurus* (Fig. 2). Because *Andesaurus* was absent from the analysis of Upchurch et al. (2004) and is one of the specifiers for the definition of Titanosauria (Wilson and Upchurch, 2003), the labeling of Titanosauria by Upchurch et al. (2004) at any node between Titanosauriformes and Lithostrotia was arbitrary. Consequently, the titanosaur membership of *Phuwiangosaurus* posited by Upchurch et al. (2004) was ambiguous according to their results.

As in previous analyses (e.g., Salgado et al., 1997), *Brachiosaurus* was found to be more closely related to titanosaurs than *Camarasaurus* in the analysis of Upchurch et al. (2004). Upchurch et al. (2004) presented the first cladistic support for Brachiosauridae, uniting the Early Cretaceous North

American *Cedarosaurus* with *Brachiosaurus* (including *Giraffatitan*). The purported *Brachiosaurus*-like Middle Jurassic sauropod *Atlasaurus* (Allain et al., 1999) was found to be a non-titanosauriform neosauropod closely allied with the contemporaneous *Jobaria* (Sereno et al., 1999). *Tehuelchesaurus* was found to be a non-neosauropod closely related to *Omeisaurus* following the original description of the former taxon (Rich et al., 1999).

The scorings for *Euhelopus* in the Upchurch et al. (2004) matrix were modified by Wilson and Upchurch (2009), with substantial consequences for the phylogenetic position of several taxa. *Euhelopus* was recovered as the sister taxon of Titanosauria in agreement with Wilson & Sereno (1998) and Wilson (2002). The sister-taxon relationship between *Brachiosaurus* and *Cedarosaurus* was unchanged, but the *Atlasaurus*–*Jobaria* clade moved outside of Neosauropoda. *Tehuelchesaurus* was deleted from the revised matrix of Upchurch et al. (2004) presented in Wilson & Upchurch (2009). Upchurch et al. (2004) recovered similar interrelationships as other analyses (e.g., Salgado et al., 1997) for titanosaurs, including a basal position for *Malawisaurus*.

Royo-Torres, 2009

Royo-Torres (2009) described a sauropod from the Early Cretaceous of Spain, *Tastavinsaurus sanzi*, and investigated its phylogenetic affinities with a matrix containing a broad sample of basal titanosauriforms and 65 new characters. This influx of novel taxon and character data resulted in substantial differences between the results of Royo-Torres (2009) and previous analyses, despite the fact that over one-quarter of the included characters (104/399) were parsimony uninformative. The topologies recovered by Royo-Torres (2009) are highly sensitive to taxon inclusion (compare Royo-Torres 2009: fig. 4.208, 4.209 and 4.212), and few steps are needed to collapse any given node. Royo-Torres (2009) included fifteen taxa traditionally regarded as non-titanosaur titanosauriforms in two separate analyses. The first analysis only included characters for anatomical regions preserved in *Tastavinsaurus*; the second contained characters sampled from the entire skeleton. The discussion below will focus on the latter, more comprehensive analysis. The data matrix (25 ingroup taxa, 399 characters) was re-run in PAUP*, which produced 5 most parsimonious trees of treelength 752, identical to the results of Royo-Torres (2009). Royo-Torres (2009) did not present a strict consensus of these trees. I computed a strict consensus computed in PAUP*, which yielded a large polytomy at the base of Titanosauriformes (Fig. 2). Royo-Torres (2009: fig. 4.212) presented a 50% majority consensus of his 5 most parsimonious trees, which included a novel clade for which he coined the name Laurasiformes. Laurasiformes was defined as a stem-based taxon containing taxa more closely related to *Tastavinsaurus* than *Saltasaurus*. The existence of Laurasiformes is highly sensitive to taxon and character inclusion — the clade is absent from the strict consensus of the tree built from 25 taxa, but is present when 28 taxa are included and many characters are excluded (Royo-Torres, 2009: fig. 4.209).

Several non-traditional relationships are hypothesized according to the strict consensus of the results of Royo-Torres (2009) that I computed in PAUP*. Most of these novel hypotheses are also present in the 50% majority rule tree computed by Royo-Torres (2009: fig. 4.212), including *Euhelopus* as the outgroup to Neosauropoda, *Tangvayosaurus* as the sister taxon of Titanosauriformes, and a close relationship between *Phuwiangosaurus* and *Brachiosaurus*. "*Pleurocoelus*" from Texas was recovered just outside of Titanosauria. The scorings for "*Pleurocoelus*" from Texas in the matrix of Royo-Torres (2009: table 4.97), include material from several specimens (i.e., dorsal and caudal vertebrae (SMU 61732), pes (FMNH PR 977)). As shown in Chapter 2, these specimens pertain to more than one species, making this operational taxonomic unit a chimera in the matrix of Royo-Torres (2009). Finally, *Andesaurus* and *Malawisaurus* are recovered as the basalmost titanosaurs in the analysis of Royo-Torres (2009).

Canudo et al. (2008) presented a restricted version of the same matrix used by Royo-Torres (2009), and obtained a different set of relationships for the Laurasiformes than any recovered by Royo-Torres (2009). Specifically, only *Venenosaurus* and *Tastavinsaurus* were members of Laurasiformes, and *Phuwiangosaurus* was not recovered as a brachiosaurid, but in a clade with *Andesaurus* and *Cedarosaurus*. One most parsimonious tree was reported by Canudo et al. (2008), but the polytomies those authors depict implies that the number of most parsimonious trees equal to at least nine. The decay indices reported by Canudo et al. (2008) are implausibly high given the data at hand (e.g., 24 for Titanosauriformes). In sum, Canudo et al. (2008) and Royo Torres (2009) presented many novel characters, yet these analyses do not result in a stable set of relationships for basal titanosauriforms. Likewise, there are problems with several of the characters in the analyses of Canudo et al. (2008) and Royo-Torres (2009), which will be discussed below (see “Characters”). The evidence for Laurasiformes is weak, and will be tested below (see “Laurasiformes” below).

González Riga et al., 2009

González Riga et al. (2009), in their description of the mid-Cretaceous Argentine taxon *Malarguesaurus florenciae*, presented a phylogenetic analysis of Titanosauriformes focusing on titanosaurs (Fig. 2). This matrix represents the latest iteration of the matrix used by González Riga and Calvo (2003), González Riga (2003), Bonaparte et al. (2006), and Calvo et al. (2007, 2008). In turn, the original matrix of Calvo and González Riga (2003) is largely based on characters culled from the previous analyses (Wilson, 2002; Upchurch et al., 2004). As such, they largely agree with the results of those cladistic analyses of Titanosauriformes, always recovering a traditional Titanosauriformes and Titanosauria, as well as positioning *Euhelopus* as the most basal somphospondyl and *Andesaurus* and *Malawisaurus* as basal titanosaurs. Several taxa not generally included in other analyses have been included in the González Riga et al. (2009) family of analyses (e.g., *Ligabuesaurus*). In these analyses, *Ligabuesaurus*, *Phuwiangosaurus*, and *Chubutisaurus* are positioned as somphospondyls outside of Titanosauria.

The results presented by González Riga et al. (2009) (2 most parsimonious trees of 199 steps) could not be reproduced when their data matrix was re-run in PAUP*. Instead, 94 most parsimonious trees were recovered of treelength 206. The reasons for this discrepancy are unknown, as the analysis was repeated with the same parameters. Eighteen of the 102 characters presented by González Riga (2009) were parsimony uninformative. A strict consensus of these trees yielded a large polytomy among *Phuwianogsaurus*, *Ligabuesaurus*, *Malarguesaurus*, *Andesaurus*, and Lithostrotia, as well as a polytomy among the node uniting those taxa, *Euhelopus*, and *Chubutisaurus*. A 50% majority rule of these trees was identical to the results of González Riga et al. (2009), except *Ligabuesaurus*, *Phuwiangosaurus*, and *Malarguesaurus* formed a polytomy. The reasons for these discrepancies are unknown.

Chure et al., 2010

Chure et al., 2010 described abundant cranial material of the Early Cretaceous North American sauropod *Abydosaurus mcintoshi* and conducted a phylogenetic analysis in which they recovered *Abydosaurus* as the sister taxon of *Brachiosaurus* (Fig. 2) (note that scorings for *Brachiosaurus altithorax* included data from *Giraffatitan brancai* in Chure et al. (2010)). The matrix was a parsed version of Wilson (2002), tailored to analyzing the phylogenetic position of *Abydosaurus* with addition and deletion of characters as necessary. Apart from the addition of *Abydosaurus*, the only other topological difference between the results of Wilson (2002) and Chure et al. (2010) is that the latter could not resolve the position of *Jobaria*, *Haplocanthosaurus*, and Diplodocoidea with respect to Neosauropoda. The decay index of Brachiosauridae is 3, whereas those for Titanosauriformes, Somphospondyli, and Lithostrotia (*Malawisaurus* + more derived forms) are 5, 4, and 5, respectively.

Carballido et al., 2011; in press

Carballido et al. (2011; in press) conducted the most taxonomically comprehensive analysis of basal titanosauriform interrelationships to date, including a substantial number of taxa included in cladistic analysis for the first time (Fig. 2). The specific aims of these analyses were to resolve the relationships of *Chubutisaurus* and *Teuhelchesaurus*.

Carballido et al. (2011) recovered a Laurasiformes that included *Tastavinsaurus*, *Venenosaurus*, *Techuelchesaurus*, and *Galvesaurus*. This result is similar to that recovered by Royo Torres (2009), who originally named Laurasiformes. In contrast, Carballido et al. (in press) only included *Janenschia* and *Tastavinsaurus* within the Laurasiformes.

Carballido et al. (2011) recovered *Euhelopus*, *Brachiosaurus* (including *Giraffatitan*), and ‘*Paluxysaurus’* (now referred to *Sauroposeidon*, see chapter 3) in a polytomy. Some taxa that were recovered outside Titanosauria (*Phuwiangosaurus*, *Malarguesaurus*) in previous analyses were recovered within it by Carballido et al. (2011). Finally, Carballido et al. (2011, in press) resolved the Late Jurassic island dwarf *Europasaurus* as a basal macronarian, in keeping with its original description (Sander et al., 2006). Support for nearly all nodes was low (decay index = 1) in the analyses of Carballido et al. (2011; in press), and results were highly influenced by taxon inclusion.

Re-running the character matrix of Carballido et al. (2011) in PAUP* showed that of the 289 characters presented by Carballido et al. (2011), 79% (227) were parsimony-informative. When the dataset of Carballido et al. (2011) was re-run in PAUP*, three unambiguous laurasiform synapomorphies were recovered. All three laurasiform synapomorphies that were recovered (characters 101, 158, 173) have a homoplastic distribution among basal titanosauriforms, and all three are mis-scored in some way. For example, a ‘supraneural camera’ (character 101) (centroprezygapophyseal fossa; Wilson et al., 2011) was scored as absent in *Brachiosaurus* and was left unscored in *Europasaurus*, but both these taxa have such fossae. Likewise, Laurasiformes was recovered with a specialized ‘platycoelous/distoplatyan’ anterior caudal vertebral centrum articulation (character 158), but anterior caudal vertebral centra with slightly concave anterior faces and concave-to-flat posterior faces are common among non-titanosaurs, including *Brachiosaurus*, *Sauroposeidon*, *Camarasaurus*, and *Haplocanthosaurus*, all of which were incorrectly scored as having different articulations than Laurasiformes. The same criticism applies to the final Laurasiform synapomorphy (character 173), ‘middle caudal vertebral neural spines vertical‘ — this feature characterizes *Camarasaurus*, *Haplocanthosaurus*, *Brachiosaurus*, and *Giraffatitan* as well as Laurasiformes, though it was scored differently for those taxa. Changing these scorings in the matrix of Carballido et al. (2011) and running it in PAUP* could not replicate results obtained with the original scorings. No result was obtained because of limitations in computing power. However, based on these scoring changes, there does not seem to be support for Laurasiformes in the corrected dataset of Carballido et al. (2011).

ANALYSIS OF LOWER-LEVEL RELATIONSHIPS OF BASAL TITANOSAURIFORM SAUROPODS

Below I present a lower-level cladistic analysis focusing on the relationships of basal titanosauriforms. I outline the operational taxonomic units employed, present the results and robustness of the analysis, and discuss its implications. See appendices for the character-taxon matrix (Appendix 1), character list (Appendix 2), synapomorphy list (Appendix 3), and autapomorphy list (Appendix 4).

OUTGROUP CHOICE

Character polarity was determined on the basis of outgroup comparison. Some ingroup taxa (e.g., Diplodocoidea, *Camarasaurus*) are universally regarded as non-titanosauriforms (e.g., Wilson, 2002; Upchurch et al., 2004), but were included in the ingroup so as to not assume the titanosauriform affinities of other ingroup taxa a priori. Two taxa were selected as outgroups: *Omeisaurus* (including *O. tianfuensis* He et al., 1988 and *O. maoianus* Tang et al., 2001) and *Jobaria tiguidensis* (Sereno et al., 1999). These taxa were selected for their completeness and because they have been recovered as non-neosauropod eusauropods by nearly all authors (Sereno et al., 1999; Wilson, 2002; Upchurch et al., 2004 when scores were corrected per Wilson & Upchurch, 2009). Scoring for *Omeisaurus* was based on He et al. (1984) and Tang et al. (2001), and scoring for *Jobaria* was based on personal observation and Sereno et al. (1999). Jobaria was originally thought to be Early Cretaceous in age (Sereno et al., 1999), but may older, perhaps Middle Jurassic (Rauhut & López-Arbarello, 2009). *Omeisaurus* is Middle Jurassic in age (Tang et al., 2001), predating any of the taxa in the ingroup with the exception of *Atlasaurus imelaki* (Allain et al., 1999).

TERMINAL TAXA

Twenty-five terminal taxa were selected for phylogenetic analysis (Table 4.3). These taxa were selected in an effort to sample the spatiotemporal distribution (Middle Jurassic–Late Cretaceous) and morphologies of possible basal titanosauriforms. Several taxa were not included in the analysis because their validity could not be evaluated or substantiated (see “Relationships of Fragmentarily Represented Taxa” below). Fragmentarily represented taxa were not excluded a priori because anatomical completeness does not necessarily equal phylogenetic informativeness (Kearney, 2002).

This analysis does not aim to resolve the relationships of all titanosauriforms, only the basal (non-titanosaur) ones. Consequently, taxonomic sampling of derived titanosaurs (i.e., lithostrotians) was limited to well-preserved taxa that are representative of several previously recovered ‘grades’ of titanosaurs. These representatives include purported basal titanosaurs (*Andesaurus*, *Phuwiangosaurus, Venenosaurus, Tangvayosaurus*) and one of the specifiers of Lithostrotia (*Malawisaurus*; Upchurch et al., 2004). *Alamosaurus* was included in order to test hypotheses surrounding the ‘sauropod hiatus’ (see Chapter 3).

All taxa were scored on the basis of personal observation and original descriptions, with the exception of *Qiaowanlong*, *Daxiatitan*, *Atlasaurus*, *Omeisaurus*, *Euhelopus*, and *Tastavinsaurus*. These latter taxa were scored on the basis of published descriptions and monographs, supplemented with photographs from collegues (see Acknowledgements). The monophyly of terminal taxa is justified with autapomorphies (see Appendix 4). Some terminal taxa require further discussion (see below) because their content and diagnosis differ from their original or traditional definition. Likewise, two ingroup taxa are composites of several sauropod genera (Diplodocoidea and ‘saltasaurini’) and one ingroup taxon contains several species (*Camarasaurus*); justification for these higher-level groupings is provided below.

Alamosaurus sanjuanensis

Alamosaurus sanjuanensis was named on the basis of a holotypic scapula and paratypic ischium from the Maastrichtian Kirtland Formation of New Mexico, USA (Gilmore, 1922). Referred remains from Utah (Gilmore, 1946) and Texas (Lehman and Coulson, 2002) are substantiated by autapomorphies among the exemplars (D’Emic et al., in press) and were included in scoring for *Alamosaurus*. Teeth (Kues, Lehman & Rigby, 1980) and an isolated pes (D’Emic et al., in press) from the holotypic area and horizon were also included in the scoring for *Alamosaurus*.

Brachiosaurus altithorax and Giraffatitan brancai

Riggs (1903) coined the name *Brachiosaurus altithorax* for what was then the world’s largest-known dinosaur. *Brachiosaurus altithorax* was founded on a single partial skeleton, from the Late Jurassic Morrison Formation of Colorado, USA, represented by several dorsal vertebrae, a sacrum with ilia, two caudal vertebrae, a coracoid, humerus, and femur, and some dorsal ribs. Some other materials from the Morrison Formation may belong to *Brachiosaurus altithorax* (see review in Taylor, 2009), but most of these materials do not overlap anatomically with the holotype, and those materials that do overlap cannot currently be united with the holotype using autapomorphies. Consequently, scoring for *Brachiosaurus altithorax* is limited to the holotype.

Janensch (1914) named two additional species of *Brachiosaurus* from the Late Jurassic Tendaguru beds of Tanzania, *B. brancai* and *B. fraasi*, which were later synonymized by Janensch (1929). Paul (1988) proposed that the Tanzanian form be regarded as a separate subgenus, *Brachiosaurus* (*Giraffatitan*) *brancai*, which Taylor (2009) formalized by referring the Tanzanian brachiosaur material to a separate genus, *Giraffatitan brancai*. Many of the differences cited by Taylor (2009) do not differ substantially between the Morrison and Tendaguru specimens when serial and individual variation is taken into account (e.g., caudal vertebral neural spine shape; compare Taylor (2009: fig. 3), with Ikejiri et al. (2005: fig. 5)). In addition, some of the differences cited in support of generic separation of the Morrison and Tendaguru brachiosaurids are erroneous due to misinterpretation of broken or deformed features (e.g., the cited tubercle on the posterior ilium of *B. altithorax* is a fragment of a sacral rib; the cited block-like hyposphene of the caudal vertebrae of *B. altithorax* is the broken remainder of the postzygapophyses; pers. obs.), or have a wider distribution among sauropods (e.g., the laterally deflected coracoid glenoid; see Wilson & Sereno 1998).

However, several features suggested by previous authors (Janensch 1950;

Paul 1988; Taylor 2009) do distinguish the Tendaguru and Morrison brachiosaurid exemplars in a substantive way. The following features do not vary within other sauropod genera when deformation, breakage, within-individual, ad within-species sources of variation are accounted for: the centra of dorsal vertebrae are broader transversely than dorsoventrally in *G. brancai*, rather than subcircular in cross-section in *B. altithorax*; anterior caudal vertebrae are about 30% taller relative to centrum length in *B. altithorax*; transverse processes are only half of the neural spine length in the posterior dorsal vertebrae of *B. altithorax*, whereas they are subequal to neural spine length in *G. brancai* (Janensch 1950; Paul 1988; Taylor 2009). These three features justify the generic separation of *Giraffatitan* and *Brachiosaurus*. Consequently, the name *Giraffatitan brancai* will be used to refer to the hypodigm brachiosaur material from Tendaguru.

Camarasaurus

The genus *Camarasaurus* is known from dozens of skeletons found across the western United States (Ikeijiri, 2005). Four species of *Camarasaurus* are currently recognized: *C. grandis*, *C. lewisi*, *C. supremus*, and *C. lentus* (Upchurch et al., 2004). Perhaps owing to its broad spatial distribution and the presence of four species in the terminal taxon, some characters are polymorphic for *Camarasaurus* in this analysis. Where polymorphisms were present, the state present in the Gunma specimen (McIntosh et al., 1996) of *Camarasaurus* was favored, because it is found stratigraphically lower than most other specimens of *Camarasaurus*, and so it more likely approximates the ancestral condition for the genus (Ikejiri, 2005).

Cedarosaurus weiskopfae

Tidwell et al. (1999) named *Cedarosaurus weiskopfae* on the basis of a partial skeleton from the Early Cretaceous Cedar Mountain Formation of Utah, USA. Chapter 3 demonstrated that a sauropod hind limb from the Glen Rose Formation of Texas (FMNH PR 977) is referable to *Cedarosaurus*, so this material is included in the scores as well.

Diplodocoidea

Diplodocoidea is a diverse, geographically-widespread clade that evolved alongside Titanosauriformes until the mid-Cretaceous. The phylogeny of the group is mostly based on their derived cranial anatomy, with few appendicular specializations (Whitlock, 2011). Scoring for Diplodocoidea was mostly based on the most primitive diplodocoid, *Haplocanthosaurus*, or the basalmost taxon available if data were missing for that genus, following the phylogeny of Whitlock (2011).

Euhelopus zdanskyi

Euhelopus zdanskyi is well-represented by cranial and postcranial materials from the Mengyin Formation of China. *Euhelopus* is likely Early Cretaceous in age, though a Late Jurassic age is possible (Wilson and Upchurch, 2009). *Euhelopus* has been the subject of several detailed descriptions (Wiman, 1929; Mateer & McIntosh, 1985) and studies of its phylogenetic affinities, which have suggested that it is a basal somphospondylan (Wilson & Upchurch, 2009). In the present analysis, exemplars ‘a’ and ‘c’ of *Euhelopus* are regarded as pertaining to one individual following Wilson & Upchurch (2009).

Europasaurus holgeri

Europasaurus is represented by multiple skeletons of different ontogenetic stage from the Late Jurassic of Germany (Sander et al., 2006). Most of this material was disarticulated when recovered, but represents a single taxon on the basis of similarity of repeated elements (Sander et al., 2006; pers. obs., 2009). Scoring for *Europasaurus* included all available parts of the hypodigm, which includes substantial cranial and postcranial material.

Janenschia robusta

Janenschia is known from fore- and hind limb material from the Late Jurassic Tendaguru beds of Tanzania (Wild, 1991; Bonaparte et al., 2000). Scoring for *Janenschia* did not include caudal vertebrae, because it is unknown whether or not these pertain to the same animal as the limb material (Bonaparte et al., 2000).

Ligabuesaurus leanzi

Bonaparte, González Riga & Apesteguía (2006) named *Ligabuesaurus leanzi* on the basis of abundant material from the Aptian Lohan Cura Formation of Argentina. Only the holotypic individual (MCF PHV 233, formerly MCF PHV 261) was considered for scoring *Ligabuesaurus* in this matrix; other, isolated materials were excluded (e.g., the tooth described by Bonaparte et al., 2006; MCF PHV 744).

Sauroposeidon proteles

Sauroposeidon proteles was named by Wedel et al. (2000) on the basis of four mid-cervical vertebrae from the Early Cretaceous Antlers Formation of Oklahoma, USA. Wedel et al. (2000a, b, 2005) tentatively referred a cervical vertebral centrum from the coeval Cloverly Formation of Wyoming to *S. proteles*. Revision of the Cloverly Formation sauropod material has confirmed this referral, as well as provided basis for referral of material from the Cloverly Formation and the Twin Mountains Formation of Texas (materials formerly referred to as *Paluxysaurus jonesi*). Autapomorphies, the absence of meaningful differences, and their similar age support referral of *Paluxysaurus* and the Cloverly Formation sauropod material to *Sauroposeidon proteles*, so all three sets of exemplars were used for scoring that taxon in this analysis (see Chapters 2 and 3).

‘Saltasaurini’

Saltasaurus, *Neuquensaurus*, and *Rocasaurus* form a clade when all three are included in cladistic analyses (e.g., Curry Rogers, 2005, González Riga et al., 2009). I informally refer to these taxa as ‘Saltasaurini’ instead of Saltasaurinae, because Saltasaurinae is a stem-based taxon and may contain some of the other terminal taxa depending on the results of the analysis. The saltasaurine status of *Bonatitan* (Martinelli & Forasieppi, 2004) remains to be adequately tested by cladistic analysis. Data for *Neuquensaurus* are based on holotypic and referred materials as outlined in D’Emic & Wilson (2011).

CHARACTERS

The data matrix includes 114 characters (Appendix 2), 3 of which are multistate (16, 30, 77; 3 character states each), all of which were ordered. These characters were ordered because state 1 is logically or developmentally intermediate in a transition between the state 0 and state 2, and so state 1 was present at some time in the transition from state 0 to 2 or vice versa. For example, somphospondylous vertebral pneumaticity (character 16: state 2) develops from coarse camellate (state 1) and camerate vertebral pneumaticity (state 0) during sauropod ontogeny (Wedel et al., 2000b), and so possession of state 2 implies that state 1 was present at some point in the lineage before the evolution of state 2.

Fifteen characters represent the cranium, 48 represent the axial column, 20 represent the pectoral and pelvic girdles, 30 represent the limbs, and one represents the dermal skeleton (Fig. 4). Previously formulated characters were selected and modified from the studies of Salgado et al. (1997), Wilson (2002), Upchurch et al., (2004), Curry Rogers (2005), González Riga et al. (2009), Royo-Torres (2009), Chure et al., (2010), Mannion (in press), and Mannion & Calvo (2011). Scoring changes to some characters outlined in Wilson (2005) and Wilson and Upchurch (2009) were implemented where appropriate. Other characters were formulated from personal observation, published diagnoses, autapomorphy lists (e.g., Wilson, 2002), and descriptions. Character states were modified for most previously formulated characters to reflect the taxonomic scope of this analysis. For example, Wilson (2002: character 80) coded the number of cervical vertebrae into five states (9 or fewer, 10, 12, 13, 15 or greater) in a cladistic analysis of Sauropoda. Because of the narrower taxonomic scope of the analysis presented herein, the number of states was reduced to two (14 or fewer, 15 or more). About 40 characters (ca. one-third) are new to this analysis. Character state scorings were examined manually for errors in the data matrix; errors were also checked for as synapomorphy optimizations were listed. Characters were worded according to standardized cladistic 'grammar' in order to facilitate comparisons with other studies (Sereno, 2007).

Some characters that have previously been recovered as synapomorphies of clades relevant to this analysis (e.g., Titanosauria) were excluded because they either displayed too much individual or ontogenetic variation to confidently score or were invariant among the ingroup or outgroup.

Many other characters purported to be relevant to basal titanosauriform phylogeny by several authors were not included in this analysis because character states could not confidently be scored. For example, several characters presented by Royo-Torres (2009) are substantially variable along single a vertebral column (e.g., characters C30, C41, C42, C84, C89, C90, C104). For such characters, scorings for vertebrae just a few positions away from one another in the column are often different. Character C30 (mislabeled as character C39 in Royo-Torres (2009: 426, translated from the Spanish) is an example of this type of character: “dorsal surface of the neural spine in dorsal vertebrae: flat or flat-convex (0), concave (1).” This character was scored as derived only for *Camarasaurus* and *Tastavinsaurus*. However, the concavity or convexity of the top of the neural spine varies substantially along the dorsal vertebral column in *Camarasaurus* (Osborn and Mook, 1921; compare Royo Torres, 2009: fig. 4.20 with fig. 4.28). When available character data are anatomically disjunct (e.g., only dorsal vertebrae 1–3 in one species versus 4–6 in another species), individual variation may be spuriously cast as taxonomically meaningful. Other characters have states that are indistinguishable when small amounts of individual variation or taphonomic deformation are taken into account (e.g., characters 154, 162, 172, 184, 213; see Royo Torres, 2009: fig. 4.162, 4.170, 4.203). Still other characters are linked (characters 192, 194).

MISSING DATA

The amount of missing data for each terminal taxon are given in Table 4.4. The average amount of missing data per taxon was 44%; this ranged from 0% (*Camarasaurus*, Diplodocoidea) to 86% (*Qiaowanlong*). In addition, *Omeisaurus*, *Giraffatitan*, *Phuwiangosaurus*, ‘Saltasaurini’, and *Alamosaurus* had less than 20% missing data; *Atlasaurus*, *Erketu*, and *Venenosaurus* had more than 70% missing data. Missing data were usually due to incompleteness of specimens, though in a few cases the data are preserved but were undescribed and could not be observed first-hand as part of this study.

TOPOLOGY

Twenty-five ingroup taxa and two outgroup taxa were scored for 114 characters (Appendix 1) in MacClade (Maddison & Maddison, 1992) and Mesquite (Maddison & Maddison, 2011) and analysed in PAUP* (Swofford, 2000). The Branch-and-Bound search algorithm was used, with stepwise addition and random branch swapping via the tree-bisection-reconnection algorithm.

Nine equally parsimonious trees of treelength 192 were found (consistency index = 0.63, retention index = 0.80); a strict consensus of these trees is given in Figure 4.5. Synapomorphies supporting a strict consensus of these nine topologies under delayed transformation (DELTRAN) optimizations are given in Appendix 3. DELTRAN optimizations are presented rather than accelerated transformation (ACCTRAN) optimizations because DELTRAN minimizes the distribution of ambiguous synapomorphies due to missing data (Table 4.4), and thus results in more phylogenetically restricted inferences of character distribution when missing data are substantial. Ambiguously-optimized synapomorphies due to missing data and/or character conflict are given in Tables 4.5 and 4.6. All nodes within the ingroup are resolved with the exception of two polytomies, each involving three taxa. Pertinent phylogenetic nomenclature is listed in Table 1.

This analysis recovered three main titanosauriform clades: Brachiosauridae, Euhelopodidae, and Titanosauria (Fig. 4.5). *Atlasaurus* is recovered as the sister-taxon to Neosauropoda, with Diplodocoidea, *Camarasaurus*, and *Tehuelchesaurus* as successive outgroups to Titanosauriformes. Titanosauriformes is composed of two sister clades, Brachiosauridae and Somphospondyli. Brachiosauridae contains a mix of Late Jurassic and Early Cretaceous Laurasian and Gondwanan taxa. Basal members of Somphospondyli include *Ligabuesaurus*, *Sauroposeidon*, and *Tastavinsaurus*. More derived somphospondylans are composed of two major clades, Euhelopodidae and the Titanosauria, with *Chubutisaurus* as outgroup to the latter. Euhelopodidae is comprised exclusively of East Asian Cretaceous genera. Two nested clades were recovered within Titanosauria: Lithostrotia and Saltasauridae. *Alamosaurus* and *Opisthocoelicaudia* were recovered as successive sister taxa of ‘Saltasaurini’.

Basal (non-titanosaur) titanosauriforms were found to be diverse in this study (16 genera), in contrast to previous studies, which recovered at most 6 genera in this part of the cladogram (Table 4.2). The topology shows general congruence with geologic age (Fig. 4.6), with basal titanosauriforms and their outgroups found in the Jurassic, basal somphospondylans in the Early and ‘middle’ Cretaceous, and titanosaurs mostly in the Late Cretaceous.

Treating the three ordered characters as unordered led to loss of all resolution within Euhelopodidae; all other relationships were identical to those recovered in the most parsimonious tree found with ordered characters. When character transformations were assumed to be unordered, the decay index of Brachiosauridae drops from 3 to 2; all other decay indices are unaffected.

ROBUSTNESS OF RESULTS

The robustness of the most parsimonious trees was evaluated in terms of Bremer support, also known as the decay index (the number of steps required for a given node to disappear from a cladogram; Bremer, 1994). Decay indices for the topology presented in Figure 4.5 are given in Table 4.7. Decay indices were calculated in MacClade (Maddison and Maddison, 1992) by writing a “Decay Index to PAUP” file, which was executed in PAUP* (Swofford, 2002). Almost half of the nodes (10 of 22) had a decay index equal to one; most of these weaker nodes were within Brachiosauridae and the Euhelopodidae. This weak support is mostly due to missing data; most members of these two clades could not be scored for more than 50% of characters (Table 4.4). The presence of very fragmentarily represented taxa near the bases of some clades (e.g., *Andesaurus* for Titanosauria, *Qiaowanlong* and *Erketu* for Euhelopodidae) also helps to explain the low decay index for those clades' basalmost nodes. These low decay indices may also be due to the close spatiotemporal association of the derived brachiosaurids and euhelopodids in this analysis, that is, if the true branch length between lineages is short. In contrast, the best supported nodes were Lithostrotia, Saltasauridae, and Titanosauriformes. The high decay indices of the former two nodes is likely due to the undersampling of Titanosauria in this analysis; the presence of more titanosaurs would likely redistribute some of the support for these nodes. Somphospondyli and Brachiosauridae are moderately supported (decay index = 3).

DISCUSSION

TOPOLOGICAL COMPARISONS WITH PREVIOUS ANALYSES

Below, I explore the topology presented in Figure 4.5 in detail, focusing on novel hypotheses of relationship presented in this analysis. Metrics and data supporting these relationships (number of additional steps required to support a given hypothesis, Templeton test statistics, synapomorphies) are given when relevant. See Templeton (1983) and Wilson (2002) for details regarding the Templeton test.

Titanosauriform outgroups

Atlasaurus is recovered as the sister-taxon to Neosauropoda, rather than a brachiosaur-relative as originally described (Monbaron et al., 1999). Eight additional steps are required to position *Atlasaurus* within Brachiosauridae, a position rejected by a Templeton test ($n = 14$; $p = 0.0003$). *Atlasaurus* lacks several expected features of neosauropods and clades therein, such as mid-dorsal vertebrae with opisthocoelous centra, horizontally-directed dorsal vertebral transverse processes, a ventrally expanded posterior centrodiapophyseal lamina, a process at the ventral base of the scapular blade, a single carpal, and a metacarpal I that is longer than metacarpal IV. Although brachiosaurid affinities for *Atlasaurus* can be ruled out, the precise phylogenetic position of *Atlasaurus* presented in Figure 4.5 should be considered preliminary, because most characters were unscored in this analysis (Table 4.4). Its completeness and Middle Jurassic age make *Atlasaurus* an important genus for understanding the origins of Neosauropoda, as it may represent the earliest known member of that clade.

Camarasaurus and Titanosauriformes are found to be more closely related to one another than either is to Diplodocoidea, as in taxonomically broader analyses of sauropod relationships (e.g., Wilson, 2002; Upchurch et al., 2004). *Tehuelchesaurus* is resolved as the sister taxon of Titanosauriformes, rather than as closely related to *Omeisaurus* as previously suggested (Rich et al,. 1999;

Upchurch et al. 2004). Two additional steps are required to position *Tehuelchesaurus* as the sister-taxon of *Omeisaurus*, and a Templeton test does not reject such a position (n = 6; p = 0.41). Several features recovered as titanosauriform synapomorphies in previous analyses such as a lateral bulge on the femur or plank-like anterior dorsal ribs (e.g., Wilson, 2002; Upchurch et al., 2004) have obsolesced to include *Tehuelchesaurus* as well.

Brachiosauridae

This analysis recovered six taxa as brachiosaurids. The fragmentary and often non-overlapping anatomy of putative brachiosaurids (e.g., *Cedarosaurus*) has yielded limited taxonomic breadth and/or resolution for this clade in previous analyses (e.g., Upchurch et al., 2004; Rose, 2007; Ksepka & Norell, 2010), though many taxa were suggested to be brachiosaurids without a cladistic analysis. In particular, cranial data are known for only three brachiosaurids (*Abydosaurus*, *Europasaurus*, *Giraffatitan*), and the only brachiosaurid for which substantial cranial and postcranial data are available is *Giraffatitan*.

The traditional (non-cladistic) content of the Brachiosauridae was maintained by this analysis (i.e., *Brachiosaurus*, *Giraffatitan*). In addition, the affinities of several putative brachiosaurids were confirmed by this analysis, including *Cedarosaurus*, *Venenosaurus*, and *Abydosaurus*. In contrast, some brachiosaurids (*Atlasaurus*, *Sauroposeidon* (including ‘*Paluxysaurus*’), *Qiaowanlong*) were recovered outside the clade, and some likely brachiosaurids

(‘French’ *Bothriospondylus*, *Sonorasaurus*) were too fragmentary to include in this analysis (but see ‘Fragmentarily Represented Taxa’ below). Five unambiguous brachiosaurid synapomorphies were recovered (wide supratemporal fenestrae, ventral triangular projection on anterior ramus of quadratojugal, maxillary teeth twisted axially, dorsal vertebrae with ‘rod-like’ transverse processes, ischium with abbreviate pubic peduncle) as well as eight more under accelerated transformation optimization (ACCTRAN; Tables 4.5 and 4.6). Under DELTRAN, these eight synapomorphies optimize either as synapomorphies of *Giraffatitan* plus more derived brachiosaurids (3, 9, 52, 78, 114), an autapomorphy of *Giraffatitan* (53), or as multiple gains and losses among various titanosauriformes (due to missing data; 67, 90).

Europasaurus was recovered as the basalmost brachiosaurid in contrast to previous hypotheses that suggested that it was a basal macronarian (Sander et al., 2006). Though strongly supported as a brachiosaurid, the affinities of *Europasaurus* within that clade are labile given the data at hand. The basal position of *Europasaurus* within the Brachiosauridae may be strongly influenced by missing data, because many of the synapomorphies that unite more derived brachiosaurids could not be scored for *Europasaurus*, because those aspects of its anatomy are unknown or undescribed (e.g., lacrimal, metatarsal IV, caudal vertebrae).

Giraffatitan and *Brachiosaurus*, once considered congeneric (e.g., Janensch, 1950), are recovered as successively more derived brachiosaurids in this analysis (Fig. 4.5). The fragmentary nature of *Brachiosaurus* weakens its position among brachiosaurids, and only a few steps are required to move it into a more or less derived position within Brachiosauridae or as the sister taxon of *Giraffatitan* as traditionally hypothesized (Janensch, 1950; Taylor, 2009). Future, confident referrals of material to *Brachiosaurus altithorax* are needed to better understand its phylogenetic position. *Cedarosaurus*, *Venenosaurus*, and *Abydosaurus*, all known from the Early Cretaceous of North America, are recovered in a polytomy as the most derived brachiosaurids. This result is in keeping with the original descriptions and other cladistic analyses dealing with these taxa (Tidwell et al., 1999; Upchurch et al., 2004; Rose, 2007; Chure et al., 2010).

Basal Somphospondyli

Three Early-middle Cretaceous sauropods make up a 'grade' of basal somphospondylans: *Ligabuesaurus*, *Sauroposeidon*, and *Tastavinsaurus*. Several features support the monophyly of Somphospondyli, for example: sub-centimeter-scale pneumatic chambers permeating the presacral vertebrae, a prespinal lamina in posterior cervical and dorsal vertebrae, anterior dorsal vertebrae with 'paddle-shaped' neural spines (anteroposteriorly flat neural spines that widen distally before tapering to a blunt or rounded distal end), a medially beveled scapular glenoid, and an embayed medial face of the proximal end of metatarsal IV. Some studies have recovered *Ligabuesaurus* and *Tastavinsaurus* as basal somphospondylans (Gomani et al., 1999; Bonaparte et al., 2006; Canudo et al., 2008; Royo-Torres, 2009; Carballido et al., 2011), but their precise relationships vary by study. This region of the cladogram presented in this study (Fig. 4.5) is likewise weakly supported, with low decay indices (Table 4.7).

A recent revision substantially augmented the hypodigm of *Sauroposeidon* with material from Texas previously referred to '*Paluxysaurus jonesi'* (Rose, 2007) and material from Wyoming (Chapters 2 and 3). Both *Sauroposeidon* and '*Paluxysaurus'* were originally described as brachiosaurids. A comparative study suggested that '*Paluxysaurus'* possibly represented a basal somphospondylan (Gomani et al., 1999), whereas a later a cladistic analysis recovered it as a brachiosaurid (Rose, 2007). Synapomorphies supporting brachiosaurid affinities for *Sauroposeidon* and '*Paluxysaurus'* in the analysis of Rose (2007) such as elongate cervical vertebrae (character 21) are inclusive of larger clades than Brachiosauridae according to the analysis presented herein. As well as possessing the somphospondylan features mentioned above, several synapomorphies support the position of *Sauroposeidon* as a somphospondylan more derived than *Ligabuesaurus* (Appendix 3). *Sauroposeidon* lacks several features including 'rod-like' dorsal vertebral diapophyses, fossae variably present in anterior and middle caudal vertebral centra, and a rounded proximolateral corner of the humerus, which would be expected in a brachiosaurid. Seven and two steps are required to position *Sauroposeidon* within Brachiosauridae or Titanosauria, respectively, and a Templeton test rejects both hypotheses (n = 13,

$p = 0.006$; $n = 37$; $p = < 0.001$).

Tastavinsaurus is recovered as slightly more derived than *Sauroposeidon*, at a node with a decay index of 2 (Table 4.7). No support for a clade of Laurasian sauropods allied with *Tastavinsaurus* is found (see below).

Euhelopodidae

Euhelopodidae was originally used to describe a clade containing *Euhelopus* and some Jurassic Chinese forms (Upchurch, 1995). The content of Euhelopodidae varies by phylogenetic analysis; *Mamenchisaurus*, *Omeisaurus*, *Shunosaurus*, and *Euhelopus* have all been considered members (see review in Wilson, 2002), and the name is not currently in widespread use (Wilson and Upchurch, 2009). Most of the fluidity in euhelopodid membership is due to conflicting placement of *Euhelopus* in different phylogenies. For example, Wilson and Sereno (1998) and Wilson (2002) recovered it as the sister-taxon of Titanosauria, whereas Upchurch (1998) and Upchurch et al. (2004) recovered it as a non-neosauropod. Recent restudy and re-scoring of the data matrices of Wilson (2002) and Upchurch et al. (2004) favored the conclusions of the former study, that *Euhelopus* is closely related to titanosaurs (Wilson and Upchurch, 2009).

The phylogenetic definition proposed by Upchurch (1995) is complex because it contains several specifying taxa, some of which are now recognized as distantly related (Wilson and Upchurch (2009). Herein Euhelopodidae is redefined as a stem-based taxon comprising all sauropods more closely related to *Euhelopus zdanskyi* than *Neuquensaurus australis* (see Table 4.1 for phylogenetic nomenclature). I have chosen to redefine and employ Euhelopodidae herein (rather than coin and define a novel name) because (1) the name with its old definition has been in disuse for over a decade, (2) coining new names instead of using old ones proliferates nomenclature, which should be avoided if possible, (3) the name does carry some of the original intended meaning with its new definition. Regarding the last point, in this analysis, a previously unrecognized group of six Early-middle Cretaceous East Asian taxa is recovered: *Qiaowanlong*, *Erketu*, *Daxiatitan*, *Euhelopus*, *Phuwiangosaurus*, *Tangvayosaurus*. Likewise, several fragmentarily represented taxa that were not included in this analysis seem to have affinities with these taxa (see 'Fragmentarily Represented Taxa' below). In this sense, Euhelopodidae still connotes a group of only East Asian sauropods closely related to *Euhelopus*, though the membership (and geologic ages of those members) differs from the original definition.

Usually the six taxa recovered as euhelopodids in this analysis have been recovered as basal somphospondylans or basal titanosaurs when considered in cladistic analyses previously (e.g., You et al., 2008, Ksepka & Norell, 2010; Suteethorn et al., 2010), but features novel to this study suggest their monophyly (see Appendix 4.2, 4.3) . Missing data, especially among basal members of the clade, weaken its support. Excluding these fragmentarily represented, basal taxa (e.g., *Erketu*, *Qiaowanlong*) from the analysis tends to increase Bremer support for more derived euhelopodid clades. New discoveries or more complete descriptions may provide character scores that support a more derived position for basal forms such as *Qiaowanlong* or *Erketu*. Euhelopodid monophyly is supported by two unambiguous synapomorphies: (1) bifid cervical vertebrae and (2) cervical vertebrae with thick, subhorizontal epipophyseal–prezygapophyseal lamina. Nine additional synapomorphies support Euhelopodidae under accelerated transformation (ACCTRAN; Tables 4.5 and 4.6).

Qiaowanlong was originally described as a brachiosaurid, a position refuted by Ksepka & Norell (2010), Mannion & Calvo (2011), and this analysis. The early identification of *Sauroposeidon* as a brachiosaurid likely contributed to the original description of *Qiaowanlong* as such, because most comparisons in its original description were focused on *Sauroposeidon* (You & Li, 2009). Three steps are required to position *Qiaowanlong* within Brachiosauridae according to this analysis, and a Templeton test rejects such a position ($n = 9$, $p = 0.004$).

The position of *Erketu* is likewise supported by two synapomorphies, and the position of more derived euhelopodids is supported by a suite of nine features, including prong-like epipophyses, ‘trifid’ posterior cervical and anterior dorsal neural spines, and a low, pointed preacetabular process of the ilium. *Tangvayosaurus* and *Phuwiangosaurus* are sister taxa within derived Euhelopodidae, in contrast to various studies that have suggested that these taxa are basal titanosaurs (Allain et al., 1999; Upchurch et al., 2004; Canudo et al., 2008; Carballido et al., 2011). Ten and three steps are required to place *Phuwiangosaurus* and *Tangvayosaurus* within the Titanosauria, respectively. Templeton tests reject the titanosaur affinities of both genera (*Phuwiangosaurus*: n = 47, p = 0.0001; *Tangvayosaurus*: n = 23, p < 0.0001).

Titanosauria

The interrelationships of Titanosauria were not the focus of this analysis, so only a small portion of its diversity (more than 65 genera; Curry Rogers, 2005; Mannion & Calvo, 2010) was sampled. The fragmentary nature of *Andesaurus* weakens the robustness of the node representing Titanosauria. More derived nodes (Lithostrotia, Saltasauridae, Saltasaurinae) are very well supported. *Alamosaurus* was recovered as a member of the Saltasaurinae, rather than the sister taxon of *Opisthocoelicaudia* as in Wilson (2002) and González Riga et al. (2008) or the outgroup to Saltasauridae as in Upchurch et al. (2004) and Carballido et al. (2011).

‘Laurasiformes’

Several authors have found support for a clade of mostly Early Cretaceous, exclusively Laurasian sauropods, termed ‘Laurasiformes’ (Canudo et al., 2008, Royo-Torres, 2009; Barco, 2009). ‘Laurasiformes’ was defined by Royo-Torres (2009) as a stem-based clade containing sauropods more closely related to

Tastavinsaurus than *Saltasaurus*, and has been found to include Laurasian taxa such as *Galvesaurus*, *Aragosaurus*, *Tastavinsaurus*, *Phuwiangosaurus*, *Cedarosaurus*, *Sonorasaurus*, *Venenosaurus,* and a single Gondwanan genus, *Tehuelchesaurus* (Carballido et al., 2011). The analysis presented herein does not support such a grouping; instead *Tehuelchesaurus* is recovered as a non-titanosauriform, *Venenosaurus, Cedarosaurus*, and *Sonorasaurus* as brachiosaurids, and *Phuwiangosaurus* as a euhelopodid (Fig. 4.5). *Aragosaurus* and *Galvesaurus* were not included in this analysis because their validity and constituency were uncertain given the data at hand (see 'Relationships of Fragmentarily Represented Taxa' below). The features supporting the monophyly of 'Laurasiformes' in each analysis are listed in Table 4.9. These features are mostly problematic in terms of definition or scoring, and revision of them erodes support for Laurasiformes' (Table 4.9). For example, the 'wrinkle' on the lateral face of middle and posterior caudal vertebrae represents a remnant of the neurocentral suture, and is present in many sauropods (e.g., *Camarasaurus*, Osborn and Mook, 1921; *Andesaurus*, Mannion and Calvo, in press). Likewise, a hyposphene-hypantrum in the middle and posterior dorsal vertebrae is present in most non-titanosaur sauropods (Wilson and Sereno, 1998). Other 'laurasiform' synapomorphies are problematic because they are not preserved in most or all 'Laurasiformes,' such as a six-degree bevel on the distal femur or a narrow sacrum. Still other features do not characterize any sauropod, such as metatarsal III equal to 30% the length of the tibia. A constraint tree containing the ‘laurasiform’ taxa in this analysis (*Tastavinsaurus*, *Cedarosaurus*, *Venenosaurus*, *Phuwiangosaurus* in a polytomy) was evaluated against the tree presented in Figure 4.5 via a Templeton test, which rejected the existence of ‘Laurasiformes’ ($n = 34$, $p < 0.0001$). Furthermore, 34 additional steps were required to accomodate the monophyly of ‘Laurasiformes’.

RELATIONSHIPS OF FRAGMENTARILY REPRESENTED TAXA

Missing data are especially problematic in some members of Titanosauriformes such as Brachiosauridae or basal Titanosauria, because in those cases the missing data often occur in non-overlapping anatomical regions among taxa. For example, only a few brachiosaurids preserve skulls. Other brachiosaurids do not preserve appendicular material. In this case, the disjunct distribution of missing data would support the monophyly of species with skulls on the one hand, and the monophyly of species with appendicular material on the other. Because the synapomorphies supporting these clades are ambiguous due to missing data, robustness of nodes (e.g., their decay index) is low. Furthermore, the few mostly complete taxa (e.g., *Giraffatitan* in the brachiosaurid case) may be simultaneously pulled towards phylogenetic relationships with several taxa by character data from different anatomical regions, depending on the data available in fragmentarily represented taxa. This ‘monophyly of the preserved’ at best leads to loss of robustness or resolution, and at worst can lead to spurious results. The ways to combat the ‘monophyly of the preserved’ are to build larger operational taxonomic units with new discoveries or referrals, or eliminate problematically-preserved taxa from the dataset.

Numerous fragmentary taxa could not be included within the cladistic analysis presented above because their validity and constituency remain to be established or verified, and/or their remains do not bear enough relevant synapomorphies to nest them in lower-level clades. Discovery of synapomorphies using more informative taxa in the cladistic analysis above allows general phylogenetic statements to be made for most fragmentarily represented taxa, as shown in Table 4.8. However, some basal titanosauriforms warrant further explication because of their interesting geographic location or age, their complex taxonomy, or differences between results of previous studies and those presented here.

Sonorasaurus thompsoni (Ratkevitch, 1998) — *Sonorasaurus* was originally described as a brachiosaurid and is important because of its Albian–?Cenomanian age, which would be on par with the youngest known North American sauropods before the start of the ‘sauropod hiatus’ (Ratkevitch, 1998; Lucas & Hunt, 1989). *Sonorasaurus* is represented by a somewhat fragmentary partial skeleton, which includes presacral and caudal vertebrae and some limb elements. *Sonorasaurus* is a titanosauriform on the basis of semicamellate presacral vertebral pneumaticity, middle caudal vertebrae with neural arches set on the anterior half of the centrum, anterior-middle caudal vertebrae with posteriorly projecting transverse processes, metacarpal I with an undivided distal condyle that is perpendicular to the shaft, other metacarpals with reduced or absent distal articular facets, and a fibula that lacks a corrugated subtriangular proximal scar (Appendix 3).

When *Sonorasaurus* is added to the data matrix and analyzed via the search parameters presented above (see 'Topology' above), it is recovered as a brachiosaurid, and all resolution within this clade disappears. Brachiosaurid affinities are suggested for *Sonorasaurus* on the basis of metatarsal IV beveled distally and metatarsal IV with medial embayment on proximal end (Appendix 3). Previous hypotheses for brachiosaurid affinities for *Sonorasaurus* were based on its elongate forelimb bones (Ratkevitch, 1998), but more recent discoveries have shown that similarly elongate limb bones are present in taxa that are here resolved as basal somphospondylans (e.g., *Ligabuesaurus*, *Sauroposeidon*) and basal titanosaurs (e.g., *Andesaurus*, *Malawisaurus*). The brachiosaurid affinities of *Sonorasaurus* are only weakly supported by the data matrix in this study — when included, the decay index for Brachiosauridae is 1, and only 1 step is required to move *Sonorasaurus* into a basal titanosauriform or basal somphospondylan position. Further data are needed to evaluate the affinities of *Sonorasaurus*.

Xenoposeidon proneneukos (Taylor and Naish, 2007) — *Xenoposeidon* was named on the basis of a single partial middle-posterior dorsal vertebra (NHMUK R2095) from the Early Cretaceous Hastings Beds of England. Six features were presented as diagnostic for *Xenoposeidon* by Taylor and Naish (2007: 1549): "(1) neural arch covers dorsal surface of centrum, with its posterior margin continuous with that of the cotyle; (2) neural arch slopes anteriorly 35 degrees relative to the vertical; (3) broad, flat area of featureless bone on lateral face of neural arch; (4) accessory infraparapophyseal and postzygapophyseal laminae meeting ventrally to form a V; (5) neural canal is asymmetric: small and circular posteriorly but tall and teardropshaped anteriorly; (6) supporting laminae form vaulted arch over anterior neural canal." Instead of representing autapomorphies, these features are the result of damage or are actually more widespread among sauropods. For example, interpreting the flush posterior neural arch-centrum as an autapomorphy (1) does not account for missing bone in the posterior centrum. The forward lean of the neural arch relative to the centrum (2) characterizes vertebrae of the pectoral region in many sauropods (e.g., *Camarasaurus*, Osborn and Mook 1921: pls. 69, 72). Likewise, the laminar pattern characters (3, 4, 6) are observed in a variety of sauropods when individual or serial variation is explored (e.g., *Camarasaurus*, Osborn and Mook, 1921; *Brachiosaurus*, Riggs, 1903; *Tehuelchesaurus*, Carballido et al., in press). The 'asymmetrical neural canal' (5) cited by Taylor and Naish (2009) misrepresents the large centroprezygapophyseal fossae (cprf) as the entire anterior neural canal, which is a feature observed in many neosauropods (e.g., *Camarasaurus*, Osborn and

Mook, 1921). The absence of diagnostic features renders *Xenoposeidon* a nomen dubium (as suggested by Mannion and Calvo, 2011). The presence of coarse camellate pneumaticity suggests that NHMUK R2095 pertains to a titanosauriform.

Brontomerus mcintoshi (Taylor et al., 2011) — *Brontomerus* was named on the basis of fragmentary dissociated material consisting of an ilium, scapula, distal caudal vertebra, ribs, and other fragmentary bones (Taylor, Wedel & Cifelli, 2011: Table 4.3) from the Early Cretaceous Burro Canyon Formation (equivalent to the Ruby Ranch Member of the Cedar Mountain Formation) of Utah. Because (1) the material is disarticulated, (2) there is substantial size variation among the known elements in the quarry, and (3) no elements from the quarry overlap with the holotype, referral of material from the holotypic quarry to *Brontomerus* is weak. Thus, the diagnosis of the species rests on the holotypic ilium (Taylor et al., 2011). Five autapomorphies were presented for the holotype of *Brontomerus*: (1) ischiadic peduncle reduced to very low bulge, (2) preacetabular lobe directed anterolaterally but not curved, (3) ilium height 52% of total length, (4) preacetabular lobe 55% of total ilium length, (5) postacetabular lobe reduced to near absence. The first two characters are present in a variety of taxa (e.g., *Tastavinsaurus*, Royo Torres, 2009; *Giraffatitan*, Janensch, 1961). The latter three characters cannot be evaluated in *Brontomerus* because the postacetabular process is broken — though Taylor et al. (2011: 81) describe this as a “genuine osteological feature not related to damage,” it is clear that this margin is not complete, and the reconstruction of the posterior curvature of the ilium is arbitrary. When reconstructed with a postacetabular process similar to that in most other sauropods, the ilium of *Brontomerus* is similar to those of brachiosaurids (e.g., *Giraffatitan*, Janensch, 1961: pl. E). *Brontomerus mcintoshi* represents a nomen dubium. Some of the material referred to *Brontomerus* by Taylor et al. (2011) appear to pertain to Titanosauriformes, based on the presence of pneumatic dorsal ribs or coarse camellate vertebral pneumaticity.

Wintonotitan wattsi (Hocknull et al., 2009) — Longmann (1933) named *Austrosaurus mckillopi* on the basis of several fragmentary dorsal vertebrae (QMF 2316) from the Early Cretaceous Allaru Mudstone of Australia. Hocknull et al. (2009) regarded *Austrosaurus* as a nomen dubium and named a new genus — *Wintonotitan* — from the slightly younger Winton Formation based on materials that had previously been referred to *Austrosaurus* (QMF 7292). *Wintonotitan* was diagnosed by a combination of many characters (see Hocknull et al., 2009: 16). Two features were cited as autapomorphies: dorsal vertebrae with ‘incipient’ spinoprezygapophyseal lamina, and cylindrical, incipiently biconvex caudal vertebrae. Both of these features characterize a wider array of basal titanosauriforms, however. An ‘incipient’ (subtle or small) spinoprezygapophyseal lamina is found in several sauropods (e.g., *Ligabuesaurus*, *Sauroposeidon*, *Giraffatitan*, *Argentinosaurus*, pers. obs.).

Likewise, weakly biconvex, cylindrical distal caudal vertebrae are found in *Giraffatitan*, *Rinconsaurus*, and *Astrophocaudia* (pers. obs.). These features may be local autapomorphies, but this awaits determination via cladistic analysis. However, the validity of *Wintonotitan* is supported by one unique feature recognized herein, distal caudal vertebrae with strongly arched ventral surfaces (see Hocknull et al., 2009: fig. 14).

Hocknull et al. (2009) recovered *Wintonotitan* as a member of Laurasiformes or the sister-taxon of *Malarguesaurus* in modified versions of the matrices of Canudo et al. (2008) and González Riga et al. (2009), respectively, but did not rule out titanosaur affinities for the genus. These results were supported by low bootstrap values (Hocknull et al., 2009: fig. 38) and the node supporting *Wintonotitan* and other titanosauriforms had a decay index of 2 in each analysis. The results of the present analysis suggest that *Wintonotitan* is a titanosauriform on the basis of reduced metacarpal phalangeal articular facets (Appendix 3), but more precise knowledge of its affinities await future discoveries and studies.

Galvesaurus herreroi (Barco et al., 2005) — *Galvesaurus herreroi* was named by Barco et al. (2005) on the basis of a holotypic middle dorsal vertebra and several referred bones from the Villar del Arzobispo Formation of Spain. These bones are thought to belong to a single individual based on their close association (Sánchez-Hernández, 2005), but the supposed left and right humeri are too disparate in size and shape to belong to a single animal, or even species (see Barco et al., 2005: fig. 4). Explaining these differences taphonomically is not feasible, because the longer humerus is shorter transversely, unlike what would be expected with flattening or shear. Further discoveries in the Villar del Arzobispo Formation would corroborate or refute referrals to *Galvesaurus*. Provisionally considering this material as a single genus, *Galvesaurus* was recently suggested to be a laurasiform macronarian outside of Titanosauriformes (Barco, 2009). Barco (2009) refuted earlier suggestions that *Galvesaurus* represented a diplodocoid (Barco et al., 2005) or non-neosauropod (Royo-Torres et al., 2006).

The lower-level phylogenetic relationships of *Galvesaurus* were sensitive to taxon sampling in the analyses of Barco (2009). The constituency and a consensus on the phylogenetic affinities of *Galvesaurus* await further discoveries, but the material from Villar del Arzobispo appears to pertain to Titanosauriformes based on a few features such as elongate cervical vertebrae and middle caudal vertebrae with anteriorly set neural arches (Appendix 3). The gracility and rounded proximolateral corner of the humeri suggest brachiosaurid affinities for those bones.

Mongolosaurus haplodon (Gilmore, 1933) — *Mongolosaurus* was collected from the Early Cretaceous of China and is based on fragmentary teeth, part of a basicranium, and three vertebrae. Wilson (2005) and Mannion (in press) established the validity of *Mongolosaurus* on the basis of several features, and both studies suggested that it was a titanosaur. In contrast, *Mongolosaurus* shares some features with *Erketu*, a Cretaceous East Asian sauropod outside of Titanosauria: tall, pillar-like epipophyses and an elongate axis with a tall ventral keel. *Mongolosaurus* also possesses bifid neural spines, as in all East Asian Cretaceous titanosauriforms. These three features suggest euhelopodid affinities for *Mongolosaurus*, in contrast to the 11 features suggesting titanosaur affinities proposed by Mannion (in press). However, many of the characters proposed by Mannion (in press) deal with parts of the skull that are unknown in almost all euhelopodids, making these comparisons equivocal. Furthermore, some cranial 'titanosaur' features proposed by Mannion (in press) have a broader distribution among sauropods. For example, mesial and distal tooth carinae and D-shaped cross-sections are features of the teeth of the non-titanosaur *Phuwiangosaurus,* and variability in tooth shape between upper and lower jaws is also present in the brachiosaurid *Abydosaurus* (Chure et al., 2010). In sum, *Mongolosaurus* displays a mix of features that suggest titanosaur or euhelopodid affinities.

Other East Asian Cretaceous sauropods — In the last decade, reports of new species in the Cretaceous of East Asia are on par with those of the rest of the world combined (Mannion, in press). Few of these new genera have been placed into a phylogenetic context via cladistic analysis, obfuscating their significance in overall sauropod evolution. Suggestions that some of these species form a clade have been made (Xu et al., 2006; Wilson and Upchurch, 2009) but no cladistic analysis has found support for a large clade of East Asian Cretaceous sauropods prior to the results presented herein. In addition to the six East Asian Cretaceous taxa recovered as a clade in this analysis (Fig. 4.5), several taxa bear features recovered as euhelopodid synapomorphies in the analysis presented herein (*Baotianmansaurus*, *Dongyangosaurus*, *Mongolosaurus*; Table 4.8). Other genera may belong to Euhelopodidae, but euhelopodid synapomorphies are not evident in them given the data at hand (*Fukuititan*, *Gobititan*, *Huanghetitan*, *Jiutaisaurus*, *Pukyongosaurus*, *Ruyangosaurus*, *Xianshanosaurus*; Table 4.8). Still other Cretaceous East Asian genera appear to lie outside Euhelopodidae, including *Opisthocoelicaudia* and *Nemegtosaurus* (Wilson, 2002), *Jiangshanosaurus*, *Sonidosaurus*, and *Qingxiusaurus* (Table 4.8). Importantly, all Cretaceous East Asian sauropods with preserved cervical vertebrae have bifid cervical neural spines. East Asia is an important area of future study for early titanosauriform evolution. Future research into the many fragmentarily represented Cretaceous genera will likely yield a core of euhelopodid taxa as well as an assemblage of more derived forms. Key to resolving the place of East Asian titanosauriforms in sauropod evolution will be taxonomic revision of several fragmentarily represented genera as well as the establishment of more precise geologic ages in various basins.

Amargatitanis macni (Apesteguíá, 2007) — Apesteguía (2007) named

Amargatitanis on the basis of fragmentary material (caudal vertebrae, scapula, femur, astragalus; MACN PV N52, 53, 34) of Neuquén, Argentina. Materials referred to *Amargatitanis* were thought to come from the Kimmeridgian Pichi Pecún Leufú Formation when they were discovered, but their preservational style suggests that they are from the Barremian La Amarga Formation. *Amargatitanis* was described as a derived titanosaur, and would constitute one of the oldest known members of that clade. However, although Apesteguía (2007) reported that the material was associated, field notebooks of J. Bonaparte indicate that the material was collected over several hundred meters of outcrop – for example, the femur and astragalus were collected over 400 meters from the caudal vertebrae (pers. obs. 2009; S. Apesteguía, pers. comm.). Some of the material referred to *Amargatitanis* may pertain to diplodocoids on the basis of complex neural arch lamination in the anterior caudal vertebrae (pers. obs., 2009).

Though presented as a titanosaur (Apesteguía, 2007), none of the material referred to *Amargatitanis* bears synapomorphies of Titanosauria according to the analysis presented herein. Several of the features cited in support of somphospondylan or titanosaur affinities by Apesteguía (2005) are instead the result of breakage. These include the medially beveled scapular glenoid, straight scapular blade, and beveled femoral condyles (i.e., these features are all broken). Likewise, fragmentary teeth from the La Amarga region cannot be ascribed to titanosaurs. A “dendritical enamel pattern” and “homogenous slenderness” were features used to refer these teeth to titanosaurs (Apesteguía, 2007: 539), but titanosaur enamel is not diagnostic, and diplodocoids and some basal titanosauriforms also have similarly slender and similarly shaped teeth (Chure et al. 2010). The purported titanosaur teeth could pertain to non-titanosauriforms similar to *Abdyosaurus* or *Ligabuesaurus* based on their shape (Apesteguía, 2007: fig. 4). The titanosaur affinities of material referred to *Amargatitanis* cannot be substantiated at present, and its validity merits re-investigation.

Janenschia robusta (Wild, 1991) — *Janenschia* is an important taxon because of its proposed titanosaur affinities (e.g., McIntosh, 1990; Bonaparte, Heinrich & Wild, 2000; Wilson, 2002; Upchurch et al., 2004) and Late Jurassic age. *Janenschia* appears to be a titanosauriform based on the absence of a proximomedial triangular scar on the fibula (Appendix 3). Bonaparte et al. (2000) pointed out that the procoelous anterior caudal vertebrae possibly referable to *Janenschia* could not strongly attest to titanosaur affinities because this feature is also present in some diplodocoids and non-neosauropods. Wilson (2002) and Upchurch et al. (2004) suggested titanosaur affinities for *Janenschia* on the basis of its robust forelimb bones and a raised ulnar olecranon process. However, similarly robust bones and a raised olecranon are found in some non-titanosaurs or non-titanosauriforms such as *Tehuelchesaurus* according to this analysis, and these features were not found to be titanosaur synapomorphies in this study. Likewise, Royo-Torres and Cobos (2009) presented evidence that some material referred to *Janenschia* pertains to non-neosauropods. Furthermore, several features of *Janenschia* are inconsistent with its placement within Titanosauria, Somphospondyli, or even Titanosauriformes: ulnar proximal arms subequally developed, the lack of an embracing proximal tibia and fibula, a divided posterior fossa on the astragalus, and a phalanx on metatarsal V (Appendix 3). Finally, the only cladistic analysis which included *Janenschia* recovered it as a non-titanosaur (Carballido et al., in press). The titanosaur affinities of *Janenschia* cannot be substantiated at present.

'Iuticosaurus' valdensis (LeLoeuff, 1993) — *Iuticosaurus* was named on the basis of two procoelous caudal vertebrae (NHMUK R151, lectotype and R146a, paralectotype; Upchurch et al., in press) and a third specimen (NHMUK R1886) was later referred (Le Loeuff, 1993). These specimens likely come from the Barremian Wessex Formation (Upchurch et al., in press). Though '*Iuticosaurus*' is regarded as a nomen dubium, its phylogenetic status is still of importance because of its early age and purported titanosaur affinities. However, like *Janenschia*, the titanosaur affinities of '*Iuticosaurus*' are problematic. LeLoeuff (1993) interpreted the holotype of *Iuticosaurus* to represent a middle caudal vertebra with autapomorphically long postzygapophyses. Reinterpreted as a more distal caudal vertebra based on its elongation, the postzygapophyses of *Iuticosaurus* (NHMUK R151) are normal and its procoely is shared with some non-titanosaurs (e.g., *Giraffatitan* HMN MB.R.5000, Janensch, 1950: pl. IV; *Malarguesaurus*, González Riga et al., 2009; Fig. 4.7). The titanosaur affinities of

‘*Iuticosaurus*’ cannot be substantiated at present.

‘*Pelorosaurus’ becklesii* (Mantell, 1852) — The complex history of the genus ‘*Pelorosaurus*’ is discussed elsewhere (Naish and Martill, 2001; Upchurch et al., 2004). ‘*Pelorosaurus*’ *becklesii* comes from the Barremian Wessex Formation of England and consists of a humerus, radius, ulna, and some skin impressions. Upchurch (1995) suggested that ‘*Pelorosaurus*’ *becklesii* was an early titanosaur on the basis of its proximally curved anteromedial process of the ulna and the presence of polygonal plates similar to those of *Saltasaurus* in its skin. However, a similarly curved anteromedial process of the ulna (and raised olecranon) are also found in non-titanosaurs (e.g., *Giraffatitan*, *Sauroposeidon*; pers. obs. of YPM 326, a cast of *‘P.’ becklesii*; Fig. 4.7) and should not be treated as a titanosaur synapomorphy in the absence of a cladistic analysis. Since the assessment of Upchurch (1995), similar polygonal dermal patterns have been reported in non-titanosaurs (e.g., *Tehuelchesaurus*, Giménez, 2007). Furthermore, ‘*P.’ becklesii* lacks one unambiguous synapomorphy of the clade uniting *Chubutisaurus* + Titanosaura: an undivided notch on the humeral radial condyle. ‘*P.’ becklesii* likely represents a titanosauriform on the basis of the anteromedial arm of the ulna being much longer than its anterolateral arm, but its titanosaur affinities cannot be substantiated at present.

TIMING OF THE ORIGIN OF TITANOSAURIA

The oldest known titanosaurs are Barremian–Albian in age (*Malawisaurus*, *Jiangshanosaurus*, NHMUK R5333; Figure 6; Table 4.8). These taxa appear to be lithostrotians, yet they predate the more basal titanosaur *Andesaurus*, which indicates an earlier origin for Titanosauria. The Barremian (ca. 128 Ma) age for these oldest titanosaurs is far younger than the Middle Jurassic (Bathonian, ca. 163 Ma) age of origin for Titanosauria inferred from wide-gauge trackways at Oxfordshire, England (Day et al., 2002; 2004). This inference was based on the proposal by Wilson and Carrano (1999) that wide-gauge trackways were produced by titanosaurs. In turn, wide-gauge trackways are thought to have been produced by titanosaurs because those clades bear synapomorphies inferred to produce such a trackway, including a proximomedially-deflected femur with a proximolateral bulge, eccentric femoral cross section, and distally beveled femoral condyles (Wilson and Carrano, 1999). Wilson and Carrano (1999) noted that several wide-gauge trackways predated the titanosaur body fossil record, and tentatively suggested that titanosaurs may have a ghost lineage leading back to the Middle Jurassic. Wide-gauge trackways are known from the Middle (Santos et al., 1994) and Late (Lockley et al., 1994) Jurassic of Portugal and the Late Jurassic of Switzerland (Lockley et al., 1994), as well as the Middle Jurassic of Oxfordshire as mentioned above (Day et al., 2002; 2004).

An alternative explanation to inference of a ghost lineage for Titanosauria into the Middle Jurassic would be if the anatomical features required to produce a wide-gauge trackway were present in non-titanosaurs as well. Wilson and Carrano (1999) noted that one of the features hypothesized to be related to wide-gauge trackmaking — a proximolateral femoral bulge — is present in Late Jurassic non-titanosaur titanosauriforms such as *Brachiosaurus*. The study presented herein recovers that feature as a synapomorphy of *Tehuelchesaurus* + Titanosauriformes, a clade whose earliest members are Late Jurassic in age (Fig. 5.6). In addition, although titanosaurs have more eccentric femoral cross sections on average than other sauropods (Wilson and Carrano, 1999: table 2), some Late Jurassic non-titanosaurs have femoral cross sections similar to those of titanosaurs (e.g., *Giraffatitan* and *Neuquensaurus*, ratio of transverse width / anteroposterior breadth of midshaft > 200%; Janensch, 1961; pers. obs.). The exact morphology required to produce a wide-gauge trackway (e.g., how prominent a proximolateral femoral bulge or eccentric a femoral shaft needs to be) is ambiguous at present. Therefore, wide-gauge trackways should not automatically be ascribed to titanosaurs — they may pertain to members of a more inclusive clade.

One other feature has been used to link trackways to titanosaurs. Day et al. (2002, 2004) suggested that the absence of a pollex claw impression in Middle Jurassic wide-gauge trackways from Oxfordshire, England indicated that the trackmaker was a titanosaur in that case. In contrast, other Jurassic wide-gauge trackways (Santos et al., 1994; Lockley et al., 1994) do possess a prominent pollux claw impression. However, even narrow-gauge sauropod trackways commonly do not possess a pollux claw impression for taphonomic or perhaps behavioral reasons (Santos et al., 1994; Wilson and Carrano, 1999). Such preservational problems could explain the absence of a pollux claw impression in the Oxfordshire wide-gauge trackways. Indeed, the Oxfordshire wide-gauge trackway lacks the pronounced heteropody observed in sauropod trackways (compare Day et al., 2002: fig 1 with Lockley et al., 1994: fig. 2). This is either the result of a true, aberrant morphology for the Oxfordshire wide-gauge trackmaker or a preservational problem. If non-preservation is indeed responsible for the absence of half of the pes impression, then the absence of a pollux claw impression might equally be explainable by non-preservation. Because the absence of a pollux claw on the Oxfordshire trackways is ambiguous, they do not demonstrably represent Middle Jurassic titanosaurs. Based on the evidence at hand, the earliest titanosaurs are known from the Early Cretaceous.

PALEOBIOGEOGRAPHIC IMPLICATIONS

During the Early Cretaceous, different titanosauriform clades developed on different continents — brachiosaurids in North America, euhelopodids in Asia, and titanosaurs in Gondwana and Asia (Fig. 4.8). The appearance of these three clades outside of their main geographic areas likely represents cases of dispersal, such as for somphospondylans in North America (*Sauroposeidon*, *Astrophocaudia*; Chapter 3) or titanosaurs in Laurasia (e.g., *Alamosaurus*; Lucas and Hunt, 1989). At the moment, more precise ages for many genera are necessary to resolve such lower-level biogeographic patterns, because the ages of many ‘middle’ Cretaceous taxa overlap given their current age uncertainty (Fig. 4.6).

The revised picture of titanosaur origins presented in this study prompts reappraisal of their possible vicariant origins related to the breakup of Pangea. Vicariance has been called upon to explain titanosaur origins by several authors (Lydekker, 1895; Bonaparte, 1999), but more recently, several authors have challenged vicariant origins for Titanosauria (Sereno, 1999; Wilson & Upchurch, 2003; Wilson & Upchurch, 2009). Instead, it has been argued that most sauropod groups were present across Pangea in the Middle and Late Jurassic, and that later geographic differences in sauropod faunas reflect differential extinction (e.g., Wilson and Sereno, 1998). This seems to be the case for Brachiosauridae, whose basal, Jurassic members are found on several continents (Figs. 4.6 and 4.8; see also Rauhut, 2006), whereas Cretaceous brachiosaurids are only found in North America.

In light of the new data presented in this paper, a vicariant origin for Titanosauria remains problematic, albeit for somewhat different reasons than previously proposed. Wilson & Upchurch (2003) rejected such a vicariant scenario for two reasons: (1) the proposed Middle Jurassic origin of Titanosauria predated the breakup of Pangea; (2) the existence of several Laurasian titanosaurs. The first objection is resolved by this study, because the revised picture of titanosaur evolution presented herein suggests that titanosaurs originated in the Early Cretaceous, during the breakup of Pangea. The second objection is ameliorated by the data presented herein, but requires further study as noted above. Some of the Laurasian taxa cited as titanosaurs by Wilson & Upchurch (2003) were shown above to be either non-titanosaurs (*Phuwiangosaurus*, *Tangvayosaurus*, Dalton Wells sauropod (Britt et al., 1998); Table 4.8). Other Laurasian titanosaurs are latest Cretaceous in age and may have dispersed from Gondwana, as they are nested within Gondwanan clades (e.g., *Opisthocoelicaudia* and *Alamosaurus*), but a dispersal origin for these and other Late Cretaceous Laurasian titanosaurs awaits a cladistic analysis that incorporates more titanosaurs and more precise age dates.

Basal titanosaurs (*Andesaurus*, *Malawisaurus*) and their closest outgroup (*Chubutisaurus*) appear in the Early Cretaceous of Gondwana, seemingly suggesting a Gondwanan origin for the group (Figure 4.6; Table 4.8). However, the earliest known titanosaurs are Barremian–Aptian forms: *Jiangshanosaurus* from China, NHMUK 5333 (middle caudal vertebrae) from England, and *Malawisaurus* from Malawi (Table 4.8). These genera all appear to be derived members within Titanosauria (i.e., lithostrotians), suggesting that the clade had achieved a wide geographic distribution well before the Aptian. Understanding the origins of Titanosauria requires new Jurassic or earliest Cretaceous discoveries.

CONCLUSIONS

This study presents a cladistic analysis focusing on the early members of the Titanosauriformes, a widespread and long-lived clade of sauropod dinosaurs. The analysis yields a cladogram for 25 ingroup taxa; many of the relationships presented herein are novel. Titanosauriformes is composed of three main clades: Brachiosauridae, Euhelopodidae, and Titanosauria. The early members of Titanosauriformes, Brachiosauridae, and outgroups to Titanosauria are found on various continents. In contrast, basal members of Titanosauria are restricted to southern continents at a time when brachiosaurids were common in North America and euhelopodids predominated in Asia. Previous claims for a Middle or Late Jurassic origin for Titanosauria are based on weak evidence. The earliest known titanosaurs are Barremian–Aptian in age, and these represent derived forms (lithostrotians), highlighting the need for new earliest Cretaceous discoveries for understanding the enigmatic origin of Titanosauria.

REFERENCES

Allain R, Taquet P, Battail B, Dejax J, Richir P, Véran M, Limon-Duparcmeur F, Vacant R, Mateus O, Sayarath P, Khenthavong B, Phouyavong S. 1999. Un nouveau genre de dinosaure sauropode de la formation de Grès supérieurs (Aptien-Albien) du Laos. *Comptes Rendus de l'Academie des Sciences de Paris, Sciences de la Terres et des Planètes* **329**: 609–616.

Antunes MT, Mateus O. 2003. Dinosaurs of Portugal. *C. R. Palevol* **2**: 77–95.

Apesteguía S. 2007. The sauropod diversity of the La Amarga Formation

(Barremian), Neuquén (Argentina). *Gondwana Research* **12:** 533–546.

Barco JL, Canudo JI, Cuenca-Bescos G, Ruiz-Omeñaca JI. 2005. Un nuevo dinosaurio saurópodo Galvesaurus herreroi gen. nov, sp. nov., del tránsito Jurásico-Cretácico en Galve (Teruel, NE de España). *Naturaleza Aragonesa* **15**: 4-17.

Barco JL. 2009. Sistemátic e implicaciones filogenéticas y paleobiogeográficas del saurópodo Galvesaurus herreroi (Formación Villar del Arzobispo, Galve, España). Unpublished D. Phil. Thesis, Universidad de Zaragoza.

Blakey RC. 2006. Global paleogeographic views of earth history—late Precambrian to Recent. Available at: http://jan.ucc.nau.edu/~rcb/globaltext2.html2006 Accessed on 06/11/11.

Bonaparte JF. 1999. Tetrapod faunas from South America and India: a palaeobiogeographic interpretation. *Proceedings of the Indian National Science Academy* **65A**: 427–437

Bonaparte JE, Heinrich WD, Wild R. Review of *Janenschia* Wild,with the description of a new sauropod from the Tendaguru beds of Tanzania and a discussion on the systematic value of procoelous caudal vertebrae in the sauropoda. *Palaeontographica Abteilung A Band* **256**: 25–76.

Bonaparte JF, González Riga BJ, Apesteguía S. 2006. *Ligabuesaurus leanzai* gen. et sp. nov. (Dinosauria, Sauropoda), a new titanosaur from the Lohan Cura Formation (Aptian, Lower Cretaceous) of Neuquén, Patagonia, Argentina. *Cretaceous Research* **27**: 364–376.

Borsuk-Bialynicka M. 1977. A new camarasaurid sauropod *Opisthocoelicaudia skarzynskii*, gen. n., sp. n. from the Upper Cretaceous of Mongolia. *Palaeontologia Polonica* **37**: 1–64.

Bremer K. 1994. Branch support and tree stability. *Cladistics* 10: 295–304.

Britt BB, Scheetz RD, McIntosh JS, Stadtman KL. 1998. Osteological characters of an Early Cretaceous titanosaurid sauropod from the Cedar Mountain Formation of Utah. *Journal of Vertebrate Paleontology* **18**: 29A.

Calvo JO, Bonaparte JF. 1991. *Andesaurus delgadoi* n. g. n. sp. (Saurischia, Sauropoda) a titanosaurid dinosaur from the Río Limay Formation (Albian-Cenomanian), Neuquén, Argentina. *Ameghiniana* **28**: 303–310.

Calvo JO, González Riga, BJ. 2003. *Rinconsaurus caudamirus* gen. et sp nov., a new titanosaurid (Dinosauria, Sauropoda) from the Late Cretaceous of Patagonia, Argentina. *Revista Geologica de Chile* **30**: 333–353.

Calvo JO, González Riga BJ, Porfiri JD. 2008. A new titanosaur sauropod from the Late Cretaceous of Neuquén, Patagonia, Argentina. *Arquivos do Museu Nacional, Rio de Janeiro* **65**: 485–504.

Canudo, J, Royo-Torres, R, Cuenca-Bescós G. 2008. A new sauropod: *Tastavinsaurus sanzi* gen et. sp. nov. from the Early Cretaceous (Aptian) of Spain. *Journal of Vertebrate Paleontology* **28**: 712–731.

Carballido JL, Pol D, Cerda I, Salgado L. 2011. The osteology of *Chubutisaurus insignis* Del Corro, 1975 (Dinosauria: Neosauropoda) from the ‘middle’ Cretaceous of central Patagonia, Argentina. *Journal of*

Vertebrate Paleontology **31**: 93–110.

Carballido JL, Pol D, Rauhut O. in press. Osteology and phylogenetic relationships of *Tehuelchesaurus benitezii* (Dinosauria, Sauropoda) from the Upper Jurassic of Patagonia. *Zoological Journal of the Linnean Society.*

Chure D, Britt BB, Whitlock, JA, Wilson, JA. 2010. First complete sauropod dinosaur skull from the Cretaceous of the Americas and the evolution of sauropod dentition. *Naturwissenschaften* **97**: 379–391.

Cope ED. 1877. On a gigantic saurian from the Dakota epoch of Colorado. *Paleontological Bulletin* **25**: 5–10.

Curry Rogers KA. 2005. Titanosauria: a phylogenetic overview. In: Curry Rogers KA, Wilson JA, eds. *The sauropods: evolution and paleobiology*. Berkeley and Los Angeles: University of California Press, 50–103.

Day JJ, Upchurch P, Norman DB, Gale AS, Powell HP. 2002. Sauropod trackways, evolution, and behavior. *Science* **296**: 1659.

Day JJ, Norman DB, Gale AS, Upchurch P, Powell HP. 2004. A Middle Jurassic dinosaur trackway site from Oxfordshire, UK. *Palaeontology* **47**: 319–348.

del Corro G. 1975. Un nuevo saurópodo del Cretácico *Chubutisaurus insignis* gen. et sp. nov. (Saurischia-Chubutisauridae nov.) del Cretácico Superior (Chubutiano), Chubut, Argentina, 12–16 August 1974. *Actas I Congreso Argentino de Paleontología y Bioestratigrafía,* Tucuman **2**: 229–240.

D’Emic MD, Wilson JA. 2011. New remains attributable to the holotype of the sauropod dinosaur *Neuquensaurus australis*, with implications for saltasaurine systematics. *Acta Palaeontologica Polonica* **56**: 61–73.

D’Emic MD, Wilson JA, Chatterjee S. 2009. The titanosaur (Dinosauria: Sauropoda) osteoderm record: review and first definitive specimen from India. *Journal of Vertebrate Paleontology* **29**: 165–177.

D’Emic MD, Wilson JA, Thompson R. 2010. The end of the sauropod dinosaur hiatus in North America. *Palaeogeography, Palaeoclimatology, Palaeoecology* **297**: 486–490.

D’Emic MD, Wilson JA, Williamson TE. in press. A sauropod dinosaur pes from the latest Cretaceous of North America and the validity of *Alamosaurus sanjuanensis* (Sauropoda: Titanosauria). Journal of Vertebrate Paleontology.

Gallina, P.A. and Apesteguía, S. 2011. Cranial anatomy and phylogenetic position of the titanosaurian sauropod *Bonitasaura salgadoi*. *Acta Palaeontologica Polonica* **56**: 45–60.

Gilmore CW. 1922. Discovery of a sauropod dinosaur from the Ojo Alamo Formation of New Mexico. *Smithsonian Miscellaneous Collections* **81**: 1–9.

Gilmore CW. 1933. Two new dinosaurian reptiles from Mongolia with notes on some fragmentary specimens. *American Museum Novitates* **679**: 1–20.

Gilmore CW. 1946. Reptilian fauna of the North Horn Formation of central Utah.

United States Geological Survey Professional Paper **210C**: 1–52.

Giménez, O. 2007. Skin impressions of Tehuelchesaurus (Sauropoda) from the Upper Jurassic of Patagonia. *Revista del Museo Argentino de Ciencias Naturales* **9**: 119–124.

Gomani E, Jacobs LL, Winkler DA. 1999. Comparison of the African titanosaurian, *Malawisaurus*, with an Early Cretaceous North American sauropod. Pp. 223–233 *in* Y. Tomida, T. H. Rich, & P. Vickers-Rich (eds) *Proceedings of the Second Gondwanan Dinosaur Symposium*, National Museum of Tokyo Monograph **15**.

González Riga BJ, Calvo JO. 2009. A new wide-gauge sauropod track site from the Late Cretaceous of Mendoza, Neuquén Basin, Argentina. *Palaeontology* 52: 631–640.

González Riga BJ, Previtera E, Pirrone CA. 2009. *Malarguesaurus florenciae* gen. et sp. nov., a new titanosauriform (Dinosauria, Sauropoda) from the Upper Cretaceous of Mendoza, Argentina. *Cretaceous Research* **30**: 135–148.

Gradstein FM, Ogg JG, Smith AG. 2004. *A geologic time scale 2004*. Cambridge: Cambridge University Press.

Haughton SH. 1928. On some reptilian remains from the Dinosaur beds of Nyasaland. *Transactions of the Royal Society of South America* **16**: 69–83.

He X, Li K, Cai K. 1988. [The Middle Jurassic Dinosaur fauna from Dashanpu, Zigong, Sichuan, Vol. IV. Sauropod dinosaurs (2), Omeisaurus tianfuensis]. Chengdu: Sichuan Scientific and Technical Publishing House. (In Chinese.)

Hocknull SA, White MA, Tischler TR, Cook AG, Calleja ND, Sloan T, Elliott DA. 2009. New mid-Cretaceous (latest Albian) dinosaurs from Winton, Queensland, Australia. PLoS ONE 4: e6190.

Ikejiri T. 2005. Distribution and biochronology of Camarasaurus (Dinosauria, Sauropoda) from the Jurassic Morrison Formation of the Rocky Mountain Region. *New Mexico Geological Society Field Conference Guidebook, Geology of the Chama Basin* **56**: 367–379.

Jacobs LL, Winkler DA, Downs WR, Gomani EM. 1993. New material of an Early Cretaceous titanosaurid sauropod dinosaur from Malawi. *Palaeontology* **36**: 523–534.

Janensch W. 1914. Übersicht über die Wirbeltierfauna der Tendaguru-Schichten, nebst einer kurzen Charakterisierung der neu aufgeführten Arten von Sauropoden. Archiv Für Biontologie **3:** 15–58.

Janensch W. 1929. Material und Formengehalt der Sauropoden in der Ausbeute der Tendaguru-Expedition. Palaeontographica (Suppl. 7) **2**: 1–34.

Janensch W. 1950. Die Wirbelsaule von *Brachiosaurus brancai*. Palaeontographica (Suppl. 7) 3:27–93.

Janensch W. 1961. Die Gliedmaßen und Gliedmassengürtel der Sauropoden der Tendaguru-Schichten. *Palaeontographica* (Supplement 7) **3:** 177–235.

Kearney M. 2002. Fragmentary taxa, missing data, and ambiguity: mistaken assumptions and conclusions. *Systematic Biology* **51:** 369–381.

Krause DW, O'Connor PM, Curry Rogers KC, Sampson SD, Buckley GA, Rogers RR. 2006. Late Cretaceous Terrestrial Vertebrates from Madagascar, Implications for Latin American Biogeography. *Annals of the Missouri Botanical Garden* **93**: 178–208.

Ksepka DT, Norell MA. 2006. *Erketu ellisoni*, a long-necked sauropod from Bor Guve (Dornogov Aimag, Mongolia). *American Museum Novitates* **3508**: 1–16.

Ksepka DT, Norell MA. **2010**. The illusory evidence for Asian Brachiosauridae: new material of *Erketu ellisoni* and a phylogenetic reappraisal of basal titanosauriformes. *American Museum Novitates* **3700**: 1–28.

Kues BS, Lehman T, Rigby JK Jr. 1980. The teeth of *Alamosaurus sanjuanensis*, a Late Cretaceous sauropod. *Journal of Paleontology* **54**: 864–868.

Lapparent AF de. 1943. Les dinosaruiens de Crétacé Supérieur du Midi de la France. *Mémoires de las Societé Géologique de France* **56**: 1–54.

Lapparent AF de. 1960. De les dinosauriens du 'continental intercalaire' du Sahara central. *Mémoires de las Societé Géologique de France* **88A**: 1–57.

Lapparent AF de, Zbyszewski G. 1957. Les dinosauriens du Portugal. *Mémoires des Services Géologiques du Portugal, nouvelle série* **2**: 1–63.

Lockley MG, Farlow JO, Meyer CA. 1994. *Brontopodus* and *Parabrontopodus ichnogen*. nov. and the significance of wide- and narrow-gauge sauropod trackways. *Gaia* **10**: 135–145.

Lehman TM, Coulson AB. 2002. A juvenile specimen of the sauropod dinosaur Alamosaurus sanjuanensis from the Upper Cretaceous of Big Bend National Park, Texas. *Journal of Paleontology* **76**: 156–172.

Le Loeuff J. 1993. European titanosaurs. *Revue de Paleobiologic* **7**: 105–117.

Longman HA. 1933. A new dinosaur from the Queensland Cretaceous. *Memoirs of the* Queensland Museum **10**: 131–144.

Lucas SG, Hunt AP. 1989. *Alamosaurus* and the sauropod hiatus in the Cretaceous of the North American western interior. Geological Society of America Special Paper **238**: 75–85.

Lydekker R. 1893. The dinosaurs of Patagonia. *Anales del Museo de La Plata* **2**: 1–14.

Lydekker R. 1895. On bones of a sauropodous dinosaur from Madagascar. *Quarterly Journal of the Geological Society of London* **51**: 329–336.

Maddison WP, Maddison DR. 1992. MacClade, Version 3.0. Sunderland, Massachusetts: Sinauer.

Maddison WP, Maddison DR. 2009. *Mesquite: a modular* system for evolutionary analysis, v2.71. Available at http://mesquiteproject.org.

Mannion, PD. 2009. A revision of the sauropod dinosaur genus '*Bothriospondylus*' with a redescription of the type material of the Middle

Jurassic form '*B. madagascariensis*. *Palaeontology* **53**, 277–296.

Mannion PD. In press. A reassessment of *Mongolosaurus haplodon* Gilmore, 1933, a titanosaurian sauropod dinosaur from the Early Cretaceous of Inner Mongolia, People's Republic of China. *Journal of Systematic Palaeontology*.

Mannion PD, Upchurch P. 2011. A re-evaluation of the 'mid-Cretaceous sauropod hiatus' and the impact of uneven sampling of the fossil record on patterns of regional dinosaur extinction. *Palaeogeography, Palaeoclimatology, Palaeoecology* **299**: 529–540.

Mannion PD, Calvo JO. In press. Anatomy of the basal titanosaur (Dinosauria, Sauropoda) *Andesaurus delgadoi* from the mid-Cretaceous (Albian–early Cenomanian) Río Limay Formation, Neuquén Province, Argentina: implications for titanosaur systematics. Zoological Journal of the Linnean Society.

Mantell, GA. 1852. On the structure of the *Iguanodon*, and on the fauna and flora of the Wealden Formation. *Proceedings of the Royal Institute of Great Britain* **1**: 141–146.

Marsh OC. 1884. Principal characters of American Jurassic dinosaurs, Part VII. On the Diplodocidae, a new family of the Sauropoda. *American Journal of Science (series 3)* **27**: 161–167.

Mateer NJ, McIntosh JS. 1985. A new reconstruction of the skull of *Euhelopus zdanskyi* (Saurischia: Sauropoda). *Bulletin of the Geological Institutions of the University of Uppsala,New Series* **11**: 125–132.

Martin V, Buffetaut E, Suteethorn V. 1994. A new genus of sauropod dinosaur from the Sao Khua Formation (Late Jurassic or Early Cretaceous) of northeastern Thailand. *Comptes Rendus de l'Academie des Sciences de Paris* **319**: 1085–1092.

Martinelli AG, Forasieppi AM. 2004. Late Cretaceous vertebrates from Bajo de Santa Rosa (Allen Formation), Río Negro Province, Argentina, with the description of a new sauropod dinosaur (Titanosauridae). *Revista del Museo Argentino de Ciencias Naturales* **6***:* 257–305.

McIntosh JS. 1990. Sauropoda. In: Weishampel DB, Dodson P, Osmólska H, eds. *The Dinosauria*, 1st edn. Berkeley:University of California Press, 345–401.

McIntosh JS, Miles CA, Cloward KC, Parker JR. 1996. A new nearly complete skeleton of *Camarasaurus*. *Bulletin of* Gunma Museum of Natural History **1**: 1–87.

Monbaron M, Russell DA, Taquet P. 1999. *Atlasaurus imelakei*, n. g., n. sp., a brachiosaurid-like sauropod from the Middle Jurassic of Morocco. *Comptes Rendus de l'Académie Des Sciences, Paris* **329**: 519–526.

Osborn HF, Mook CC. 1921. *Camarasaurus*, *Amphicoelias*, and other sauropods of Cope. *Memoirs of the American* Museum of Natural History **3**: 247–387.

Ostrom JH, McIntosh JS. 1966. Marsh's Dinosaurs. Yale University Press, New

Haven, 388 pp.

Paul GS. 1988. The brachiosaur giants of the Morrison and Tendaguru with a description of a new subgenus, Giraffatitan, and a comparison of the world's largest dinosaurs. Hunteria **2**: 1–14.

Powell, J.E. 1992. Osteología de *Saltasaurus loricatus* (Sauropoda–Titanosauridae) del Cretácico Superior del noroeste Argentino. In: J Sanz, A Buscalioni eds. *Los Dinosaurios y Su Entorno Biotico: Actas del Segundo Curso de Paleontología en Cuenca*, 165–230.

Ratkevitch R. 1998. New Cretaceous brachiosaurid dinosaur, *Sonorasaurus thompsoni* gen. et sp. nov, from Arizona. *Journal of the Arizona-Nevada Academy of Science* **31**: 71–82.

Rauhut OWM. 2006. A brachiosaurid sauropod from the Late Jurassic Cañadón Calcáreo Formation of Chubut, Argentina. *Fossil Record* **9**: 226–237.

Rauhut OWM, Lopez-Arbarello A. 2009. Considerations on the age of the Tiouaren Formation (Iullemmeden Basin, Niger, Africa): implications for Gondwanan Mesozoic terrestrial vertebrate fauna. *Palaeogeography, Palaeoclimatology, Palaeoecology* 271: 259–267.

Rich TH, Vickers-Rich P, Gimenez O, Cúneo R, Puerta P, Vacca R. 1999. A new sauropod dinosaur from Chubut Province, Argentina. *National* Science Museum Monographs **15**: 61–84.

Riggs ES. 1903. Structure and relationships of opisthocoelian dinosaurs. Part I: *Apatosaurus* Marsh. *Field Columbian* Museum Geological Series **2:** 165–196.

Rose P. 2007. A titanosauriform (Dinosauria: Saurischia) from the Early Cretaceous of Central Texas and its phylogenetic relationships. *Palaeontologica Electronica* **10**: 1–65. Royo Torres 2009

Royo Torres R, Cobos A. 2009. Turiasaur sauropods in the Tendaguru beds of Tanzania. *Journal of Vertebrate Paleontology* **29**: 173A.

Salgado L, Calvo JO. 1997. Evolution of titanosaurid sauropods. II: The cranial evidence. *Ameghiniana* **34**: 33–48.

Salgado L, Azpilicueta C. 2000. Un nuevo saltasaurino (Sauropoda, Titanosauridae) de la provincia de Río Negro (Formación Allen, Cretácico Superior), Patagonia, Argentina *Ameghiniana* **37**: 259–264.

Salgado L, Coria RA, Calvo J. 1997. Evolution of titanosaurid sauropods. I: phylogenetic analysis based on the postcranial evidence. *Ameghiniana* **34**: 3–32.

Sánchez-Hernández B. 2005. *Galveosaurus herreroi*, a new sauropod dinosaur from Villar del Arzobispo Formation (Tithonian-Berriasian) of Spain. *Zootaxa* **1034**: 1–20.

Sander PM, Mateus O, Laven T, Knötschke N. 2006. Bone histology indicates insular dwarfism in a new Late Jurassic sauropod dinosaur. *Nature* **441**: 739–741.

Santos VF, Lockley MG, Meyer CA, Carvalho J, Galopim de Carvalho AM, Moratalla JJ. 1994. A new sauropod tracksite from the Middle Jurassic of

Portugal. *Gaia* **10**: 5–14.

Sereno PC. 1999. Dinosaurian biogeography: vicariance, dispersal and regional extinction. In: Tomida Y, Rich TH, Vickers-Rich P, eds. Proceedings of the second Gondwanan *dinosaur symposium*. Tokyo: National Science Museum Monographs, 249–257.

Sereno PC. 2007. Logical basis for morphological characters in phylogenetics. *Cladistics* **23**: 565–587.

Sereno PC. 2009. Comparative cladistics. *Cladistics* **25**: 624–659.

Sereno PC, Beck AL, Dutheil DB, Larssen HCE, Lyon GH, Moussa B, Sadleir RW, Sidor CA, Varricchio DJ, Wilson GP, Wilson JA. 1999. Cretaceous sauropods from the Sahara and the uneven rate of skeletal evolution among dinosaurs. *Science* 286: 1342–1347.

Stein K, Cziki Z, Curry Rogers KC, Weishampel DB, Redelstorff R, Carballido JL, Sander PM. 2010. Small body size and extreme cortical bone remodeling indicate phyletic dwarfism in *Magyarosaurus dacus* (Sauropoda: Titanosauria). *Proceedings of the National Academy of Sciences* **107**: 9258–9263.

Sullivan RM, Lucas SG. 2000. Alamosaurus (Dinosauria: Sauropoda) from the Late Campanian of New Mexico and its significance. *Journal of Vertebrate Paleontology* **20**: 400–403.

Swofford DL. 2002. PAUP*: phylogenetic analysis using parsimony (*and other methods), Version 4.0b10. Sunderland: Sinauer Associates.

Tang F, Jing X, Kang X, Zhang G. 2001. *[Omeisaurus maoianus*: a complete sauropod from Jingyuan, Sichuan]. Beijing: China Ocean Press. (In Chinese.)

Taylor M. 2009. A reevaluation of *Brachiosaurus altithorax* Riggs, 1903 (Dinosauria, Sauropoda) and its generic separation from *Brachiosaurus brancai* (Janensch, 1914). *Journal of Vertebrate Paleontology* **29**: 787–806.

Taylor MP, Naish D. 2007. An unusual new neosauropod dinosaur from the Lower Cretaceous Hastings Beds Group of East Sussex, England. *Palaeontology* **50**: 1547–1564.

Taylor MP, Wedel MJ, Cifelli RL. 2011. A new sauropod dinosaur from the Lower Cretaceous Cedar Mountain Formation, Utah, USA. *Acta Palaeontologica Polonica* 56: 75–98.

Templeton A. 1983. Phylogenetic inference from restriction endonuclease cleavage site maps with particular reference to the evolution of humans and apes. *Evolution* 37: 221–244.

Tidwell V, Carpenter K, Brooks W. 1999. New sauropod from the Lower Cretaceous of Utah, USA. *Oryctos* **2**: 21–37.

Tidwell V, Carpenter, K, Meyer S. 2001. New titanosauriform (Sauropoda) from the Poison Strip Member of the Cedar Mountain Formation (Lower Cretaceous), Utah. In: D. Tanke & K. Carpenter, eds. *Mesozoic Vertebrate Life: New Research Inspired by the Paleontology of Phillip J. Currie.*

Bloomington: Indiana University Press, 139–165.

Tidwell V, Wilhite DR. 2005. Ontogenetic variation and isometric growth in the forelimb of the Early Cretaceous sauropod *Venenosaurus*. In: K. Carpenter & V. Tidwell eds. *Thunder-Lizards: The Sauropodomorph Dinosaurs.* Indiana University Press, Bloomington, 187–196.

Upchurch P. 1995. The evolutionary history of sauropod dinosaurs. Philosophical Transactions of the Royal Society of *London* **349:** 365–390.

Upchurch P. 1998. The phylogenetic relationships of sauropod dinosaurs. Zoological Journal of the Linnean Society **124:** 43–103.

Upchurch P, Barrett PM, Dodson P. 2004. Sauropoda. In: Weishampel DB, Dodson P, Osmólska H, eds. *The Dinosauria*, 2nd edn. Berkeley: University of California Press, 259–322.

Upchurch P, Hunn CA, Norman DB. 2002. An analysis of dinosaurian biogeography: evidence for the existence of vicariance and dispersal patterns caused by geological events. *Proceedings of the Royal Society of London B* **269:** 613–621.

Upchurch, P, Mannion, PD, Barrett, PM. in press. Sauropod dinosaurs. In: Wealden Fossils. ed. D. Batten.The Palaeontological Association, Fieldguides To Fossils.

Wedel MJ, Cifelli RL, Sanders RK. 2000a. *Sauroposeidon proteles*, a new sauropod from the Early Cretaceous of Oklahoma. *Journal of Vertebrate Paleontology* **20**: 109–114.

Wedel MJ, Cifelli R, Sanders RK. 2000b. Osteology, paleobiology, and relationships of the sauropod dinosaur *Sauroposeidon*. *Acta Paleontologica Polonica* **45**: 343–388.

Wedel MJ, Cifelli R. 2005. *Sauroposeidon*: Oklahoma's Native Giant. *Oklahoma Geology Notes* **65**: 40–57.

Whitlock JA, D'Emic MD, Wilson JA. 2011. Cretaceous diplodocids in Asia? Re-evaluating the affinities of a fragmentary specimen. Palaeontology **54**: 351–364.

Wild R. 1991. *Janenschia* n. g. *robusta* (E. Fraas 1908) pro *Tornieria robusta* (E. Fraas 1908) (Reptilia, Saurischia, Sauropodomorpha). Stuttgarter Beiträge zur Naturkunde, Serie B (Geologie und Paläontologie) **173**: 1–4.

Wilson JA. 1999. A nomenclature for vertebral laminae in sauropods and other saurischian dinosaurs. *Journal of Vertebrate* Paleontology **19:** 639–653.

Wilson JA. 2002. Sauropod dinosaur phylogeny: critique and cladistic analysis. Zoological Journal of the Linnean Society **136:** 217–276.

Wilson JA. 2005. Redescription of the Mongolian sauropod *Nemegtosaurus mongoliensis* Nowinski (Dinosauria: Saurischia) and comments on Late Cretaceous sauropod diversity. Journal of Systematic Paleontology **3:** 283–318.

Wilson JA, Sereno PC. 1998. Early evolution and higher level phylogeny of sauropod dinosaurs. *Society of Vertebrate* Paleontology Memoir **5:** 1–68.

Wilson JA, Carrano MT. 1999. Titanosaurs and the origin of 'wide-gauge' trackways: a biomechanical and systematic perspective on sauropod locomotion. *Paleobiology* **25**: 252–267.

Wilson JA, Upchurch P. 2003. A revision of Titanosaurus Lydekker (Dinosauria-Sauropoda), the first dinosaur genus with a 'Gondwanan' distribution. *Journal of Systematic Palaeontology* **1**: 125–160.

Wilson JA, Upchurch P. 2009. Redescription and reassessment of the phylogenetic affinities of *Euhelopus zdanskyi* (Dinosauria: Sauropoda) from the Early Cretaceous of China. *Journal of Systematic Palaeontology* **7**: 199–239.

Wilson JA, D'Emic, MD, Ikejiri T, Moacdieh E, Whitlock JA. 2011. A nomenclature for vertebral fossae in sauropods and other saurischian dinosaurs. PLOS One, e17114.

Wiman C. 1929. Die Kreide-Dinosaurier aus Shantung. *Palaeontologia Sinica (series C)* **6**: 1–67.

Xu, X, Zhang, X, Tan, Q, Zhao, X, Tan, L. 2006. A new titanosaurian sauropod from Late Cretaceous of Nei Mongol, China. *Acta Geologica Sinica* **80**: 20–26.

You H-L, Li D-Q, Zhou L-Q, Ji Q. 2008. *Daxiatitan binglingi*: a giant sauropod dinosaur from the Early Cretaceous of China. *Gansu Geology* 17: 1–10.

You H-L, Li D-Q. 2009. The first well-preserved Early Cretaceous brachiosaurid dinosaur in Asia. *Proceedings of the Royal Society of London, Series B*: doi:10.1098/rspb.2009.1278.

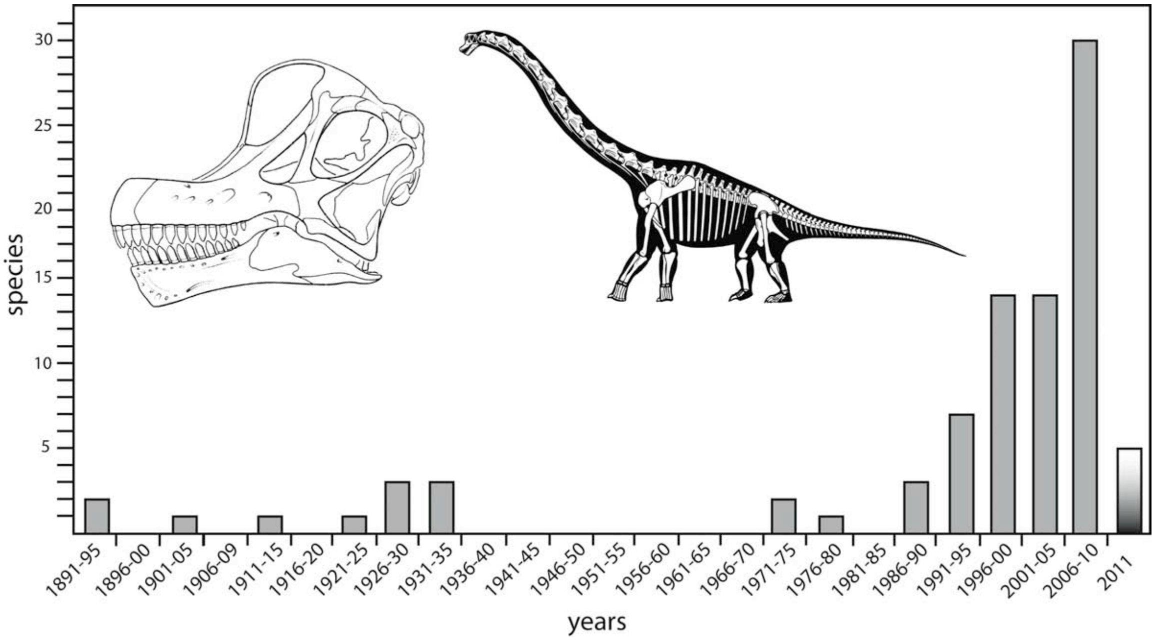

Figure 4.1. Titanosauriform discoveries plotted in five-year bins. Note the dramatic increase in naming in recent years. The skull and body of *Giraffatitan* (modified from Wilson and Sereno, 1998) highlight basal titanosauriform anatomy.

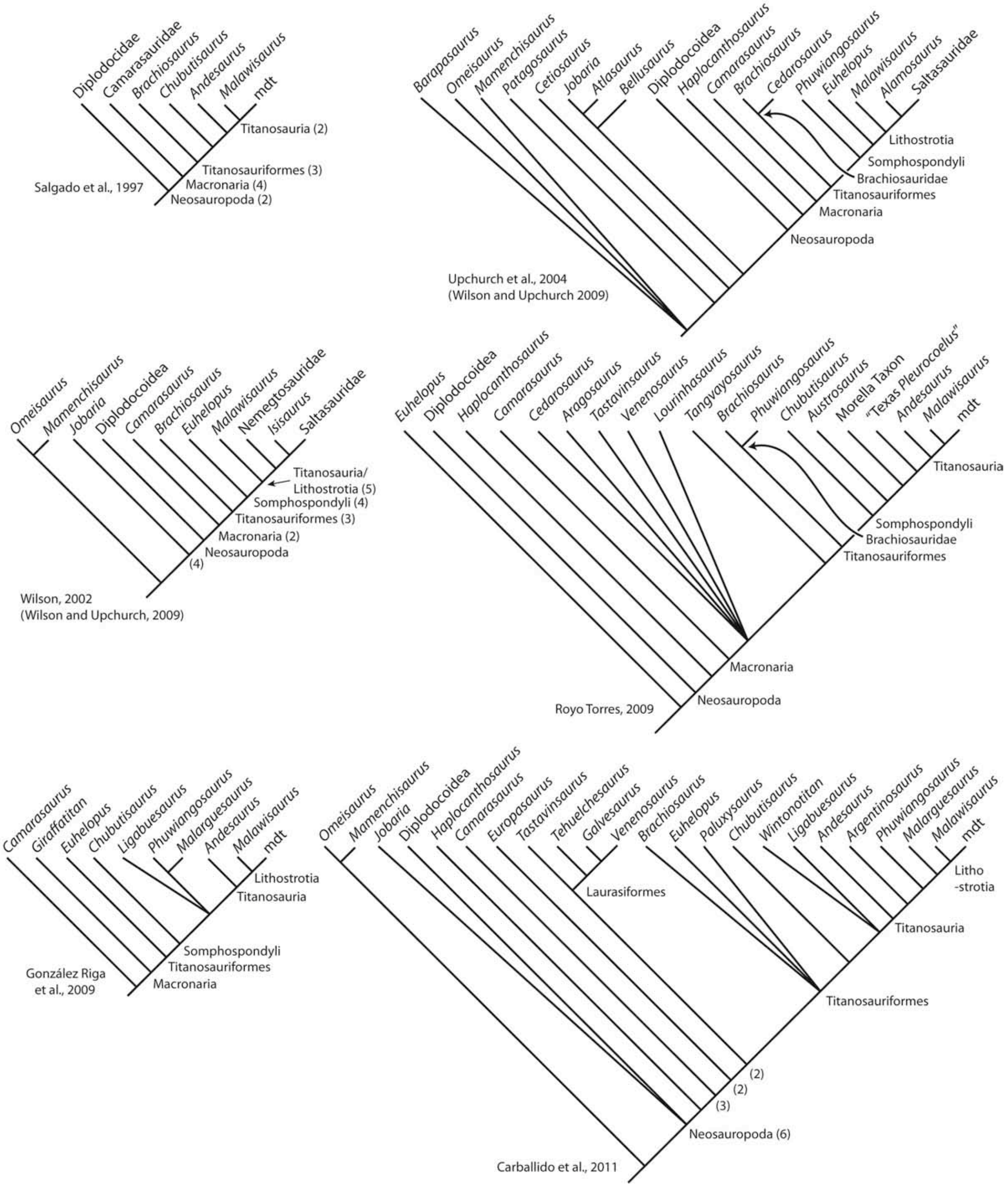

Figure 4.2. Select previous cladistic hypotheses for the relationships of basal titanosauriforms, with their authors listed near their root. Numbers near each node indicate decay indices calculated in PAUP*. Abbreviations: mdt, more derived titanosaurs.

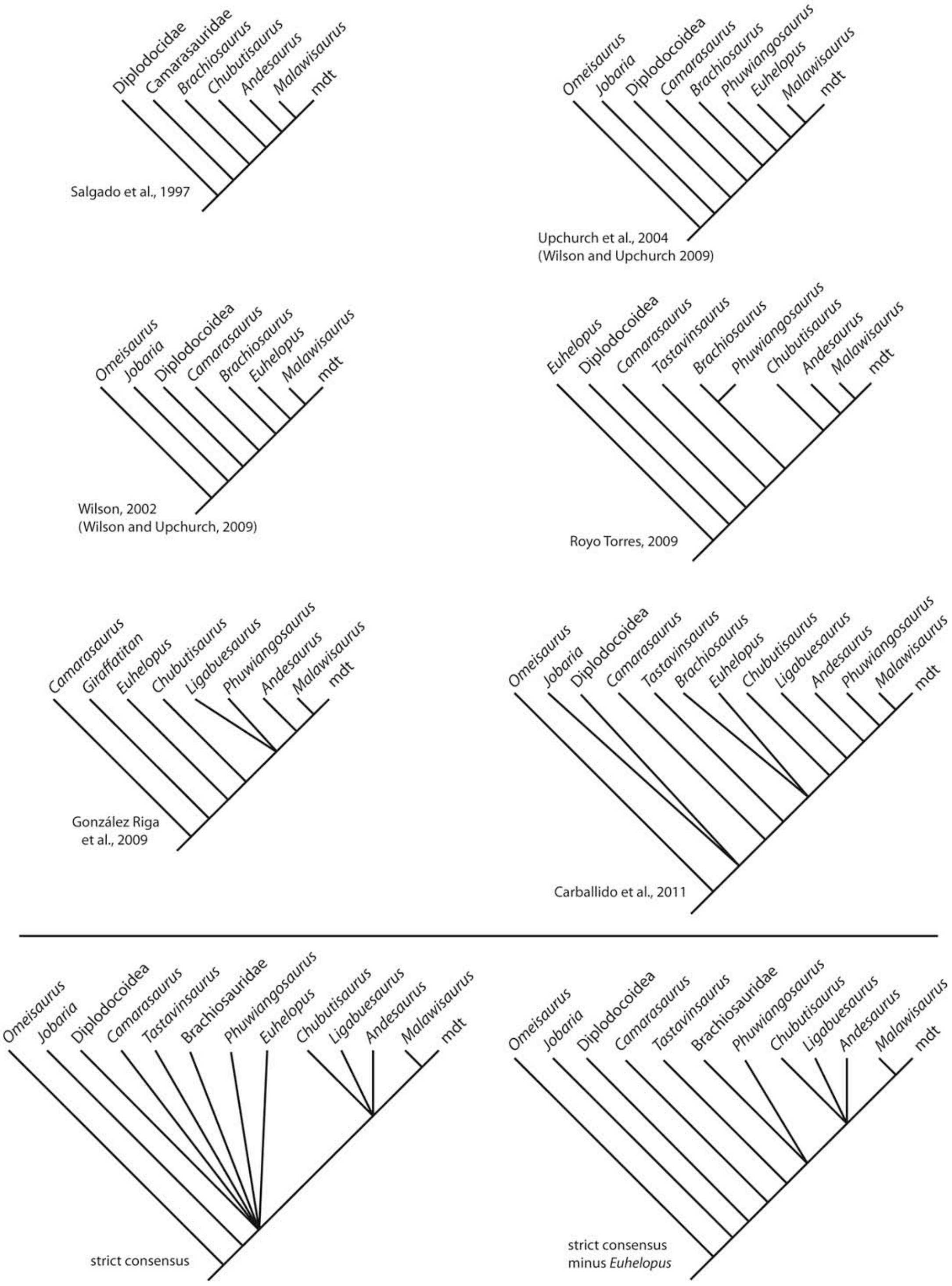

Figure 4.3. Parsed versions of the cladograms presented in Figure 4.2, with their authors listed near their root. Only taxa appearing in at least half of those analyses are included here. A strict consensus of these analyses with and without *Euhelopus* are shown below.

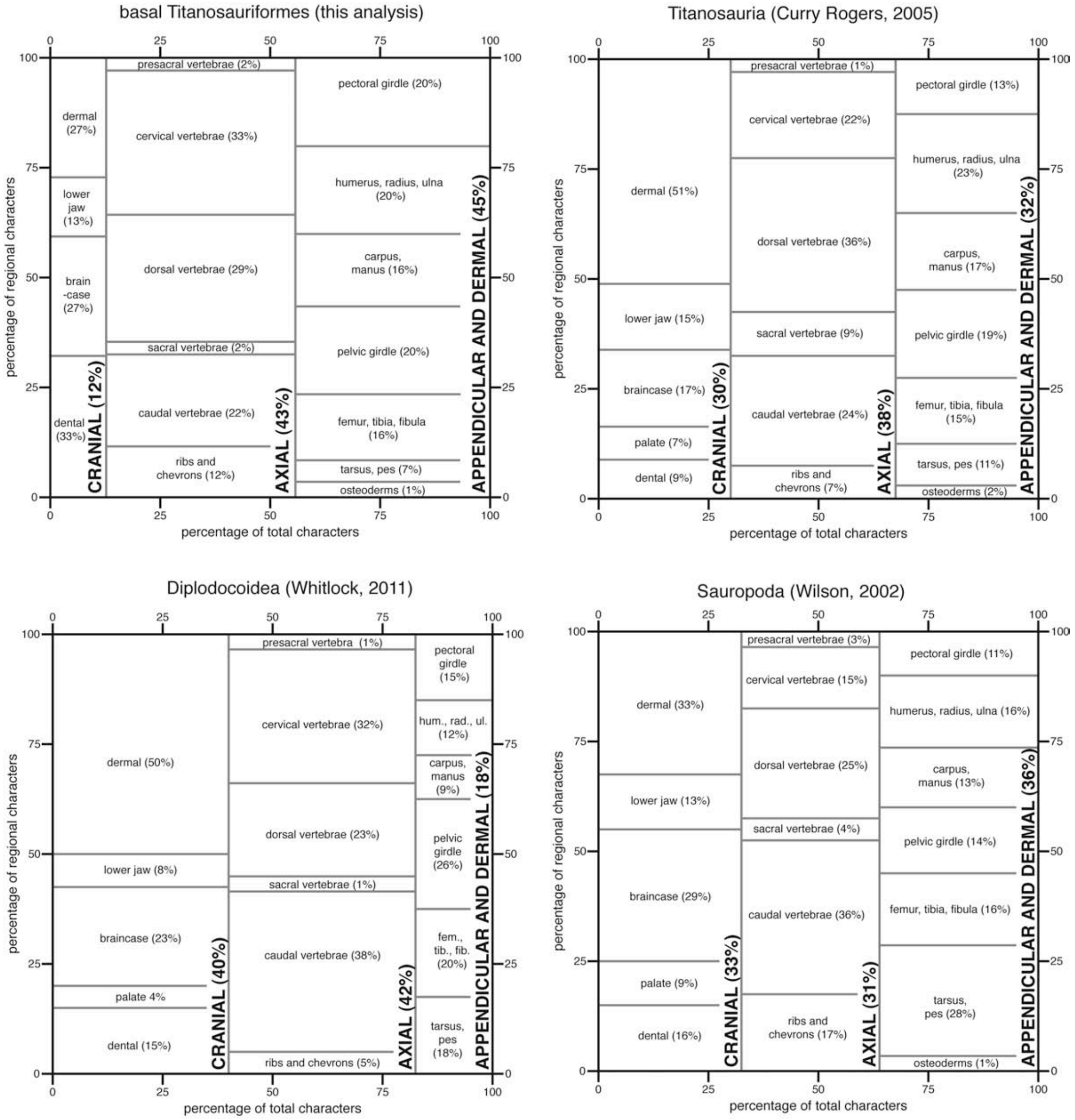

Figure 4.4. Character maps for some cladistic analyses of sauropod dinosaurs. The analysis presented in this study incorporates few cranial characters, reflecting the poor fossil record for titanosauriform skulls and standing in contrast to the pattern of character distribution in Diplodocoidea. Analyses that are wider in scope such as that of Wilson (2002) have a more even distribution of characters throughout the body.

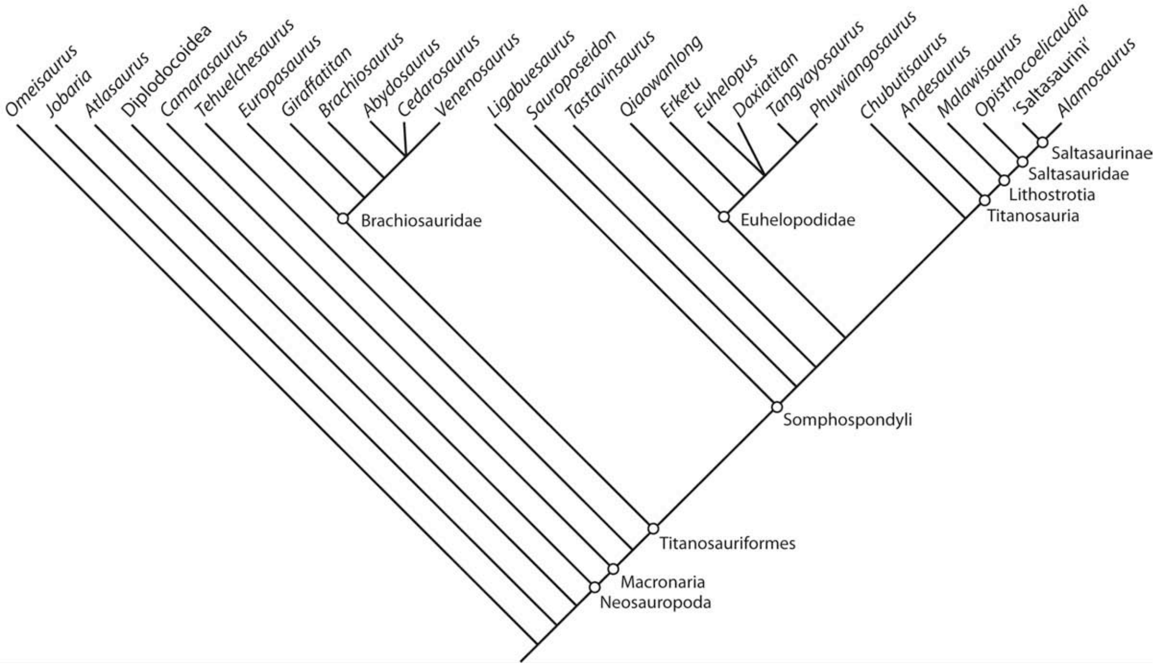

Figure 4.5. Cladistic hypothesis presented in this study. The cladogram is a strict consensus of 9 equally parsimonious trees. Clade names as defined by phylogenetic taxonomy (Table 4.1; Wilson and Upchurch, 2003) are listed beside each node.

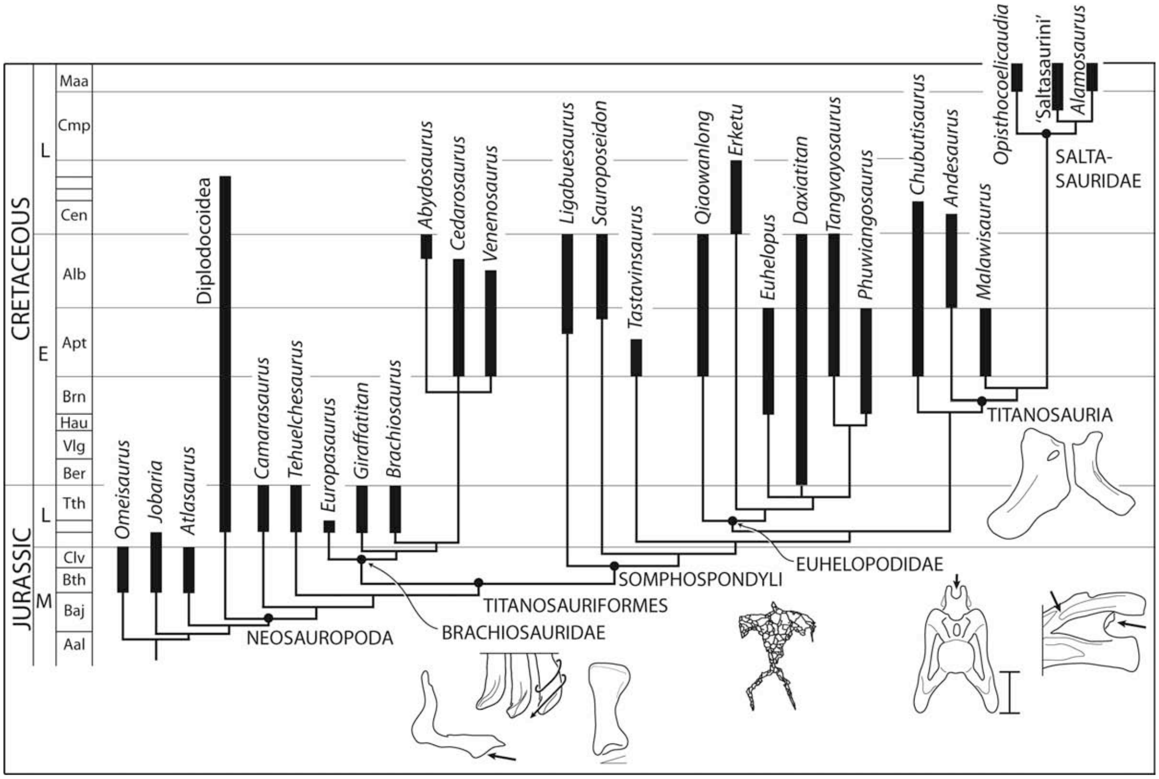

Figure 4.6. Phylogenetic hypothesis presented in this study plotted on a geologic timescale (Gradstein, 2004), with relevant clade names (Table 4.1) labeled. Select synapomorphies highlighting some nodes are highlighed. Brachiosauridae: quadratojugal with triangular ventral prong (shown here in *Europasaurus*), twisted maxillary teeth (shown here in *Giraffatitan*), beveled distal end of metatarsal IV (shown here in *Sonorasaurus*). Somphospondyli: somphospondylus vertebral pneumaticity, consisting of sub-centimeter and sub-millimeter cells and walls, respectively, that permeate the vertebra (shown here in *Saruoposeidon*). Euhelopodidae: cervical vertebrae with bifid neural spines, pendant cervical ribs, a thick, vertically oriented epipophyseal–prezygapophyseal lamina (eprl), a 'kinked' intrapostzygapophyseal lamina (shown here in *Erketu*). Titanosauria: platelike ischium (shown here in *Andesaurus*). Also shown here are a short ischium (a synapomorphy of *Sauroposeidon* plus more derived somphospondyls) and a raised tubercle on the lateral ischium (a titanosauriform synapomorphy).

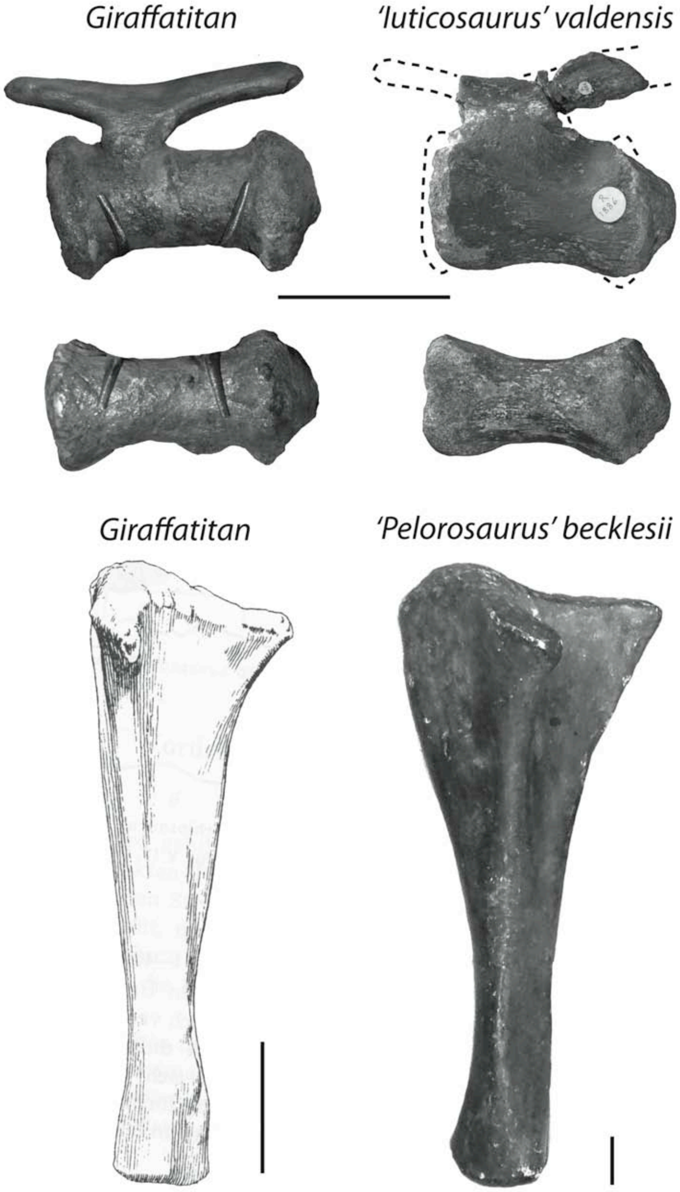

Figure 4.7. Purported early 'titanosaur' species in comparison with a basal titanosauriform (*Giraffatitan*). The caudal vertebral procoely of '*Iuticosaurus*' and curved/raised ulnar olecranon of '*Pelorosaurus*' *becklesii* are indistinguishable from the situation in *Giraffatitan*. Scale bar equals 5 cm in A, 10 cm in B–D.

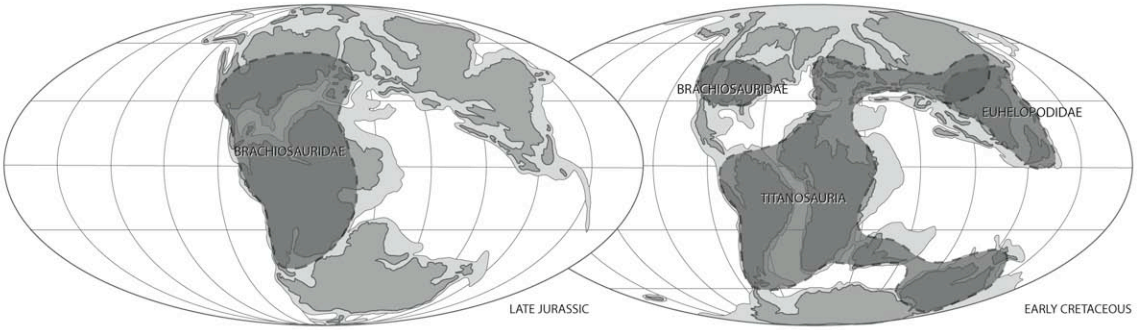

Figure 4.8. Titanosauriform paleobiogeography. The Early Cretaceous is characterized by some endemism, with mostly brachiosaurids in North America, mostly euhelopodids in Asia, and mostly titanosaurs in South America. Dark grey signifies geographic range, medium grey indicates land, and light grey indicates shallow seas. Paleogeographic reconstructions modified from Blakey, 2006.

Table 4.1. Recommended phylogenetic nomenclature for select clades within Titanosauriformes and its outgroups. Definitions follow Wilson and Sereno (1998), Wilson and Upchurch (2003), and Taylor (2009). Abbreviations: MRCA = most recent common ancestor

clade	**definition**	**reference/author**
Neosauropoda	*Diplodocus longus*, *Saltasaurus loricatus*, MRCA and all its descendants	Bonaparte, 1986
Macronaria	neosauropods more closely related to *Saltasaurus loricatus* than to *Diplodocus longus*	Wilson and Sereno, 1998
Euhelopodidae	neosauropods more closely related to *Euhelopus zdanskyi* than to *Neuquensaurus australis*	new definition
Titanosauriformes	*Brachiosaurus altithorax*, *Saltasaurus loricatus*, MRCA and all its descendants	Salgado, Coria, and Calvo 1997
Brachiosauridae	neosauropods more closely related to *Brachiosaurus altithorax* than to *Saltasaurus loricatus*	Riggs, 1903
Somphospondyli	neosauropods more closely related to *Saltasaurus loricatus* than to *Brachiosaurus altithorax*	Wilson and Sereno, 1998
Titanosauria	*Andesaurus delgadoi*, *Saltasaurus loricatus*, MRCA and its descendants	Bonaparte and Coria, 1986
Lithostrotia	*Malawisaurus dixeyi*, *Saltasaurus loricatus*, MRCA and its descendants	Upchurch et al., 2004

Table 4.2. Comparison of seven recent cladistic analyses including a substantial number of basal titanosauriform sauropod dinosaurs. Character numbers in parentheses indicate the total number of characters included (i.e., including constant and parsimony-uninformative ones). Abbreviations: CI = consistency index; MPTs = most parsimonious trees; RI = retention index, TSFs, Titanosauriformes

Analysis	**Ingroup taxa**	**# recovered as non-titanosaur TSFs**	**# char-acters**	**MPTs**
Salgado et al., 1997	10	2	38	1
Wilson, 2002 (Wilson and Upchurch, 2009)	27	2	234	3
Canudo et al., 2008	17	3	217 (246)	9
González Riga et al., 2009	22	6	84 (102)	2
Upchurch, 2004 (Wilson and Upchurch, 2009)	34	4	309 (311)	97
Royo Torres, 2009	24	6	295 (399)	5
Carballido et al., 2011	28	6	227 (289)	12
This analysis	**25**	**16**	**114**	**9**

Table 4.3. Geological age, geographical range, percent missing data, and original reference for two outgroups (*Omeisaurus*, *Jobaria*) and 25 terminal taxa analysed

Taxon	**geological age (stage)**	**geographic range**	**Original reference**
Omeisaurus	Middle Jurassic (Bathonian–Callovian	Asia (China)	Young, 1939
Jobaria tiguidensis	Middle of Late Jurassic (Bathonian–Oxfordian	Africa (Niger)	Sereno et al., 1999
Atlasaurus imelaki	Middle Jurassic (Bathonian–Callovian	Africa (Morocco)	Monbaron et al., 1999
Diplodocoidea	Late Jurassic–Late Cretaceous (Kimmeridgian–Coniacian)	North America (United States), Europe (various), Africa (Niger), South America (Argentina)	Marsh, 1884; Upchurch, 1995
Camarasaurus	Late Jurassic (Kimmeridgian–Tithonian)	North America (United States)	Cope, 1877
Tehuelchesaurus benitezii	Late Jurassic (Kimmeridgian–Tithonian)	South America (Argentina)	Rich et al., 1999
Europasaurus holgeri	Late Jurassic (Kimmeridgian)	Europe (Germany)	Sander et al., 2006
Giraffatitan brancai	Late Jurassic (Kimmeridgian–Tithonian)	Africa (Tanzania)	Janensch, 1914; Paul, 1988
Brachiosaurus altithorax	Late Jurassic (Kimmeridgian–Tithonian)	North America (United States)	Riggs, 1903
Cedarosaurus weiskopfae	Early Cretaceous (Aptian–Albian)	North America (United States)	Tidwell et al., 1999
Venenosaurus dicrocei	Early Cretaceous (Aptian–Albian)	North America (United States)	Tidwell et al., 2001
Abydosaurus mcintoshi	Early Cretaceous (late Albian)	North America (United States)	Chure et al., 2010
Ligabuesaurus leanzi	Early Cretaceous (Aptian–Albian)	South America (Argentina)	Bonaparte et al., 2006
Sauroposeidon proteles	Early Cretaceous (Aptian–Albian)	North America (United States)	Wedel et al., 2000a

Taxon	**geological age (stage)**	**geographic range**	**Original reference**
Chubutisaurus insignis	Early or Late Cretaceous (Aptian–Cenomanian)	South America (Argentina)	del Corro, 1975
Tastavinsaurus sanzi	Early Cretaceous (Aptian)	Europe (Spain)	Canudo et al., 2008
Qiaowanlong kangxii	Early Cretaceous (Aptian–Albian)	Asia (China)	You and Li, 2009
Erketu ellisoni	Late Cretaceous (Cenomanian–Santonian)	Asia (Mongolia)	Ksepka and Norell, 2006; 2010
Daxiatitan binglingi	Early Cretaceous	Asia (China)	You et al., 2008
Euhelopus zdanskyi	Early Cretaceous (Barremian–Aptian)	Asia (China)	Wiman, 1929
Phuwiangosaurus sirindhornae	Early Cretaceous (Barremian–Aptian)	Asia (Thailand)	Martin et al., 1994
Tangvayosaurus hoffeti	Early Cretaceous (Aptian–Albian)	Asia (Laos)	Allain et al., 1999
Andesaurus delgadoi	Early or Late Cretaceous (Albian–Cenomanian)	South America (Argentina)	Calvo and Bonaparte, 1991
Malawisaurus dixeyi	Early Cretaceous (Aptian)	Africa (Malawi)	Haughton, 1928; Jacobs et al., 1993
Opisthocoelicaudia skarzynskii	Late Cretaceous (Maastrichtian)	Asia (Mongolia)	Borsuk-Bialynicka, 1977
Alamosaurus sanjuanensis	Late Cretaceous (Maastrichtian)	North America (United States)	Gilmore, 1922
‘Saltasaurini’ *(Saltasaurus, Neuquensaurus, Rocasaurus)*	Late Cretaceous (Campanian–Maastrichtian)	South America (Argentina)	Powell, 1992; Lydekker, 1893; Salgado & Azpilicueta, 2000

Table 4.4. Missing data in the outgroups and terminal taxa analysed, broken down by anatomical region

Taxon	**Cranial**	**Axial**	**Appendicul ar/dermal**	**Total**
Omeisaurus	0.0	11.8	9.8	8.8
Jobaria tiguidensis	6.7	0.0	1.9	1.8
Atlasaurus imelaki	60.0	76.5	88.2	78.9
Diplodocoidea	0.0	0.0	0.0	0.0
Camarasaurus	0.0	0.0	0.0	0.0
Tehuelchesaurus benitezii	100.0	56.9	47.1	58.8
Europasaurus holgeri	13.3	37.3	50.9	39.5
Giraffatitan brancai	0.0	9.8	1.9	5.3
Brachiosaurus altithorax	100.0	56.9	66.7	65.8
Cedarosaurus weiskopfae	100.0	49	49.0	55.3
Venenosaurus dicrocei	100.0	70.6	62.7	71.9
Abydosaurus mcintoshi	0.0	76.5	80.4	67.5
Ligabuesaurus leanzi	93.3	64.7	47.1	62.3
Sauroposeidon proteles	93.3	13.7	17.6	26.3
Chubutisaurus insignis	100.0	56.9	47.1	58.8
Tastavinsaurus sanzi	100.0	43.1	60.8	57.0
Qiaowanlong kangxii	100.0	86.3	82.4	85.9
Erketu ellisoni	100.0	78.4	84.3	83.3
Daxiatitan binglingi	100.0	52.9	80.4	71.1
Euhelopus zdanskyi	46.7	31.4	29.4	33.3
Phuwiangosaurus sirindhornae	46.7	0.0	25.5	17.5
Tangvayosaurus hoffeti	100.0	60.8	66.7	67.5
Andesaurus delgadoi	100.0	50.9	76.5	67.5

Taxon	**Cranial**	**Axial**	**Appendicular/dermal**	**Total**
Malawisaurus dixeyi	33.3	13.7	41.2	26.3
Opisthocoelicaudia skarzynskii	100.0	31.4	11.8	32.5
Alamosaurus sanjuanensis	86.7	7.8	5.9	17.5
'Saltasaurini' *(Saltasaurus, Neuquensaurus, Rocasaurus)*	73.3	7.8	15.7	20.2
Average	**65**	**39**	**43**	**44**

Table 4.5. Ambiguous character state optimizations attributable to missing data based on two optimization strategies in PAUP* (Swofford, 2000). Delayed transformations (DELTRAN) favour parallelism over reversals; accelerated transformations (ACCTRAN) favour reversals over parallelisms. Abbreviations: mdb, more derived brachiosaurids; mde, more derived euhelopodids; mdn, more derived neosauropods; mdsa, more derived sauropods; mdso, more derived somphospondylans; mdt, more derived titanosaurs. Italicization indicates characters that have ambiguous changes in other parts of the cladogram that are instead due to character conflict (Table 6)

Character number	**ACCTRAN**	**DELTRAN**
41, 61, 110	*Atlasaurus* + Neosauropoda	Neosauropoda
36, 38	Neosauropoda	Macronaria
21, 49, 54, 55, 62, 64, 87–89, 92–94, 96, 108	*Tehuelchesaurus* + Titanosauriformes	Titanosauriformes
29, *113*	*Tehuelchesaurus* + Titanosauriformes	Somphospondyli
31, 33	Titanosauriformes, Euhelopodidae	Somphospondyli, *Euhelopus* + mde
3, 9, 52, 78, 114	Brachiosauridae	*Giraffatitan* + mdb
53	Brachiosauridae	*Giraffatitan*
90	*Giraffatitan* + mdb	*Abydosaurus* + mdb
95	*Giraffatitan* + mdb, (*Chubutisaurus* + Titanosauria)	*Giraffatitan*, Saltasaurinae
10	*Brachiosaurus* + mdb	*Abydosaurus*
13	*Brachiosaurus* + mdb; Somphospondyli	*Abydosaurus* + mdb; (*Chubutisaurus* + Titanosauria) + Euhelopodidae
5, 14	Somphospondyli	Euhelopodidae + (*Chubutisaurus* + Titanosauria)
98	Somphospondyli	*Sauroposeidon* + mdso
17	Somphospondyli	*Euhelopus* + mde
85	Somphospondyli	Saltasauridae

Character number	ACCTRAN	DELTRAN
71	*Tastavinsaurus* + mdso	Euhelopodidae + (*Chubutisaurus* + Titanosauria)
73	*Tastavinsaurus* + mdso	Lithostrotia
24	Euhelopodidae	*Erketu* + mde
29, 30, 31, 32, 46	Euhelopodidae	*Euhelopus* + mde
112	Euhelopodidae	*Euhelopus*
53, 62	Euhelopodidae	*Phuwiangosaurus* + *Tangvayosaurus*
92	*Erketu* + mde	*Euhelopus* + mde
66, *74*	*Phuwiangosaurus* + *Tangvayosaurus*	*Phuwiangosaurus*
6, 7, 26, 69, 114	*Chubutisaurus* + Titanosauria	Lithostrotia
18, 25	*Chubutisaurus* + Titanosauria	Saltasaurinae
68, 110	*Chubutisaurus* + Titanosauria	Saltasauridae
72	(Chubutisaurus + Titanosauria), –*Opisthocoelicaudia*	*Malawisaurus*, *Alamosaurus*
77, 105	Titanosauria	Saltasauridae

Table 4.6. Ambiguous character optimizations attributable to character conflict, based on two optimization strategies in PAUP* (Swofford, 2000). Abbreviations: mdsa, more derived sauropods; mdso, more derived somphospondylans. Italicization indicates characters that have ambiguous changes in other parts of the cladogram that are instead due to missing data (Table 5)

Character number	**ACCTRAN**	**DELTRAN**
12	(*Atlasaurus* + Neosauropoda), –Camarasaurus	Diplodocoidea, Titanosauriformes
90	Macronaria, –Brachiosauridae	*Camarasaurus*, Saltasauridae
112	–*Giraffatitan*	*Venenosaurus*
67	–(*Tehuelchesaurus* + Titanosauriformes), Brachiosauridae	–*Tehuelchesaurus*, –Somphospondyli
74	–*Europasaurus*, Titanosauriformes, –*Tastavinsaurus* + mdso	*Giraffatitan* + mdb, *Ligabuesaurus*, *Sauroposeidon*
28	*Tastavinsaurus* + mdso, Saltasauridae	*Malawisaurus, Euhelopus* + mde
15	*Tastavinsaurus* + mdso, –*Euhelopus*	Lithostrotia, *Phuwiangosaurus*
65	Titanosauria, –‘Saltasaurini’	*Opisthocoelicaudia*, *Alamosaurus*
19	–(Chubutisaurus + Titanosauria), ‘Saltasaurini’	*Malawisaurus*, *Alamosaurus*

Table 4.7. Decay indices (Bremer, 1994) for the nodes in the topology presented in this study (Figure 5), calculated using MacClade (Maddison and Maddison, 1994) and PAUP* (Swofford, 2000). If no decay index is listed for a node shown in Figure 5, decay index = 1

Node	**Decay index**	**Rank**
Neosauropoda	2	4
Macronaria	2	4
Tehuelchesaurus + Titanosauriformes	2	4
Titanosauriformes	4	2
Brachiosauridae	3	3
Somphospondyli	3	3
Sauroposeidon + more derived somphospondyls	2	4
Tastavinsaurus + more derived somphospondyls	2	4
Euhelopodidae	2	4
Lithostrotia	5	1
Saltasauridae	5	1
Saltasaurinae	3	3

Table 4.8. Age, provenance, and taxonomic assignment of 36 fragmentary basal titanosauriform–basal titanosaur sauropods. The list includes purported basal titanosauriforms and is limited to valid genera. Numbers refer to characters (Appendix 2) supporting and refuting higher-level assignments (Appendix 4) that were recovered as synapomorphies under delayed transformation. An exclamation point before a clade name means that the genus probably does not belong to that clade based on the absence of some synapomorphies; those characters are also preceded by an exclamation point. When affinities with more than one clade are suggested, the largest encompassing clade is listed. Age abbreviations: EJ = Early Jurassic; EK = Early Cretaceous; LJ = Late Jurassic; LK = Late Cretaceous; LTr = Late Triassic; MJ = Middle Jurassic. Area abbreviations: AF = Africa; AS = Asia; AU = Australia; EU = Europe; I = India; NA = North America; SA = South America; MA = Madagascar. Clade/validity abbreviations: Br, Brachiosauridae; Euh, Euhelopodidae; mdso, more derived somphospondylans, nd = nomen dubium; Neo, Neosauropoda; So, Somphospondyli; Ti, Titanosauria; TSF, Titanosauriform

Taxon	**Age**	**Area**	**Clade/validity**	**Characters**
Agustinia ligabuei	EK	SA	nd	—
Amargatitanis macni	EK	SA	nd	—
Angolotitan adamastor	LK	AF	Lithostrotia	79
Aragosaurus ischiaticus	LJ–EK	EU	TSF; !Titanosauria	101; !98
Argentinosaurus hunculensis	LK	SA	*Tastavinsaurus* + mdso; !Euhelopodidae; !Lithostrotia	34; !20; !45
Astrophocaudia slaughteri	EK	NA	*Sauroposeidon* + msdo; !Titanosauria	66, !98
Baotianmansaurus henanensis	LK	AS	*Euhelopus* + mde	28
Brontomerus mcintoshi	EK	NA	nd	—
Daanosaurus zhangi	LJ	AS	Macronaria	36
Diamantinasaurus matildae	EK	AU	Saltasauridae	105
Dongbeititan dongi	EK	AS	Somphospondyli	64
Dongyangosaurus sinensis	LK	AS	*Euhelopus* + mde	28, 92

Taxon	**Age**	**Area**	**Clade/validity**	**Characters**
Fukuititan nipponensis	EK	AS	Macronaria	85
Fusuisaurus zhaoi	EK	AS	*Tehuelchesaurus* + Titanosauriformes	60
‘French Bothiospondylus’/ Damparis sauropod	LJ	EU	*Giraffatitan* + mdb	74, 75, 77, 89
Galvesaurus herreroi	LJ–EK	EU	TSF; !Titanosauria	21, 54, 101; !98
Gobititan shenzhouensis	EK	AS	*Sauroposeidon* + mdso	106
Huabeisaurus allocotus	LK	AS	*Euhelopus* + mde	92
Huanghetitan liujiaxiaensis	EK	AS	Somphospondyli	65
Huanghetitan ruyangensis	LK	AS	Euhelopodidae + (*Chubutisaurus* + Titanosauria)	47
Janenschia robusta	LJ	AF	TSF; !TSF; !(*Sauroposeidon* + mdso); !(*Euhelopus* + (*Chubutisaurus* + Titanosauria))	107; !82; !106; !111
Jiangshanosaurus lixianensis	EK	AS	Saltasauridae	68, 70
Jiutaisaurus xidiensis	EK	AS	TSF	63
Lusotitan atalaiensis	LJ	EU	*Brachiosaurus + mdb*	74, 75
Malarguesaurus florenciae	LK	SA	*Tehuelchesaurus* + TSF; !Lithostrotia	102; !51
Mongolosaurus haplodon	EK	AS	Euhelopodidae + (*Chubutisaurus* + Titanosauria)	6, 20
NHMUK R5333	EK	EU	Lithostrotia	51

Taxon	Age	Area	Clade/validity	Characters
'Pelorosaurus' becklesii	EK	EU	TSF; !(*Chubutisaurus* + Titanosauria)	81, !79
Pukyongosaurus milleniumi	EK	AS	Somphospondyli	16
Qingxiusaurus youjiangensis	LK	AS	Lithostrotia	79*
Ruyangosaurus giganteus	LK	AS	Somphospondyli	16
Sonidosaurus saihangaobiensis	LK	AS	Euhelopodidae + (*Chubutisaurus* + Titanosauria)	28, 45
Sonorasaurus thompsoni	EK/LK	NA	*Giraffatitan* + mdb	74, 113
Wintonotitan wattsi	EK	AU	TSF; !(*Abydosaurus* + mdb); !Titanosauria	91; !89; !50
Xenoposeidon proneneukos	EK	EU	nd	—
Xianshanosaurus shijiagouensis	LK	AS	TSF	59

**Qingxiusaurus* also shares the presence of a posteriorly expanded sternal plate (character 72) with *Alamosaurus* and *Malawisaurus*. This is recovered as a Lithostrotian synapomorphy under ACCTRAN.

Table 4.9. Synapomorphies published in support of the monophyly of Laurasiformes (*Galvesaurus*, *Phuwiangosaurus*, *Aragosaurus*, *Tastavinsaurus*, *Venenosaurus*), with supporting references. Problematic features of each character are listed on the right

Character state	Analysis	comments
'lateral' pneumatic fossae of anterior cervical vertebrae undivided; those of posterior cervical vertebrae subdivided	Barco (2009)	serial variability in the subdivision of vertebral fossae is present in several neosauropods (Wilson et al., 2011)
hyposphene–hypantrum articulations only present in middle and posterior dorsal vertebrae	Barco (2009)	characterizes most saurischians; absent in derived titanosaurs
anterior caudal vertebrae (excluding the first) weakly procoelous	Barco (2009)	feature common to most non-lithostrotian sauropods, e.g., *Patagosaurus*, *Giraffatitan*, *Astrophocaudia*, *Chubutisaurus*; subtlety is serially variable
anterior caudal hemal canals bridged; middle hemal canals open	Barco (2009)	also present in some diplodocoids, *Jobaria*, and some specimens of *Camarsaurus* (Wilson and Sereno, 1998)
spol separated from spdl in dorsal vertebrae	Royo Torres (2009)	contact between these laminae varies along the vertebral series in most eusauropods
sacrum narrow (width 50–70% length)	Royo Torres (2009)	only *Tastavinsaurus* has this feature among neosauropods
anterior caudal vertebral centra concave anteriorly, flat posteriorly	Royo Torres (2009)	feature common to most non-lithostrotian sauropods, e.g., *Patagosaurus*, *Giraffatitan*, *Chubutisaurus*; subtlety is serially variable
'wrinkle' on lateral face of neural arch of middle-posterior caudal vertebrae	Royo Torres (2009)	remnant of neurocentral suture; present in all sauropods at some ontogenetic stage
neural spines of anterior caudal vertebrae bulbous	Royo Torres (2009)	displays variation within some genera (e.g., *Camarasaurus*); also present in some brachiosaurids

Character state	Analysis	comments
anterior caudal neural spines straight, directed posteriorly, vertically, or anteriorly, with anterodorsal edge anterior of postzygapophyses	Royo Torres (2009)	uninformative; character states span known morphologies for sauropods
angle between distal condyles and shaft of femur 6 degrees	Royo Torres (2009)	angle not preserved in *Tastavinsaurus*, *Cedarosaurus*, *Venenosaurus*, *Sonorasaurus*, similar angle found amongst many titanosauriforms
metatarsal III more than 30% tibia length	Royo Torres (2009)	not found in any sauropod

APPENDIX 4.1. Character-taxon scorings.

Omeisaurus
000000000000000010101000?00000000001010000000?000?00010000??0000
??0000000000000000000000000000000000000?00?000?000

Jobaria
000000000?000000001001010000000000000000000000000000001000000000
001000000000000000000000000000?0000000000000000000

Diplodocoidea
0001000000001201000100000000000000000000100000000000000000001000
00100000000000000010000000000000000000000000100000

Camarasaurus
0001010001101000000110000001000000010100100000000000000000001000
00100000001000000001100001000000000000000000100000

Tehuelchesaurus
???????????????0????????????1?00?00?1010100000????0???????01????
000000???0100000000????????????0000001000????????0

Atlasaurus
???0100?????1?00?0???00???0????????00000??0?0???????????????????
0??????????????????0?0??0?0??????????????????????0

Giraffatitan
11100001111110100101000000??0???10111011000000001001111000111010
101000000011020001101111?0111111000111000010100010

Brachio_altithorax
???????????????1?????????????0???10111011000000??00??1?0??11????
???000???10020?0???????????11?1??????1000????????0

Cedarosaurus
???????????????1?????????????0???1?1?101?00000?0?001?11100?1101?
10?00000010020001?0?1???1?1?????00???101?????????0

Abydosaurus
1110000110112101?01?1???0??????????????1????????1001?11?????????
??????????0??0?0??????????1??????????1010???????10

Europasaurus
00?00001?111110???101000000??0?0??01110110000?0??00??1?000??1?1?
?0?00?00?010?0?01?????1?0?11101??001?100?????????0

‘Saltasaurini’
???1111????????2?110?000110?1011101100111111101?0110111011111011
1101111110110111111?????0?111111111011111111011??1

Alamosaurus
????????????2?12?1001000110??011101101111111110?10110111011111011
210111111011?111111211110111111??11011111111011101

Opisthocoelicaudia
???????????????????????????0?11?011101101110111101?0111000111?11
200111101011011010121111011?1??111?0110011110111??

Malawisaurus
?0?1111???112012??001000?10110111011010111111?10011001100011101?
????10111010?010110?1?11??1??????1101101?1110????1

Daxiatitan
???????????????2???111?1?011???000?1?1?0??010????????1?01?110???
1?0000???????????????????????????????1010????????0

Erketu
???????????????2?0111011001?????????????????????????????????????
??????10?????????????????????????????????111001???

Euhelopus
??0???00?10200210111101?0110200001101011001?11????????????11???1
110000???0101000???????????01?10000011010111001000

Chubutisaurus
???????????????2??????????????????110?0??01?00???000011?00111???
110??????0101010?10?11110?1??????000?1010??????10?

Phuwiangosaurus 0???100????
1201010111111001102000011010010010110100011100011111110000?0?0?11
010001?0?????0?10101110001101011100???0

Sauroposeidon
??????????????02??101000000010111101?10100000000?00001100011???1
2100000001101000110?1???0?1110111000110101100????0

Tangvayosaurus
???????????????0???????1???????0???1??01????01?0?00011?000??111?
????????????????????????0?1????11000?1010110001???

Tastavinsaurus
???????????????2?????????????????011?1011000000010000110001?101?
???????????????????????????110111000110101110??10?

Venenosaurus
??1001?111001?1010
?0??????????????110?1???101????100011????????0011?

Qiaowanlong
??????????????????11101??00?????????????????????????????????????
???????????????????????????110111000??????????????

Andesaurus
???????????????2?????????????????111?101?0??00?01100011000?1101?
?????????01??0????????11??1????111001?????????????

Ligabuesaurus
??????????????02???????????0101111?101?1?00?0??????????????????1
100000???1101000??????????1??????????101001010?100

APPENDIX 4.2 Characters ordered by anatomical region. The original author or modifications to preexisting characters are listed where appropriate.

1. Premaxilla–maxilla suture, shape: planar (0); twisted along its length, giving the contact a sinuous appearance in lateral view (1). (Chure et al., 2010).
2. Premaxilla, premaxillary process near anteromedial corner of external naris: absent (0); present (1).
3. Lacrimal, anteriorly-projecting vertical plate of bone: absent (0); present (1). (modified from Chure et al., 2010).
4. Parietal, distance separating supratemporal fenestrae: less than (0) or twice (1) the long axis of supratemporal fenestra. (Wilson, 2002).
5. Supraoccipital, height: twice (0) subequal to or less than (1) height of foramen magnum. (Wilson, 2002).
6. Basal tubera, width relative to occipital condyle: less than 1.4 (0); greater than 1.6 (1) (modified from Mannion, 2010).
7. Paroccipital process, ventral non-articular process: absent (0); present (1). (Wilson, 2002).
8. Quadradojugal, anterior ramus, ventral triangular projection: absent (0); present).
9. Dentary, posteroventral process, shape: single (0); divided (1). (modified from Chure et al., 2010).
10. Surangular depth: less than twice (0) or more than two and one-half times (1) maximum depth of the angular (Wilson, 2002).
11. Dentary teeth, number: greater than 20 (0); 17 or fewer (1). (Wilson, 2002).
12. Tooth crowns, orientation: aligned anterolingually, tooth crowns overlap (0); aligned along jaw axis, crowns do not overlap (1). (modified from Wilson, 2002).
13. Marginal tooth denticles: present on anterior and posterior edges of tooth (0); only present in posteriormost few teeth (1); absent on both anterior and posterior edges (2). (modified from Wilson, 2002).
14. Maxillary teeth, shape: straight along axis (0); twisted axially through an arc of 30-45 degrees (1). (modified from Chure et al., 2010).
15. Teeth, average slenderness index (= crown height/crown width): > 3.0 (0); < 3.0 (1).
16. Presacral neural arch bone texture: camerate, with a few, large cavities (0); spongy, with centimeter-scale internal cells and walls, “semicamellate” (Wedel et al., 2000b) (1); camellate to somphospondylus, with sub-centimeter scale cells and walls (Wedel et al., 2000b). (Wilson, 2002).
17. Cervical vertebrae, number: 14 or fewer (0); 15 or more (1) (modified from Wilson, 2002).
18. Axis, centrum, shape: over two and a half times as long as tall (0); less than twice as long as tall (1).
19. Cervical pneumatopores (pleurocoels), shape: complex, divided by bony septa (0); simple, undivided (1). (Wilson, 2002).
20. Middle cervical neural spines, shape: single (0); bifid (1). (Wilson, 2002).
21. Middle cervical centra, anteroposterior length/average of width and height of posterior face: < 2.5 (0); > 3.0. (modified from Wilson, 2002; Chure et al., 2010).

22. Cervical vertebrae, epipophyses, shape: stout, pillar-like expansions above prezygapophyses (0); posteriorly projecting prongs (1).
23. Cervical vertebrae, eprl, morphology: thin lamina passing nearly horizontally across the neural arch (0); thick, subvertically oriented strut that joins the spol at the neural spine (1).
24. Cervical vertebrae, tpol, shape: has little or no relief past margin of cpol when viewed laterally (0); projects beyond cpol in lateral view, with distint 'kink' (1).
25. Middle cervical vertebrae, neural canal, shape: roughly same diameter throughout length (0); mediolaterally narrows towards mid-length of vertebra (1). (Curry Rogers, 2005).
26. Middle and posterior cervical vertebrae, parapophyses, shape: subcircular or only slightly longer than tall (0); elongate, making up more than half the functional centrum length in posterior cervical vertebrae.
27. Cervical vertebrae, parapophyses, shape and orientation: weakly developed, project laterally or slightly ventrally from the centrum (0); broad and project ventrally such that cervical ribs are displaced ventrally more than the height of the centrum (1). (modified from Wilson and Upchurch, 2009).
28. Posterior cervical and anterior dorsal vertebrae, neural spines, height: tall, length approaches or exceeds centrum height (0); very short, length less than centrum height (1).
29. Posterior cervical and anterior dorsal vertebrae, spdls: single (0); divided, with low relief on the front of the neural spine (1). (modified from Salgado et al., 1997).
30. Posterior cervical and anterior dorsal vertebrae, neural spine, shape: single (0); bifid (1); trifid (2).
31. Posterior cervical and anterior dorsal vertebrae, prespinal lamina: absent (0), present (1). (Salgado et al., 1997).
32. Posteriormost cervical vertebrae, region between centrum and prezygapophyses, height: tall, around centrum height (0); low, much less than centrum height (1). (Bonaparte et al., 2006).
33. Anterior dorsal vertebrae, neural spines, shape: taper along their length (0), expand distally and end in a rounded, anteroposteriorly thin blade ('paddle-shaped').
34. Middle dorsal vertebrae, posterior centrodiapophyseal lamina (pcpl): single (0); double, with low relief (1).
35. Middle and posterior dorsal vertebrae, spol: divided (0); single (1). (Wilson, 2002).
36. Posterior dorsal centra, articular face shape: amphicoelous (0); opisthocoelous (1). (Wilson, 2002).
37. Middle and posterior dorsal vertebrae, diapophyses, shape: short and dorsoventrally tall (0); long and dorsoventrally short, rod-like (1). (Janensch, 1950).
38. Middle dorsal vertebrate, diapophyses, orientation: directed dorsally at an angle of about 45 degrees (0); directed horizontally (1). (Wilson, 2002).
39. Middle dorsal vertebrae, podl: present (0); absent (1). (Sanz et al., 1999).
40. Middle and posterior dorsal vertebrae, pcdl: single and of constant width (0); ventrally widened or forked (1). (Salgado et al., 1997).
41. Middle and posterior dorsal neural spines, breadth: much narrower (0); equal to or broader (1) transversely than anteroposteriorly. (modified from Wilson, 2002).

42. Middle and posterior dorsal vertebrae, prespinal lamina, shape: present and bifurcates toward its ventral end (0); present and remains a single lamina throughout its length (1). (Upchurch *et al.*, 2004).
43. Middle and posterior dorsal neural spines, orientation: vertical (0); posterior, neural spine summit approaches level of diapophyses (1). (Wilson, 2002).
44. Middle and posterior dorsal vertebrae, diapophyses: dorsal surface grades smoothly towards face of centrum (0); dorsal surface flat and set off from rest of diapophysis by a lip (1). (modified from Sanz et al., 1999).
45. Posterior dorsal neural arches, hyposphene-hypantrum articulations: present (0); absent (1). (Wilson, 2002).
46. Middle and posterior dorsal vertebral centra, keel: absent (0); present (1).
47. Sacral vertebrae, number: 5 (0); 6 (1). (modified from Wilson, 2002).
48. Anterior caudal vertebrae, transverse processes, ventral ‘bulge’ or ‘kink’ visible in anteroposterior views: absent (0); present (1). (modified from Chure et al., 2010).
49. Caudal vertebrae, number: more than 50 (0); less than 35 (1). (Wilson, 2002).
50. Anterior and middle caudal centra, ventral longitudinal hollow: absent (0); present (1) (Wilson, 2002).
51. Anterior and middle caudal vertebral centra, articular faces, shape: anterior face concave and posterior face weakly concave to flat; anterior more concave (0); procoelous (1). (modified from Wilson, 2002).
52. Anterior and middle caudal vertebrae, blind fossae in lateral centrum: absent (0); present, often sporadically along the vertebral series (1).
53. Anterior caudal vertebrae, tubercle or subtle blade-like process on spinoprezygapophyseal lamina (sprl) near prezygapophysis: absent (0); present (1).
54. Anterior and middle caudal vertebrae, neural arches, location: over the midpoint of the centrum with approximately subequal amounts of the centrum exposed at either end (0), on the anterior half of the centrum (1). (Salgado et al., 1997; Upchurch et al., 2004).
55. Middle caudal vertebrae, transverse processes, orientation: roughly perpendicular (0); swept backwards, usually reaching posterior margin of centrum (excluding posterior ball if present) (1).
56. Middle caudal vertebrae, neural spines, orientation: upright or lean posteriorly (0); lean anteriorly (1). (modified from Rose, 2007).
57. Middle and distal caudal vertebral centra, articular shape: amphiplatyan (0); procoelous (1). (Wilson, 2002).
58. Distal caudal vertebral centra, shape: subcircular (0); around twice as wide as tall (1).
59. Dorsal ribs, proximal pneumatocoels: absent (0); present (1). (Wilson, 2002).
60. Anterior dorsal ribs, cross-sectional shape: subcircular (0); plank-like, anteroposterior breadth more than three times mediolateral breadth (1). (Wilson, 2002).
61. Chevrons, ‘crus’ bridging dorsal margin of hemal canal: present (0); absent (1). (Wilson, 2002).
62. Anterior and middle chevrons, articular facets: contiguous (0); each facet divided into an anterior and posterior section, separated by a furrow (1).

63. Anterior chevrons excluding the first, haemal canal, depth: short, approximately 25 percent (0) or long, approximately 50 percent (1) chevron length. (Wilson, 2002).
64. Scapular glenoid, orientation: relatively flat or laterally facing (0); beveled medially (1). (Wilson, 2002).
65. Scapula, processes on ventral margin near base of blade, number: zero (0); one (1), two (2).
66. Scapular blade, cross-section near base: D-shaped, wide lateral ridge present (0); flat or slightly curved, no lateral ridge (1). (modified from Wilson, 2002).
67. Scapula, acromial side of blade, shape: straight (0); curved, flaring (1).
68. Scapulocoracoid suture, shape: suture ends before dorsal margin of acromion and coracoid (0); suture extends to dorsal margin of acromion and coracoid (= flush dorsal margin).
69. Coracoid, shape: anteroposterior dimension more than 1.5 times proximodistal dimension (0); anteroposterior dimension less than proximodistal dimension (1). (modified from Wilson, 2002).
70. Coracoid, anteroventral margin: rounded (0); square (1). (Wilson, 2002).
71. Sternal plate, shape: oval with nearly straight lateral margin (0); crescentic, lateral margin strongly curved (1). (Wilson, 2002).
72. Sternal plate, shape: posterolateral margin curved (0); posterolateral margin expanded as a corner (1).
73. Sternal plate length/humerus length: about 0.5 (0); more than 0.7 (1).
74. Humerus, robustness: robust (length/midshaft width < 7) (0); gracile (length/midshaft width > 7.5 (1).
75. Humerus, proximolateral corner, shape: forms an obtuse angle, head of humerus raised (0); forms a right angle or acute angle, head of humerus flat (1). (modified from Wilson, 2002).
76. Humerus, strong posterolateral bulge on around level of the deltopectoral crest, absent (0); present (1).
77. Humerus-to-femur ratio: <= 0.80 (0); 0.85 to 0.95 (1); > 1.0. (2). (modified from Wilson, 2002).
78. Humerus, deltopectoral crest, shape: narrow throughout length (0); strongly expanded distally (1). (modified from Wilson, 2002).
79. Humerus, radial and ulnar condyles, shape: radial condyle divided on anterior face by a notch (0); undivided (1).
80. Humerus, distal condyles, shape: flat or convex (0); concave/divided distally (1). (modified from Wilson, 2002).
81. Ulna, proximal arms, shape: anterior and medial arms subequal in development (0); anterior arm longer and wider than medial arm (1) (modified from Wilson, 2002).
82. Ulna, distal end: expanded posteriorly (0); unexpanded (1).
83. Radius, distal end, orientation: perpendicular to (0) or beveled approximately 20 degrees proximolaterally (1) relative to long axis of shaft (1). (Wilson, 2002).
84. Carpal bones, number: 3 or more (0); 2 or fewer (1); none (2). (modified from Wilson, 2002).
85. Longest metacarpal-to-radius ratio: close to 0.3 (0); 0.45 or more (1). (Wilson, 2002).

86. Metacarpal I, length: less than (0) or subequal to/longer than (1) metacarpal IV. (modified from Wilson, 2002).
87. Metacarpal I, distal condyle shape: divided (0); undivided (1). (Wilson, 2002).
88. Metacarpal I distal condyle, transverse axis orientation: beveled approximately 20 degrees proximodistally (0) or perpendicular (1) with respect to axis of distal shaft (i.e., not angled due to bowing of bone). (modified from Wilson, 2002).
89. Metacarpal IV, articulation for metacarpal V, shape: anteroposteriorly long, broad articular surface (0); articular surface forms a near-right angle, transverse and anteroposterior dimensions of proximal end subequal (1).
90. Metacarpal V, proximal end, size: much smaller than proximal end of metacarpal I (0); subequal to or larger than proximal end of metacarpal I (1).
91. Metacarpals, distal articular facets, shape: present and extend well onto external/ anterior face of bone (0); reduced almost entirely to distal face of the bone except in metatarsal IV (1). (modified from Wilson, 2002).
92. Ilium, preacetabular process, shape: dorsoventrally short and tapering anteriorly (0); expanded into a semicircle anteriorly (1).
93. Ilium, preacetabular process, orientation: directed anteriorly (0); flared laterally (1). (Wilson, 2002).
94. Ilium, preacetabular process, kink on ventral margin, absent (0); present (1).
95. Ilium, pubic peduncle, shape: anteroposterior and transverse dimensions subequal (0); transverse dimension more than 1.5 times anteroposteior dimension (1).
96. Pubis, length relative to puboischial contact: greater than or equal to 3 (0); less than or equal to 2.5 (1) (modified from Wilson, 2002).
97. Ischial blade, length: equal to or longer than (0) or shorter than (1) pubic blade (modified from Wilson, 2002).
98. Ischial blade, shape: emarginated distal to pubic peduncle (0); no emargination distal to pubic peduncle (1). (Wilson, 2002).
99. Ischium, acetabular margin, shape: margin forms short, obtuse angle (0); margin strongly embayed, forming acute angle with tall pubic peduncle (1).
100. Ishium, pubic peduncle, shape: anteroposteriorly long, large ischial contribution to acetabulum (0); anteroposteriorly abbreviate, short ischial contribution to acetabulum (modified from Wilson, 2002).
101. Ischium, tubercle on lateroventral face, shape: set in fossa (0); raised on surface (1).
102. Femoral shaft, lateral margin shape: straight (0); proximal one-third deflected medially (1). (Wilson, 2002).
103. Femur, longitudinal ridge on anterior face: absent (0); present (1). (Otero, 2010).
104. Femur, fourth trochanter, shape: raised ridge, projects prominently in lateral view (0); low ridge or absent, barely or not visible in anterior view (1).
105. Femur, distal condyles: roughly perpendicular to long axis of shaft (0); beveled dorsomedially approximately 10 degrees (1) (Wilson, 2002).
106. Fibula, proximal end, anterior crest: absent or poorly developed (0); well developed, creating interlocking proximal crus (1) (modified from Wilson and Upchurch, 2009; Royo Torres, 2009).
107. Fibula, proximomedial end, raised triangular scar, present (0); absent (1).

108. Fibula, shaft, shape: straight (0); sigmoid, such that proximal and distal faces are angled relative to midshaft (1). (Royo Torres, 2009).
109. Fibula, distal end, shape: unexpanded or gently expanding distally (0); abruptly expands to form a medial lip (1). (modified from Wilson, 2002).
110. Astragalus, shape: at least 1.5 times wider than anteroposteriorly long (0); anteroposterior and transverse dimensions subequal.
111. Astragalus, posterior end of proximal face, tubercle: present (0); absent (1).
112. Metatarsal IV, proximomedial end, shape: flat or slightly convex (0); possesses a distinct embayment (1).
113. Metatarsal IV, distal end, orientation: roughly perpendicular to long axis of bone (0); beveled upwards medially (1).
114. Osteoderms: absent (0); present (1). (Wilson, 2002).

Appendix 4.3 Synapomorphies. Shared derived features supporting various neosauropod clades are listed below in order of decreasing inclusiveness. Characters are optimized according to delayed transformations (DELTRAN). See Tables 4.5 and 4.6 for ambiguous synapomorphies due to character conflict or missing data. Numbers in brackets refer to characters in Appendix 4.2.

Atlasaurus + Neosauropoda

1. Marginal tooth denticles present only in posteriormost few teeth (modified from Wilson, 2002). [13]

Neosauropoda (Bonaparte, 1986)

1. Distance separating supratemporal fenestrae twice long axis of fenestra (Wilson, 2002). [4]
2. Middle and posterior dorsal vertebral neural spines broader transversely than anteroposteriorly (modified from Wilson, 2002). [41]
3. Chevrons open proximally (Wilson, 2002). [61]
4. Only one carpal bone (modified from Wilson, 2002). [84]
5. Fibula abruptly expanded distally to form medial lip. (modified from Wilson, 2002). [109]

Macronaria (Wilson and Sereno, 1998)

1. Surangular tall, forming coronoid eminence (Wilson, 2002). [10]
2. Dentary teeth 17 or fewer in number (Wilson, 2002). [11]
3. Middle and posterior dorsal vertebrae opisthocoelous (Wilson, 2002). [36]
4. Middle dorsal vertebral diapophyses project horizontally (Wilson, 2002). [38]
5. Humerus with squared proximolateral corner (modified from Wilson, 2002). [75]
6. Longest metacarpal at least 45% radius length (Wilson, 2002). [85]

Tehuelchesaurus + Titanosauriformes

1. Middle and posterior dorsal vertebrae with ventrally widened or forked posterior centrodiapophyseal lamina (pcdl) (modified from Salgado et al., 1997). [40]
2. Anterior dorsal ribs plank-like, at least three times wider than broad (Wilson, 2002). [60]
3. Femur with proximolateral bulge, proximal one-third deflected medially (McIntosh, 1990; Salgado et al., 1997). [102]

Titanosauriformes (Salgado et al., 1997)

1. Tooth crowns do not overlap (Wilson and Sereno, 1998). [12]
2. Presacral vertebrae ‘semicamellate’, branching centimeter to decimeter-scale cells do not fully permeate centrum. [16]
3. Middle cervical vertebral centra, anteroposterior length/average of width and height of posterior face > 3.0. (modified from Wilson, 2002; Chure et al., 2010). [21]
4. Middle dorsal vertebrae with divided posterior centroparapophsyeal lamina (pcpl). [34]
5. Anterior caudal vertebrae with bulge or ‘kink’ on ventral margin of transverse process (Chure et al., 2010). [49]

6. Anterior and middle caudal vertebrae with neural arches set on anterior half of centrum (Salgado et al., 1997). [54]
7. Middle caudal vertebrae with posteriorly-projecting transverse processes. [55]
8. Dorsal ribs pneumatic (Wilson and Sereno, 1998). [59]
9. Anterior chevrons (excluding the first) with hemal canal at least 50% the length of the bone (Wilson, 2002). [63]
10. Scapula with tubercle on ventral margin of base of blade. [65]
11. Humerus length between 85% and 95% femur length (modified from Wilson, 2002). [77]
12. Ulna with anterior arm much longer and wider than medial arm (modified from Wilson, 2002). [81]
13. Ulna with unexpanded posterodistal end. [82]
14. Metacarpal I subequal to or longer than metacarpal IV (modified from Wilson, 2002). [86]
15. Metacarpal I distal condyle undivided (Wilson, 2002). [87]
16. Metacarpal I distal condyle perpendicular to long axis of shaft (Wilson, 2002). [88]
17. Metacarpal distal articular facets reduced (excepting metacarpal IV). [91]
18. Ilium preacetabular process expanded, semicircular (Salgado et al., 1997). [92]
19. Ilium preacetabular process flared laterally 45 degrees or more (modified from Salgado et al., 1997) [93]
20. Iliac pubic peduncle more than 1.5 times wider than long anteroposteriorly. [95]
21. Pubis at least three times as long as puboischial contact (modified from Wilson, 2002). [96]
22. Ischium with raised tubercle on lateroventral face. [101]
23. Fibular proximomedial end lacks corrugated triangular scar. [107]

Brachiosauridae (Riggs, 1903)

1. Distance separating supratemporal fenestrae less than long axis of fenestra (Wilson, 2002). [4]
2. Quadratojugal with ventral triangular projection on anterior ramus. [8]
3. Maxillary teeth twisted axially through an arc of 30–45 degrees (modified from Chure et al., 2010). [14]
4. Middle and posterior dorsal vertebrae with long, dorsoventrally short transverse processes, ‘rod-like’. [37]
5. Ischium with abbreviate pubic peduncle (Wilson, 2002). [100]

Giraffatitan + ((Brachiosaurus + (Abydosaurus, Cedarosaurus, Venenosaurus))

1. Premaxilla–maxilla suture sinuous. (Chure et al. 2010). [1]
2. Premaxilla with small, fingerlike process near anteromedial corner of external naris. [2]
3. Lacrimal with anteriorly projecting plate of bone at dorsal end (modified from Chure et al., 2010). [3]
4. Dentary with divided posteroventral process (modified from Chure et al., 2010). [9]
5. Anterior and middle caudal vertebrae with sporadically distributed, shallow fossae in lateral faces of centrum. [52]
6. Humerus gracile, length/midshaft width > 7.5. [74]

7. Humerus length more than 95% femur length. (modified from McIntosh, 1990; Wilson, 2002) [77]
8. Metatarsal IV with distal end beveled upwards medially. [111]

Brachiosaurus + (Abydosaurus, Cedarosaurus, Venenosaurus)

1. Humerus with rounded proximolateral corner (modified from Wilson, 2002). [75]

Abydosaurus, Cedarosaurus, Venenosaurus

1. Middle caudal vertebrae with neural spines that lean anteriorly (modified from Rose, 2007). [56]
2. Metacarpal IV embraces metacarpal V; proximal articular surface forms a near-right angle. [89]
3. Femoral fourth trochanter reduced to subtle bulge. [104]

Somphospondyli (Wilson and Sereno, 1998)

1. Presacral vertebrae with sub-centimeter scale pneumatic chambers that permeate the entire vertebra. [16]
2. Posterior cervical and anterior dorsal vertebrae with spinodiapophyseal laminae that are low in relief on the front of the neural spine (modified from Salgado et al., 1997). [29]
3. Posterior cervical and anterior dorsal vertebrae with a prespinal lamina (modified from Salgado et al., 1997). [31]
4. Posteriormost cervical vertebrae with low ‘infrazygapophyseal region’; region between centrum and prezygapophyses shorter than centrum height (modified from Bonaparte et al., 2006). [32]
5. Anterior dorsal vertebrae with plate-like, ‘paddle shaped’ neural spines. [33]
6. Scapular glenoid beveled medially (Wilson, 2002). [64]
7. Scapular blade straight on acromial side. [67]
8. Femoral fourth trochanter reduced to subtle bulge. [104]
9. Metatarsal IV with embayed medial face of proximal end. [112]

Sauroposeidon + (Tastavinsaurus + (Euhelopodidae + (Chubutisaurus + Titanosauria)))

1. Scapular blade flat in cross-section (modified from Wilson, 2002). [66]
2. Ischial blade shorter than pubic blade (modified from Wilson, 2002). [97]
3. Fibula with anterior crest on proximal end that is embraced by the cnemial crest of the tibia (modified from Wilson and Upchurch, 2009; Royo Torres, 2009). [106]
4. Fibula with distal end that is unexpanded, or gradually and subtly expanded; medially-facing lip absent. [109]

Tastavinsaurus + (Euhelopodidae + (Chubutisaurus + Titanosauria))

1. Middle dorsal vertebrae, posterior centroparapophyseal lamina (pcpl) undivided. [34]
2. Middle and posterior dorsal vertebrae with single spinopostzygapophyseal lamina (spol). [35]
3. Fibula sigmoid; proximal and distal faces angled relative to shaft (Royo Torres, 2009). [108]

Euhelopodidae + (Chubutisaurus + Titanosauria)

1. Supraoccipital subequal to or less than height of foramen magnum (Wilson, 2002). [5]
2. Tooth denticles absent (modified from Wilson, 2002). [13]
3. Middle and posterior dorsal vertebrae with flat-topped diapophyses (modified from Sanz et al., 1999). [44]
4. Six sacral vertebrae. (Wilson, 2002). [47]
5. Sternal plate crescentic (Wilson, 2002). [71]
6. Astragalus lacks tubercle on posterior proximal face. [113]

Euhelopodidae

1. Middle cervical neural spines bifid (Wilson, 2002). [20]
2. Cervical vertebrae with thick, subvertically oriented epipophsyeal–prezygapophyseal lamina (eprl). [23]

Erketu + (Euhelopus, Daxiatitan + (Tangvayosaurus + Phuwiangosaurus))

1. Cervical vertebrae with ‘kinked’ intrapostzygapophyseal lamina (tpol); tpol visible in lateral view. [24]
2. Cervical vertebrae with pendant parapophyses; cervical ribs displaced ventrally more than the height of the centrum (modified from Wilson and Upchurch, 2009). [27]

Euhelopus, Daxiatitan + (Tangvayosaurus + Phuwiangosaurus)

1. Fifteen or more cervical vertebrae. [17]
2. Cervical vertebral epipophyses form long, posteriorly-projecting prongs. [22]
3. Posterior cervical and anterior dorsal vertebrae with neural spines shorter than centrum height. [28]
4. Posterior cervical and anterior dorsal vertebrae with single spinodiapophyseal laminae that are sharp in relief on the side of the neural spine (modified from Salgado et al., 1997). [29]
5. Posterior cervical and anterior dorsal vertebral neural spines trifid. [30]
6. Posterior cervical and anterior dorsal vertebrae lack prespinal lamina. [31]
7. Posteriormost cervical vertebrae with tall ‘infrazygapophyseal region’; region between centrum and prezygapophyses exceeds centrum height (modified from Bonaparte et al., 2006). [32]
8. Anterior dorsal neural spines (metapophyses) taper along their length. [33]
9. Middle and posterior dorsal vertebral centra with ventral keel. [46]
10. Ilium with pointed, low preacetabular process (modified from Wilson, 2002). [92]

Tangvayosaurus + Phuwiangosaurus

1. Presacral vertebrae lack camellae; internal pneumaticity restricted to one or a few large chambers in the centrum. [16]
2. Anterior caudal vertebrae with tubercle on dorsal margin of prezygapophyses. [53]
3. Anterior and middle caudal vertebral chevrons with proximal articular facets divided into anterior and posterior segments. [62]

Chubutisaurus + Titanosauria

1. Dorsal vertebrae with reclined neural spines (Wilson, 2002) [43].

2. Humerus with undivided radial condyle (condyle lacks ‘notch’). [79]

Titanosauria (Bonaparte and Coria, 1993)

1. Anterior and middle caudal vertebrate with ventral longitudinal hollow (Wilson, 2002). [50]
2. Ischium platelike, no emargination distal to pubic peduncle (Wilson, 2002). [98]

Lithostrotia (Upchurch et al., 2004)

1. Basal tubera width more than 1.6 times occipital condyle width (modified from Mannion, 2010). [6]
2. Paroccipital processes with ventral, non-articular processes (Wilson, 2002). [7]
3. Teeth slender, average slenderness index less than 3. [15]
4. Middle and posterior cervical vertebrae with elongate parapophyses; parapophyses make up more than half the functional centrum length in posterior cervical vertebrae [26]
5. Middle and posterior dorsal vertebrae with a single prespinal lamina (Upchurch et al., 2004). [42]
6. Posterior dorsal neural arches lack hyposphene-hypantrum articulations (Wilson, 2002). [45]
7. Anterior caudal vertebrae with bulge or ‘kink’ on ventral margin of transverse process (Chure et al., 2010). [49]
8. Anterior and middle caudal vertebrae procoelous (Wilson, 2002). [51]
9. Coracoid proximodistally long (modified from Wilson, 2002). [69]
10. Sternal plate more than 70% humerus length. [73]
11. Ischial margin of acetabulum strongly embayed, margin acute. [99]
12. Osteoderms present. [114]

Saltasauridae (Powell, 1992)

1. Middle dorsal vertebrae lack postzygapophyseal-diapophyseal lamina (podl) (modified from Salgado et al., 1997). [39]
2. Thirty five or fewer caudal vertebrae (Wilson, 2002). [48]
3. Anterior caudal vertebrae with tubercle on dorsal margin of prezygapophyses. [53]
4. Scapulocoracoid suture flush, no embayment at suture. [68]
5. Coracoid anteroventral margin square (Wilson, 2002). [70]
6. Humerus with strong posterolateral bulge around level of deltopectoral crest. [76]
7. Humerus length less than 85% femur length (modified from Wilson, 2002). [77]
8. Humeral deltopectoral crest strongly expanded distally (Wilson, 2002). [78]
9. Radius distal end beveled approximately 20 degrees proximolaterally relative to shaft (Wilson, 2002). [83]
10. Carpus unossified or absent (Wilson, 2002). [84]
11. Metacarpal V proximal end subequal in size to proximal end of metacarpal I. [90]
12. Femoral distal condyles beveled 10 degrees dorsomedially relative to shaft (Wilson, 2002). [105]
13. Astragalus transversely narrow (modified from Wilson, 2002). [110]

Alamosaurus + ‘Saltasaurini’

1. Axis short, less than twice as long as tall. [18]
2. Middle cervical vertebrae, neural canal dramatically narrows at mid-length of centrum (Curry Rogers, 2005). [25]
3. Middle and distal caudal vertebrae procoelous (Wilson, 2002). [57]
4. Distal caudal vertebral centra about twice as wide as tall. [58]
5. Humeral radial and ulnar condyles divided distally (Wilson, 2002). [80]
6. Ilium with kink on ventral margin of preacetabular process. [94]
7. Femur with longitudinal ridge on anterior face of shaft (Otero, 2010). [103]

APPENDIX 4.4 Autapomorphies diagnosing each taxon are listed below. Numbers in brackets refer to autapomorphies resolved in the phylogenetic analysis and correspond to character numbers given in Appendix 4.2. Features listed without a number following them are unique autapomorphies and are absent from the data matrix

Omeisaurus (Young, 1939)

1. Maxillary ascending ramus with dorsoventrally expanded distal end (Wilson & Sereno, 1998).
3. More than fifteen cervical vertebrae. [17]
4. Middle cervical vertebral centra, anteroposterior length/average of width and height of posterior face > 3.0. [21]
5. Posterior dorsal vertebral centra opisthocoelous. [36]
6. Middle dorsal vertebral diapophyses directed horizontally. [38]
7. Anterior and middle caudal vertebrae with neural arches situated anteriorly on the centrum. [54]
8. Distalmost caudal chevrons fused to anteriormost portion of ventral centrum (Wilson, 2002).
9. Scapular blade unexpanded on acromial side. [67]

Jobaria tiguidensis (Sereno et al., 1999)

1. Cervical vertebral epipophyses form long, posteriorly-projecting prongs. [22]
2. Cervical vertebrae with 'kinked' intrapostzygapophyseal lamina (tpol); tpol visible in lateral view. [24]
3. Cervical ribs with secondary anterior projection. (Wilson, 2002).
4. Dorsal neural arches with well developed, paired coels below diapophysis (Sereno et al., 1999).
5. Anterior caudal neural spines with circular depression at base of prespinal lamina (Sereno et al., 1999).
6. Middle caudal vertebrae with posteriorly-projecting transverse processes. [55]
7. U-shaped first caudal chevron (Sereno et al., 1999).
8. Middle caudal chevrons with pronounced ligamentous scar encircling distal end (Sereno et al., 1999).

Atlasaurus imelaki (Monbaron et al., 1999)

1. Paroccipital processes extend nearly horizontally (Monbaron et al., 1999).
2. Width of paroccipital processes nearly half mandible length (Monbaron et al., 1999).
3. Jugal process of postorbital orthogonal to dorsal ramus.
4. Supratemporal fenestrae occupy over 80% of skull width.
5. Ulna 115% length of tibia (Monbaron et al., 1999).

Diplodocoidea (Marsh, 1884; Upchurch, 1995)

1. Tooth crowns do not overlap (Wilson and Sereno, 1998). [12]
2. Marginal tooth denticles present only in posteriormost few teeth (modified from Wilson, 2002). [13]
3. Teeth slender, average slenderness index less than 3. [15]
4. Cervical ribs short, not overlapping posterior centra (Berman & McIntosh, 1978).

5. Fibular facet of astragalus faces posterolaterally (Whitlock, 2011).

Camarasaurus (Cope, 1877)

1. Lacrimal with long axis directed anterodorsally (Wilson & Sereno, 1998).
2. Quadratojugal with short anterior ramus that does not extend anterior to the laterotemporal fenestra (Wilson & Sereno, 1998).
3. Quadratojugal anterior process shorter than dorsal process. (Wilson, 2002).
4. Pterygoid with dorsomedially orientated basipterygoid hook (Wilson, 2002).
5. Basal tubera width more than 1.6 times occipital condyle width (modified from Mannion, 2010). [6]
6. Splenial posterior process separating anterior portions of angular and prearticular (Wilson, 2002).
7. Middle cervical neural spines bifid (Wilson, 2002). [20]
8. Posterior cervical and anterior dorsal neural spines bifid. [30]
9. Conspicuous groove passing anteroventrally from the surangular foramen to the ventral margin of the dentary (Wilson & Sereno, 1998).
10. Forked chevrons restricted to distal tail (Wilson, 2002).
11. Metacarpal V proximal end subequal in size to proximal end of metacarpal I. [90]
12. Ischial blade directed posteriorly so that the long axis of its shaft passes though the pubic peduncle (Wilson & Sereno, 1998).

Tehuelchesaurus benitezii (Rich et al., 1999)

1. Posterior cervical vertebrae with neural spines less than centrum height. [28]
2. Dorsal vertebrae with very short diapophyses.
3. Middle and posterior dorsal vertebral neural spines broader transversely than anteroposteriorly [41]
4. Acromion process of scapula tall, over four times minimum height of scapular blade. (Carballido et al., in press)
5. Scapular blade unexpanded on acromial side. [68]
6. Humerus subcircular in cross-section (Upchurch et al., 2004).

Europasaurus holgeri (Sander et al., 2006)

1. Small body size.
2. Premaxilla with anteriorly projecting nasal process (Sander et al., 2006).

Giraffatitan brancai (Janensch, 1914)

1. Snout elongate. (Wilson, 2002).
2. Posterior dorsal vertebral centra about twice as wide as tall.
3. Anterior caudal vertebrae with tubercle on dorsal margin of prezygapophyses. [53]
4. Ilium with kink on ventral margin of preacetabular process [94]
5. Pubis with well-developed ambiens process.

Brachiosaurus altithorax (Riggs, 1903)

1. Posterior dorsal vertebral column long relative to humerus length (Paul, 1988).

Cedarosaurus weiskopfae (Tidwell et al., 1999)

1. Radius with well-developed flange lateral to ulnar articulation (Tidwell et al., 1999).
2. Radius with subtle tubercle on anterior face of shaft, one-third of the way from proximal end.
3. Metatarsal II with well-developed medial and lateral tubercles at mid-shaft.
4. Metatarsal V rod-like, unexpanded proximally.
5. Metatarsal V longer than metatarsals II or III.
6. Phalanx on metatarsal V.

Venenosaurus dicrocei (Tidwell et al., 2001)

1. Anterior and posterior faces of anterior and middle caudal vertebrae equally flat to slightly concave.
2. Metatarsal II with collateral ligament pits.
3. Metacarpal I proximal end more than twice as broad as wide.
4. Metacarpals II–IV with distal articular facets divided.
5. Metatarsal IV with embayed medial face of proximal end. [110]

Abydosaurus mcintoshi (Chure et al., 2010)

1. Foramen on lateral aspect of postorbital at juncture of the three processes.
2. Lacrimal angled anteriorly in lateral view.
3. Two exits for cranial nerve V.
4. Surangular short, lacking coronoid eminence. [10]
5. Tooth denticles absent. [13]
6. Caudal vertebral transverse processes with deep fossa into ventral face.
7. Collateral ligament pits on metatarsals II–IV.

Ligabuesaurus leanzi (Bonaparte et al., 2006)

1. Distal scapular blade with rounded dorsal expansion.
2. Humeral head expanded posteriorly.
3. Humerus gracile, length/midshaft width > 7.5. [74]
4. Fossae on proximoventral faces of metatarsals II and III.
5. Deep pit on ventrodistal face of manual phalanx I.1.

Sauroposeidon proteles (Wedel et al., 2000)

1. Middle cervical vertebrae with elongation index greater than 6 (Wedel et al., 2000)
2. Pneumatic fossa developed posteriorly to the cotyle in middle cervical vertebrae (Wedel et al., 2000).
3. Neural spines perforated in middle cervical vertebrae (Wedel et al., 2000).
4. Top of neural spine with broad midline ridge flanked by small fossae at its anterior and posterior ends.
5. Narrow middle and posterior dorsal neural spines that taper distally. [41]
6. Spinoprezygapophyseal laminae (sprl) divergent, forming wide spinoprezygapophyeal fossa (sprf) in anterior caudal vertebrae.
7. Anterior caudal vertebral centra roughly square in cross-section.
8. Scapula with two processes at the base of the blade. [65]
9. Humerus gracile, length/midshaft width > 7.5. [74]

Tastavinsaurus sanzi (Canudo et al., 2008)
1. Distal neural spines of dorsal vertebrae with small fossae and foramina.
2. Distal neural spines of dorsal vertebrae with upwardly-directed hook-like processes.
3. Sacrum narrow.
4. Sacricostal yoke projects well below ventral margin of sacral centra.
5. Fifth sacral rib dorsoventrally deep, flaring distally.
6. Metatarsal I with ventrally expanded distal condyles.
7. Metatarsal I without ventrally expanded proximal articular surface.
8. Metatarsals II–IV divided distally.
9. Metatarsal IV with divided distal articular surface.
10. Metatarsal V with proximoventral flange.
11. Pedal phalanx I.1 subrectangular.

Qiaowanlong kangxii (You and Li, 2009)
1. Cervical vertebral centra large, taller than the neural arch and spines.
2. Pubic articulation of ischium more than 50% ischium length (You and Li, 2009).

Erketu ellisoni (Ksepka and Norell, 2006)
1. Axis extremely elongate (more than 3 times longer than tall).
2. Spinodiapophyseal (sdf) and centrodiapophyseal (cdf) neural arch fossae extremely subdivided in cervical vertebrae.

Euhelopus zdanskyi (Wiman,1929)
1. Maxillary ascending process flush with anterior margin of bone; subnarial fossa reduced.
2. Teeth procumbent with asymmetrical crown-root margin (i.e. the mesial margin closer to the apex of the crown). (Wilson and Upchurch, 2009).
3. Tooth crowns overlap [12]
4. Third cervical vertebral neural spine with laterally compressed, anteriorly projecting triangular process (Wilson and Upchurch, 2009).
5. Anterior cervical vertebrae with three costal spurs on tuberculum and capitulum. (Wilson and Upchurch, 2009).
6. Cervical vertebrae with thin, horizontally oriented epipophsyeal–prezygapophyseal lamina. [23]
7. Ilium pneumatic (Wilson and Upchurch, 2009).
8. Pubis less than 2.5 times as long as puboischial contact. [96]
9. Ischial blade longer than pubic blade. [97]
10. Metatarsal IV with straight medial face of proximal end. [112]

Daxiatitan binglingi (You et al., 2008)
1. Middle and posterior dorsal vertebrae with single, unexpanded posterior centrodiapophyseal lamina (pcdl). [40]
2. Middle and distal caudal vertebrae procoelous. [57]
3. Chevrons closed proximally. [61]
4. Femoral distal condyles beveled 10 degrees dorsolaterally with respect to shaft (You et al., 2008).

Phuwiangosaurus sirindhornae (Martin et al., 1994)
1. Quadrate with kinked posteromedial margin of quadrate fossa.
2. Teeth slender, average slenderness index less than 3. [15]
3. Axial centrum without paramedian fossae on anterior half of ventral centrum.
4. Posterior cervical and anterior dorsal vertebrae with tubercle on prdl.
5. Middle dorsal vertebrae with dorsally acuminate pneumatic openings.
6. Middle and posterior dorsal vertebrae with single, unexpanded posterior centrodiapophyseal lamina (pcdl). [40]
7. Middle caudal vertebrae with kinked neural arch pedicle below postzygapophyses.
8. Scapular blade D-shaped (with expanded lateral ridge) in cross-section. [66]
9. Humerus gracile, length/midshaft width > 7.5. [74]

Tangvayosaurus hoffeti (Allain et al., 1999)
1. Fibular shaft straight. [108]

Chubutisaurus insignis (DelCorro, 1975)
1. Centroprezygapophyseal fossa (cprf) subdivided in anterior dorsal vertebrae (Carballido et al., 2011).
2. Metacarpal I with posteriorly expanded distal condyle.
3. Metacarpal III with distomedial flange.

Andesaurus delgadoi (Calvo and Bonaparte, 1991)
1. Middle dorsal vertebrae with divided posterior centroparapophsyeal lamina (pcpl). [34]
2. Posterior dorsal vertebrae with neural spines more than twice height of centrum (Mannion and Calvo, 2011).
3. Caudal vertebral centra transversely narrow.
4. Metacarpals I and V with elongate ridges on their internal faces (Mannion and Calvo, 2011).

Malawisaurus dixeyi (Haughton, 1928)
1. Abbreviate premaxillary portion of snout, dentary arched ventrally (Wilson, 2002).
2. Surangular notch and groove on dentary (Wilson, 2002).
3. Cervical vertebrae with undivided pleurocoels. [19]
4. Posterior cervical vertebrae with neural spines less than centrum height. [28]
5. Neural spines of anterior caudal vertebrae very short.
6. Sternal plate with squared posterolateral margin. [73]

Opisthocoelicaudia skarzynskii (Borsuk-Bialynicka, 1977)
1. Posterior cervical and anterior dorsal neural spines bifid. [30]
2. Anterior dorsal vertebrae with plate-like, ‘paddle shaped’ neural spines. [33]
3. Middle dorsal vertebrae with divided posterior centroparapophsyeal lamina (pcpl). [34]
4. Middle and posterior dorsal vertebrae with single, unexpanded posterior centrodiapophyseal lamina (pcdl). [40]

5. Middle and posterior dorsal vertebrae lack flat-topped diapophyses (modified from Sanz et al., 1999). [44]
6. Middle and posterior dorsal vertebral centra with ventral keel. [46]
7. Scapula with two processes at the base of the blade. [66]
8. Scapular blade D-shaped (with expanded lateral ridge) in cross-section. [66]
9. Ulna with expanded posterodistal end. [82]
10. Femoral fourth trochanter raised as a prominent ridge. [104]
11. Femoral fourth trochanter positioned at midshaft, near midline of femur.
12. Second muscle attachment surface lateral to fourth trochanter on femur.

Alamosaurus sanjuanensis (Gilmore, 1922)

1. Cervical vertebrae with undivided pleurocoels. [19]
2. Biconvex first caudal vertebra with circumferential depression on anterior condyle limited to ventral half of bone (D'Emic et al., in press).
3. Cross section of scapular blade asymmetrical, thicker ventral margin (D'Emic et al., in press).
4. Scapula with two processes at the base of the blade. [65]
5. Ventral edge of scapular blade nearly straight, dorsal edge expanded distally (D'Emic et al., in press).
6. Sternal plate with squared posterolateral margin. [72]
7. Ilium pneumatic.

'Saltasaurini'

1. Zygapophyses of cervical vertebrae set posteriorly; postzygapophyses overhang the centrum.
2. Middle dorsal vertebral diapophyses directed horizontally. [38]
3. Posterior caudal centra dorsoventrally flattened, breadth of posterior centrum at least twice height (Wilson, 2002).
4. Scapula with medial tuberosity on acromial side (Wilson, 2002).
5. Femoral distal condyles exposed on anterior portion of femoral shaft (Wilson, 2002).

CHAPTER 5

OSTEOCYTES AS PROXIES OF PHYSIOLOGY IN EXTINCT ANIMALS

Introduction

Reconstructing the physiology of extinct tetrapods is a branch of paleontology with a rich history, commonly focused on comparisons of bone histology (e.g., Enlow, 1956, Reid, 1993, Horner et al., 2000, Chinsamy-Turan, 2005). In cases where the animals' long bones (e.g., femur, humerus) contain lines of arrested growth, mass-versus-age growth curves can be constructed, yielding both the overall pattern and quantitative growth rates for a given species (e.g., Erickson et al., 2001). However, for some extinct animals such as sauropod dinosaurs, growth lines in long bones are rare (Sander, 2000), making this type of skeletochronology often inapplicable. Other efforts to reconstruct the growth patterns and rates of extinct animals include the creation of histological ontogenetic growth stages (e.g., Horner et al. 2000; Klein and Sander, 2008) and relationships between bone vascularity patterns and growth rates (e.g., de Margerie et al., 2002). However, these proxies are either qualitative or yield inconsistent or imprecise results (Starck and Chinsamy, 2002). Aside from lines of arrested growth, no bone histological proxy has been developed to reliably estimate an animal's growth rate in a quantitative sense.

The morphology of bone-forming cells is a logical and unexplored candidate for reconstructing bone growth rates, because the size and shape of these cells vary within and among bones of animals that grow at different rates (Marotti, 1976; Feretti et al., 1998). Bone-forming cells (called osteoblasts) are embedded within bone via the differential secretion of bone by neighboring cells (Franz-Odenaal et al., 2006). Once mature, osteoblasts are referred to as osteocytes. Osteocytes have a variety of functions, including ion regulation, mechano-sensing, and bone repair (Aarden et al., 1994). Osteocytes reside in small spaces within bone called lacunae and are connected to one another via networks of cellular projections located inside tubes within bone called canaliculi. Because lacunae and canaliculi correspond well with osteocyte shape and size (Marotti 1979, 1980) and are generally well-preserved in fossils (e.g., Reid, 1993; Organ et al., 2007), they provide a window into one aspect of cellular biology in deep time.

Osteocytes vary in size (ca. 0.1–1.0 μm^3; see below), shape, and density depending on the sample. Research into osteocyte morphology has largely fallen into two fields: modern anatomy and paleontology. Modern anatomical studies have largely focused on a few model organisms (e.g., chicken, human, dog) and the within-bone variation in osteocyte morphology (e.g., Marotti, 1996). These studies found that osteocyte volume varies with bone identity (e.g., femur versus scapula), bone tissue organization (e.g., woven versus lamellar; Marotti, 1980), location within a bone (e.g., midshaft versus metaphysis; Cané et al., 1982), and distance from a vascular canal (Ardizzoni, 2001). Zallone (1977) and Volpi et al. (1981) studied the relationship between bone growth rate and osteocyte size in trabecular bone of the tibia of the dog and chick, respectively. Both studies reported a strong positive relationship between osteoblast ‘secretory territory’ (i.e., the volume of the osteoblast divided by the area touching the growth surface, equivalent to the shortest axis of the cell) and the thickness of osteoid (unmineralized bone) deposited. Marotti (1976) found a positive relationship between osteoblast volume and bone growth rate, and further suggested that total osteocyte volume was proportional to bone growth rate.

In contrast, paleontological studies have largely investigated osteocyte variation using broad taxonomic samples, ignoring the lower-level sources of variation (intraspecific, within-individual, within-bone). To date, two studies have measured osteocyte volume in a wide variety of amniotes (Organ et al. 2007; 2009), and both reported a large (nearly ten-fold) degree of variation among taxa. Because these studies focused on questions in a broad phylogenetic context, some possible factors contributing to osteocyte variation were not controlled for (e.g., within- or among-bone variation within an individual). Organ et al. (2007) reported a relationship between osteocyte volume and genome size in amniotes ($R^2 = 0.56$; $R^2 = 0.32$ under a generalized least-squares regression accounting for phylogeny) and applied that relationship to calculate genome size in several non-avian dinosaurs. They reported that non-avian theropod dinosaurs had small osteocytes (and thus genomes), and inferred that theropods may have had bird-like metabolisms due to their small cell size (Organ et al., 2007). Organ et al. (2007) argued that organisms with smaller red-blood cell size should have higher metabolisms because their cells have a higher surface area to volume ratio. Organ et al. (2007) assumed that small osteocyte size in theropod dinosaurs meant that they had small red blood cell size. This reasoning is supported by the data of Gregory (2002), who found a relationship between growth rate and red blood cell size after correcting for body mass (but not the phylogenetic relatedness of the taxa concerned). Organ et al. (2009) reported moderate osteocyte volumes for several sauropodomorph dinosaurs, and suggested that osteocyte volume was not related to body size.

Data from these modern and paleontological studies suggest opposing hypotheses for the relationship between osteocyte volume and bone growth rate. Marotti (1976) suggested that larger osteocytes develop from larger osteoblasts, which deposit bone faster due to their comparably large volume. In contrast, the data presented by Organ et al. (2007) suggest that animals with smaller osteocytes have higher basal metabolic rates due to their higher surface area-to-volume ratio. These reports conflict because in amniotes, growth rate is proportional to metabolic rate (Montes et al., 2007).

Recently, several studies have integrated data from cellular biology, ecology, and physiology in order to investigate the evolution of metabolism across large clades such as mammals or birds (e.g., Kozlowski et al., 2003; Savage et al., 2007). Models have been developed to study interactions among the number and size of cells and cellular metabolic rates, which combine to produce organismal attributes such as basal metabolic rate and body mass (Savage et al., 2007). Savage et al. (2007) identified two types of cells: those with constant cellular mass and varying cellular metabolic rates (type i; e.g., erythrocytes, fibrocytes, hepatocytes, most cells of the lung), and those with cellular masses proportional to body mass with invariant metabolic rates (type ii; e.g., adiposites, neurons). It is unknown which type of cell osteocytes are. Because osteocytes are the only cells commonly observable in deep time, they represent an opportunity to trace the evolution of metabolism in deep time in different clades. However, first the basic relationships among osteocyte volume, body mass, and physiology must be understood. In this chapter, I explore the relationships among osteocyte volume, red blood cell volume, growth rate, basal metabolic rate, and genome size using a broad sample of modern birds. I attempt to discover relationships among these factors that could be applied to understand the paleobiology of extinct animals.

Methods

Osteocyte measurement.—The problems associated with obtaining threedimensional measurements from two-dimensional thin-sections are well known (e.g., Marotti, 1980; Fig. 5.1), but they have not been taken into account in many studies. For example, Organ et al. (2007, 2009) assumed a prolate ellipsoid shape (i.e., cigar-shaped, with intermediate axis = short axis < long axis) when calculating osteocyte volumes. This model is inappropriate because the three axes of osteocyte lacunae are almost always unequal for parallel-fibered bone (Marotti, 1979, 1980; McCreadie et al., 2004). Osteocytes in parallel-fibered bone are generally scalene ellipsoids, which have three unequal axes (Marotti 1980; McCreadie et al., 2004). In this chapter, a best-fit ellipsoid was used as the model for volume calculation, using the formula: volume = 4/3 * π * long axis * intermediate axis * short axis. Canaliculi were excluded from volumetric measurements because their contribution to osteocyte volume is negligible (McCreadie et al., 2004) and they are not consistently observable due to problems of preparation and preservation. Surface area was approximated using a formula (surface area = $4 * \pi * ((a^p b^p + a^p c^p + b^p c^p) / 3))^{1/p}$ where $p = 1.605$). Osteocytic osteolysis, a process by which osteocytes have been proposed to increase the size of their lacunae through resorption, was not considered a significant source of morphological bias following previous studies (Boyde, 1980; Teti and Zallone, 2008). Furthermore, osteocytic osteolysis is usually reported for osteocytes in ‘statically formed’ (woven) bone (e.g., Belanger, 1969), which was excluded from the dataset (see below).

In order to observe all three axes of the osteocyte lacunae, thin-sectioned bones in two orthogonal dimensions were prepared, which correspond to a transverse and a sagittal section for each long bone (Fig. 5.1). Because osteocyte lacunae align themselves with the predominant collagen fiber orientation in bone (Marotti, 1980) and this fiber orientation can be observed under cross- or circularly polarized light (Bromage et al., 2003), one can discern whether or not the long axis of an osteocyte lacuna is visible in a given thin-section. Specifically, areas where thin-sections appear dark under polarized light have osteocytes with their longest axis perpendicular to the plane of section (i.e., extending into and out of the plane), whereas areas where thin-sections appear bright have osteocytes with the longest axis visible in the section. For the diaphyses of long bones, osteocytes were generally observed to have their long axis parallel to that of the entire bone.

Thin sections were photographed under 20x magnification with cross-polarized light. Osteocyte axes were measured in ImageJ (Rasband, 1997–2011; http://rsbweb.nih.gov/ij/). Measuring osteocyte axes in this manner resulted in four sets of axes, one long and one short axis for the longitudinally-cut osteocytes and one long and one short axis for the transversely-cut osteocytes. Only two of these sets were nearly equal (within 10% of one another) and represented the shortest axes of the osteocytes, as expected for a scalene ellipsoid. Means and variances for each axis and a best estimate of osteocyte volume and surface area were calculated for each bone. Because each volume or surface area was calculated only after data for each axis were averaged, variances for volumes could not be calculated straightforwardly (i.e., by calculating a volume for each cell and then calculating the variance of that sample of volumes). In order to calculate variance of the volumes of osteocytes, a program was written in R (www.r-project.org) to randomly sample (with replacement) each set of osteocyte axes (i.e., long, intermediate, short). Once each axis was sampled, a volume and a surface area were calculated. This process was repeated 10,000 times and variance was calculated from that bootstrapped population of volumes or surface areas.

Data.– Species-specific data were gathered from the CRC Handbook of Avian body masses (Dunning, 2008), Starck and Ricklefs (1998), and the Animal Cell Size database (http://www.genomesize.com/cellsize). Because several of the species in the dataset were sexually dimorphic, average body mass for each sex was selected for the appropriate sex (if known). The most widely available data on growth rate are in the form of the growth parameter K (day^{-1}), which is proportional to overall growth rate in models fitted to plots of age versus mass (Stark and Ricklefs, 1998). The K calculated from a logistic growth model was selected because it is the most often provided (Starck and Ricklefs, 1998). If K were unknown for a species that had been thin-sectioned but did not vary substantially (less than 10%) among other species in the same genus, then the average generic value for K was used. Species for which I could not find data on genome size, growth rate K, or basal metabolic rate were appropriately omitted prior to computation of regressions or phylogenetic independent contrasts (see below).

Seventy-three bird bones were thin-sectioned twice orthogonally to produce 156 thin-sections. The sample was broad in terms of phylogeny (Fig. 5.2) and body size (range: approximately 10 g–100 kg). Bird bones and their thin sections are reposited in the University of Michigan Museums of Zoology and Paleontology, and specimen data are available through Ornisnet (www.ornisnet.org). The sample includes 43 femora from 35 species and 11 humeri from ten species. For nine species, more than one femur or humerus was sectioned. The femur and humerus sectioned were from the same individual for eight species, and 21 bones were sectioned from a single skeleton of the emu (*Dromaius novaehollandae*) in order to assess within-individual variation in osteocyte morphology.

Numerous procedural controls were employed in order to reduce potential sources of variation in osteocyte volume. For long bones, thin sections were only taken at the midshaft and osteocytes were only measured on the anterior and posterior sides of the bone. Only osteocytes in primary, parallel-fibered bone from the middle of the cortex were measured: osteocytes in secondary, endosteal, periosteal, trabecular, medullary, woven, and lamellar bone were excluded. Osteocytes formed by static bone formation (i.e., those representing the first stage of bone formation, Palumbo et al., 2004) were also excluded from the dataset.

Testing hypotheses via regression analysis.— Osteocyte volume or surface area was regressed onto body mass, growth rate, basal metabolic rate, and genome size. All variables were log-transformed prior to regression. Linear and multiple ordinary least squares regressions were calculated using Microsoft Excel. Because the datapoints are not independent, phylogenetic independent contrasts (Felsenstein, 1985) were computed using the PDAP module of Mesquite (Maddison and Maddison, 2009; Midford et al., 2010). Independent contrasts were standardized by dividing each contrast by the square root of its standard deviation (Garland et al. 1992). A single best-estimate topology was based on the phylogenies in Barker et al. (2001, 2004), and Ericson et al. (2006), and branch lengths (in millions of years) were taken from the latter. Relationships and branch lengths for species not included in Barker et al. (2001, 2004) or Ericson et al. (2006) were interpolated from the closest relatives that were included in that dataset. All regressions of phylogenetic contrasts were repeated with all branch lengths set equal to one another.

Results

General comments on variation.—Orthogonal thin-sectioning indicated that the vast majority of measured osteocytes were best approximated as a scalene ellipsoid ($x \neq y \neq z$), rather than a prolate ellipsoid ($x = y < z$). These osteocytes must be scalene ellipsoids because (1) only two sets of the four measured axes (two each in two orthogonal thin sections) were equal, and (2) those two equal sets of axes were smaller than the other axes. Observed osteocyte volumes spanned nearly an order of magnitude, from 105 μm^3 in the femur of the black-capped chickadee (*Poecile atricapillus atricapillus*) to 939 μm^3 in the ostrich (*Struthio camelus*) (Appendix 1). The range of observed osteocyte surface areas was also broad, from 131 to 684 um^2 in these two species, respectively. No strong relationships exist among the three axes of the osteocyte (Fig. 5.3), in keeping with the results of McCreadie et al. (2004). Standard deviations range from 3–14% of the mean osteocyte volume for each bone. Standard deviations are even more constrained among long bones; they are always below 10% of the mean osteocyte volume for humeri and femora (Appendix 1). Osteocytes generally appeared larger in the metaphyses and epiphyses of long bones, in keeping with the results of Cané et al. (1982).

Within-individual variation.—Variation in osteocyte volume among the bones of an individual emu (*Dromaius novaehollandae*) was substantial, ranging from 130 um^3 in the metacarpals to 789 um^3 in the frontal (Fig. 5.4). Surface area also varied substantially (Appendix 1). The average and standard deviation of osteocyte volumes in all 21 sectioned emu bones was 418 and 177 um^3, respectively. The average value was similar to the value for the femur, humerus, and ischium, but very different from most other bones, which were either lower or higher. Bone size or cortical thickness was also poorly related to osteocyte volume as shown by comparisons between the largest bone in the body (tibiotarsus, osteocyte volume = 248 um^3) with one of the smallest (pedal phalanx, osteocyte volume = 345 um^3).

For eight bird species, a femur and humerus were sectioned from the same individual. Difference in osteocyte volumes was high between these bones for a given individual, ranging from 7–105%, with an average of 29% (Table 5.1).

Within-species variation.— For eight species, femora from two individuals were sectioned, and from one species, humeri from two individuals were sectioned. Difference in osteocyte volumes was low between homologous bones of individuals of the same species, ranging from 4–24%, with an average difference of 12% (Table 5.2).

Relationship between osteocyte volume, osteocyte surface area, and body size.—The results of linear regression show that osteocyte volume (N = 35 species; $R^2 = 0.78$; $p = 2E^{-12}$; Table 5.3) and surface area (N = 35 species; $R^2 = 0.7$; $p = 5E^{-12}$; Table 5.3) are each strongly dependent on body mass in the femur and humerus. When accounting for the non-independence of the datapoints due to shared ancestry using phylogenetic independent contrasts (Felsenstein, 1985), the relationship between body mass and osteocyte volume is still significant ($p < 0.05$) but is much weaker ($R^2 = 0.15$). Using a topology with all branch lengths set equal to one (rather than using best estimates of branch length from molecular and fossil data, Ericson et al. 2006) did not alter the significance of the regression model (i.e., move the p-value below or above 0.05) for any of these relationships. Because osteocyte volume scales with body mass, osteocytes represent a type ii cell of Savage et al. (2007), that is, osteocytes relate to body mass as do neurons and adipocytes, rather than erythrocytes and fibrocytes.

Relationship between osteocyte volume, osteocyte surface area, and growth rate.—Growth rate was dependent on both osteocyte volume and surface area (N = 16 species; $R^2 \sim= 0.45$, $p < 0.01$; Table 5.4). However, this dependence disappeared in both cases when phylogeny was taken into account (Table 5.4). Using best-estimates of branch length rather than setting branch lengths equal to one did not alter the significance of the regression model for any of these relationships. The length of the osteocyte short axis was inversely proportional to growth rate K ($R^2 = 0.34$; $p = 0.02$), in conflict with the results of Zallone (1977), Marotti (1980), and Volpi et al. (1981), whose data suggested that this axis is proportional to bone growth rate. Such a relationship was not significant when phylogenetic relatedness of the datapoints was accounted for (Table 5.4).

Because of the strong dependence of osteocyte volume and surface area on body mass mentioned above, it is possible that body mass is driving the observed relationship between these factors and growth rate. Multivariate regressions performed with osteocyte volume, surface area, surface area/volume, short axis, and body mass as independent variables and growth rate as the dependent variable were almost all insignificant (Table 5.4). Only the regression model between body mass and osteocyte volume or surface area remained significant (Table 5.4), suggesting that this relationship drives the observed growth rate–osteocyte volume relationship. This interpretation was tested by regressing the residuals of a regression between growth rate and body mass upon the residuals of a regression between osteocyte volume and body mass. The results of this regression were not significant. Accounting for phylogeny by using independent contrasts further decreased the strength of these relationships (Table 5.4).

Relationship between osteocyte volume, osteocyte surface area, and basal metabolic rate.—Mass-specific metabolic rate (i.e., metabolic rate/body mass$^{0.75}$) was dependent on osteocyte volume and surface area (N = 18 species; R^2 ~= 0.44; $p < 0.005$; Table 5.5). Similar to the relationships between osteocyte volume and growth rate described above, these relationships were insignificant when phylogeny was taken into account. Using best-estimates of branch length rather than setting branch lengths equal to one did not alter the significance of the regression model for any of these relationships.

Using mass-specific metabolic rate (= body mass/metabolic rate$^{0.75}$) is one way to factor body mass out of metabolic rate when performing regressions;

another way is to perform a multiple regression using raw basal metabolic rate, body mass, and osteocyte volume. The results of this multiple regression (accounting for phylogeny or not) indicate that only body mass and osteocyte volume or surface area have a significant relationship; there is no independent relationship between these osteocyte parameters and basal metabolic rate (Table 5.5).

Relationship between osteocyte volume and genome size.—A strong and significant relationship was found between osteocyte volume and genome size (N = 20 species; $R^2 = 0.62$; $p = 4E-5$; Table 5.6). This relationship was not significant using phylogenetic independent contrasts with best estimates of branch length but was significant with all branch lengths set equal to one. This indicates that estimated divergence times are important to the significance of the regression results presented herein. When genome size and body mass were simultaneously regressed on osteocyte volume, neither of these relationships was significant ($p = 0.78$ and 0.18, respectively; Table 5.6), suggesting that the dependence of genome size on osteocyte volume is mostly due to the effect of body mass. The significance of all other regression models of the relationships among these parameters was unaltered by setting branch lengths equal to one.

Discussion

Data presented above show that variation in osteocyte volume and surface area is low among homologous bone tissue types, regions within bones, and homologous bones of the same species. In contrast, variation in osteocyte volume among the bones of an individual is high and not related to bone size or function. Osteocyte volume and surface area are strongly dependent on body mass, mass-specific metabolic rate, and the growth rate constant K. Genome size is strongly dependent on osteocyte volume. However, these relationships are all weakened (and most are rendered insignificant) when phylogenetic relatedness is taken into account. Relationships among osteocyte volume or surface area and metabolic rate, growth parameter K, or genome size disappear when correcting for body mass. The results of this study suggest that body mass is the strongest control on osteocyte volume and surface area, and that no strong relationships exist between metabolic or growth rates and osteocyte morphology. This study indicates that osteocytes represent a ‘type ii’ cell according to Savage et al (2007). This signifies that osteocytes scale with body mass rather than metabolic rate. Osteocytes are thus fundamentally different from erythrocytes in their relationship to organismal body mass, which explains the problems with (and cautions future studies to) relate osteocytes to physiological, molecular, or morphological parameters (e.g., Organ et al., 2009).

The results presented above stand in contrast to those presented by Zallone (1977), Marotti (1980), Volpi et al. (1988), and Organ et al. (2007), who proposed relationships between bone growth rate, metabolism, and osteocyte size or morphology. The strong relationship between body mass and osteocyte volume discovered herein also contradicts the results of Organ et al. (2009), who concluded that osteocyte volume was unrelated to body mass over a broad sample of archosaurs.

Differences between the results and conclusions of previous studies and those presented herein are attributable to several factors. Discrepancies between the results presented herein and those of Zallone (1977), Marotti (1980), and Volpi et al. (1981) may be partially explained by differences in the bone tissue type sampled; those authors primarily sampled lamellar trabecular bone, whereas this study examined parallel fibered cortical bone. Growth rate may relate differently to osteocyte morphology in these different bone types. Furthermore, the 'growth rate' considered in this study was for an entire individual, rather than for particular bone accretion rates studied by Zallone, (1977), Marotti (1980), and Volpi et al. (1981). Differences among bone growth rates should balance one another to produce a whole organismal growth rate. However, it is clear that the relationships drawn from a single bone cannot be scaled up to predict growth rates in an individual.

Discrepancies between the results presented above and those of Organ et al. (2007, 2009) can be attributed to a combination of two factors. First, Organ et al. (2007) compared a variety of bones and tissue types (compare Organ et al. (2007: suppl. table 1 with Table 5.1), making their results for osteocyte volumes among bones and taxa incomparable. Second, Organ et al. (2007) assumed a prolate ellipsoid shape when calculating osteocyte volumes, which introduced substantial error in volume calculation, especially when the long-axis of the osteocyte was not visible in the section (e.g., Organ et al., 2007: fig. 1a). Despite the methodological problems of Organ et al. (2007, 2009), they recovered a signal congruent with amniote phylogeny. However, this signal is likely driven by the strong relationship between osteocyte size and body size reported herein.

In addition, Organ et al. (2009) may have failed to discover a strong relationship between osteocyte volume and body mass because they did not always use adult femur lengths when calculating body mass, again suggesting that their results per taxon are incomparable with one another (Organ et al., 2009:suppl. table 1; pers. obs.). The data presented herein using accurate measurement techniques, as well as accounting for body size and phylogenetic independence, cast doubt on the utility of osteocytes for calculating genome size or physiological parameters in extinct vertebrates.

Conclusions

Osteocyte lacunae currently represent the most commonly available source of data for studying cellular biology in fossils, and thus the only data available for direct observation of cellular evolution over long timescales. This paper explores the potential of osteocyte lacunae as a proxy for physiology using recent birds. Avian osteocytes in parallel-fibered bone are scalene ellipsoids, so a single thin-section is insufficient to calculate osteocyte volume. The strongest controls on osteocyte volume or surface area are bone element (e.g., femur vs. rib), bone tissue type (e.g., woven vs. lamellar), and body mass. Osteocyte volume displays low variation between homologous bones in individuals of the same species. Genome size is not strongly related to osteocyte volume when the effects of body mass and/or phylogeny are removed. Growth rate and basal metabolic rate are unrelated to osteocyte volume or surface area. Changes in bone growth rate may be attributable to osteocyte density (Bromage et al., 2008) or the efficacy of bone formation per osteocyte.

References

Aarden E. M., Burger, E. H., Nijweide, P.J. 1994. Function of Osteocytes in Bone. Journal of Cellular Biochemistry 55: 287–299.

A. Ardizzoni, A. 2001. Osteocyte Lacunar Size–Lamellar Thickness Relationships in Human Secondary Osteons. Bone 28: 215–219.

Barker, F. K., Cibois, A., Schikler, P., Feinstein, J., Cracraft, J. 2004. Phylogeny and diversification of the largest avian radiation. Proceedings of the National Academy of Sciences 101: 11040–11045.

Barker, F. K., Barrowclough, G. F., Groth, J. G. 2001. A phylogenetic hypothesis for passerine birds: taxonomic and biogeographic implications of an analysis of nuclear DNA sequence data. Proceedings of the Royal Society of London B 269: 295–308.

Boyde, A. 1980. Evidence against osteocytic osteolysis. Metabolic Bone Disease Related Research 25:239–255.

Bromage T. G., Goldman H. M., McFarlin S., Warshaw J., Boyde A., Riggs C. 2003. Circularly polarized light standards for investigations of collagen fiber orientation in bone. Anatomical Record New Anatomist 274B: 157–168.

Bélanger, L. F. 1969. Osteocytic Osteolysis. Calcified Tissue Research 4: 1–12.

Cané, V., Marotti, G., Volpi, G., Zaffe, D., Palazzini, S., Remaggi, F., Muglia, M. A. 1982. Size and Density of Osteocyte Lacunae in Different Regions of Long Bones Calcified Tissue International 34: 558–563.

Chinsamy-Turan, A. 2005. The microstructure of dinosaur bone. Johns Hopkins University Press, Baltimore.

de Margerie, E., Cubo, J., Castanet, J. 2002. Bone typology and growth rate: testing and quantifying “Amprino’s rule” in the mallard (*Anas platyrhynchos*). Comptus Rendus Biologies 325: 221–230.

Dunning, J. B. 2007. CRC Handbook of Avian Body Masses. CRC Press, Boca Raton, Florida. 655 pp.

Enlow, D. H., Brown, S. O. 1957. A comparative histological study of fossil and recent bone tissues. Part II. Texas Journal of Science 9: 186–214.

Erickson, G. M., Curry Rogers K. A., Yerby, S. A. 2001. Dinosaurian growth patterns and rapid avian growth rates. Nature 412: 429–433.

Ericson, P. G. P., Anderson, C. L., Britton, T., Elzanowski, A., Johansson, U. S., Källersjö, M., Ohlson, J. I., Parsons, T. J., Zuccon, D., Mayr, G. 2006. Diversification of Neoaves: integration of molecular sequence data and fossils. Biology Letters 2: 543–547.

Felsenstein, F. 1985. Phylogenies and the comparative method. The American Naturalist 125: 1–15.

Franz-Odendaal T.A, Hall B. K., Witten P. E. 2006. Buried alive: how osteoblasts become osteocytes. Developmental Dynamics 235: 176–190.

Garland, T., Harvey, P. H., Ives, A. R. 1992. Procedures for the analysis of comparative data using phylogenetically independent contrasts. Systematic Biology 41: 18–32.

Gregory, T. R. 2002. Genome size and developmental parameters in the homeothermic vertebrates. Genome 45: 833–838.

Klein, N., Sander, P. M. 2008. Ontogenetic stages in the long bone histology of sauropod dinosaurs. Paleobiology 34: 248–264.

Kozlowski, J., Konarzewski, M., Gawelczyk, A. T. 2003. Cell size as a link between noncoding DNA and metabolic rate scaling. Proceedings of the National Academy of Sciences 100: 14080–14085.

Horner, J. R., Ricqles, A. de, Padian, K. 2000. Long bone histology of the hadrosaurid dinosaur *Maiasaura peeblesorum*: growth dynamics and physiology based on an ontogenetic series of skeletal elements. Journal of Vertebrate Paleontology 20: 115–129.

Maddison W. P., Maddison D. R. 2009. Mesquite: a modular system for evolutionary analysis, v2.71. Available at http://mesquiteproject.org.

Marotti, G. 1976. Decrement in volume of osteoblasts during osteon formation and its effects on the size of the corresponding osteocytes. In: Meunier P. J. (ed.), Bone histomorphometry. Armour Montagu, Paris, pp. 385–397.

Marotti, G., Zambonin Zallone, A. 1980. Changes in the vascular network during the formation of the haversian system. Acta Anatomica 106: 84–100.

Marotti, G. 1979. Osteocyte orientation in human lamellar bone and its relevance to the morphometry of periosteocytic lacunae. Metabolic Bone Disease Related Research 1: 325–333.

Marotti, G. 1996. The structure of bone tissues and the cellular control of their deposition. Italian Journal of Anatomy and Embryology 101: 25–79.

McCreadie, B. R., Hollister, S. J., Schaffler, M. B., Goldstein, S. A. 2004. Osteocyte lacuna size and shape in women with and without osteoporotic fractures. Journal of Biomechanics 37: 563–572.

Midford, P. E., Garland, T. Jr., Maddison, W. P. 2010. PDAP Package version 1.15. Organ, C. L., Shedlock, A. M., Meade, A., Pagel, M., Edwards, S. V. 2007. Origin of avian genome size and structure in non-avian dinosaurs. Nature 446: 180–184.

Montes, L., Le Roy, N., Perret, M., de Buffrenil, V., Castanet, J., Cubo, J. 2007. Relationships between bone growth rate, body mass and resting metabolic rate in growing amniotes: a phylogenetic approach. Biological Journal of the Linnean Society 92: 63–76.

Organ, C. L., Brusatte, S. L., Stein, K. 2009. Sauropod dinosaurs evolved moderately sized genomes unrelated to body size. Proceedings of the Royal Society B. 1677: 4303–4308.

Rasband W. S. 1997–2011. ImageJ. Bethesda, Maryland, USA: U. S. National Institutes of Health.

Reid, R. 1993. Dinosaur blood cells rediscovered. Nature 366: 24

Teti, A., Zallone, A. 2009. Do osteocytes contribute to bone mineral homeostasis? Osteocytic osteolysis revisited. Bone 44: 11–16.

Sander, P. M. 2000. Long bone histology of the Tendaguru sauropods: Implications for growth and biology. Paleobiology 26:466-488.

Savage, V. M., Allen, A. P., Brown, J. H., Gillooly, J. F., Herman, A. B., Woodruff, W. H., West, G. B. 2007. Scaling of number, size, and metabolic rate of cells with body size in mammals. Proceedings of the National Academy of Sciences 104: 4718–4723.

Starck, J. M., Ricklefs, R. E., 1998. Patterns of development: The Altricial-Precocial Spectrum. In: Starck, J.M., Ricklefs, R.E. (eds.), Avian Growth and Development. Oxford University Press, Oxford, pp. 3–26.

Starck, J. M., Chinsamy, A. 2002. Bone microstructure and developmental plasticity in birds and other dinosaurs. Journal of Morphology 254: 232–246.

Stein, K. Sander, P. M. 2009. Histological core drilling: a less destructive method for studying bone histology. In: Methods In Fossil Preparation: Proceedings of the First Annual Fossil Preparation and Collections Symposium. Brown, M.A., Kane, J.F., and Parker, W.G., Eds. pp. 69–80.

Volpi, G., Palazzini, S., Cané, V., Remaggi, F., Muglia, M. A. 1981. Morphometric Analysis of Osteoblast Dynamics in the Chick Embryo Tibia. Anatomy and Embryology 162: 393–401.

Zallone, A. Z. 1977. Relationships between Shape and Size of the Osteoblasts and the Accretion Rate of Trabecular Bone Surfaces. Anatomy and Embryology 152: 65–72.

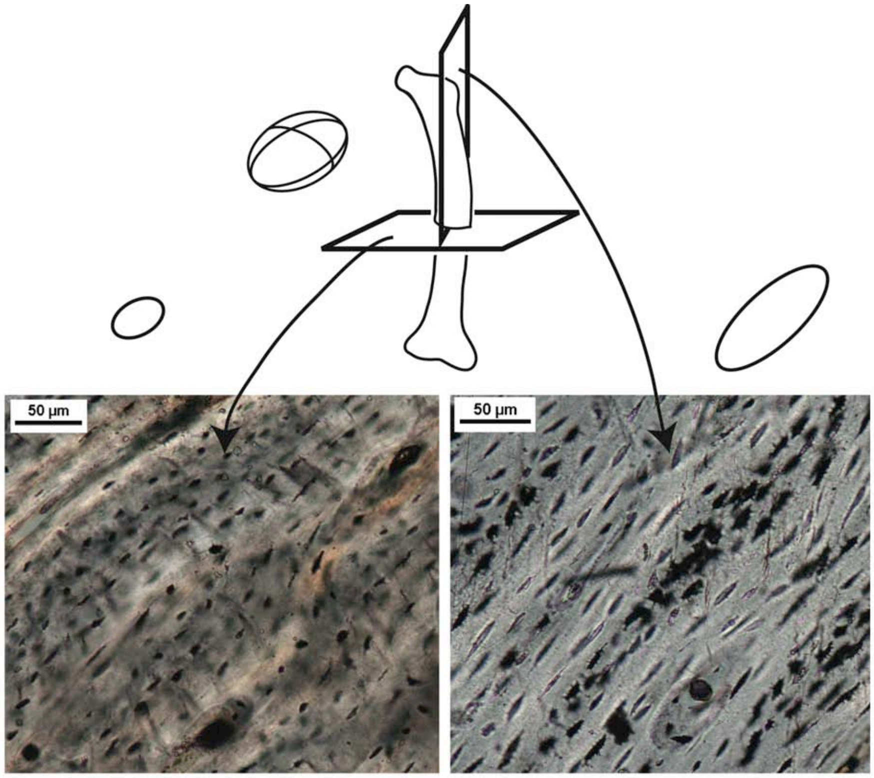

Figure 5.1. Apparent osteocyte size when cut in different planes. Diagram shows two planes of section that were used in this study to observe all three osteocyte axes. Photos below illustrate how osteocyte appearance varies based on plane of section in the femur of a rhea (UMMZ 223136).

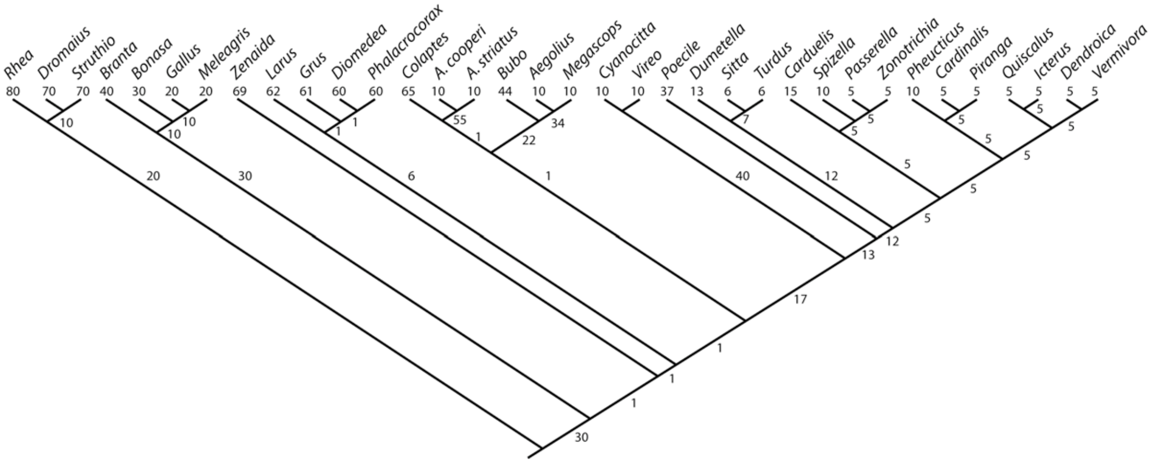

Figure 5.2. Best estimate phylogeny of birds used in this study, based on the phylogenies presented in Barker et al. (2001, 2004), and Ericson et al. (2006). Branch lengths (in millions of years) are shown on each branch, and were taken from Ericson et al. (2006). Relationships and branch lengths for taxa not included in Barker et al. (2001, 2004) or Ericson et al. (2006) were interpolated from the closest relatives that were included in that dataset.

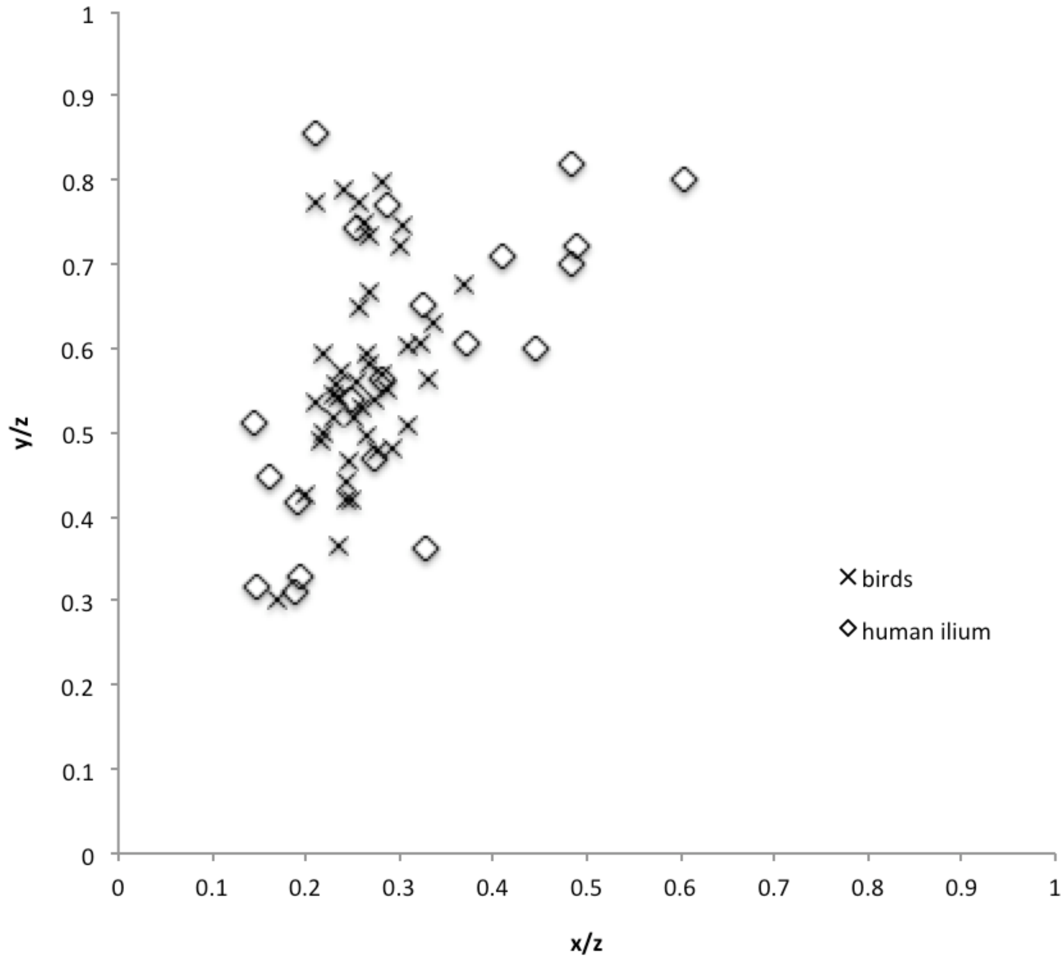

Figure 5.3. Osteocyte shape variability in human ilia and bird femora. x, y, and z represent the long, intermediate, and short axes of the osteocyte. All osteocytes in the sample are scalene ellipsoids (none of the axes are equal). Data for human ilia are from McCreadie et al. (2004).

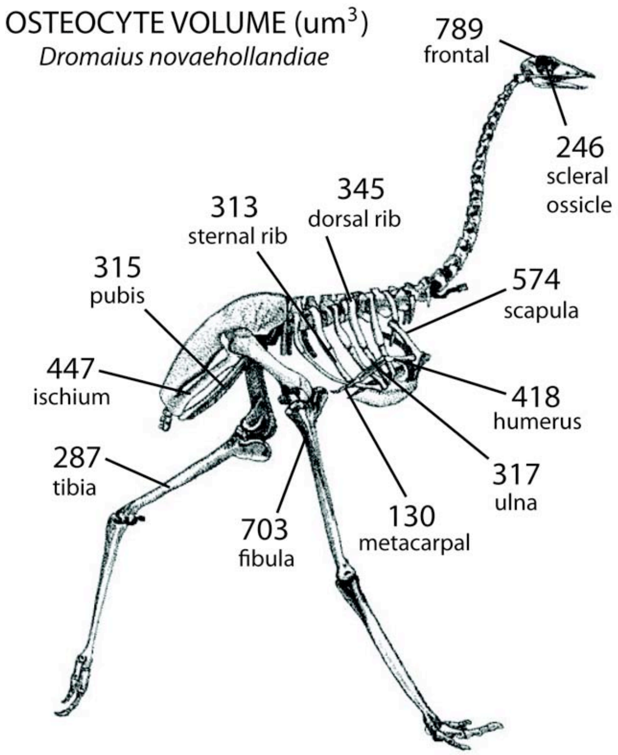

Figure 5.4. Osteocyte size variability in the emu (UM R1717). All bones were sampled at their mid-shafts or centers.

Table 5.1. Within-individual variation in osteocyte volume for eight species of bird.

species	bone	osteocyte volume mean (um^3)	osteocyte volume standard deviation (um^3)	% difference between bones
Aegolius acadius	femur	210	11.9	28
	humerus	269	11.4	
Bonasa umbellus	femur	231	8.2	29
	humerus	179	7.8	
Colaptes auratus	femur	199	7.7	7
	humerus	186	11.3	
Gallus domesticus	femur	326	16.7	21
	humerus	394	17.9	
Megascops ‘Otus’ asio	femur	194	6.6	6
	humerus	206	9.1	
Megascops ‘Otus’ asio	femur	157	9.6	27
	humerus	199	18.6	
Parus atricapillus	femur	114	4.8	9
	humerus	124	6.2	
Struthio camelus	femur	939	76.7	105
	humerus	458	26.2	

Table 5.2. Variation in osteocyte volume between homologous bones of individuals of the same species. Unless otherwise noted, data are for femoral osteocytes.

species	osteocyte volume mean (um^3)	osteocyte volume standard deviation (um^3)	% difference between individuals
Accipiter cooperi	332	17.4	12
	297	13.2	
Accipiter striatus	260	10.9	8
	281	18.4	
Cyanocitta cristata	216	10.3	18
	183	6.5	
Dendroica pensylvanica	162	12.5	5
	170	9.0	
Megascops 'Otus' asio	157	6.6	24
	194	9.6	
Megascops 'Otus' asio (humerus)	206	9.1	4
	199	18.6	
Phalacrocorax idahoensis	290	18.0	13
	328	26.4	
Pheucticus ludovicianus	108	7.9	19
	129	7.5	
Piranga olivacea	105	9.3	9
	114	4.8	

Table 5.3. Linear regressions among osteocyte volume, osteocyte surface area, body mass, femur length, and red blood cell area. All values were log-transformed prior to regression. Phylogenetic independent contrasts (PICs) were standardized prior to regression following Garland et al. (1992). Significant p-values (= F-statistic by the F-test) are shown in bold; all p-values are for the two-tailed case.

y variable (dependent)	x variable (independent)	R^2	standard error	F	two-tailed p-value
osteocyte volume	body mass	0.78	0.10	118.10	**1.90E-12**
osteocyte surface area	body mass	0.70	0.63	122.67	**4.70E-10**
osteocyte volume	red blood cell area	0.56	0.15	75.68	**4.30E-05**
PIC osteocyte volume	PIC body mass	0.17	0.09	26.42	**0.015**
PIC surface area	PIC body mass	0.16	0.09	5.99	**0.020**

Table 5.4. Regressions among the growth rate parameter (K, 1/day), body mass, osteocyte volume, and osteocyte surface area. All values were log-transformed prior to regression. Phylogenetic independent contrasts (PICs) were standardized prior to regression following Garland et al. (1992). Significant p-values are shown in bold; all p-values are for the two-tailed case. The F-statistic for the bivariate regressions is equivalent to the *p*-value listed. SE = standard error of the regression model.

x variable 1	x variable 2	y variable	R^2	p-value for x var 1	p-value for x var 2	SE	F	F-statistic
osteocyte volume	—	growth rate K	0.46	**0.004**	—	0.33	11.88	—
osteocyte surface area	—	growth rate K	0.42	**0.007**	—	0.34	10	—
short axis of osteocyte	—	growth rate K	0.34	**0.02**	—	0.05	6.83	—
osteocyte surface area/ volume	—	growth rate K	0.42	**0.009**	—	0.04	9.30	—
PICs of osteocyte volume	—	PICs of growth rate K	0.01	0.713	—	0.05	0.14	—
PICs of surface area	—	PICs of growth rate K	0.03	0.574	—	0.05	0.33	—
PICs of short axis of osteocyte	—	PICs of growth rate K	0.01	0.78	—	0.01	0.08	—
PICs of osteocyte surface area/ volume	—	PICs of growth rate K	0.01	0.78	—	0.01	0.08	—
osteocyte volume	body mass	growth rate K	0.7	0.59	**0.007**	0.25	14.9	4E-04
osteocyte surface area	body mass	growth rate K	0.69	0.86	**0.005**	0.26	14.5	5E-04
short axis of osteocyte	body mass	growth rate K	0.72	0.44	**0.002**	0.25	15.7	4E-04
osteocyte surface area/ volume	body mass	growth rate K	0.73	0.4	**0.003**	0.25	16	4E-04

x variable 1	**x variable 2**	**y variable**	**R^2**	**p-value for x var 1**	**p-value for x var 2**	**SE**	**F**	**F-statistic**
PICs of osteocyte volume	PICs of body mass	PICs of growth rate K	0.32	0.39	**0.04**	0.05	2.78	0.102
PICs of surface area	PICs of body mass	PICs of growth rate K	0.3	0.56	**0.06**	0.05	2.33	0.14
PICs of short axis of osteocyte	PICs of body mass	PICs of growth rate K	0.32	0.36	**0.04**	0.05	2.81	0.1
PICs of osteocyte surface area/volume	PICs of body mass	PICs of growth rate K	0.32	0.36	**0.04**	0.05	2.84	0.1

Table 5.5. Regressions among the basal metabolic rate, body mass, osteocyte volume, and osteocyte surface area. In some cases, basal metabolic rate was normalized for body mass (mass-specific metabolic rate; Gillooly et al. 2006). All values were log-transformed prior to regression. Phylogenetic independent contrasts (PICs) were standardized prior to regression following Garland et al. (1992). Significant p-values are shown in bold; all p-values are for the two-tailed case. The F-statistic for the bivariate regressions is equivalent to the *p*-value listed. SE = standard error of the regression model.

x variable 1	x variable 2	y variable	R^2	p-value for x var 1	p-value for x var 2	SE	F	F-statistic
osteocyte volume	—	mass-specific metabolic rate	0.46	**0.002**	—	0.15	13.46	—
surface area	—	mass-specific metabolic rate	0.41	**0.004**	—	0.16	10.93	—
PIC osteocyte volume	—	PIC mass-specific metabolic rate	0.014	0.650	—	0.08	0.21	—
PIC surface area	—	PIC mass-specific metabolic rate	0.003	0.840	—	0.08	0.04	—
osteocyte volume	body mass	basal metabolic rate (uncorrected)	0.56	0.87	0.08	0.14	9.56	0.002
surface area	body mass	basal metabolic rate (uncorrected)	0.56	0.87	**0.037**	0.14	9.56	0.002
PICs of osteocyte volume	PICs of body mass	PICs of basal metabolic rate (uncorrected)	0.84	0.58	**6E-05**	0.03	37.87	2E-06
PICs of surface area	PICs of body mass	PICs of basal metabolic rate (uncorrected)	0.84	0.66	**7E-05**	0.03	37.50	2E-06

Table 5.6. Regressions among genome size, body mass, osteocyte volume, and osteocyte surface area. All values were log-transformed prior to regression. Phylogenetic independent contrasts (PICs) were standardized prior to regression following Garland et al. (1992). Significant *p*-values are shown in bold; all *p*-values are for the two-tailed case. The F-statistic for the bivariate regressions is equivalent to the *p*-value listed. SE = standard error of the regression model.

x variable 1	**x variable 2**	**y variable**	**R^2**	***p*-value for var 1**	***p*-value for var 2**	**SE**	**F**	**F-statistic**
genome size	—	osteocyte volume	0.62	**4.27E-05**	—	0.03	28.82	—
PIC genome size	—	PIC osteocyte volume	0.02	0.537	—	0.01	0.40	—
PIC of genome size	PICs of body mass	PICs of osteocyte volume	0.13	0.771	0.181	0.02	1.18	0.33

Appendix 5.1. Osteocyte size measurements.

	taxon	common name	element	long axis avg	long axis std	int axis avg	int axis std	short axis av	short axis st	long radius	long rad sd	int radius	int rad sd	short rad	short rad sd	VOLUME
241009	*Accipiter cooperii*	Cooper's hawk	femur	14.20537931	2.477439958	10.98019608	2.131638544	3.6351	0.563744614	**7.10268966**	1.238719979	**5.49009804**	1.065819272	**1.81755**	0.281872307	**297**
242198	*Accipiter cooperii*	Cooper's hawk	femur	14.95484314	3.557005034	11.797	4.292409195	3.596542169	0.726745742	**7.47742157**	1.778502517	**5.8985**	2.146204598	**1.79827108**	0.363372871	**332**
240638	*Accipiter striatus velo*	Sharp-shinned hawk	femur	13.20227273	2.405305351	9.515119048	1.749888208	3.955268041	0.659470708	**6.60113636**	1.202652676	**4.75755952**	0.874944104	**1.97763402**	0.329735354	**260**
242034	*Accipiter striatus velo*	Sharp-shinned hawk	femur	13.99434615	2.428402766	10.27228125	3.018330742	3.735189655	0.725004451	**6.99717308**	1.214201383	**5.13614063**	1.509165371	**1.86759483**	0.362502226	**281**
241878	*Aegolius acadicus*	Northern saw-whet owl	femur	14.47997368	3.020069298	7.191133333	2.315610793	3.851131579	0.765291577	**7.23998684**	1.510034649	**3.59556667**	1.157805397	**1.92556579**	0.382645789	**210**
241878	*Aegolius acadicus*	Northern saw-whet owl	humerus	14.41549091	3.1018694	9.54	2.056792028	3.741041096	0.475977199	**7.20774545**	1.5509347	**4.77000**	1.028396014	**1.87052055**	0.2379886	**269**
242039	*Bonasa umbellus*	Ruffled grouse	femur	14.11659155	2.235099784	7.176333333	1.341993093	4.359833333	0.742809759	**7.05829577**	1.117549892	**3.58816667**	0.670996546	**2.17991667**	0.371404879	**231**
242039	*Bonasa umbellus*	Ruffled grouse	humerus	18.74819608	3.774992482	5.478903846	1.11681763	3.323067961	0.58987603	**9.37409804**	1.887496241	**2.73945192**	0.558408815	**1.66153398**	0.294938015	**179**
227638	*Branta canadensis*	Canada goose	femur	16.43055556	4.740909982	7.671793103	1.345828288	4.041166667	0.533692715	**8.21527778**	2.370454991	**3.83589655**	0.672914144	**2.02058333**	0.266846358	**267**
UM R 1452	*Bubo virginianus occid*	Western great horned owl	femur	15.5594717	2.656984667	8.361155172	2.726019133	4.268072727	0.708258592	**7.77973585**	1.328492334	**4.18057759**	1.363009567	**2.13403636**	0.354129296	**291**
UM 241794	*Cardinalis cardinalis*	Northern Cardinal	femur	12.844875	3.892397899	6.171657143	1.555833361	3.771490196	0.876966077	**6.4224375**	1.946198949	**3.08582857**	0.77791668	**1.8857451**	0.438483038	**157**
241809	*Carduelis tristis*	American goldfinch	femur	13.59489744	2.217439892	7.4155	1.320359551	3.12615	0.533539664	**6.79744872**	1.108719946	**3.70775**	0.660179775	**1.563075**	0.266769832	**165**
241887	*Colaptes auratus*	Northern flicker	femur	11.90647273	1.832656419	8.878823529	1.967025955	3.601358491	0.480159402	**5.95323636**	0.91632821	**4.43941176**	0.983512978	**1.80067925**	0.240079701	**199**
241887	*Colaptes auratus*	Northern flicker	humerus	13.59213953	3.18356495	8.464869565	1.963365756	3.086033708	0.632481035	**6.79606977**	1.591782475	**4.23243478**	0.981682878	**1.54301685**	0.316240518	**186**
241803	*Cyanocitta cristata bro*	Bluejay	femur	13.12484783	2.060151245	7.616603448	1.518114539	3.504182692	0.680563584	**6.56242391**	1.030075623	**3.80830172**	0.759057269	**1.75209135**	0.340281792	**183**
242057	*Cyanocitta cristata bro*	Bluejay	femur	13.70402817	2.641719856	7.818975	1.911299417	3.841261261	0.805079744	**6.85201408**	3.426007042	**3.9094875**	0.955649708	**1.92063063**	0.402539872	**216**
240871	*Dendroica pensylvanic*	Chestnut-sided warbler	femur	13.28484615	2.829780611	6.357326923	1.687212258	3.659215385	0.761317864	**6.64242308**	1.414890306	**3.17866346**	0.843606129	**1.82960769**	0.380658932	**162**
241982	*Dendroica pensylvanic*	Chestnut-sided warbler	femur	18.51114286	3.448778136	5.565606557	1.101742246	3.152170732	1.084249616	**9.25557143**	1.724389068	**2.78280328**	0.550871123	**1.57608537**	0.542124808	**170**
210390	*Diomedea exulans*	Wandering albatross	femur	18.3387561	3.69489857	9.513306122	2.291464144	4.228277778	2.899245293	**9.169378**	1.847449285	**4.75665**	1.145732072	**2.114139**	1.449622647	**386**
UM R1717	*Dromaeus novaehollan*	Emu	caudal vert	15.83328	4.879325923	13.21027273	4.991628694	4.383396552	0.911234577	**7.91664**	7.91664	**6.60513636**	2.495814347	**2.19169828**	0.455617288	**480**
UM R1717	*Dromaeus novaehollan*	Emu	cervical vert	18.33615556	4.469633389	17.0125	4.107457819	4.192327869	0.713636783	**9.16807778**	2.234816695	**8.50625**	2.053728909	**2.09616393**	0.356818391	**685**
UM R1717	*Dromaeus novaehollan*	Emu	coracoid	12.758625	2.838177551	11.395	1.707370744	3.546358974	0.657130264	**6.3793125**	1.419088775	**5.6975**	0.853685372	**1.77317949**	0.328565132	**270**
UM R1717	*Dromaeus novaehollan*	Emu	dorsal rib	15.42615385	3.021713582	11.65608108	3.231702126	3.66808	0.651903112	**7.71307692**	1.510856791	**5.82804054**	1.615851063	**1.83404**	0.325951556	**345**
UM R1717	*Dromaeus novaehollan*	Emu	femur	19.13281356	3.104500956	11.34112857	2.076141474	4.193108527	0.914644007	**9.56640678**	1.552250478	**5.67056429**	1.038070737	**2.09655426**	0.457322004	**476**
UM R1717	*Dromaeus novaehollan*	Emu	fibula	17.23836	4.860107551	13.45829412	5.285729062	5.783666667	2.147819923	**8.61918**	2.430053775	**6.72914706**	2.642864531	**2.89183333**	1.073909962	**703**
UM R1717	*Dromaeus novaehollan*	Emu	frontal	16.91028205	4.926233043	17.77177419	3.525331178	5.012328571	1.086905243	**8.45514103**	2.463116522	**8.8858871**	1.762665589	**2.50616429**	0.543452621	**789**
UM R1717	*Dromaeus novaehollan*	Emu	furcula	13.96558333	2.266181147	12.079375	2.578388031	4.4041	0.626703901	**6.98279167**	1.133090574	**6.0396875**	1.289194016	**2.20205**	0.31335195	**389**
UM R1717	*Dromaeus novaehollan*	Emu	humerus	18.76669565	4.623230929	10.25895349	2.064982335	4.144893939	0.597566787	**9.38334783**	2.311615464	**5.12947674**	1.032491168	**2.07244697**	0.298783394	**418**
UM R1717	*Dromaeus novaehollan*	Emu	ischium	16.434	7.768343181	11.69573684	2.833519657	4.439894737	0.744317056	**8.217**	3.88417159	**5.84786842**	1.416759829	**2.21994737**	0.372158528	**447**
UM R1717	*Dromaeus novaehollan*	Emu	manual phalan	15.34948148	3.706410646	9.975416667	2.739343414	3.759	0.598766265	**7.67474074**	1.853205323	**4.98770833**	1.369671707	**1.8795**	0.299383132	**301**
UM R1717	*Dromaeus novaehollan*	Emu	metacarpals	9.041339623	1.737472379	9.223	1.930464315	2.976140845	0.677560378	**4.52066981**	0.868736189	**4.6115**	0.965232157	**1.48807042**	0.338780189	**130**
UM R1717	*Dromaeus novaehollan*	Emu	pedal phalanx	17.87848889	4.064236989	7.907660377	1.625901808	4.922581633	0.855716881	**8.93924444**	2.032118494	**3.95383019**	0.812950904	**2.46129082**	0.42785844	**364**
UM R1717	*Dromaeus novaehollan*	Emu	publs	17.68577273	3.255533706	7.110714286	1.942047864	4.78562069	0.707932877	**8.84288636**	1.627766853	**3.55535714**	0.971023932	**2.39281034**	0.353966438	**315**
UM R1717	*Dromaeus novaehollan*	Emu	radius	15.34886207	2.852520686	9.809066667	1.52689415	4.020810811	0.730173927	**7.67443103**	1.426260343	**4.90453333**	0.763447075	**2.01040541**	0.365086964	**317**
UM R1717	*Dromaeus novaehollan*	Emu	scapula	17.88089655	4.670569156	13.30230435	2.379354332	4.610019231	0.809066237	**8.94044828**	2.335284578	**6.65115217**	1.189677166	**2.30500962**	0.404533119	**574**
UM R1717	*Dromaeus novaehollan*	Emu	scleral ossicle	11.02965385	1.760671757	10.90065	2.233578089	3.905673913	0.567746933	**5.51482692**	0.880335878	**5.450325**	1.116789045	**1.95283696**	0.283873467	**246**
UM R1717	*Dromaeus novaehollan*	Emu	sternal rib	15.12807407	5.487202593	9.7455	2.25624303	4.049529412	0.875284282	**7.56403704**	2.743601297	**4.87275**	1.128121515	**2.02476471**	0.437642141	**313**
UM R1717	*Dromaeus novaehollan*	Emu	tarsometatarsu	16.755	3.660312874	7.664548387	1.913267185	4.26627027	0.882742369	**8.3775**	1.830156437	**3.83227419**	0.956633593	**2.13313514**	0.441371185	**287**
UM R1717	*Dromaeus novaehollan*	Emu	tibia	14.31188889	3.443496393	9.017183673	2.30819275	3.663013158	0.663752514	**7.15594444**	1.721748197	**4.50859184**	1.154096375	**1.83150658**	0.331876257	**248**
UM R1717	*Dromaeus novaehollan*	Emu	ulna	17.06406897	4.179957296	14.08126667	3.773338144	5.382554054	1.022557057	**8.53203448**	2.089978648	**7.04063333**	1.886669072	**2.69127703**	0.511278529	**677**
242013	*Dumetella carolinensis*	Gray catbird	femur	15.49195918	2.568464992	6.851432432	1.474089522	3.755941176	0.884429482	**7.74597959**	3.872989796	**3.42571622**	0.737044761	**1.87797059**	0.442214741	**209**
UM R1719	*Gallus*	Chicken	femur	13.56083019	3.417042332	9.166383333	2.12716876	5.012553571	1.246780234	**6.78041509**	1.708521166	**4.58319167**	1.06358438	**2.50627679**	0.623390117	**326**
UM R1719	*Gallus*	Chicken	humerus	15.781	2.874082657	9.9589	2.333375015	4.782567568	1.013312521	**7.8905**	3.94525	**4.97945**	1.166687508	**2.39128378**	0.506656261	**394**
116250	*Grus canadensis*	Sandhill crane	femur	15.39904082	3.671967836	8.633930233	1.968305664	3.898290323	5.522290863	**7.69952041**	1.835983918	**4.31696512**	0.984152832	**1.94914516**	2.761145432	**271**
241804	*Icterus galbula*	Baltimore oriole	femur	15.29965	2.541015136	6.446089286	1.414918093	3.336657895	0.612220038	**7.649825**	1.270507568	**3.22304464**	0.707459047	**1.66832895**	0.306110019	**172**
8771	*Larus philadelphia*	Herring gull	femur	14.02819149	2.998881187	7.272759259	1.403609578	3.53363	0.890701139	**7.01409574**	3.507047872	**3.63637963**	0.701804789	**1.766815**	0.445350569	**189**
240864	*Megascops Otus asio*	Screech owl	femur	12.76978947	2.889303183	8.497481481	2.261903154	3.412198198	0.608606782	**6.38489474**	1.444651592	**4.24874074**	1.130951577	**1.7060991**	0.304303391	**194**
241793	*Megascops Otus asio*	Screech owl	femur	13.22214286	2.094034695	7.374785714	1.460916594	3.081415584	0.634076688	**6.61107143**	1.047017347	**3.68739286**	0.730458297	**1.54070779**	0.317038344	**157**
240864	*Megascops Otus asio*	Screech owl	humerus	15.27968627	3.264931941	6.970513514	1.80123108	3.693032	0.575914461	**7.63984314**	1.632465971	**3.48525676**	0.90061554	**1.846516**	0.287957231	**206**
241793	*Megascops Otus asio*	Screech owl	humerus	11.87086667	3.920674648	8.747096154	1.701350735	3.661567164	0.798464667	**5.93543333**	1.960337324	**4.37354808**	0.850675368	**1.83078358**	0.399232334	**199**
UM R1718	*Meleagris gallopavo*	Turkey	femur	13.3827191	3.528765139	8.085380952	1.8839061	4.126328244	1.111895885	**6.69135955**	1.76438257	**4.04269048**	0.94195305	**2.06316412**	0.555947942	**234**
241934	*Parus atricapillus atric*	Black-capped chickadee	femur	10.8046087	2.231991482	5.960631579	1.288660037	3.106071429	1.114481513	**5.40230435**	2.701152174	**2.98031579**	0.644330018	**1.55303571**	0.557240757	**105**
241963	*Parus atricapillus atric*	Black-capped chickadee	femur	10.95743548	1.915168474	7.111459459	1.422890789	2.805635135	0.435488061	**5.47871774**	2.739358871	**3.55572973**	0.711445394	**1.40281757**	0.217744031	**114**
241963	*Parus atricapillus atric*	Black-capped chickadee	humerus	10.91572	2.174188441	7.34220339	1.33382628	2.960964286	0.468424492	**5.45786**	2.72893	**3.67110169**	0.66691314	**1.48048214**	0.234212246	**124**
242058	*Passerella iliaca iliaca*	Fox sparrow	femur	11.68024528	3.074988342	6.587603448	1.575833636	3.853225225	0.849376827	**5.84012264**	1.537494171	**3.29380172**	0.787916818	**1.92661261**	0.424688414	**155**
UMMP 63156	*Phalacrocorax idahoensis*		femur	15.21861538	3.338551565	9.042212121	2.484852143	4.021905882	0.871482079	**7.60930769**	1.669275783	**4.52110606**	1.242426071	**2.01095294**	0.43574104	**290**
UMMP 74435	*Phalacrocorax idahoensis*		femur	18.16042553	4.963347112	7.652755556	2.6920334	4.504804348	1.658543398	**9.08021277**	2.481673556	**3.82637778**	1.3460167	**2.25240217**	0.829271699	**328**
241935	*Pheucticus ludovicianu*	Rose-breasted grosbeak	femur	13.36905263	3.1944419	4.900326923	1.330033653	3.160478873	0.64315912	**6.68452632**	3.342263158	**2.45016346**	0.665016827	**1.58023944**	0.32157956	**108**
241952	*Pheucticus ludovicianu*	Rose-breasted grosbeak	femur	13.43597959	2.954025597	5.642238095	1.683728974	3.250868132	0.563005846	**6.7179898**	1.477012799	**2.82111905**	0.841864487	**1.62543407**	0.281502923	**129**
241960	*Piranga olivacea*	Scarlet Tanager	femur	13.8841	3.545285017	6.918350877	1.7717529	3.051880342	6.076973146	**6.94205**	1.772642509	**3.45917544**	0.88587645	**1.52594017**	3.038486573	**153**
8725	*Podilymbus podiceps*	Pied-billed grebe	humerus	17.68678378	4.127290638	7.93678	1.888711506	4.319367816	0.713850615	**8.84339189**	2.063645319	**3.96839**	0.944355753	**2.15968391**	0.356925307	**317**
241885	*Quiscalus quiscula*	Common grackle	femur	11.48618462	1.666398656	7.236902439	1.888711506	3.870792453	0.591933936	**5.74309231**	0.833199328	**3.61845122**	0.944355753	**1.93539623**	0.295966968	**168**
223136	*Rhea americana*	Rhea	femur	21.96155556	3.316934641	9.33375	1.802426834	4.411690909	0.894509194	**10.9807778**	1.65846732	**4.666875**	0.901213417	**2.20584545**	0.447254597	**474**
241799	*Sitta carolinensis cook*	White breasted nuthatch	femur	12.28645455	1.774307879	9.215	2.276502418	3.214084746	0.657580132	**6.14322727**	0.88715394	**4.6075**	1.138251209	**1.60704237**	0.328790066	**191**
241938	*Spizella arborea arbor*	American tree sparrow	femur	11.45389655	2.555570274	6.934915493	1.822704237	3.700968992	0.777178369	**5.72694828**	1.277785137	**3.46745775**	0.911352119	**1.8504845**	0.388589185	**154**
UM R1716	*Struthio camelus*	Ostrich	femur	22.2952037	5.306567764	17.23378571	6.052319496	4.668037037	1.194219886	**11.1476019**	2.653283882	**8.61689286**	3.026159748	**2.33401852**	0.597109943	**939**
UM R1716	*Struthio camelus*	Ostrich	humerus	26.28013636	6.670173983	8.064047619	1.922911664	4.127697674	0.748680032	**13.1400682**	3.335086991	**4.03202381**	0.961455832	**2.06384884**	0.374340016	**458**
241899	*Turdus migratorius*	American robin	femur	14.55237931	2.030329537	7.804732143	1.539329801	3.070325301	0.592196019	**7.27618966**	1.015164769	**3.90236607**	0.7696649	**1.53516265**	0.296098009	**183**
242012	*Vermivora pinus*	Blue-winged warbler	femur	13.62146512	1.999316995	7.210903846	1.713161786	3.535789474	0.987079109	**6.81073256**	0.999658497	**3.60545192**	0.856580893	**1.76789474**	0.493539555	**182**
240779	*Vireo olivaceus*	Red-eyed vireo	femur	11.3574	1.953056852	9.062068966	1.889846785	3.201030612	0.571477854	**5.6787**	0.976528426	**4.53103448**	0.944923393	**1.60051531**	0.285738927	**173**
241897	*Zenaida macroura car*	Mourning dove	femur	11.18207547	1.612450308	6.407162162	1.645393224	2.649966292	0.746527468	**5.59103774**	0.806225154	**3.20358108**	0.822696612	**1.32498315**	0.373263734	**144**
241280	*Zonotrichia albicollis*	White throated sparrow	femur	13.5666	1.748743371	7.347967742	0.880345973	3.191634146	0.508134813	**6.7833**	0.874371686	**3.67398387**	0.440172987	**1.59581707**	0.254067406	**167**
									MIN	**4.52066981**	**0.80622515**	**2.45016346**	**0.44017299**	**1.32498315**	**0.21774403**	**105**
									MAX	**13.1400682**	**7.91664**	**8.8858871**	**3.02615975**	**2.89183333**	**3.03848657**	**939.128561**
									AVG	**7.49783368**	**1.99992978**	**4.49478101**	**1.0811666**	**1.93582858**	**0.51022639**	**294.945182**
										2.906663997	9.819390977	3.626650726	6.874932903	2.182543485	13.95439666	8.966308255

std dev	% stdDev is	Surface area	log surface area	
17.4	0.059	288.600	2.460	
13.2	0.040	321.394	2.507	
10.9	0.042	244.324	2.388	
18.4	0.065	270.527	2.432	
11.9	0.057	211.257	2.325	
11.4	0.042	261.255	2.417	
8.2	0.035	215.263	2.333	
7.8	0.044	210.503	2.323	
15.0	0.056	253.195	2.403	
14.8	0.051	261.599	2.418	
10.1	0.065	167.954	2.225	
6.5	0.039	192.155	2.284	
7.7	0.038	204.945	2.312	
11.3	0.061	213.792	2.330	
10.3	0.056	196.066	2.292	
6.5	0.030	214.010	2.330	
12.5	0.077	175.050	2.243	
9.0	0.053	206.706	2.315	
17.3	0.045	335.992	2.526	
46.3	0.096	389.949	2.591	
49.3	0.072	553.784	2.743	
19.7	0.073	268.987	2.430	
25.3	0.073	328.527	2.517	
16.8	0.035	403.083	2.605	
99.4	0.141	459.700	2.662	
59.4	0.075	553.722	2.743	
35.8	0.092	323.081	2.509	
27.1	0.065	363.151	2.560	
58.7	0.131	364.517	2.562	
23.3	0.077	287.624	2.459	
7.0	0.054	157.933	2.198	
16.4	0.045	299.525	2.476	
34.9	0.111	272.523	2.435	
15.1	0.048	288.423	2.460	
38.1	0.066	443.140	2.647	
14.6	0.059	233.064	2.367	
28.0	0.090	283.647	2.453	
18.4	0.064	262.221	2.419	
15.1	0.061	246.352	2.392	
45.0	0.066	463.489	2.666	
9.8	0.047	215.126	2.333	
16.7	0.051	262.156	2.419	
17.9	0.045	314.681	2.498	
14.2	0.052	258.644	2.413	
8.3	0.048	195.703	2.292	
9.4	0.050	201.481	2.304	
6.6	0.034	207.492	2.317	
9.6	0.061	185.731	2.269	
9.1	0.044	213.976	2.330	
18.6	0.093	202.827	2.307	
13.1	0.056	219.950	2.342	
9.3	0.089	130.666	2.116	
4.8	0.042	148.012	2.170	
6.2	0.050	153.571	2.186	
8.1	0.052	162.887	2.212	
18.0	0.062	267.849	2.428	
26.4	0.081	287.543	2.459	
7.9	0.073	138.798	2.142	
7.5	0.058	155.660	2.192	
7.4	0.048	184.125	2.265	
17.7	0.056	284.125	2.454	
6.3	0.037	172.458	2.237	
23.7	0.050	396.468	2.598	
9.5	0.050	211.396	2.325	
6.7	0.044	163.950	2.215	
76.7	0.082	683.870	2.835	
26.2	0.057	412.891	2.616	
7.8	0.043	212.613	2.328	
8.3	0.046	194.825	2.290	
7.3	0.042	193.868	2.288	
7.1	0.049	136.378	2.135	
7.6	0.046	191.395	2.282	
SD MAX	0.141			
SD MIN	0.030			
SD AVG	0.060			

CHAPTER 6

CONCLUSION

In this chapter I summarize the research results and conclusions of the preceding dissertation. In the past decade, the number of named titanosauriforms has greatly outpaced both taxonomic revision of preexisting genera and phylogenetic studies of their interrelationships, leaving a large unresolved pool of genera as ‘basal titanosauriforms.’ This dissertation utilized comparative anatomy in museum collections research, geologic and paleontological fieldwork, bone histology, and cladistic analysis to better understand the evolution and systematics of early titanosauriform dinosaurs.

In Chapter 2 I resolved the taxonomic affinities of Early Cretaceous titanosauriforms from the Trinity Group of Texas. I first showed that a lack of autapomorphies in their holotypes and definitive skeletal associations among their hypodigms renders *Astrodon johnstoni, Pleurocoelus altus*, and *Pleurocoelus nanus* nomina dubia, precluding referral of Texan material to those taxa as has been common practice historically. I showed that although representative individuals of one Texan genus, *Paluxysaurus,* were not near adult size at the time of death. The similar provenance, lack of morphological differences, and shared unique features support referral of *Paluxysaurus* to *Sauroposeidon*. Other titanosauriform materials from the Trinity Group represent the holotype of a new basal titanosauriform diagnosed by a hyposphene-hypantrum system in the caudal vertebrae. A titanosauriform hind limb previously referred to "*Pleurocoelus*" is instead referable to the brachiosaurid *Cedarosaurus weiskopfae* based on shared features of the pes. I showed that the Trinity Group of Texas and laterally-equivalent Antlers Formation of Oklahoma exhibit a similar dinosaur fauna at the generic level with the Cloverly Formation of Wyoming. This homogeneity with respect to latitude stands in marked contrast to the latitudinal variation in dinosaur faunas that developed later in the Cretaceous.

In Chapter 3, I redescribed and presented new sauropod material from the Early Cretaceous Cloverly Formation that I refered to the titanosauriform *Sauroposeidon proteles*. In contrast to previous hypotheses that it was a brachiosaurid, I asserted that *Sauroposeidon* is a member of Somphospondyli on the basis of numerous features including fine camellate pneumaticity in presacral vertebrae, a medially beveled scapular glenoid, and an interlocking proximal tibia and fibula. Thus, the disappearance of sauropods from the North American fossil record (the start of the 'sauropod hiatus') concerned both brachiosaurids and somphospondylans. I found claims for titanosaurs in the Early Cretaceous of North America to be unsubstantiated. My field observations augment previous reports that indicate that the latest register of *Sauroposeidon* and other Early Cretaceous North American sauropods occurs in or below the near-coastal units marking major transgression of the Western Interior Seaway, whereas seven ecologically disparate dinosaur lineages are present just below and above this boundary. The presence of these through-ranging lineages with sauropods before and after sauropod disappearance suggests that appropriate sauropod-bearing environments were present into the early Late Cretaceous, in turn suggesting that the disappearance of sauropods is not attributable to taphonomic bias or uneven sampling. Furthermore, my field observations of the Cloverly Formation indicate that sauropods inhabited near-coastal environments, which were abundant in the western United States well after sauropods' disappearance. I interpret the start of the sauropod hiatus as the result of a genuine continent-wide extinction, perhaps attributable to competition with ornithischian herbivores and/or the incursion of the Western Interior Seaway.

In Chapter 4, I investigated the phylogenetic relationships of basal titanosauriforms via a cladistic analysis in which 25 terminal taxa were scored for 114 characters, over one-third of which were new. Analysis of these characters resulted in the recovery of three main clades: Brachiosauridae, a cosmopolitan mix of Late Jurassic and Early Cretaceous forms, Euhelopodidae, an endemic clade of 'middle' Cretaceous East Asian sauropods, and Titanosauria, a large Cretaceous clade made up of mostly Gondwanan genera. Early titanosauriforms and their outgroups display cosmopolitanism, but towards the middle of the Cretaceous, brachiosaurids and euhelopodids display endemism. Titanosauriform paleobiogeographic history is the result of several factors, including differential extinction patterns and dispersal. Several putative brachiosaurids were instead found to represent non-titanosauriforms or more derived taxa, and no support for a Laurasia-wide clade of titanosauriforms was found. This analysis establishes robust synapomorphies for many titanosauriform subclades. A reevaluation of the phylogenetic affinities of fragmentarily represented taxa based on these synapomorphies finds no body fossil evidence for titanosaurs before the middle Cretaceous (Aptian), in contrast to previous reports of Late Jurassic taxa. Purported titanosaur tracks from the Middle Jurassic either represent a 35-million-year ghost lineage for the group (longer than their entire body fossil record) or — more likely — represent non-titanosaurs. This study provides a foundation for future study of basal titanosauriform phylogeny and the origins of Titanosauria. The latter topic remains enigmatic, as the geologically oldest titanosaurs are already derived forms.

In Chapter 5, I investigated the morphology of bone-forming cells (osteocytes), which are the only cells whose morphology is readily observable in the fossil record. Previous studies had linked osteocyte morphology with genome size and bone growth rates, and had suggested that osteocyte volume was unrelated to body size. I showed that results of previous studies are suspect due to their design, sample scope, or analysis, using a large sample of modern birds and orthogonal thin sectioning. I demonstrated that avian osteocytes in parallel-fibered bone are best modelled as scalene ellipsoids, and that the strongest controls on osteocyte volume or surface area are bone element (e.g., femur vs.

rib), bone tissue type (e.g., woven vs. lamellar), and body mass. Osteocyte volume displays low variation between homologous bones in individuals of the same species. Genome size is not strongly related to osteocyte volume when the effects of body mass and/or phylogeny are removed. Growth rate and basal metabolic rate are unrelated to osteocyte volume or surface area. Changes in bone growth rate instead may be attributable to osteocyte density or the efficacy of bone formation per osteocyte.

This dissertation synthesized data and methods from several disciplines to investigate the evolution of titanosauriform sauropod dinosaurs. I presented several taxonomic revisions and a framework of their early evolution via cladistic analysis. I also showed that osteocyte morphology is not a suitable proxy for reconstructing the growth rates, metabolic rate, or genome sizes of extinct animals as had been previously concluded. Further work is needed to reconstruct the growth rates of titanosauriforms via bone histology.